ANNEXE 1 – Liste des posters

Posters présentés lors du Forum
(seuls figurent ici les posters dont les doctorants concernés autorisent la diffusion)

APIL 2017

Annual PhD students conference
IAEM Lorraine

Actes des posters
Journée d'automne de l'école doctorale
IAEM Lorraine

16 octobre 2017

Edités par Didier Maquin

Université de Lorraine
ED IAEM Lorraine, Faculté des Sciences et Technologies
Bâtiment du 2ème cycle – Atrium, BP 70239
54506 Vandoeuvre-lès-Nancy Cedex, France
ed-iaem-dir@univ-lorraine.fr
http ://www.iaem.univ-lorraine.fr

Préface

Ce document rassemble les posters présentés par les doctorants inscrits en troisième année (année académique 2017–2018) de préparation du doctorat de l'Université de Lorraine au sein de l'Ecole Doctorale IAEM Lorraine. Chaque poster a été évalué par deux membres du comité de programme et les doctorants ont déposé une version finale tenant compte des remarques des relecteurs. Cet exercice contribue au suivi des doctorants au cours de la préparation du doctorat. Les posters ont été présentés le 26 octobre 2017 au cours de la Journée d'Automne de l'Ecole Doctorale IAEM Lorraine dont le programme est donné à la page suivante.

Journée d'automne de l'Ecole Doctorale IAEM Lorraine
Annual PhD students conference IAEM Lorraine
APIL 2017

Jeudi 26 octobre 2017
Amphithéâtre 8 de la Faculté des Sciences et Technologies de Vandœuvre-lès-Nancy (Campus Aiguillettes)

9h00 – 9h10	Accueil des participants (Didier Maquin) **Clotilde Boulanger, Vice-Présidente déléguée à la Stratégie doctorale** La place du doctorat au sein de l'Université de Lorraine
9h10 – 9h40	**Didier Maquin, Directeur de l'ED IAEM Lorraine** L'Ecole Doctorale IAEM – Dispositions du nouvel arrêté Informations diverses
9h40 – 10h10	**Marc Dalaut, Responsable du service des Etudes Doctorales** Le service des études doctorales Le Collège Lorrain des Etudes Doctorales
10h10 – 11h00	Pause café – Séance Poster
11h00 – 11h15	**Badr-El-Boudour Bidouche, doctorante en génie électrique** Le rôle des élus étudiants au sein du conseil de l'ED et du CLED
11h15 – 11h45	**Corentin Kerbiriou, chargé de projet au PEEL** **Natacha Hauser-Costa et Lisa Mougenot, Incubateur Lorrain** Le doctorat et l'entrepreneuriat
11h45 – 12h05	**Mayank Shekkar Jha, maître de conférences UL** Témoignage sur le parcours d'un docteur
12h05 – 13h30	Séance Poster – Buffet

Comité de programme

Amar Rouane	Université de Lorraine, IJL
Horatiu Cirstea	Université de Lorraine, LORIA
Bernard Davat	Université de Lorraine, GREEN
Thierry Divoux	Université de Lorraine, CRAN
Pierrick Gaudry	Université de Lorraine, LORIA
Imed Kacem	Université de Lorraine, LCOMS
Hoai An Le Thi	Université de Lorraine, LITA
Didier Maquin	Université de Lorraine, CRAN
Jean-Yves Marion	Université de Lorraine, LORIA
Dominique Mery	Université de Lorraine, LORIA
Mustapha Nadi	Université de Lorraine, IJL
Hervé Oyono-Oyono	Université de Lorraine, IECL
Stéphane Raël	Université de Lorraine, GREEN
Nidhal Rezg	Université de Lorraine, LGIPM
Alain Richard	Université de Lorraine, CRAN
Jean-Rodolphe Roche	Université de Lorraine, IECL
Stéphane Vialle	CentraleSupelec, UMI Georgia Tech
Laurent Vigneron	Université de Lorraine, LORIA

Table des matières

Méthode de décomposition de domaines pour la résolution numérique d'une équation non linéaire

Nahed Naceur

co-directeurs: Moez Khenissi et Jean R. Roche

Institut ÉLIE CARTAN de Lorraine

Objectifs

1. Développer et étudier une méthode de décomposition de domaines pour résoudre numériquement une équation parabolique non linéaire.
2. Démontrer la convergence des méthodes numériques étudiées pour la résolution de ce type d'équation.
3. Réaliser une implémentation informatique des algorithmes étudiés dans le cas d'une et deux dimensions.

Introduction

On s'intéresse à l'étude théorique de solution faible positive des équations aux dérivées partielles non linéaires. On décrit après un algorithme numérique qui calcule une approximation numérique de cette solution. Dans une première étape on calcule, à l'aide de la méthode de décomposition de domaines une sur-solution positives pour ce type de problème:

$$(\mathcal{P})\begin{cases} u_t(x,t) - Au(x,t) + G(x, Du(x,t)) = F(x, u(x,t)) + f(x,t) & \text{dans } Q_T \\ u(x,t) = 0 & \text{dans } \Sigma_T \\ u(x,0) = u_0(x) & \text{dans } \Omega, , \end{cases}$$

- $Q_T = \Omega \times]0,T]$, $\Sigma_T = \partial\Omega \times]0,T]$,
- Ω un ouvert borné de $\mathbb{R}^d$ $(d = 1, 2)$, $T > 0$.
- A un opérateur elliptique ($\frac{\partial^2}{\partial x^2}$ pour $d = 1$ et Δ pour $d = 2$),
- $F, G : \Omega \times \mathbb{R} \to [0, +\infty[$ sont mesurables et continues par rapport à Du et u
- f une fonction positive.

Sous-problème elliptique

On commence par l'étude de l'existence de la solution positive de ce problème elliptique:

$$(E)\begin{cases} -Au(x) + G(x, Du(x)) = F(x, u(x)) + f(x) & \text{dans } \Omega \\ u(x) = 0 & \text{dans } \partial\Omega \end{cases}$$

S'il existe une sur-solution positive w de (E) alors il existe une unique solution positive u de ce problème tel que $0 \leq u \leq w$. u est la limite de la suite u_n solution de:

$$\begin{cases} u_{n+1} \in W_0^{1,\infty}(\Omega) \\ -Au_{n+1}(x) + G_{n+1}(x, Du_{n+1}(x)) = F(x, u_n(x)) + f(x) \text{ dans } \mathcal{D}'(\Omega) \end{cases} \quad (1)$$

avec $u^0 = w$, $0 \leq u_{n+1} \leq u_n \leq w$, et G_n approximation de Yosida de G.

Méthodes Numériques

1) Calculer $w \in H_0^1(\Omega)$ telle que:

$$-Aw(x) = F(x, w) + f \text{ dans } \mathcal{D}'(\Omega). \quad (2)$$

2) Pour une donnée $u_0 = w$, calculer, pour $n = 1, 2, \ldots$ convergence, la suite $\{u_n\}_n$, est solution dans $H_0^1(\Omega)$ de l'équation non linéaire:

$$-Au_{n+1}(x) + G_{n+1}(x, Du_{n+1}(x)) = F(x, u_n(x)) + f(x) \text{ dans } \mathcal{D}'(\Omega). \quad (3)$$

On applique la méthode de Newton pour résoudre (2). Soit $w^0 = 0$, on définit $w^{k+1} = w^k + \delta$, où δ est la solution du problème linéaire suivant:

$$\begin{cases} -A\delta(x) - \dfrac{\partial F(x, w^k)}{\partial r}\delta(x) = Aw^k(x) + F(x, w^k) + f(x) & \forall x \in \Omega \\ \delta(x) = 0 & \text{sur } \partial\Omega. \end{cases}$$

Ce problème est elliptique dans $H_0^1(\Omega)$ si $\text{mes}(\Omega) \leq \frac{\sqrt{2}}{c_\infty}$, où $c_\infty = \| \frac{\partial F(x, w^k)}{\partial r} \|_\infty$.

Méthode de décomposition de domaines en 1 D

Soit $\overline{\Omega} = \bigcup_{i=1}^{m} [\alpha_i, \alpha_{i+1}] = \bigcup_{i=1}^{m} \overline{\Omega_i}$, $\Omega_i \cap \Omega_j = \emptyset$, $i = 1, \ldots, m$, et $\text{mes}(\Omega_i) \leq \frac{\sqrt{2}}{c_\infty}$.

Pour $i = 1, .., m$ et pour $j = 0, ..,$ convergence, on résout les problèmes suivants:

$$\begin{cases} -A\delta_i^{j+1}(x) + c(x)\delta_i^{j+1}(x) = g(x) \text{ dans } \Omega_i \\ \dfrac{\partial \delta_i^{j+1}(\alpha_i)}{\partial n} - \lambda\delta_i^{j+1}(\alpha_i) = \dfrac{\partial \delta_{i-1}^{j+1}(\alpha_i)}{\partial n} - \lambda\delta_{i-1}^{j+1}(\alpha_i) = r_{i-1}^{j+1}(\alpha_i) \\ \dfrac{\partial \delta_i^{j+1}(\alpha_{i+1})}{\partial n} + \lambda\delta_i^{j+1}(\alpha_{i+1}) = \dfrac{\partial \delta_{i+1}^{j}(\alpha_{i+1})}{\partial n} + \lambda\delta_{i+1}^{j}(\alpha_{i+1}) = l_{i+1}^{j}(\alpha_{i+1}) \end{cases}$$

Cette méthode converge dans $H_0^1(\Omega)$.

Algorithmes Numériques

Une fois la sur-solution calculée, on va résoudre le problème non linéaire obtenu par l'approximation de Yosida G_n de G:

$$-Au_n(x) + G_n(x, Du_n(x)) = F(x, u_{n-1}(x)) + f(x) \quad \forall x \in \Omega \quad (4)$$

A chaque itération en n le problème (4) est résolu par la méthode de Newton:

- $u_0 = w$,
- Pour $n = 1, ..,$ convergence, $u_n^0 = u_{n-1}$ $\theta = 0$
- Pour $j = 1, \ldots,$convergence, $\theta = u_n^{j+1} - u_n^j$ est la solution du problème linéaire:

$$\begin{cases} -A\theta(x) + \dfrac{\partial G_n(x, Du_n(x))}{\partial r}D\theta(x) = Au_n(x) - G_n(x, Du_n^j) \\ \qquad +F(x, u_{n-1}(x)) + f(x) \ \forall x \in \Omega \\ \theta(x) = 0 \quad \text{sur } \partial\Omega \end{cases}$$

Résultat Numérique

$$\begin{cases} -u''(x) = \beta \mid u(x) \mid^3 - \mid u(x)' \mid^3 + 2\delta_{\frac{1}{3}} & \forall x \in]0,1[\\ u(0) = u(1) = 0. \end{cases} \quad (5)$$

où δ_x désigne la mesure de Dirac au point x.

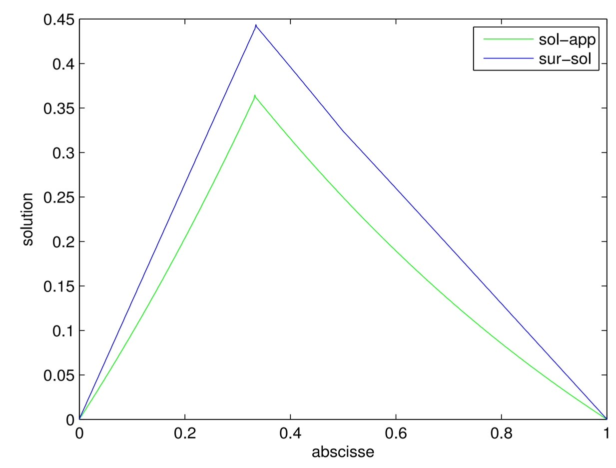

Figure 1: $\| c \|_\infty = 0.885$, $m = 2$, $err = 6.6\,10^{-5}$

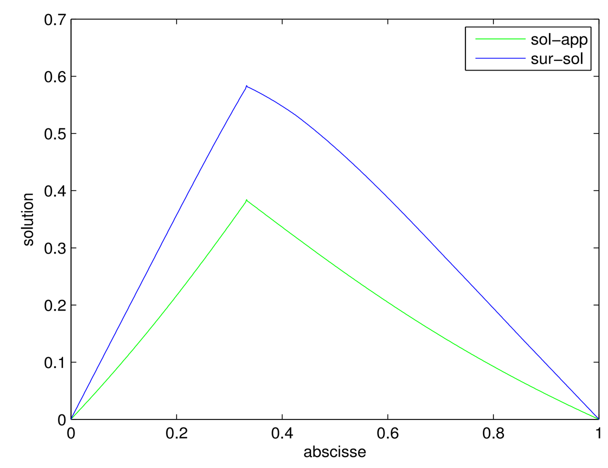

Figure 2: $\| c \|_\infty{=}6.644$, $m = 7$, $err = 3.6\,10^{-5}$

On remarque que le nombre de sous domaine dépend de $\| c \|_\infty$. Par ailleurs plus on a des sous domaines, plus l'erreur est réduite.

Problème Parabolique

On considère le problème de Fujita suivant:

$$(\mathcal{P}')\begin{cases} u_t(x,t) - Au(x,t) = |u(x,t)|^p + f(x,t) & \text{dans } Q_T \\ u(x,t) = 0 & \text{dans } \Sigma_T \\ u(x,0) = u_0(x) & \text{dans } \Omega, \end{cases}$$

avec $p > 1$, $f \geq 0$. Pour $u_0 \in L^2(\Omega)$, $f \in L^\infty_{loc}(L^2(\Omega), [0, \infty[)$, alors il existe une unique solution maximale $u \in C(L^2(\Omega), [0, T_{max}[)$ de $(\mathcal{P}')$. On a $T_{max} > 0$ et si $T_{max} < \infty$ alors $\lim_{t \nearrow T_{max}} \| u(t) \|_\infty = \infty$.

Perspectives

Si maintenant on considère l'équation:

$$(\mathcal{P}'')\begin{cases} u_t(x,t) - Au(x,t) + |\nabla u(x,t)|^q = |u(x,t)|^p + f(x,t) & \text{dans } Q_T \\ u(x,t) = 0 & \text{dans } \Sigma_T \\ u(x,0) = u_0(x) & \text{dans } \Omega, \end{cases}$$

avec $p > 1$, $f \geq 0$.

- Développer et montrer la convergence de la méthode de décomposition des domaines ainsi que l'approximation de Yosida pour résoudre $(\mathcal{P}'')$.
- Étudier le comportement de la solution approchée dans le cas d'explosion en fonction de p et q.
- Compléter le codage des algorithmes dans le cas de deux dimensions.

Références

[1] A. Valli A. Quarteroni.
Domain Decomposition Methods for Partial Diferential Equations, volume 1.
Oxford Science Publications, 1999.

[2] J.R. Roche N.Alaa.
Theoretical and numerical analysis of a class of nonlinear elliptic equations.
Mediterr. J. Math, 2:327–344, 2005.

David FEUTRIE (Doctorant en Mathématiques)

david.feutrie@univ-lorraine.fr

Encadrants : Cécile Dartyge & Gérald Tenenbaum

Cribler par une progression arithmétique

Institut Élie Cartan de Lorraine

Mon travail est consacré à l'étude d'une formule asymptotique pour le nombre des entiers $\leqslant x$ n'admettant aucun diviseur dans une progression arithmétique donnée. Mon objectif pour cela est de parvenir à une amélioration du résultat de Narkiewicz et Radziejewski [2], et même à une généralisation des résultats obtenus.

Préliminaires :

Fixons un entier $q \geqslant 3$ et une classe résiduelle $a(\bmod q)$ telle que $\mathrm{PGCD}(a, q) = 1$.

Landau [3], en 1909, a d'abord montré que tous les entiers $\leqslant x$, sauf $o(x)$ exceptions, possèdent un diviseur congru à a modulo q. Par la suite, plusieurs mathématiciens se sont intéressés à

$$\mathcal{N}_{a,q}(x) := \left|\left\{2 \leqslant n \leqslant x : \big(d \mid n,\ d > 1\big) \Longrightarrow d \not\equiv a \,(\bmod q)\right\}\right|.$$

Dans cette direction, en 2008, Banks, Friedlander et Luca [1] ont étudié le cas où q est premier. Trois ans plus tard, Narkiewicz et Radziejewski ont étudié le cas général et ont obtenu

Théorème.

$$\mathcal{N}_{a,q}(x) = \big(C(a,q) + o(1)\big)\frac{x(\ln_2 x)^{\alpha(a,q)}}{(\ln x)^{1-\beta(a,q)}}$$

où $C(a,q) > 0$, $\alpha(a,q) > 0$ et $0 \leqslant \beta(a,q) < 1$. Ces trois constantes dépendent de certaines propriétés de $G_q := (\mathbb{Z}/q\mathbb{Z})^\times$ et peuvent être calculées, mais leur formulation est assez complexe.

- *Lorsque $a = 1$, $C(1,q)$ et $\alpha(1,q)$ sont assez simples à expliciter et $\beta(1,q) = 0$.*
- *Lorsque $a \neq 1$, $\beta(a,q) = B(a,q)/\varphi(q) > 0$ où $B(a,q)$ est le cardinal du plus grand sous-groupe de G_q ne contenant pas $a\,(\bmod q)$.*

L'article précise que le terme d'erreur peut être remplacé par $O\big(1/\ln_2 x\big)$.

Nous notons $s = \sigma + i\tau \in \mathbb{C}$ où $\sigma, \tau \in \mathbb{R}$.

L'outil principal utilisé pour la démonstration est le théorème de Selberg-Delange dans une version de 1953 [6]. Nous utilisons pour notre étude ce théorème, mais dans une version actualisée (chapitre II.5. de [5]).

Définition. *La fonction* **Gamma d'Euler** *est définie sur $\sigma > 0$ par*

$$\Gamma(s) := \int_0^\infty t^{s-1}\mathrm{e}^{-t}\,\mathrm{d}t$$

et est prolongeable en une fonction méromorphe sur $\mathbb{C}$ avec des pôles en 0 et pour les entiers négatifs.

Lemme. [5] *Soit $F(s) := \sum_{n\geqslant 1} a_n/n^s$ une série de Dirichlet telle que, pour $z \in \mathbb{C}$, $c_0 > 0$, $0 < \delta < 1$, $M > 0$, la série de Dirichlet $G(s,z) := F(s)\big(\sum_{n\geqslant 1} 1/n^s\big)^{-z}$ est prolongeable en une fonction holomorphe pour $\sigma \geqslant 1 - c_0/(1 + \max\{0, \ln|\tau|\})$ et vérifie dans ce domaine*

$$|G(s;z)| \leqslant M(1 + |\tau|)^{1-\delta}.$$

Alors pour $x \geqslant 3$, $A > 0$, $|z| \leqslant A$, on a

$$\sum_{n\leqslant x} a_n = x(\ln x)^{z-1}\left\{\frac{G(s,z)}{\Gamma\big(z/\varphi(q)\big)} + O\Big(\frac{1}{\ln_2 x}\Big)\right\}.$$

L'autre outil utilisé pour notre étude est le théorème de Hankel.

Lemme. [5] *Pour tout $z \in \mathbb{C}$ et tout $r > 0$, nous avons*

$$\frac{1}{\Gamma(z)} = \frac{1}{2i\pi}\int_{\mathcal{H}(r)} \xi^{-z}\mathrm{e}^{\xi}\mathrm{d}\xi$$

où $\mathcal{H}(r)$ est un contour de Hankel défini par

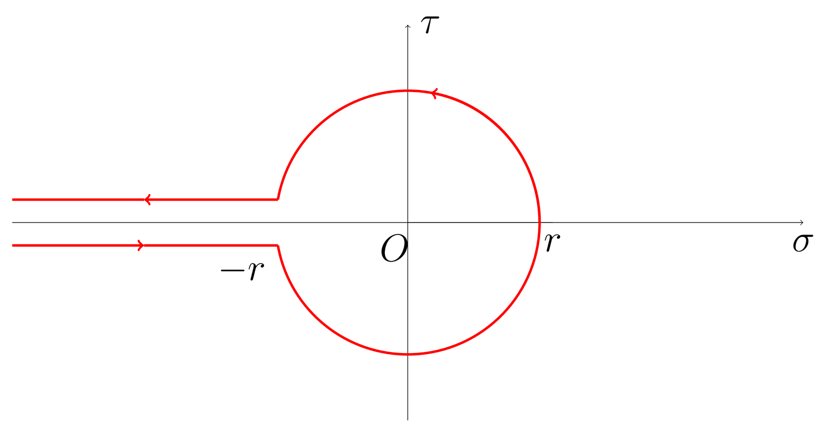

Nos notations :

Notations.

- *$\boldsymbol{\nu} = (\nu_j)_{j\in G_q} \in [\![0; \varphi(q)]\!]^{\varphi(q)}$ non nul est dit* **admissible** *si*

$$\forall(\mu_j)_{j\in G_q} \in \prod_{j\in G_q}[\![0;\nu_j]\!] : \quad \sum_{j\in G_q}\mu_j > 0 \Longrightarrow \prod_{j\in G_q} j^{\mu_j} \not\equiv a\,(\bmod q)$$

  et on pose $\mathcal{E}_q$ l'ensemble de ces éléments.
- *Pour $\boldsymbol{\nu} = (\nu_j)_{j\in G_q} \in \mathcal{E}_q$, on pose $I_q(\boldsymbol{\nu}) \subseteq G_q$ l'ensemble des classes j vérifiant $\nu_j = \varphi(q)$.*
- *Pour $\boldsymbol{\nu} = (\nu_j)_{j\in G_q} \in \mathcal{E}_q$, on note*

$$\mathsf{s}(\boldsymbol{\nu}) := \sum_{j\in G_q\smallsetminus I_q(\boldsymbol{\nu})}\nu_j; \qquad \boldsymbol{\nu}! := \prod_{j\in G_q\smallsetminus I_q(\boldsymbol{\nu})}\nu_j!$$

- *On pose $\mathfrak{J}_a := \max\{|I_q(\boldsymbol{\nu})| : \boldsymbol{\nu} \in \mathcal{E}_q\}$, $\mathfrak{K}_a := \max\{\mathsf{s}(\boldsymbol{\nu}) : |I_q(\boldsymbol{\nu})| = \mathfrak{J}_a\}$.*
- *Pour $\boldsymbol{\nu} \in \mathcal{E}_q$ et χ_0 le caractère principal, on pose*

$$C(q,\boldsymbol{\nu}) := \Big(\frac{q}{\varphi(q)}\Big)^{1-|I_q(\boldsymbol{\nu})|/\varphi(q)}\prod_{\chi\neq\chi_0}\prod_p\Big(1-\frac{1}{p}\Big)^{-\chi(p)\sum_{j\in I_q(\boldsymbol{\nu})}\overline{\chi(j)}/\varphi(q)}.$$

Notre résultat :

Théorème. [7] *Il existe un polynôme P tel que l'on ait, uniformément par rapport à x, pour $0 < \varepsilon < 1/\varphi(q)$,*

$$\mathcal{N}_{a,q}(x) = \Big\{P(\ln_2 x) + O\Big(\frac{1}{(\ln x)^{(1-\varepsilon)/\varphi(q)}}\Big)\Big\}\frac{x}{(\ln x)^{1-\mathfrak{J}_a/\varphi(q)}}.$$

- *Si $1 < a < q$, alors $\mathfrak{J}_a > 0$, P est de degré $\mathfrak{K}_a$ et son coefficient dominant vaut*

$$\frac{1}{\Gamma\big(\mathfrak{J}_a/\varphi(q)\big)\varphi(q)^{\mathfrak{K}_a}}\sum_{\substack{\boldsymbol{\nu}\in\mathcal{E}_q\\ |I_q(\boldsymbol{\nu})|=\mathfrak{J}_a\\ \mathsf{s}(\boldsymbol{\nu})=\mathfrak{K}_a}}\frac{C(q,\boldsymbol{\nu})}{\boldsymbol{\nu}!}.$$

- *Si $a = 1$, alors $\mathfrak{J}_a = 0$, $\mathfrak{K}_a > 0$, P est de degré $\mathfrak{K}_a - 1$ et son coefficient dominant vaut*

$$\frac{q\mathfrak{K}_a}{\varphi(q)^{\mathfrak{K}_a+1}}\sum_{\substack{\boldsymbol{\nu}\in\mathcal{E}_q\\ \mathsf{s}(\boldsymbol{\nu})=\mathfrak{K}_a}}\frac{1}{\boldsymbol{\nu}!}.$$

Remarque. [7] *On a un résultat similaire en remplaçant a par une suite de résidus $\boldsymbol{a} = \{a_1 \dots, a_k\}$, en distinguant les cas $1 \in \boldsymbol{a}$ et $1 \notin \boldsymbol{a}$.*

Références

[1] Banks, W., Friedlander, J. and Luca, F., Integers without divisors, *Forum mathematicum*, 20 : 1005-1037, 2008.

[2] Narkiewicz, W. and Radziejewski, M., Integers without divisors in a given progression, *Monatsh Math.*, (164) : 75-85, 2011.

[3] Landau, E., *Handbuch der Lehre von der Verteilung der Primzahlen*, Taubner, 1909. Reprint Chelsea (1953).

[4] Erdös, P., On the distribution of divisors of integers in the residue classes (mod d), *Bull. Soc. Math. Grèce*, 6 Fasc. 1 : 27-36, 1965.

[5] Tenenbaum, G., *Introduction à la théorie analytique et probabiliste des nombres*, quatrième édition, coll. Échelles, Belin, 2015.

[6] Delange, H., Sur la distribution des entiers ayant certaines propriétés, *Ann. Sci. Ecole Norm. Sup.*, **73**(3) : 15-74, 1956.

[7] Feutrie, D., Cribler par une progression arithmétique, Prépublication.

Secure operation of virtualized Named Data Networks

Xavier Marchal, Thibault Cholez, Olivier Festor
LORIA, UMR 7503 (University of Lorraine, CNRS, INRIA)
Vandoeuvre-les-Nancy, F-54506, France
{xavier.marchal, thibault.cholez, olivier.festor}@loria.fr

Introduction to Named-Data Networking (NDN)

- New networking architecture (Information-Centric Networking) instead of current Host-Centric Networking
- Layer-3 Protocol (can replace IP) but routes on content names instead of IP addresses: **/alice/pictures/paris_1.jpg**

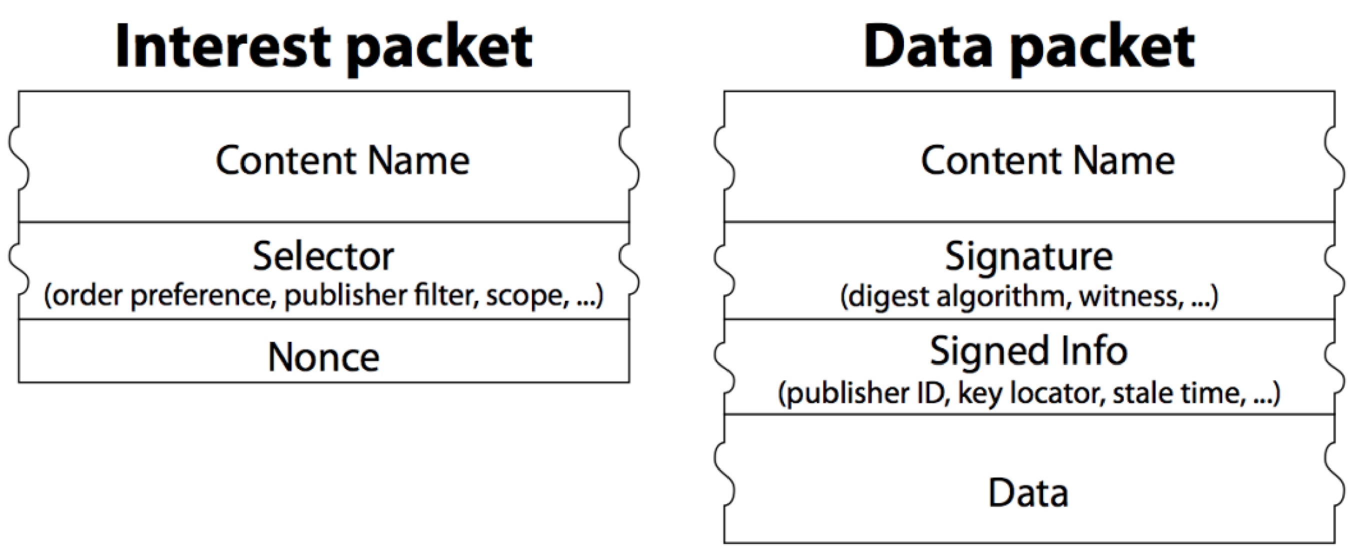

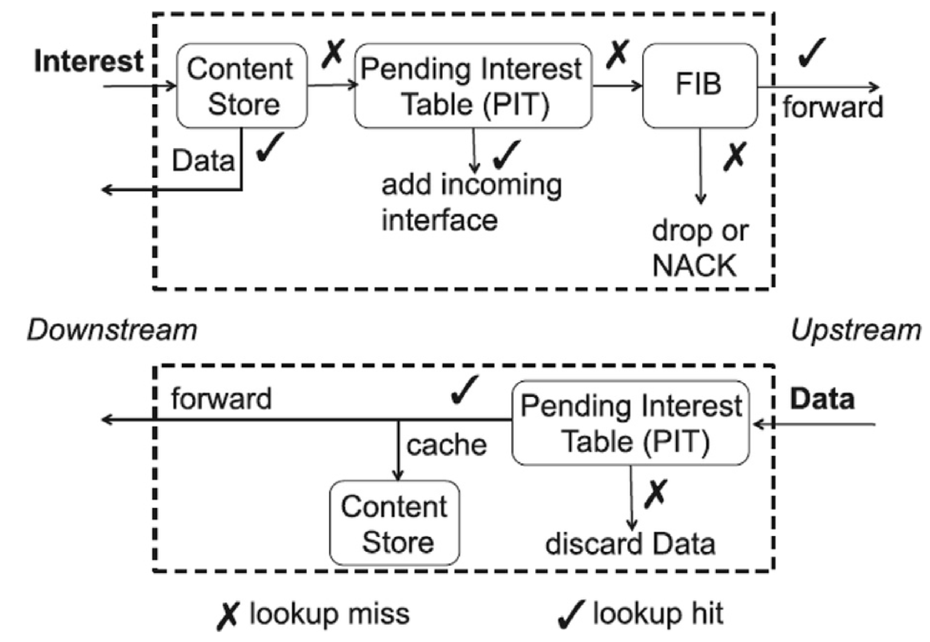

- Optimized for massive content diffusion:
  - In-network cache (CS) and Interest concatenation (PIT)
  - Rely on digital signature for content authentication

- Objectives of the thesis: Improve security, interoperability and deployment of NDN networks
  - Deploy a solution that allows IP and NDN networks to communicate for web contents (HTTP)
  - Deployment and orchestration of NDN virtual network functions (VNF)

Security of Named-Data Networking

- New kind of networks = new kind of attacks
- Content Poisoning attack
  - Recognized as a major threat
  - Insert malicious Data in routers' CS
- Timed Data from unregistered producer
  - Undetectable by the legitimate producer
  - Data flooding on a specific content
  - Self-answering (can inject any content)
  - Can be patched easily

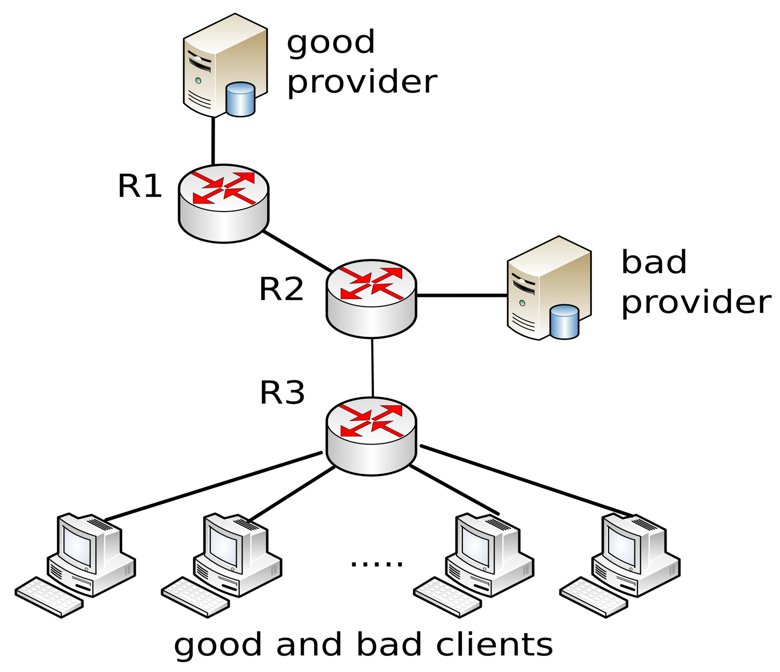

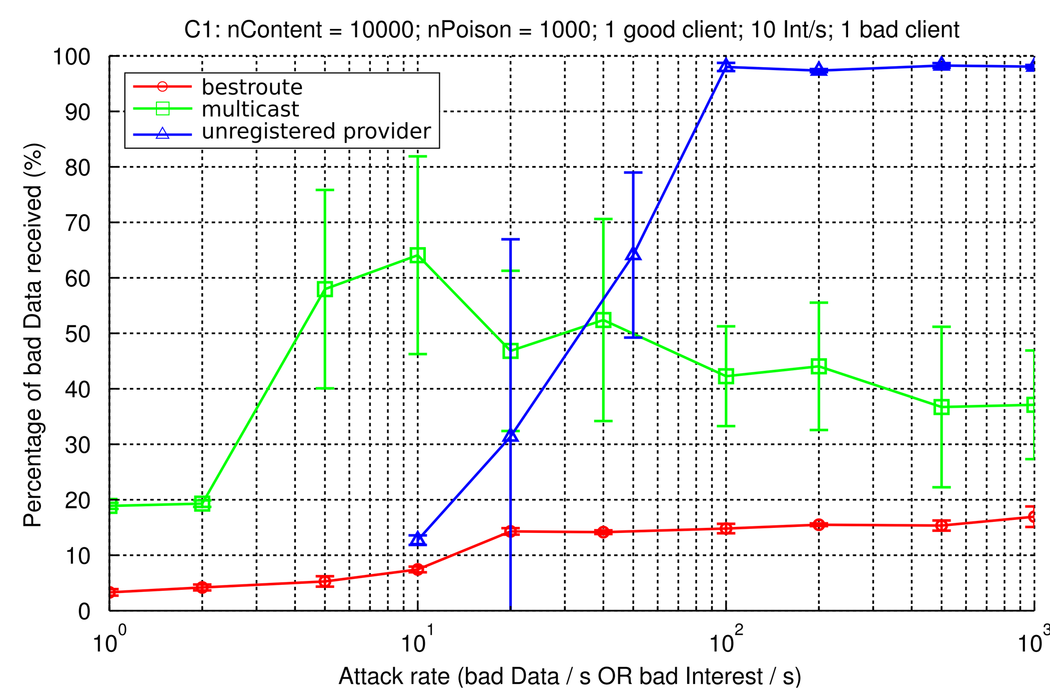

IP to Named-Data Networking HTTP Gateway

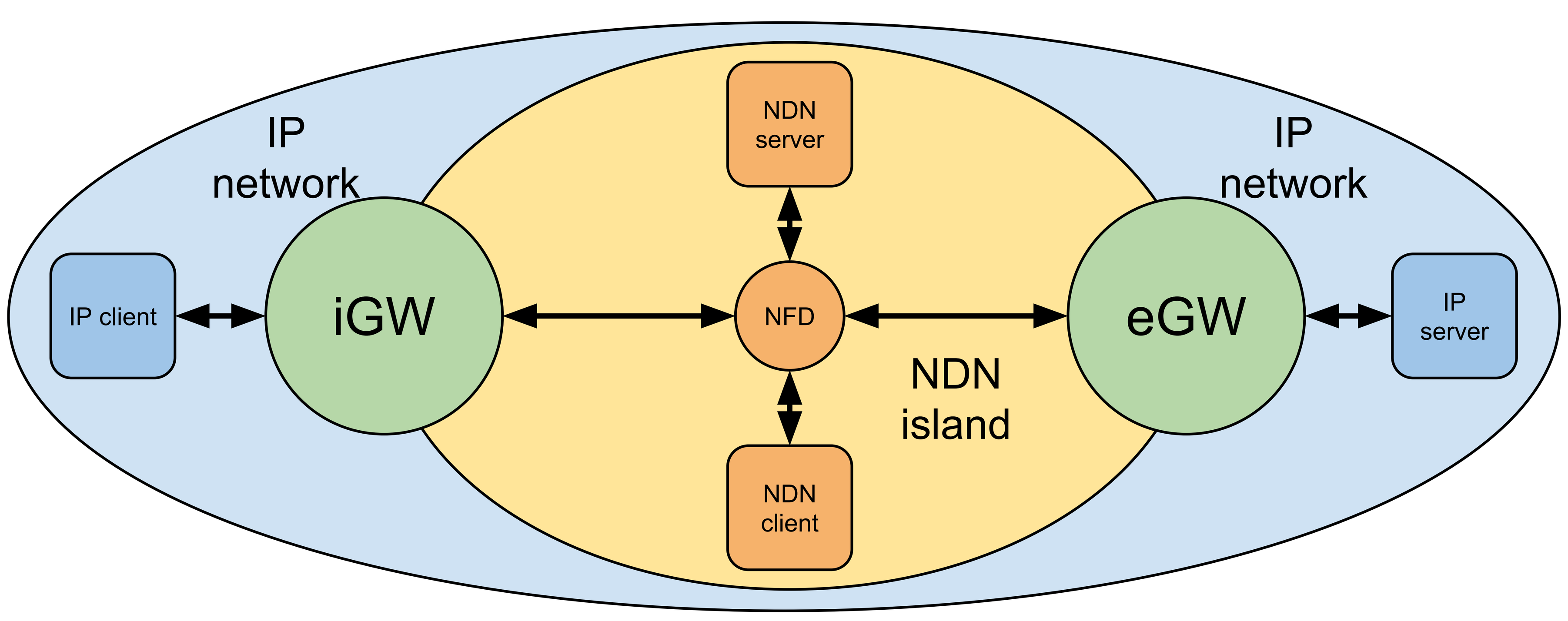

- Enable smooth transition from IP to NDN for web contents
- Requirements:
  - Forward HTTP requests from IP clients to NDN network
  - Forward HTTP requests from NDN clients to IP network
  - Ingress gateway (iGW) or NDN clients can transparently reach any NDN servers or egress gateway (eGW)
- Example: http://detectportal.firefox.com/success.txt
  - Consumer notifies the request to producer: /http/com/firefox/detectportal/success.txt/%07%0B%08%04http%08%03iGW/1E6...
  - Producer asks the request: /http/iGW/success.txt/1E6...
  - Consumer asks the response: /http/com/firefox/detectportal/success.txt/1E6...

Named-Data Networking as Virtual Elementary Modules

- Network Function Virtualization (NFV)
  - Common hardware, hosting various software components
  - Aims at reducing investment cost (CAPEX/OPEX)
  - Improve reliability and flexibility

- NFV concept aims to split network functions
  - The CS table represents a caching function
  - The PIT table represents a multiplexing function
  - The FIB table represents a routing function

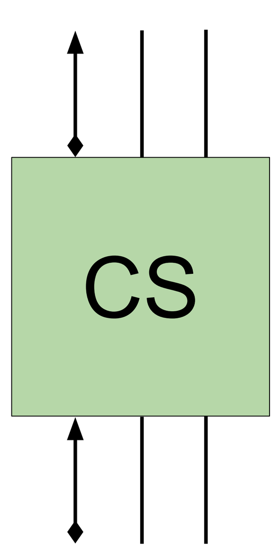

- Like a network proxy
  - Each "input" has its own "output"
  - Transparent for users
  - Cache forwarded Data packets

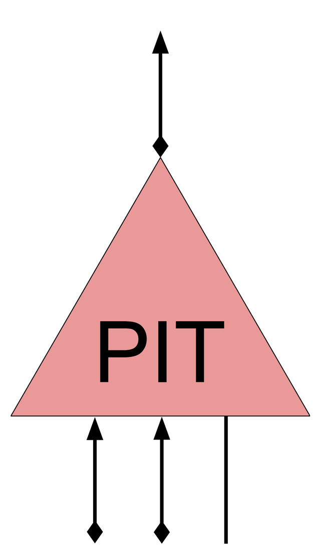

- Stateful multiplexer
  - N "inputs" and 1 "output"
  - Forward Data to all "inputs" that have sent at least 1 matching Interest
  - Don't resend same Interests before a given time

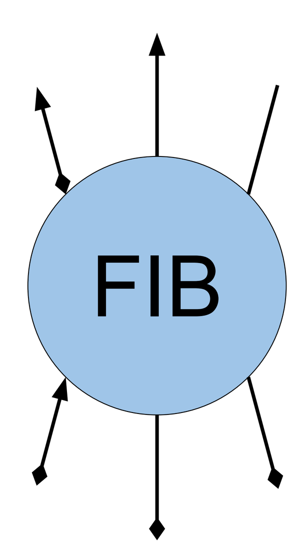

- Multi-path router/demultiplexer
  - N "inputs" and M "outputs"
  - Forward Interest to all "outputs" that have a prefix of the packet
  - Forward Data to all "inputs"
  - Edit or show table with JSON requests

Implementing Delaunay Triangulations of the Bolza Surface

Iordan Iordanov and Monique Teillaud

Summary

We present an implementation for the computation of Delaunay triangulations on the Bolza surface. To our best knowledge, there is no other available software for the case of the Bolza surface. Our work is based on theoretical results and an incremental algorithm proposed recently [BTV16], and our implementation is based on CGAL [CGAL].

Delaunay triangulation of point set $\mathcal{P}$

Simplicial complex: set of simplices K with

1. $\sigma \in K, \tau \leq \sigma \Rightarrow \tau \in K$
2. $\sigma, \tau \in K \Rightarrow \sigma \cap \tau \in K$
3. local finiteness

Delaunay property: the interior of the *circumscribing ball* of any triangle does not contain any point of $\mathcal{P}$

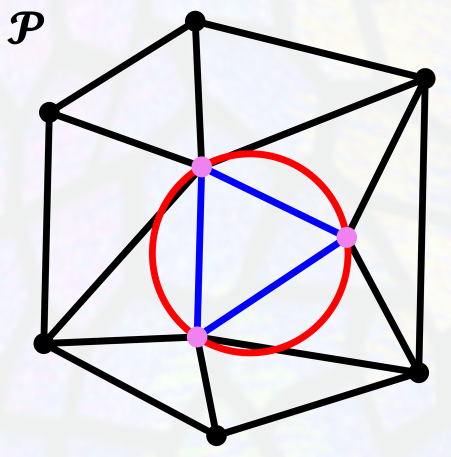

Delaunay triangulation: *Simplicial complex with the Delaunay property*

The Bolza surface $\mathcal{M}$

is the most symmetric *hyperbolic* surface of genus 2; can be obtained by identifying the opposite sides of a hyperbolic octagon with angles π/4

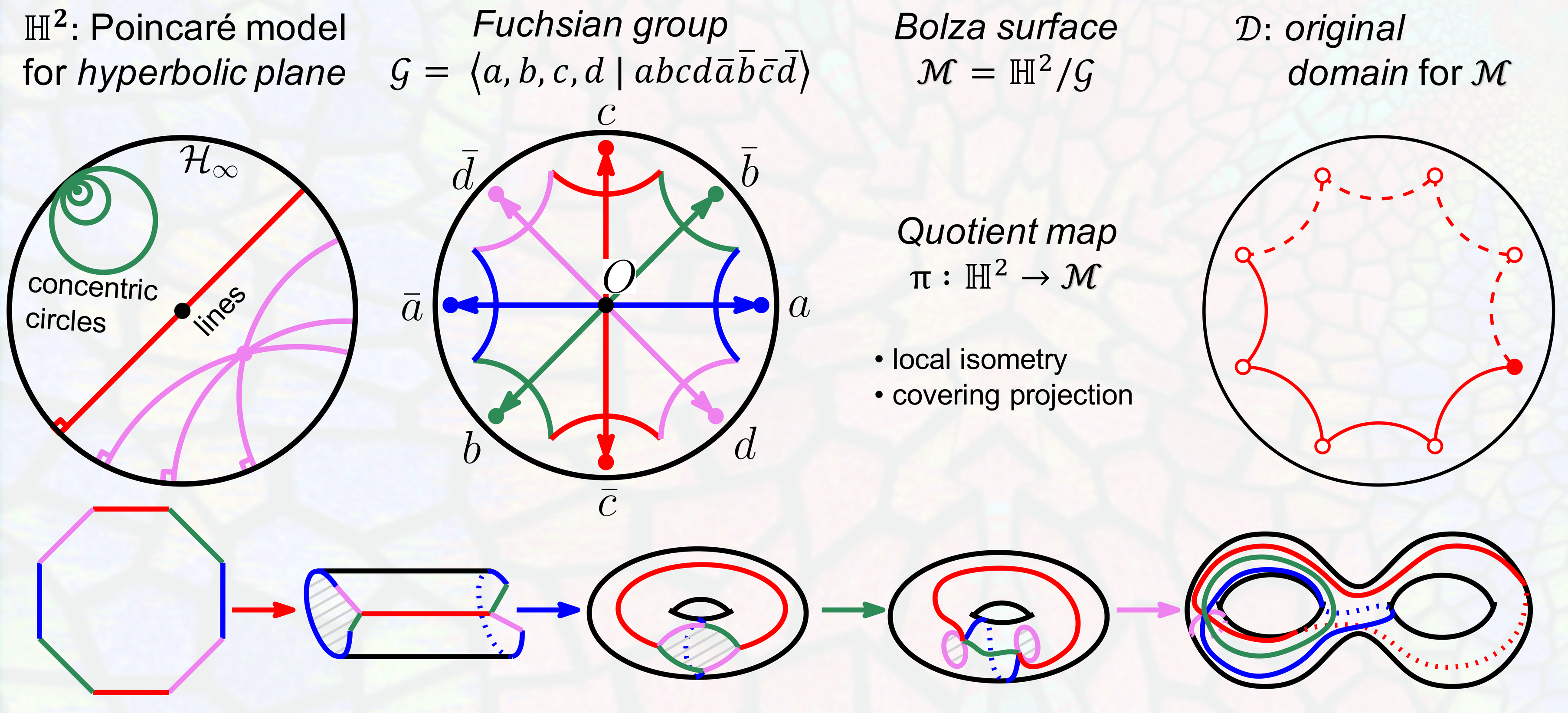

Delaunay triangulation of $\mathcal{M}$ [BTV16]

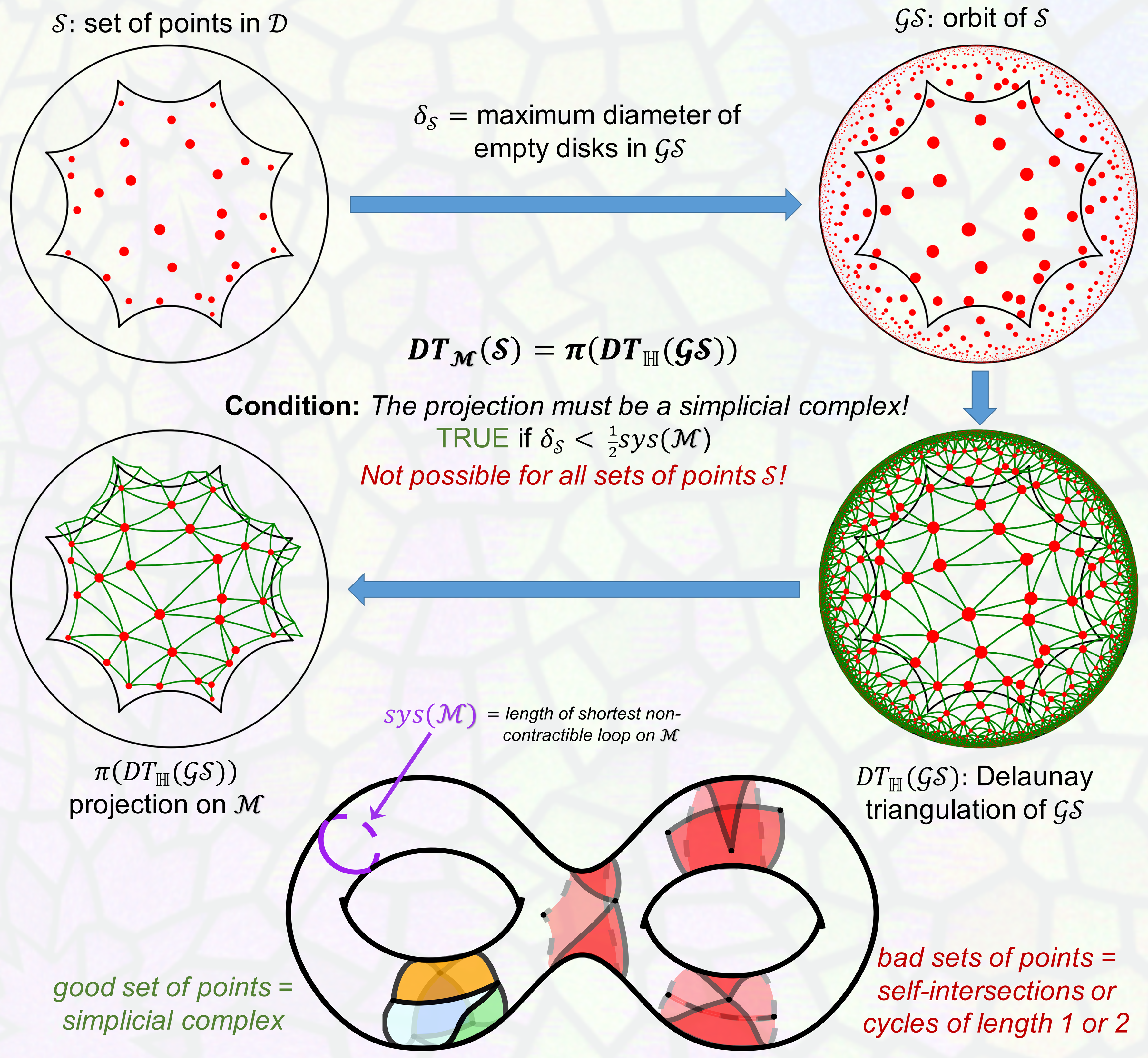

Algorithm [BTV 16]

Use set $\mathcal{Q}$ of 14 *dummy points* to guarantee that the triangulation is always a simplicial complex*:*

1. Construct $DT_\mathcal{M}(\mathcal{Q})$
2. Insert points of $\mathcal{S}$
3. Remove points of $\mathcal{Q}$

Attention: removal allowed only if condition holds!

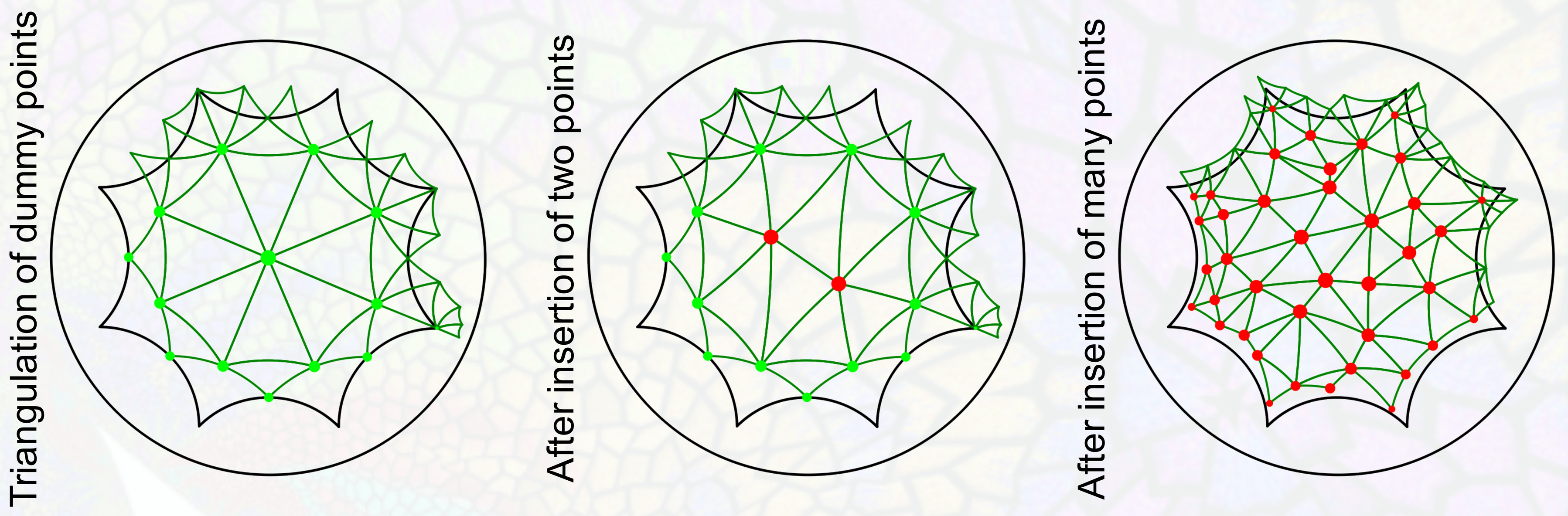

Implementation [IT17]

Points in Poincaré disk

- all input points are in $\mathcal{D}$
- points outside $\mathcal{D}$ addressed by an element g of $\mathcal{G}$

Property: if a face σ of $DT_\mathcal{M}(\mathcal{S})$ has at least one vertex in $\mathcal{D}$, then the vertices of σ outside $\mathcal{D}$ are addressed by an element of $\mathcal{N} \subset \mathcal{G}$ with $|\mathcal{N}|$= 48

Canonical representative: unique image in $DT_\mathbb{H}(\mathcal{GS})$ of a 2-face of $DT_\mathcal{M}(\mathcal{S})$, stored in the data structure

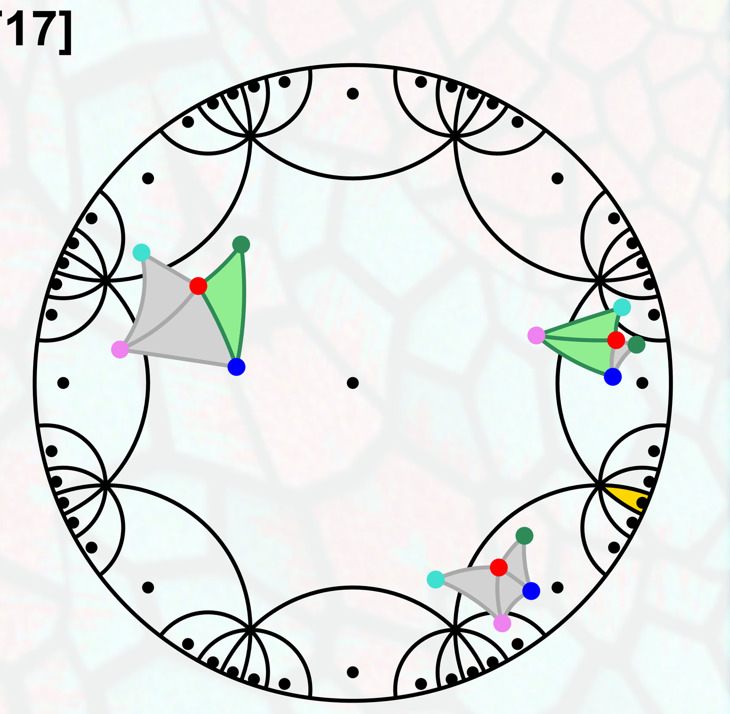

Images of $\mathcal{D}$ for all elements of $\mathcal{N}$

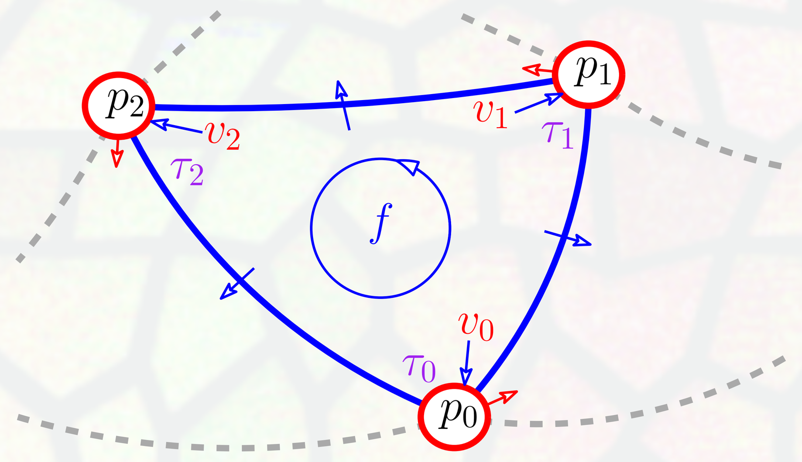

Data structure

- based on the CGAL 2D Triangulation Data Structure
- extra information in every 2-face
  - one translation of $\mathcal{N}$ for every vertex

Representation of translations

- words on the generators of $\mathcal{G}$
- operations on translations
- Dehn's algorithm for word reduction

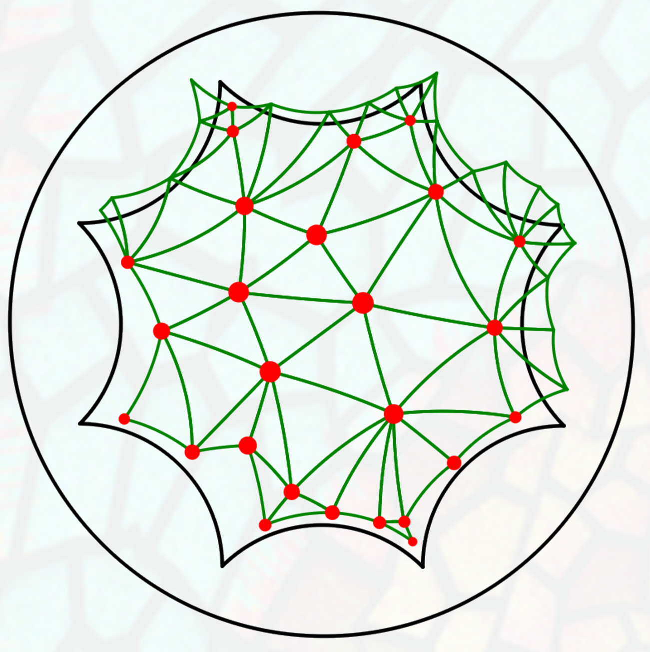

Algebraic complexity of predicates

- *Orientation*: maximum algebraic degree 20
- *InCircle*: maximum algebraic degree up to 72
- Implementation with CORE::Expr

Results

- Fully dynamic implementation
- Computation of dual Voronoi diagram

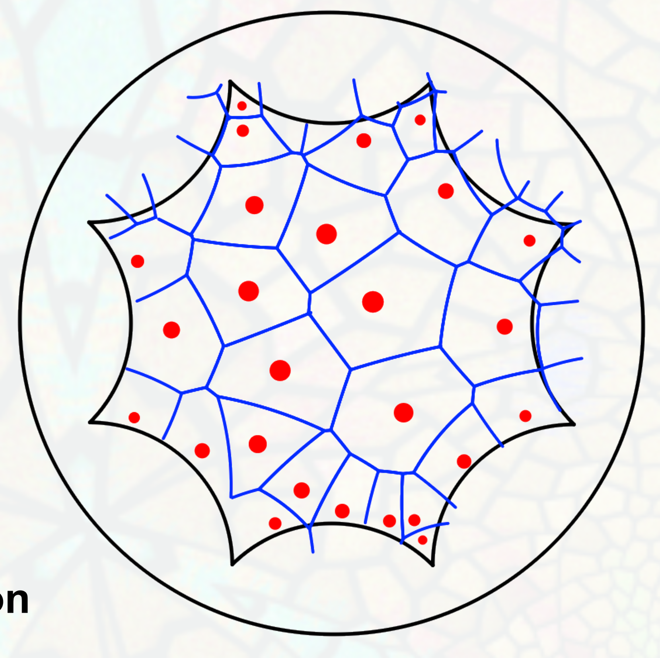

Experiments

- Insertion of 1 million random points:
  - Euclidean (CORE::Expr) in 12 seconds
  - hyperbolic (CORE::Expr) in 34 seconds
- All dummy points removed: 12 ~ 72 random points

Submission to CGAL upon documentation completion

Future work

Generalization for

- other surfaces of genus 2 (not as symmetric as $\mathcal{M}$, different/unknown systole…)
- surfaces of higher genus

References

[CGAL] CGAL, Computational Geometry Algorithms Library, http://www.cgal.org

[BTV16] M. Bogdanov, M. Teillaud, and G. Vegter. **Delaunay triangulations on orientable surfaces of low genus**. In *Proceedings of the Thirty-second International Symposium on Computational Geometry*, pages 20:1-20:17, 2016.

[IT17] I. Iordanov and M. Teillaud. **Implementing Delaunay triangulations of the Bolza surface**. In *Proceedings of the Thirty-third International Symposium on Computational Geometry*, pages 44:1-44:15, 2017.

ECOLE DOCTORALE IAEM LORRAINE

Problème de dimensionnement de lots sous contrat buyback avec production par batch

Mlouka FARHAT

Directrice de thèse : Nathalie SAUER

Co-directrices de thèse : Ayse AKBALIK & Atidel B.HADJ-ALOUANE

Contexte général

- Problème de planification d'approvisionnement : Problème de Dimensionnement de Lots (**PDL**) mono-produit avec contrat buyback et production par batch complet (PDL-BBC)
- Contrat buyback : Le détaillant a la possibilité de retourner au fournisseur un certain pourcentage des articles inutilisés

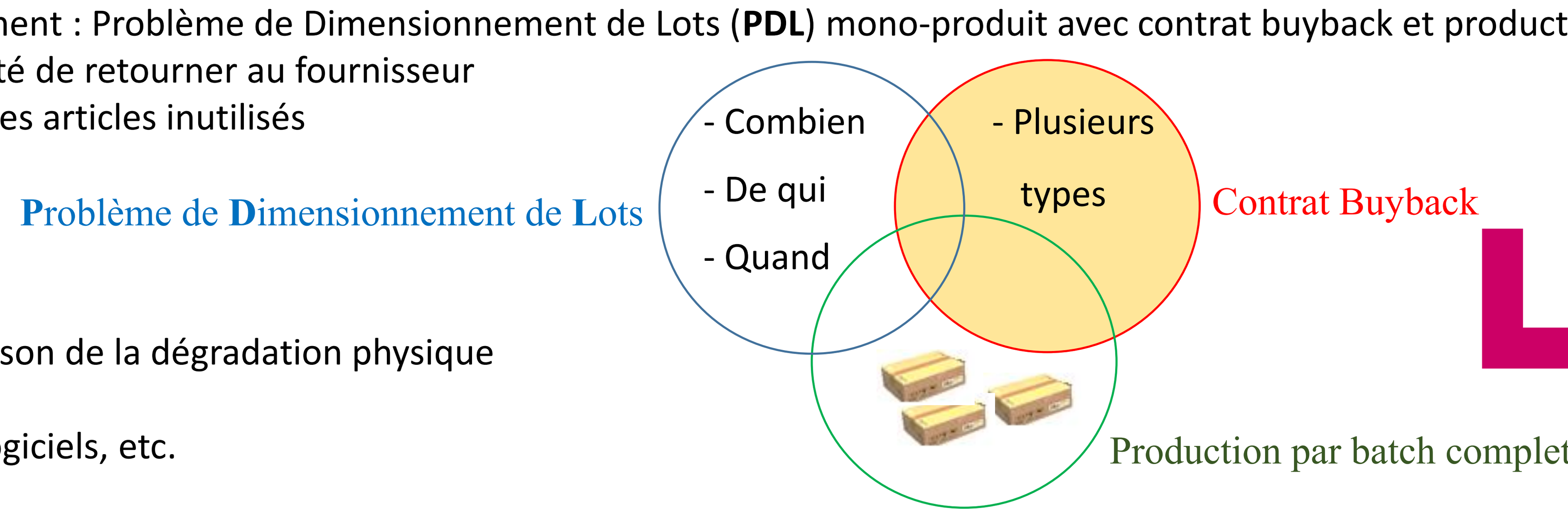

- Produit avec une durée de vie limitée en raison de la dégradation physique
- Produit avec un risque d'obsolescence
- Exemple : vêtements de mode, livres, CD, logiciels, etc.

Problématique et objectifs du PDL-BBC

Pour t = 1, …, T

- **Commander** une quantité unitaire $\mathbf{x_t}$ dans des $\mathbf{A_t}$ batches de taille constante V avec un coût par commande $\mathbf{f_t}$, un coût d'achat unitaire $\mathbf{p_t}$ et un coût par batch $\mathbf{a_t}$
- **Stocker** à la fin de t une quantité $\mathbf{s_t}$ avec le coût $\mathbf{h_t}$
- **Retourner** une quantité $\mathbf{q_t}$ à la fin de chaque période w_i à un revenu de retour $\mathbf{p^b_t}$ tel que $\max_{t \in \{1,\dots,T\}} p^b_t < p_t$, i = 1, …, N et N est le nombre de retours
- Pourcentage de retour $0 \leq \rho \leq 1$
- Périodes de retour w_i peuvent être connues ou inconnues
- Demande d_t déterministe

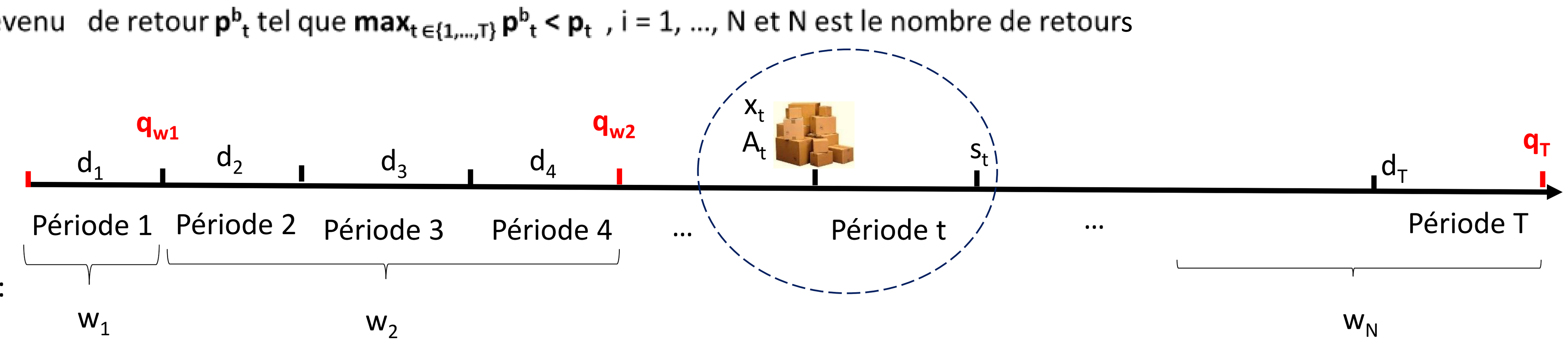

Résoudre 3 sortes de problèmes avec retour complète ou partielle :

- **PDL-BBC avec des périodes de retour connues**
- **PDL-BBC avec une durée de retour limitée**
- **PDL-BBC avec possibilité de retour uniquement dans les périodes d'approvisionnement**

Périodes de retour inconnues

Modèle générale du PDL-BBC

→ **Minimiser** {les coûts de **setup** + **approvisionnement** + **stockage** - les revenues de **retour**} **tout en satisfaisant** ces différentes contraintes :

- Equilibrage des quantités entrantes et sortantes à chaque période
- Génération des variables de setup à chaque période
- Nombre de batches complets pour la quantité commandée
- Conditions de contrat buyback

PDL-BBC avec des périodes de retour connues		**PDL-BBC avec une durée de retour limitée**		**PDL-BBC avec possibilité de retour uniquement dans les périodes d'approvisionnement**	
Retour complète	Retour partielle	Retour complète	Retour partielle	Retour complète	Retour partielle
-Pas de retour autorisé pour les périodes différentes de celles de retour -Pas de stock à la période de retour		-Détaillant retourne, juste au cours des premières t périodes, un maximum de $\rho\ \sum_{i=1}^{t} x_t$		-Détaillant peut retourner à chaque période t une quantité qui ne dépasse pas $\rho\ x_t$	

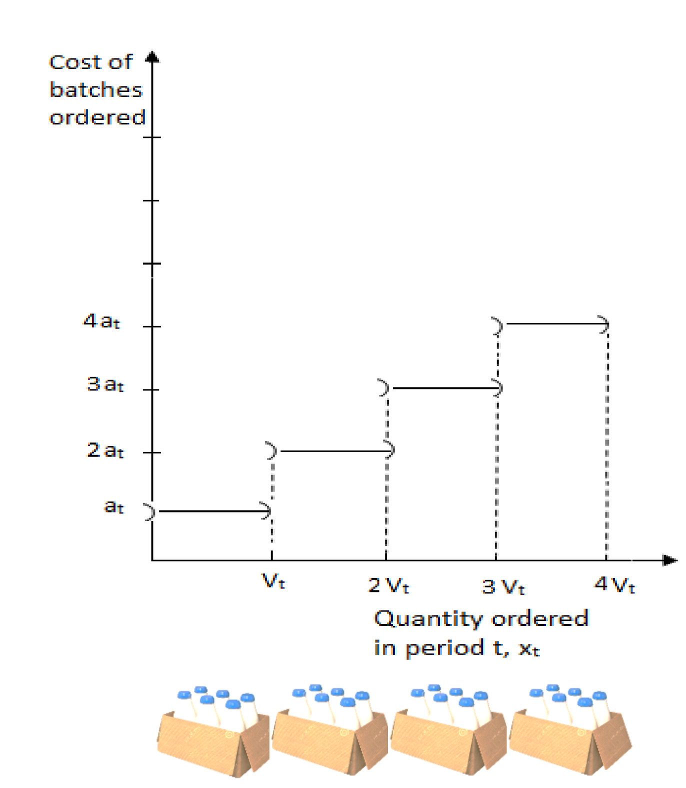

Résultats des PDL-BBC

Proposition des algorithmes polynomiaux de programmation dynamique de différentes complexités :

- PDL-BBC avec des périodes de retour connues : $O\left(\sum_{i=0}^{N-1}(w_{i+1} - w_i)^2\right), O\left(2\ \sum_{i=0}^{N-1}(w_{i+1} - w_i)^2\right), O\left(\sum_{i=0}^{N-1}(w_{i+1} - w_i)^4\right)$
- PDL-BBC avec une durée de retour limitée : $O(T^4)$, $O(T^5)$
- PDL-BBC avec possibilité de retour uniquement dans les périodes d'approvisionnement : $O(T^4)$, $O(T^5)$, $O(T^6)$

Conclusion & perspectives

- Différentes formes de contrat buyback sont fusionnées avec PDL
- Complexités des algorithmes proposés pour le PDL avec périodes de retour connues sont inférieures à celle de PDL sans politique de retour
- Complexités des PDL avec une durée de retour limitée et avec possibilité de retour uniquement dans les périodes d'approvisionnement sont supérieures à celle de PDL sans politique de retour
- Perspectives : LSP-BB avec d'autres formes de contrat de réservation de capacité : contrat de flexibilité de quantité, backup, minimum commitment, partage des revenus, réservation déductible, take-or-pay et pay-to-delay

ECOLE DOCTORALE IAEM LORRAINE

UNIVERSITÉ DE LORRAINE

Decision Support for Interoperability Readiness in Networked Enterprises

Da Silva Serapião Leal, Gabriel

(gabriel.leal@list.lu, gabriel.da-silva-serapiao-leal@univ-lorraine.fr)

Supervisor: Prof. Hervé Panetto

Co-supervisor: Dr. Wided Guédria

CRAN CNRS UMR 7039

LUXEMBOURG INSTITUTE OF SCIENCE AND TECHNOLOGY LIST

Fonds National de la Recherche Luxembourg

Research Context

Networked Enterprise

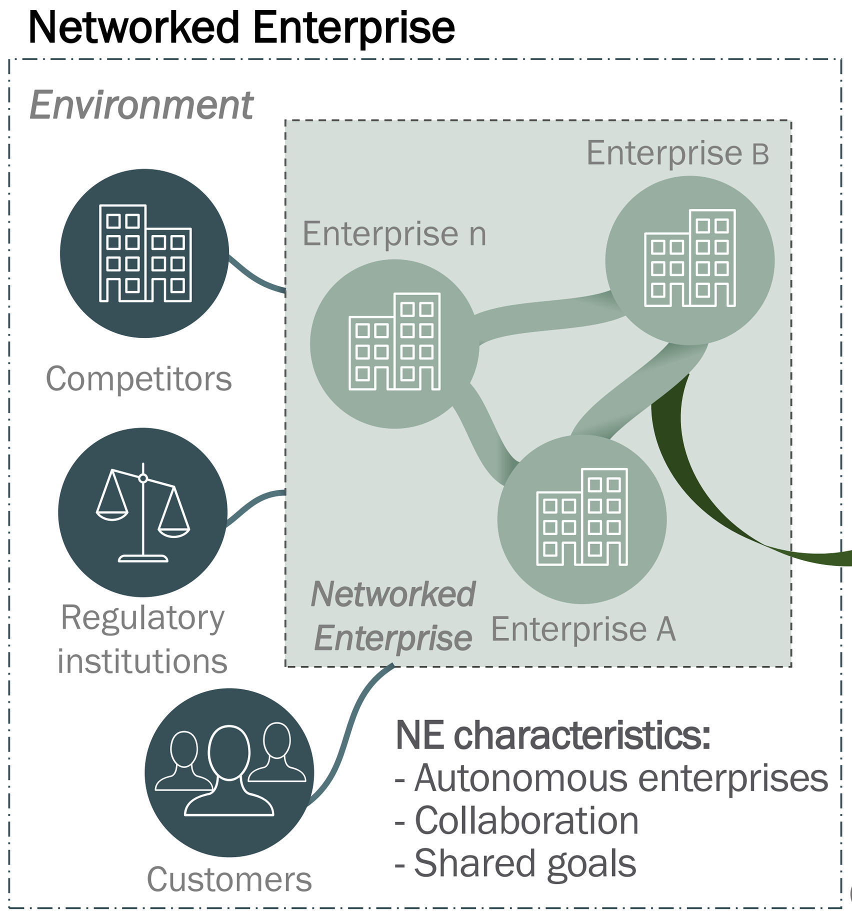

(Camarinha-Matos et al. 2005)

Enterprise Interoperability (EI)

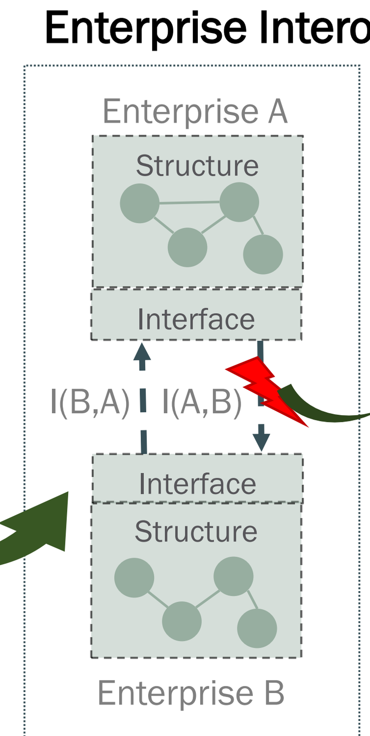

E.g. of barriers:
- Different semantics
- Incompatible IT tools
- Responsibilities not defined

EI aspects:
- Technical
- Conceptual
- Organizational

EI concerns:
- Data - Process
- Service -Business

(INTEROP 2007), (EURO 2017)

Interoperability Assessment

It is a support for:

- Identifying impacts due to envisioned transformation,
- Identifying negative impacts caused by interoperability barriers;

Application contexts:

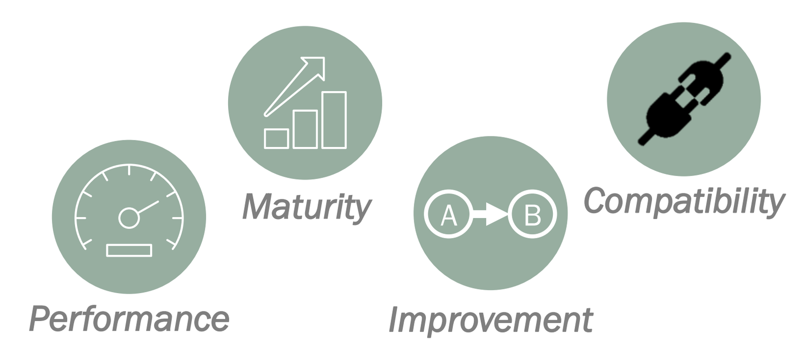

Gaps

(i) Lack formal definition of evaluation criteria and need a high level of expertise to be applied in an industrial context.

(ii) Lack of an approach dealing with multiple aspects of interoperability and considering the different contexts.

(Guédria et al. 2015), (Panetto et al. 2016)

Research Contribution

An ontology-based interoperability assessment approach for supporting decision making in the Networked Enterprise.

Issues

Questions

(Q1) What are the existing interoperability requirements, their interdependencies and their potential impacts in the overall system? And how to represent it?

(Q2) How to assess the interoperability, when dealing with different interoperability aspects and different application contexts, in the Networked Enterprise?

Hypothesis

(H1) A Networked Enterprise is as a System-of-Systems composed of at least two autonomous systems (enterprises) that collaborate and interoperate during a period of time to reach a shared objective that cannot be reached by a system alone.

(H2) There are interdependencies between the interoperability requirements derived from different interoperability aspects and concerns.

Research Approach

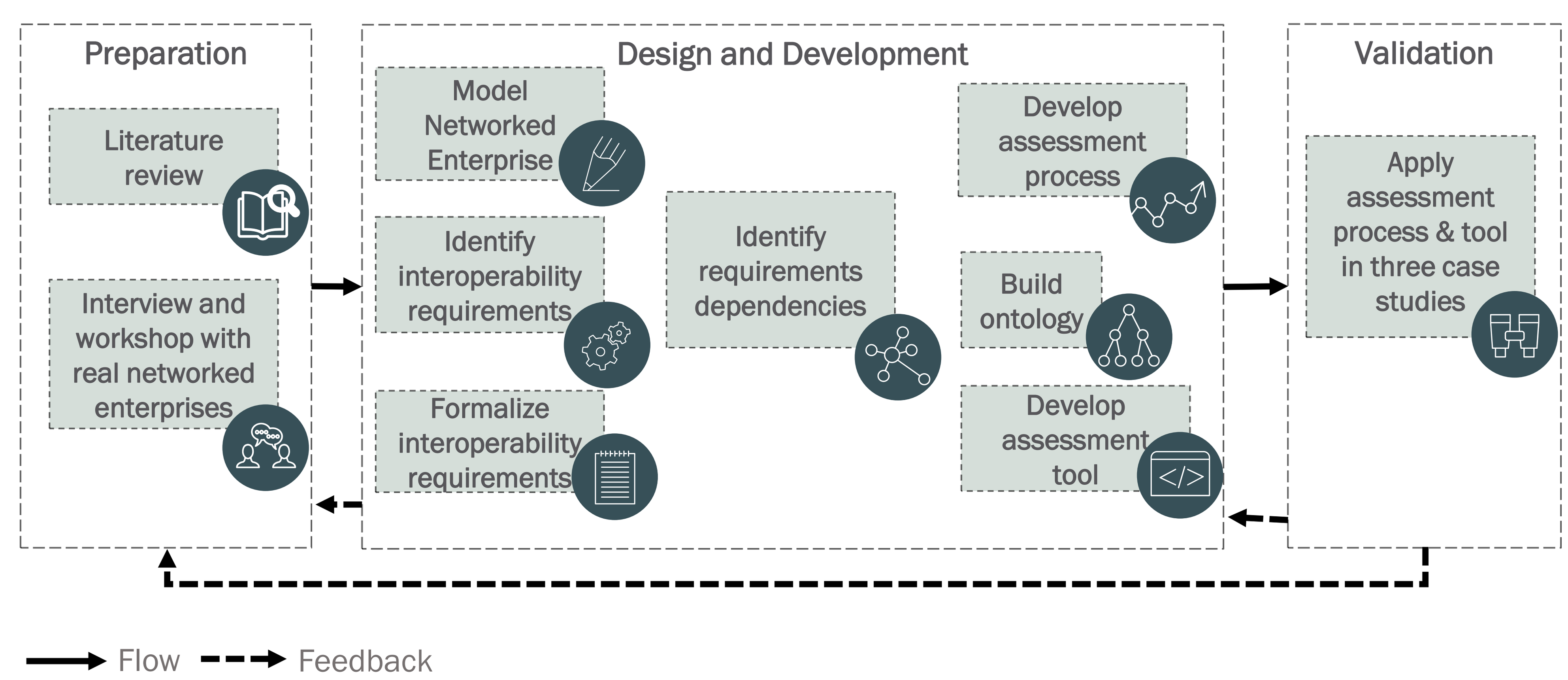

Preliminary Results

Model-Based System Engineering: Networked Enterprise

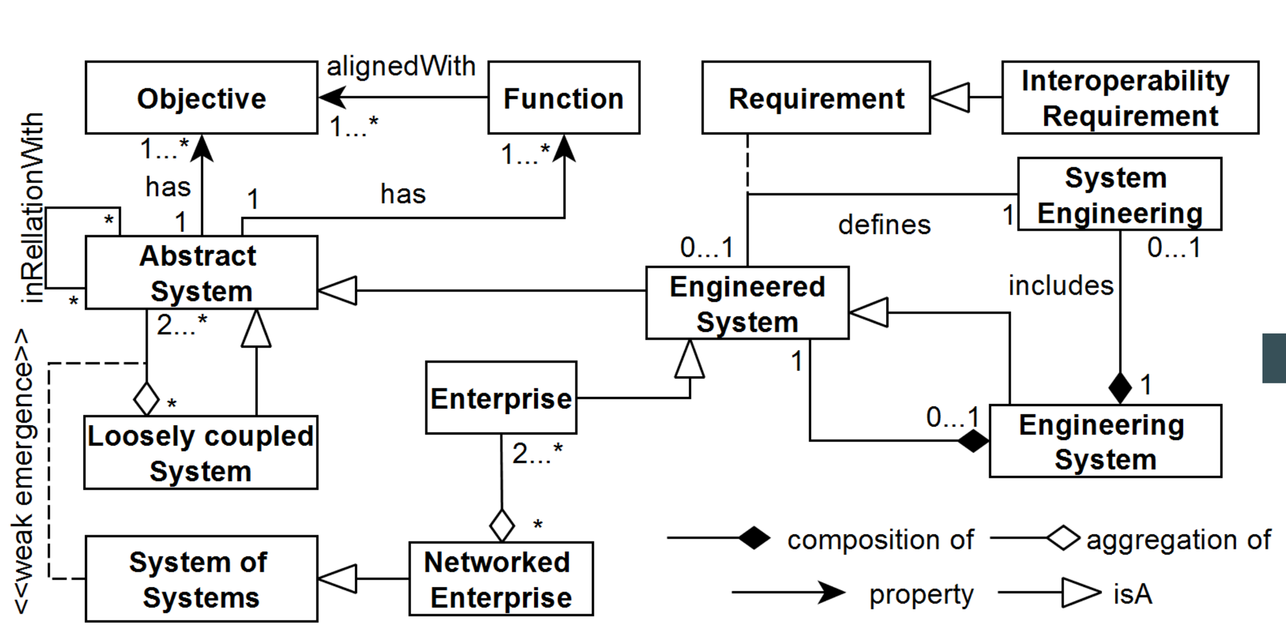

adapted from (Morel et al. 2007)

Example of interoperability requirement	
System of Systems Characteristic	Requirement
Connectivity	DT1: Data storage devices are connectable; and simple electronic exchange is possible
Formalization	
(DT1.1 ∪ ((DT1.2 ∪ DT1.3) ∧ (DT1.4 ∪ DT1.5))) ∪ DT1.6 ; *where ∪ = requires / ∧ = and*	

Extract of the ontology for interoperability assessment

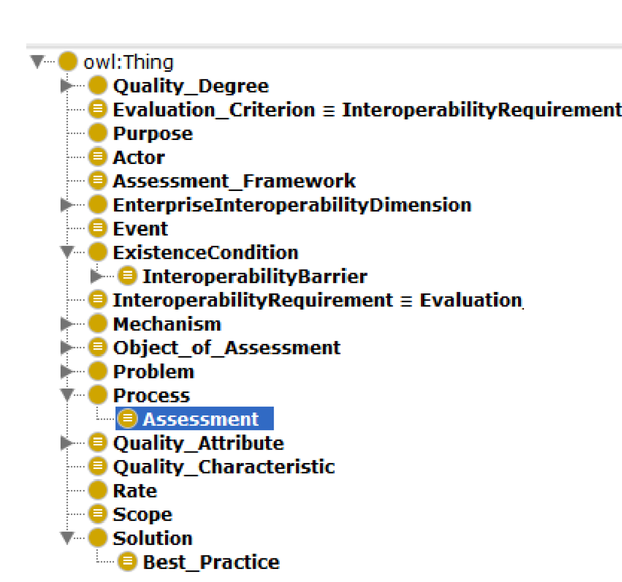

Case Study: Tool validation

A real Networked Enterprise

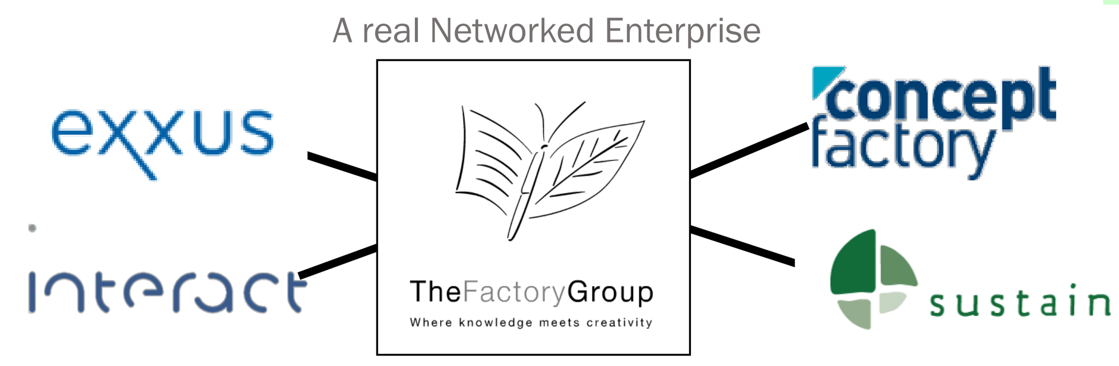

The assessment tool architecture

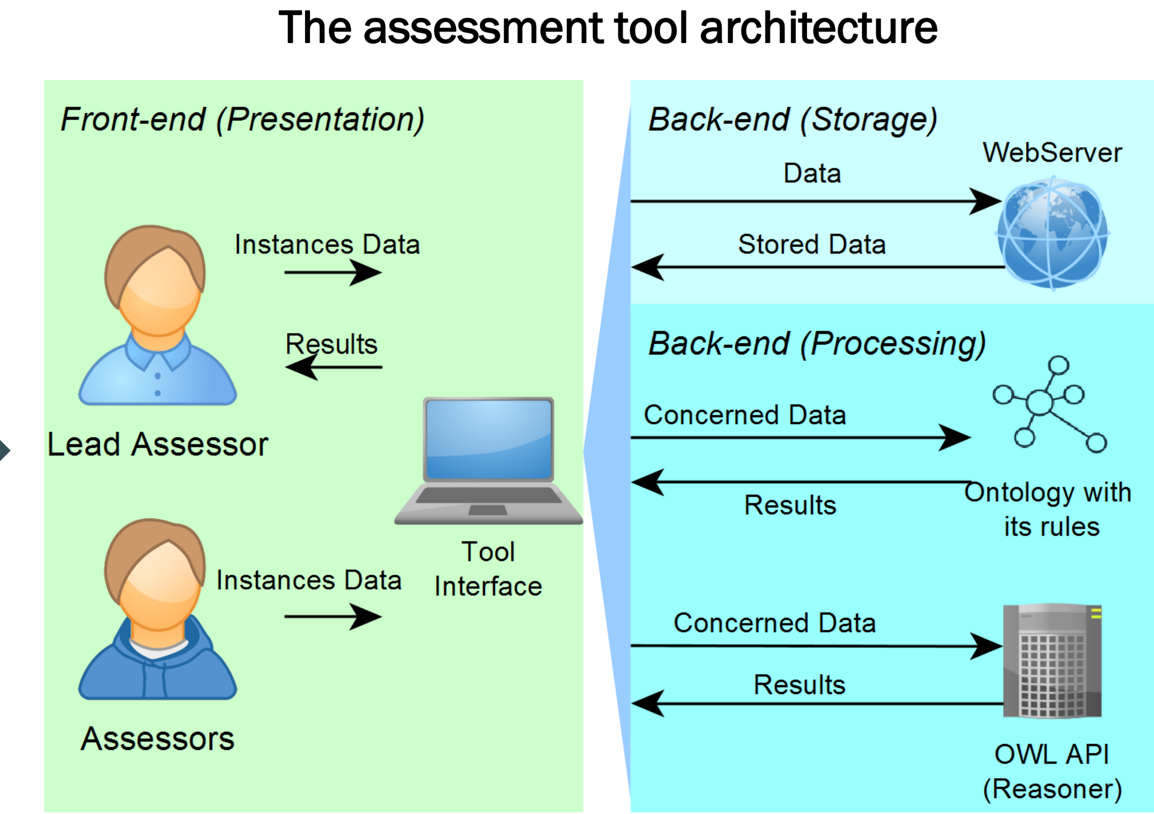

References:

Camarinha-Matos, L.M. and Afsarmanesh, H., 2005. Collaborative networks: a new scientific discipline. In *Journal of intelligent manufacturing,* 16(4-5), pp.439-452.

INTEROP., 2007. Enterprise Interoperability – Framework and Knowledge Corpus – Final Report, INTEROP NOE, Contact n 508011, Deliverable DI.3.

European Commission. 2017. European Interoperability Framework - Implementation Strategy. In *Annex of to the communication from the commission to the European parliament, the council, the European economic and social committee and the committee of the regions*.

Morel, G., Panetto, H., Mayer, F. and Auzelle, J.P., 2007, October. System of enterprise-Systems integration issues: an engineering perspective. In IFAC Conference on Cost Effective Automation in Networked Product Development and Manufacturing, IFAC-CEA'07 . Elsevier.

Panetto, H., Zdravkovic, M., Jardim-Goncalves, R., Romero, D., Cecil, J. and Mezgár, I., 2016. New perspectives for the future interoperable enterprise systems. In *Computers in Industry*, 79, pp.47-63.

Guédria, W., Naudet, Y. and Chen, D., 2015. Maturity model for enterprise interoperability. In *Enterprise Information Systems*, 9(1), pp.1-28.

Publications:

G. Leal, W. Guédria, H. Panetto, E. Proper., 2016. Towards a Meta-Model for Networked Enterprise. In *the 21st international conference on exploring modelling methods for systems analysis and design (EMMSAD 2016)*, Slovenia. In LNBP, Springer, 2016, vol.248, pp.417-431

G. Leal, W. Guédria, H. Panetto, M. Lezoche., 2016. Towards a comparative analysis of interoperability assessment approaches for collaborative enterprise systems. In *23rd IPSE International Conference on Transdisciplinary Engineering, Curitiba, Brazil. IOS Press, 4, pp.45-54, Advances in Transdiciplinary Engineering.*

G. Leal, W. Guédria, H. Panetto, E. Proper., 2017. An approach for interoperability assessment in networked enterprises. In *the 20th World Congress of the International Federation of Automatic Control (IFAC*), Toulouse, France

G. Leal, W. Guédria, H. Panetto, E. Proper., 2017. Towards a semi-automated tool for interoperability assessment: an ontology-based approach. In the 17th International SPICE (Software Process Improvement and Capability Determination) Conference

This work has been conducted in the context of the PLATINE project (PLAnning Transformation Interoperability in Networked Enterprises), financed by the National Fund of Research of the Grand Duchy of Luxembourg (FNR), under the grant C14/IS/8329172/R2.

A SERIES ARC FAULT LOCATION ON ELECTRICAL HOME NETWORKS

E. CALDERON, P. SCHWEITZER, S. WEBER
Jean Lamour Institute, Lorraine University, Sciences Faculty, 54506 Vandœuvre-lès-Nancy, France
edwin-milton.calderon-mendoza@univ-lorraine.fr

Introduction

Nowadays electric arc fault location represents a great challenge for researchers. The accurate fault location in an electric transmission line can save time for technicians and avoid hard damage in electrical networks. Finally it can be extended to aircraft systems, automotive and telecommunication systems. In this work we present different developed algorithms to estimate a series arc fault in an experimental indoor power line.

Electric arc fault

An arc-fault occurs when loose or corroded connections make intermittent contact and causes sparking or arcing between the connections. This translates into heat which will break down the insulation of the wire and can initiate an electrical fire.

Home

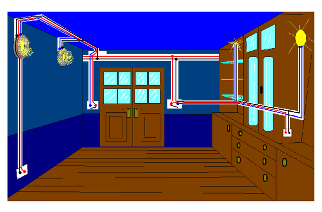

Aircraft

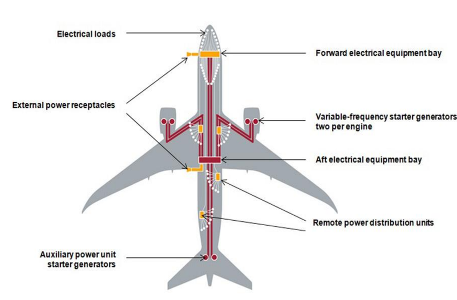

Automotive

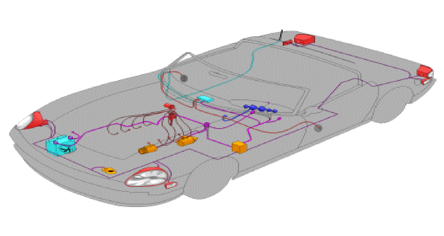

Damaged cable

Experimental environment

Experimental transmission line (49 m)

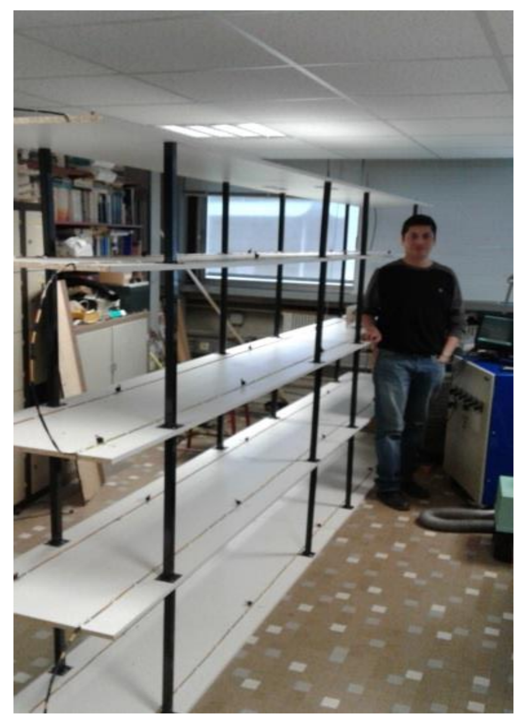

Carbonized path

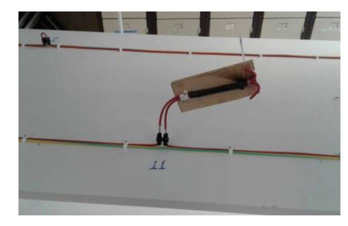

Oscilloscope

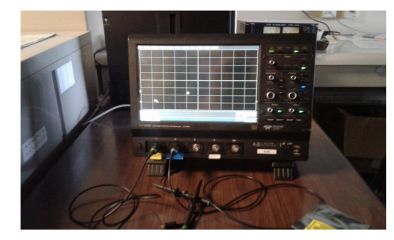

Experimental loads

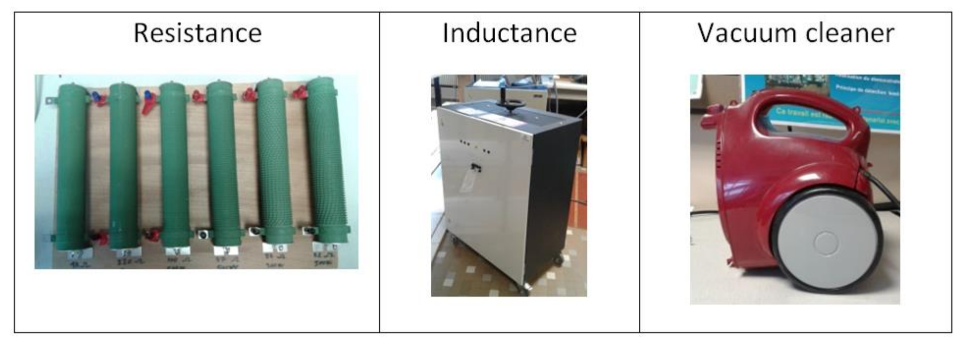

DEVELOPED ALGORITHMS FOR A SERIES ARC FAULT LOCATION

Algorithm based on Wavelet transform

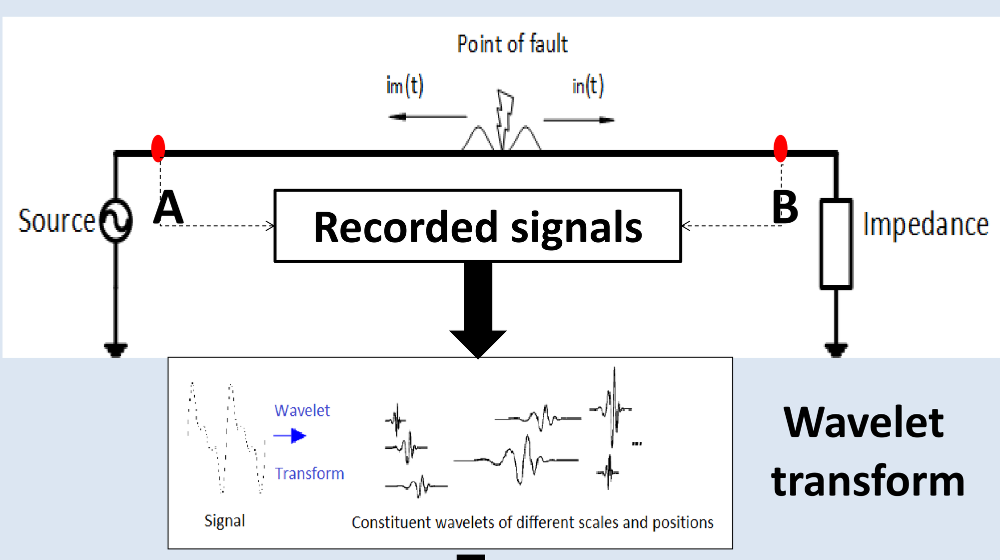

Wavelet transform

Calcul of td

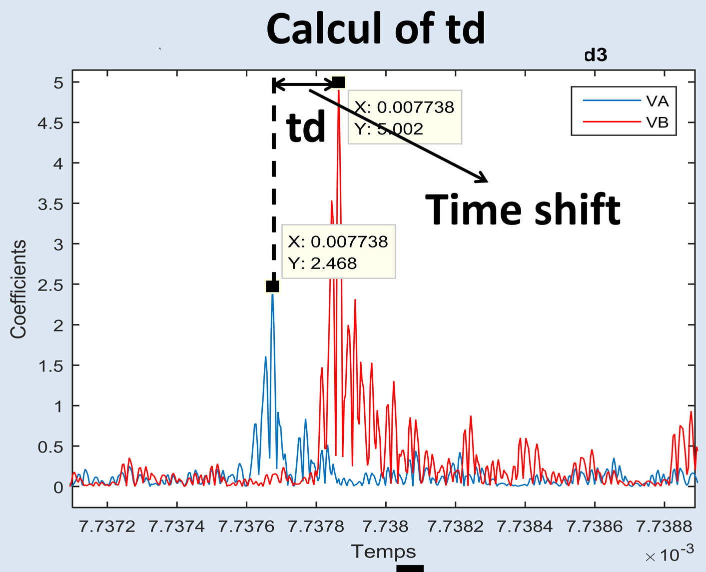

Chosen decomposition at scale (D3)

$$Fault\ distance = \frac{total\ length\ line - v * t_d}{2}$$

Fault location algorithm

Series arc fault location			
Real distance	8.13m	26.34m	42.08m
Estimation Using algorithm	5.14m	24.5m	40.43m

Performance

Algorithm based on impedance parameters

Transmission line model:

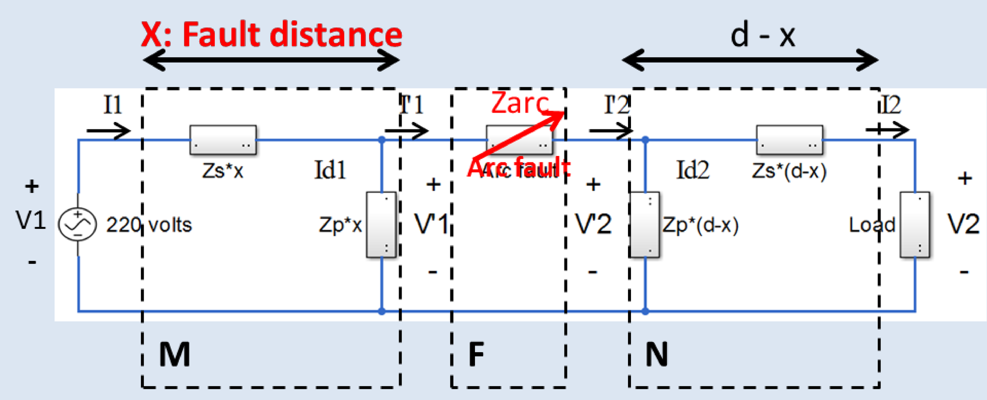

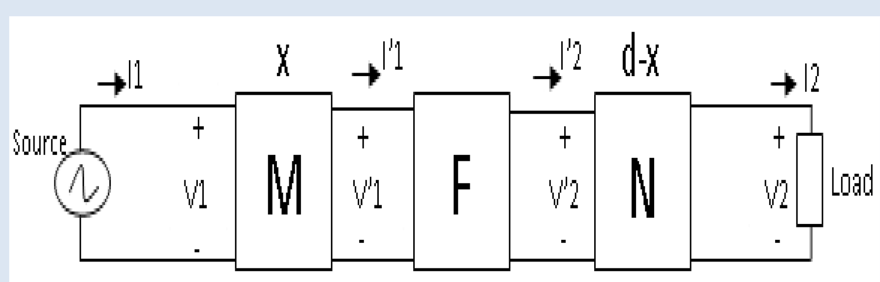

Obtention of the fundamental equation based on currents:

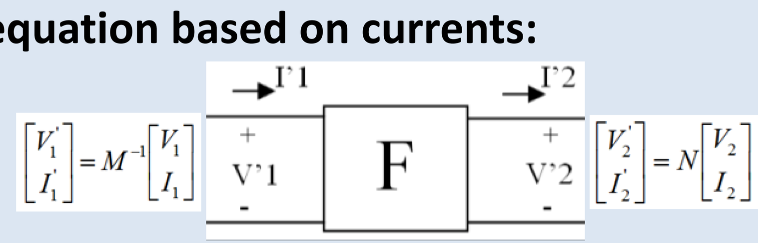

$$I_1^{'} - I_2^{'} = M_{21}^{-1} * V_1 + M_{22}^{-1} * I_1 - N_{21} * V_2 - N_{22} * I_2$$

Series arc fault generation:

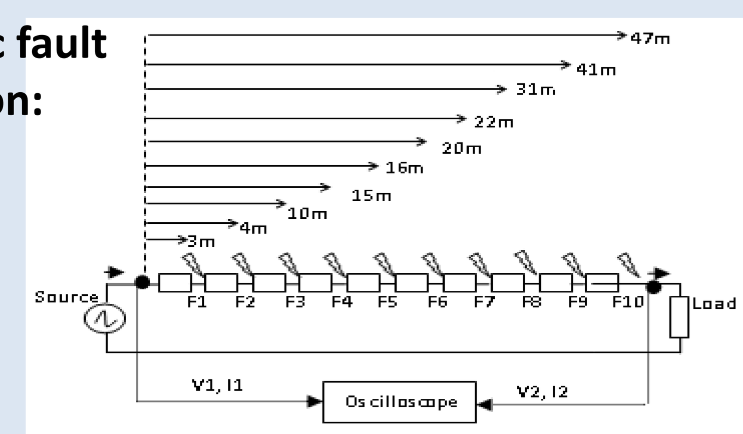

Algorithm description:

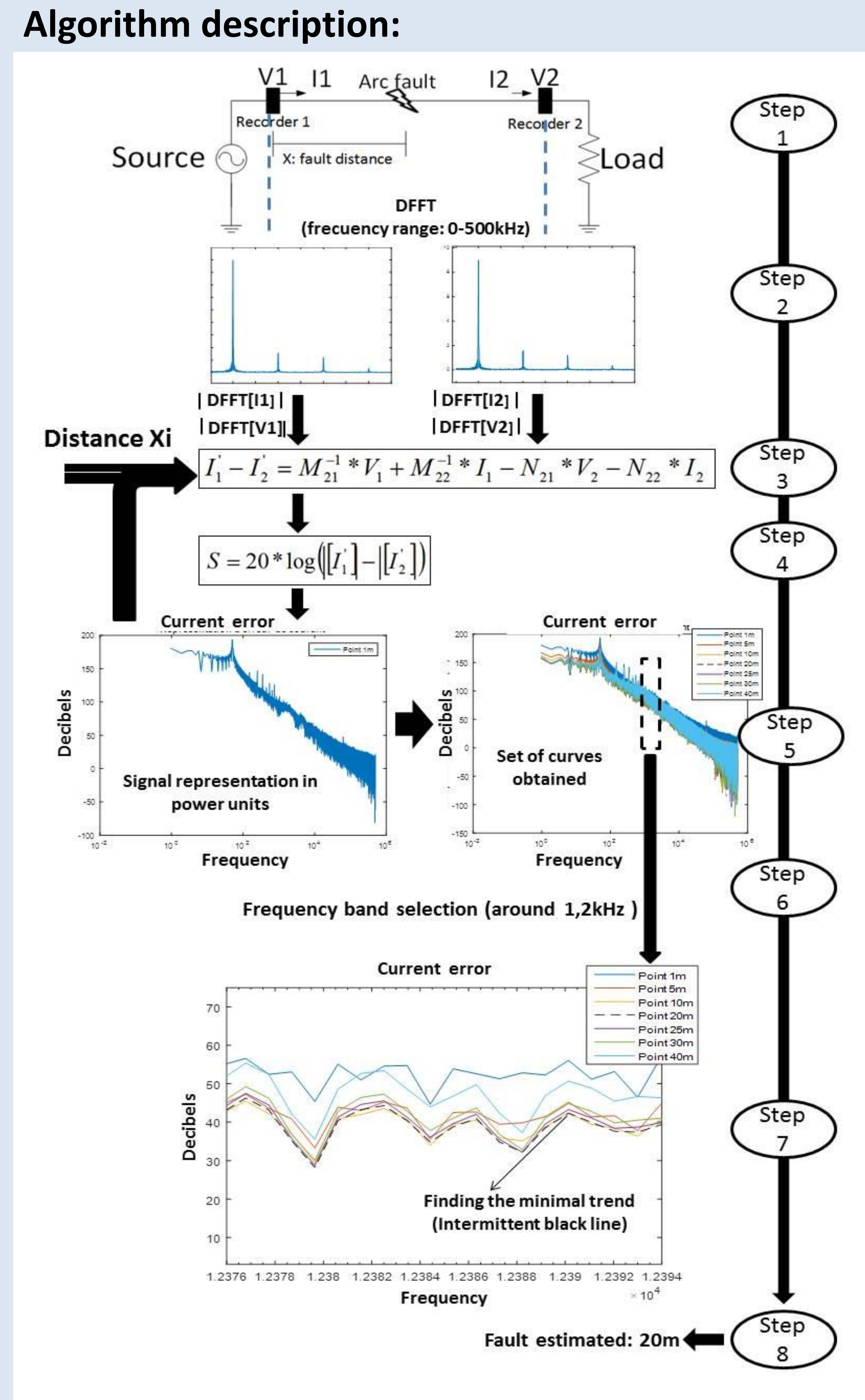

Algorithm based on impedance parameters and neural network

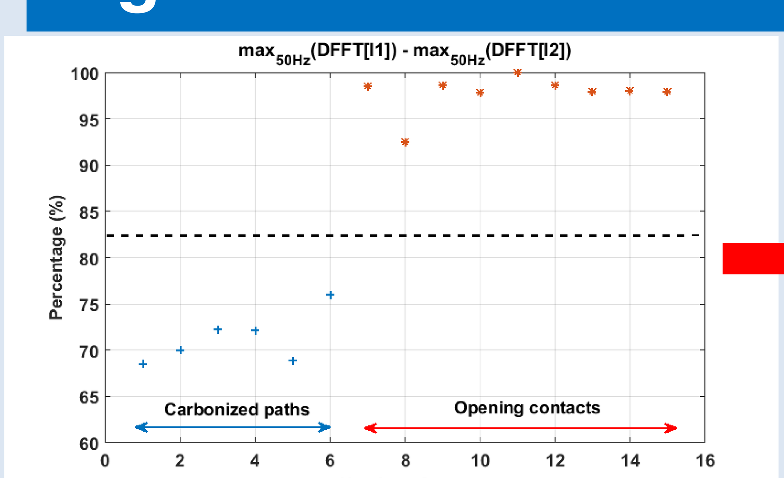

Classification criterion (real series arc fault data)

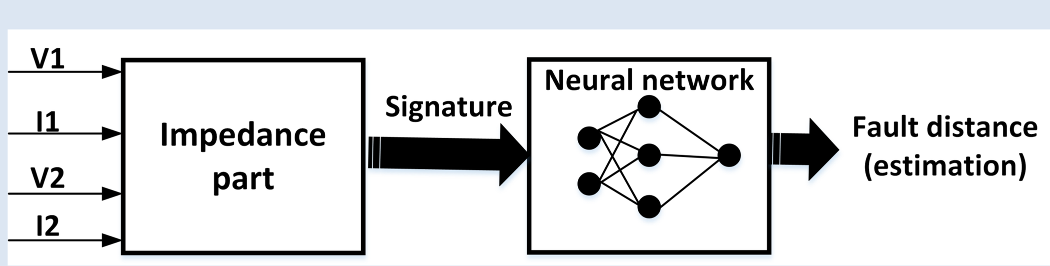

Algorithm
(Application in a simulated trasnmission line)

Results

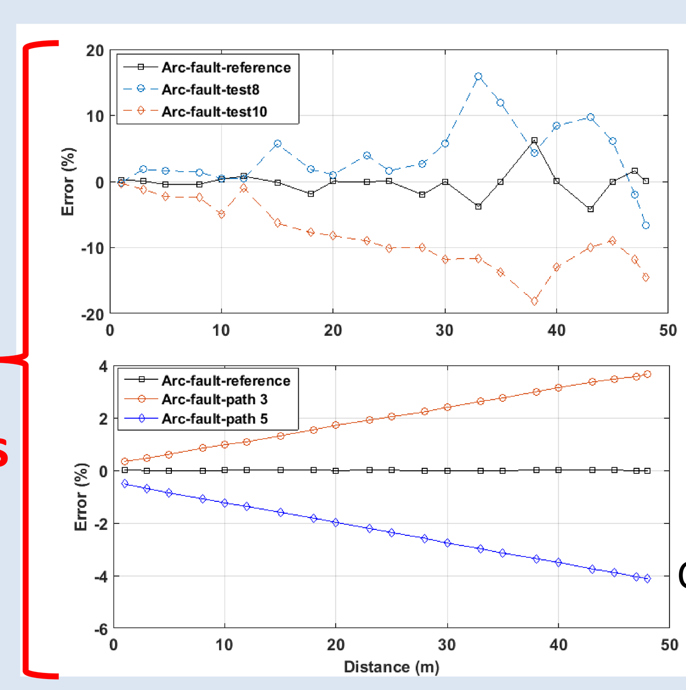

Performance

Composition	Path	Error min(%)	Error max(%)	PD (m)
Carbonized paths	Test1	0.35	3.66	1
	Test3	0.51	4.12	1
	Test4	0.50	28.33	1
	Test5	0.26	24.24	1
Opening contacts	Test7	0.18	15.96	25
	Test9	0.28	18.13	12
	Test10	0.41	16.26	18
	Test11	1.03	25.18	25
	Test12	0.06	11.10	30
	Test13	0.31	13.55	25
	Test15	0.17	9.51	5

Series arc fault characterization

Samples used

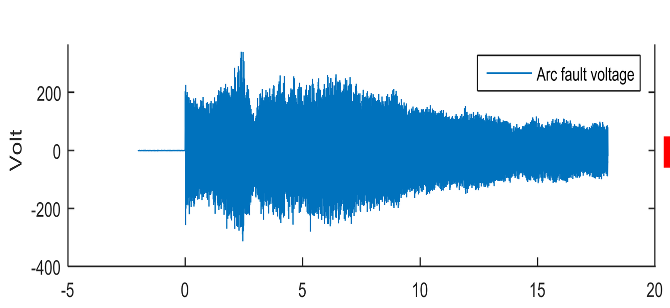

A series arc fault voltage

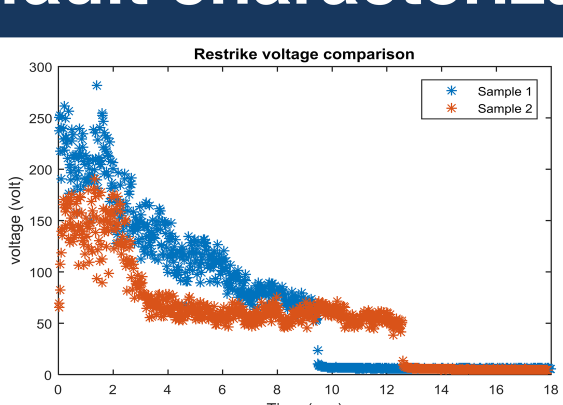

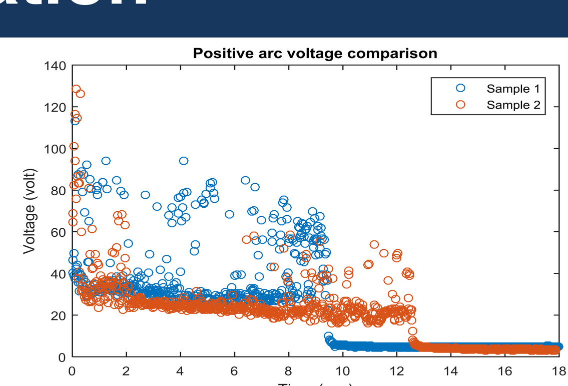

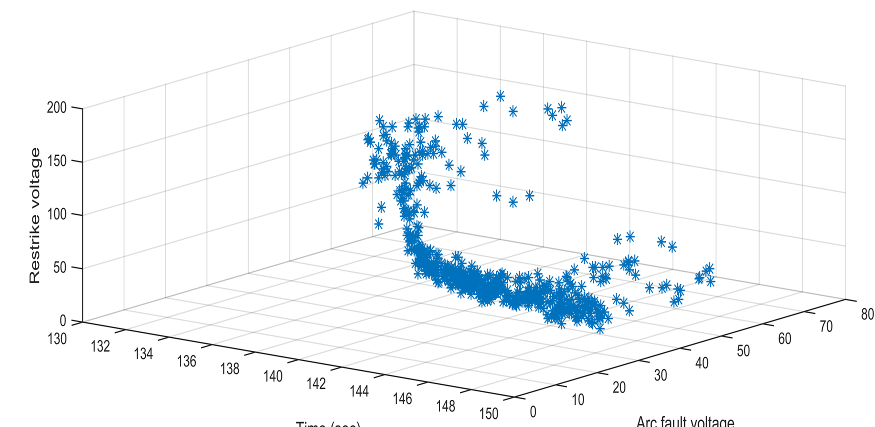

Analyse of restrike voltage and arc fault voltage

This work is sponsored by Peruvian government (Beca Presidente de la República - PRONABEC)

INTRA OPERATIVE AUGMENTED REALITY FOR HEPATIC SURGERY

Garcia Guevara J., Peterlik I., Cotin S., Berger M O
Contact: jaime.garcia guevara@inria.fr

Abstract
Augmented reality hepatic surgery needs pre and intra operative image non rigid registration. The registration pipeline, the improved graph matching, the mechanical model that simulates realistic and large deformations and experimental results on cone beam CT (CBCT) and 3D ultrasound (3DUS) images are described here.

Introduction
Accurate liver tumour resection improves surgery's outcome. To cope with big intra operative liver deformation a non rigid registration based on biomechanical models that fit intra operative vessels is done. The pipeline consists of extracting the vascular trees [1] from both pre and intra operative images, and then automatically match the graphs. Finally the biomechanical model is used to select the best hypothesis and extrapolate the displacement field over the entire organ.

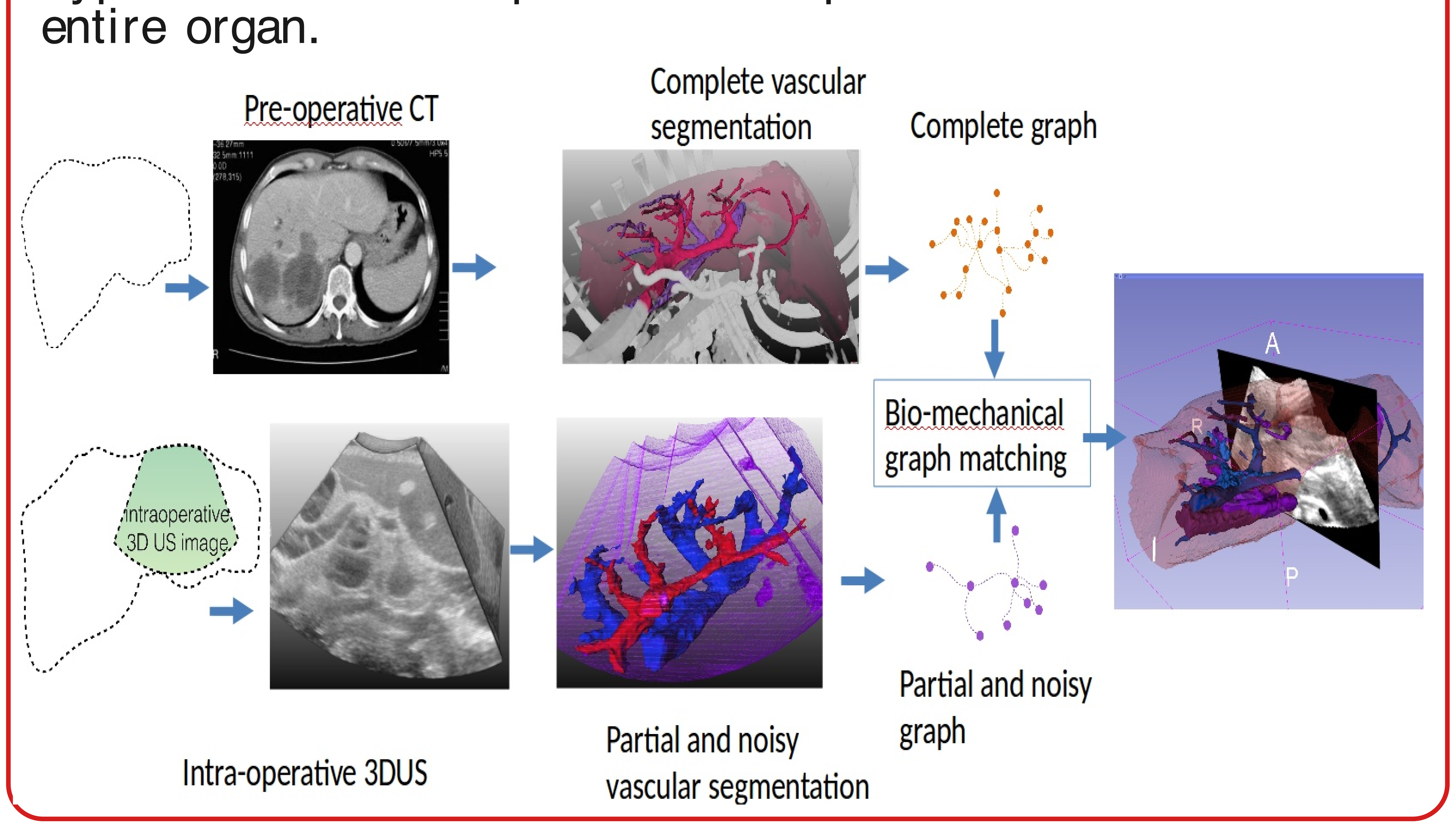

Graph matching
Based on the Gaussian process regression (GPR) graph matching method [2]. It does not require initialization and handles partial matching and topological differences. It iteratively constructs a set of hypotheses associated with a number of inliers quality measure

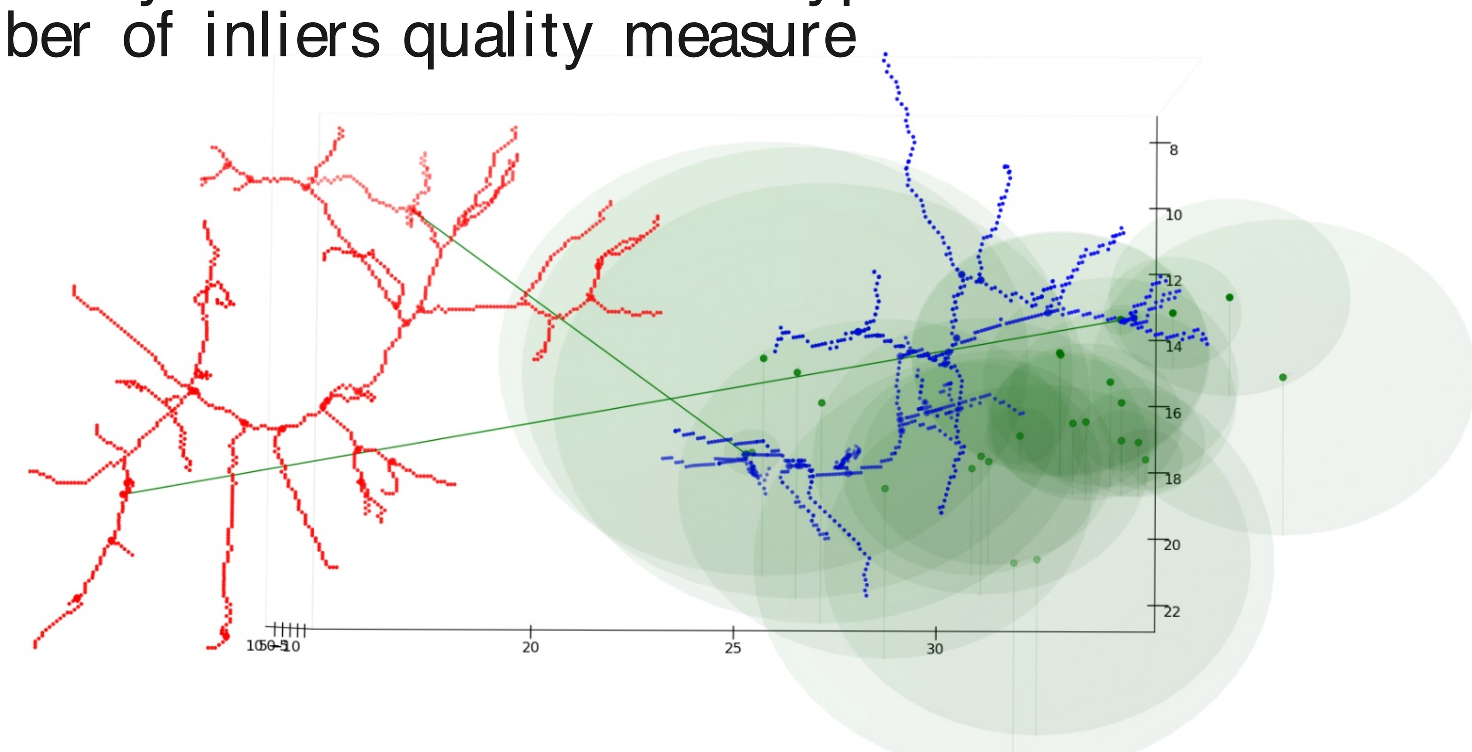

Graph matching initialized with covariance plotted.

Biomechanical model
The graph matching algorithm is improved with a very efficient biomechanical model of liver based on a co rotational linear elastic formulation [3]. The model tolerates large deformations, deals with geometric non linearities and augments the intra operative view.

Hypothesis selection
The original graph matching method [2] results in a set of hypothesis, we improve it with two different methods:

GP + FEM method, the best hypothesis given by the GPR is used to drive physically coherent elastic registration based on the biomechanical model.

Selected FEM method, first rank the generated hypothesis according to the number of inliers estimated from the GPR. Then the top ranked hypotheses are used to drive biomechanical deformations and recompute the number of inliers metric for every top ranked hypothesis. From the set of top ranked hypothesis the one with the largest recomputed inliers metric is kept as the best solution and used to augment the intra operative image.

Results
The original graph mathcing method [2] and our two improved methods are evaluated with two intraoperative modalities with large deformations.

CBCT swine with different pose, pneumoperitoneum and laparoscopic surgical manipulation.

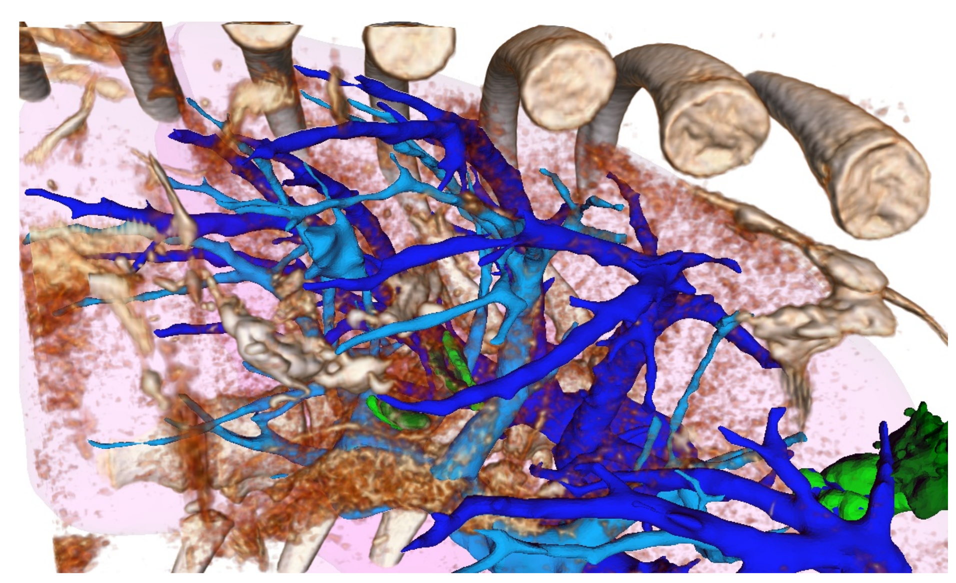

Augmented CBCT, showing clearly the vascular tree (in blue) and the target and registered landmarks (in dark and light green respectively).

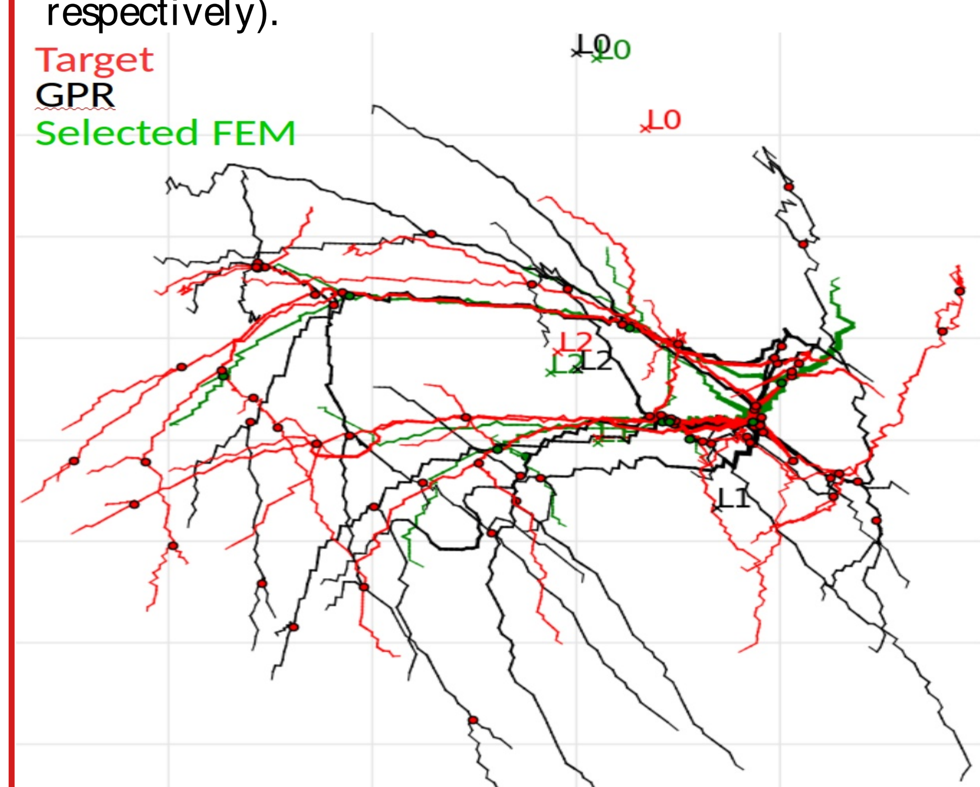

Comparison of target and registered graphs with original GPR matching and selected FEM.

Three inserted landmarks, up to 7.61 cm distant from bifurcations used to compute TRE.

Original GPR matching [2] TRE = 13.7 mm
GPR + FEM TRE = 8.62 mm
Selected FEM TRE = 7.64 mm

3DUS like CT probed images from 2 poses.

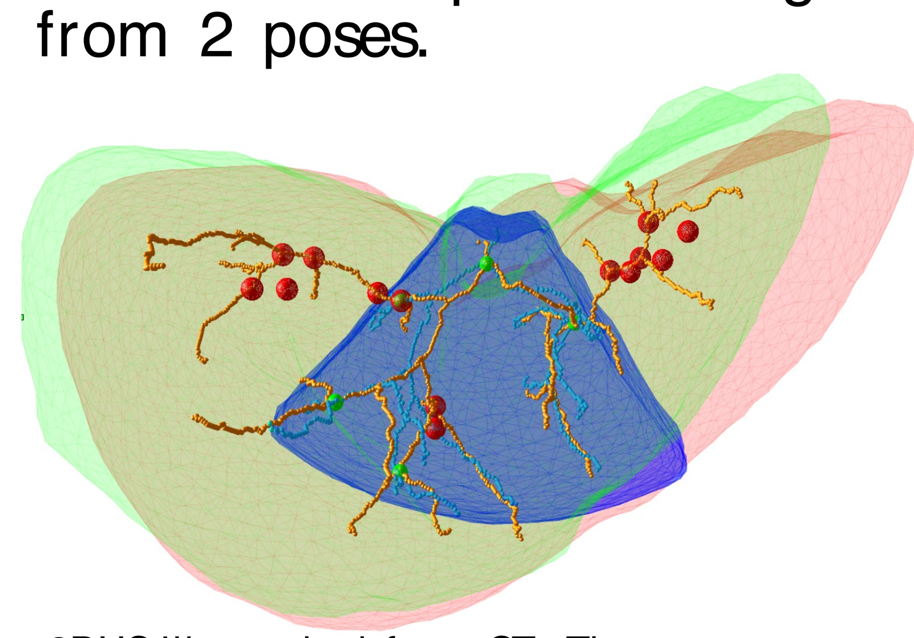

3DUS like probed from CT. The target registration error (TRE) landmarks are the bifurcations outside the 3DUS in red.

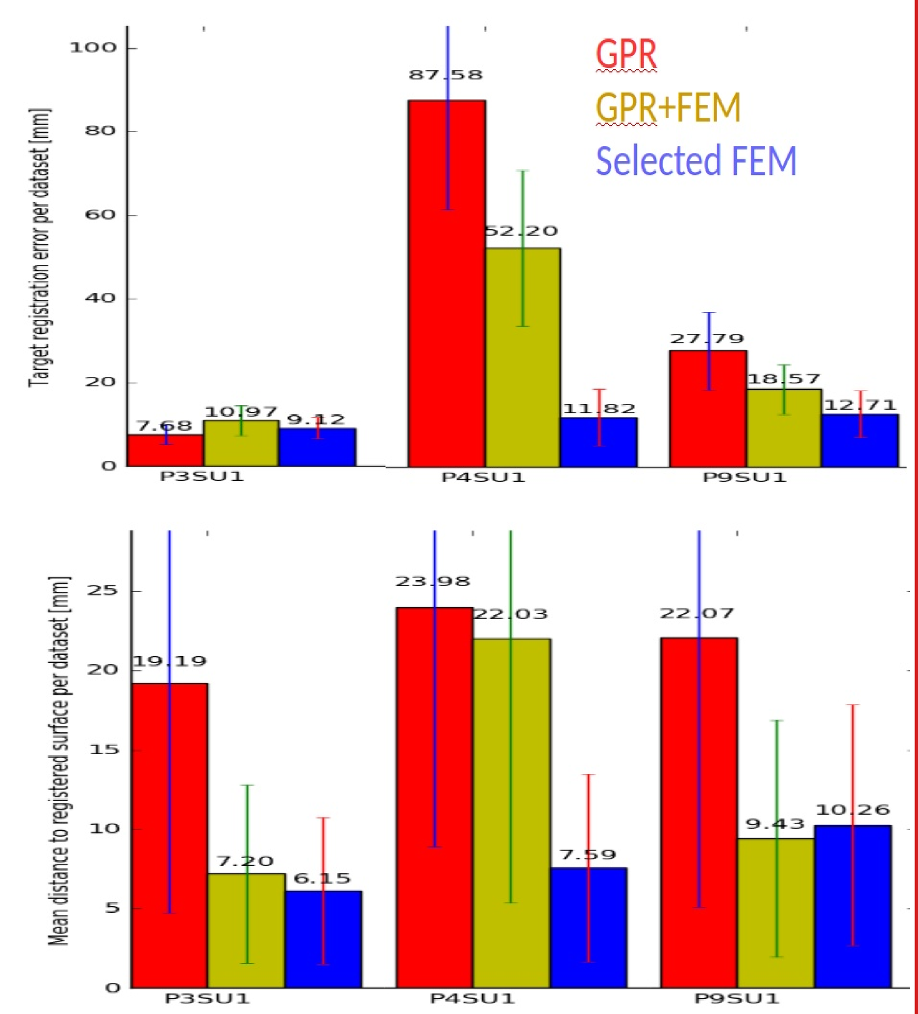

3DUS like evaluation (TRE and mean distance to surface) on 3 human datasets. For the original GPR, the GPR+FEM and selected FEM methods.

Conclusion
We have demonstrated that the use of a biomechanical model noticeably improves the evaluation of the matching hypotheses compared to state of the art grap matching.

References
[1] E. Smistad, A. C. Elster et F. Lindseth. GPU accelerated segmentation and centerline extraction of tubular structures from medical images. IJCARS 2014.

[2] E. Serradell, M. A. Pinheiro, R. Sznitman, J. Kybic, F. Moreno Noguer, and P. Fua. Non rigid graph registration using active testing search. IEEE Transactions on Pattern Analysis and Machine Intelligence, 37(3):625–638, 2015.

[3] I. Peterlik, C. Duriez, and S. Cotin. Modelling and real time simulation of a vascularized liver tissue. In International Conference on Medical Image Computing and Computer Assisted Intervention, pages 50–57. Springer, 2012.

Metric Entropy and Rademacher Complexity of Margin Multi-category Classifiers

Khadija Musayeva, Fabien Lauer, Yann Guermeur

LORIA, CNRS, University of Lorraine, France
Email: khadija.musayeva@loria.fr

UNIVERSITÉ DE LORRAINE

Preliminaries

Problem of pattern classification

- $\mathcal{X}$: description space, $\mathcal{Y}$: finite set of C (> 2) categories
- Random pair (X, Y) taking values in $\mathcal{X} \times \mathcal{Y}$ with distribution P
- The only source of information about P is an m-sample $\mathbf{Z}_m = ((X_i, Y_i))_{1 \leqslant i \leqslant m} \sim P^m$
- Learn the link between descriptions $x \in \mathcal{X}$ and their categories $y \in \mathcal{Y}$

Learning process

- $\mathcal{G} = \prod_{k=1}^{C} \mathcal{G}_k$: a class of functions $g = (g_k)_{1 \leqslant k \leqslant C}$ from $\mathcal{X}$ into $[-M_{\mathcal{G}}, M_{\mathcal{G}}]^C$
- Assumption: $\forall k \in \{1, \ldots, C\}$, $\mathcal{G}_k$ is a uniform Glivenko-Cantelli class [3]
- Decision rule: $\forall g = (g_k)_{1 \leqslant k \leqslant C} \in \mathcal{G}, \forall x \in \mathcal{X}, \mathrm{dr}_g(x) = \arg\max_{1 \leqslant k \leqslant C} g_k(x)$
- Function selection: Minimize over $\mathcal{G}$ the *probability of error* or *risk*

$$L(g) = P\left(\mathrm{dr}_g(X) \neq Y\right)$$

Margin classification

To estimate the classification accuracy of $g \in \mathcal{G}$, use its margin:

$$f_g(x, k) = \frac{1}{2}\left(g_k(x) - \max_{l \neq k} g_l(x)\right), \quad (x, k) \in \mathcal{X} \times \mathcal{Y}.$$

Select a margin loss function

$$\phi_\gamma(t) = \mathbb{1}_{\{t \leqslant 0\}} + \left(1 - \frac{t}{\gamma}\right) \mathbb{1}_{\{t \in (0, \gamma]\}}, \quad \gamma \in (0, 1], t \in \mathbb{R}.$$

Focus on relevant information using a piecewise-linear squashing function

$$\pi_\gamma(t) = t\mathbb{1}_{\{t \in (0,\gamma]\}} + \gamma \mathbb{1}_{\{t > \gamma\}}, \quad \gamma \in (0, 1], t \in \mathbb{R}.$$

Define the class $\mathcal{F}_{\mathcal{G},\gamma} = \left\{ f_{g,\gamma} = \pi_\gamma \circ f_g : g \in \mathcal{G} \right\}$.

Minimize over $\mathcal{G}$ the *empirical margin risk*

$$L_{\gamma,m}(g) = \frac{1}{m} \sum_{i=1}^{m} \phi_\gamma \circ f_{g,\gamma}(X_i, Y_i).$$

Goal

Derive an upper bound on $\sup_{g \in \mathcal{G}} \left(L(g) - L_{\gamma,m}(g)\right)$ in terms of the **number** C **of categories** and the **sample size** m.

Approach (inspired by [6])

1. Derive a guaranteed risk as a function of the Rademacher complexity $R_m\left(\mathcal{F}_{\mathcal{G},\gamma}\right)$:

Theorem (from [8])

For fixed $\gamma \in (0, 1]$ and $\delta \in (0, 1)$, with P^m-probability at least $1 - \delta$, uniformly for every function $g \in \mathcal{G}$,

$$L(g) \leqslant L_{\gamma,m}(g) + \frac{2}{\gamma} R_m\left(\mathcal{F}_{\mathcal{G},\gamma}\right) + \sqrt{\frac{\ln\left(\frac{1}{\delta}\right)}{2m}}.$$

2. Link the Rademacher complexity $R_m\left(\mathcal{F}_{\mathcal{G},\gamma}\right)$ to the metric entropy of $\mathcal{F}_{\mathcal{G},\gamma}$ via chaining [2]:

Theorem (from [4])

Let $N \in \mathbb{N}^*$ and $h : \mathbb{N} \to \mathbb{R}_+$, a decreasing function with $h(0) \geqslant \mathrm{diam}(\mathcal{F}_{\mathcal{G},\gamma})$. Then

$$\hat{R}_m\left(\mathcal{F}_{\mathcal{G},\gamma}\right) \leqslant h(N) + 2\sum_{j=1}^{N} (h(j) + h(j-1)) \sqrt{\frac{\ln \mathcal{N}\left(h(j), \mathcal{F}_{\mathcal{G},\gamma}, d_{2,\mathbf{z}_m}\right)}{m}},$$

with $d_{p,\mathbf{z}_m}$ the empirical pseudo-metric on $\mathbf{z}_m = ((x_i, y_i))_{1 \leqslant i \leqslant m} \in (\mathcal{X} \times \mathcal{Y})^m$ derived from the L_p-norm.

3. Link the metric entropy of $\mathcal{F}_{\mathcal{G},\gamma}$ to that of $\mathcal{G}_k$, $1 \leqslant k \leqslant C$, via a decomposition lemma :

Lemma (from [4])

For any $\epsilon \in \mathbb{R}_+^*$ and $p \in [1, \infty]$,

$$\ln \mathcal{N}\left(\epsilon, \mathcal{F}_{\mathcal{G},\gamma}, d_{p,\mathbf{z}_m}\right) \leqslant \sum_{k=1}^{C} \ln \mathcal{N}\left(\frac{\epsilon}{C^{\frac{1}{p}}}, \mathcal{G}_k, d_{p,\mathbf{x}_m}\right),$$

with $\mathbf{x}_m = (x_i)_{1 \leqslant i \leqslant m} \in \mathcal{X}^m$.

4. Link the metric entropy of $\mathcal{F}_{\mathcal{G},\gamma}$ to the fat-shattering dimensions $\epsilon\text{-dim}\left(\mathcal{G}_k\right)$, $1 \leqslant k \leqslant C$, via decomposition + generalized Shauer-Shelah lemmas ([7], [5], [1]). Several choices:

- **Dimension-free** bounds in L_2-norm:

$$\ln \mathcal{N}\left(\epsilon, \mathcal{F}_{\mathcal{G},\gamma}, d_{2,\mathbf{z}_m}\right) \leqslant 20C\, d\left(\frac{\epsilon}{96\sqrt{C}}\right) \ln\left(\frac{14 M_{\mathcal{G}}\sqrt{C}}{\epsilon}\right), \quad (1)$$

$$\ln \mathcal{N}\left(\epsilon, \mathcal{F}_{\mathcal{G},\gamma}, d_{2,\mathbf{z}_m}\right) \leqslant 3C\, d\left(\frac{\epsilon}{16}\right) \ln^2\left[\frac{K\left(2M_{\mathcal{G}}\right)^3 \gamma^2 C^{\frac{3}{2}} d\left(\frac{\epsilon}{192\sqrt{C}}\right)}{\epsilon^5}\right] \quad (2)$$

- **Sample-size dependent** bound in L_∞-norm:

$$\ln \mathcal{N}\left(\epsilon, \mathcal{F}_{\mathcal{G},\gamma}, d_{2,\mathbf{z}_m}\right) \leqslant \ln \mathcal{N}\left(\epsilon, \mathcal{F}_{\mathcal{G},\gamma}, d_{\infty,\mathbf{z}_m}\right) \leqslant 3C\, d\left(\frac{\epsilon}{4}\right) \ln^2\left(\frac{16 M_{\mathcal{G}}^2 m}{\epsilon^2}\right), \quad (3)$$

with $d(\epsilon) = \max_{1 \leqslant k \leqslant C} \epsilon\text{-dim}\left(\mathcal{G}_k\right)$.

5. Make a hypothesis regarding the growth rate of the fat-shattering dimensions:

There exists a pair $(d_{\mathcal{G}}, K_{\mathcal{G}}) \in \left(\mathbb{R}_+^*\right)^2$ such that $\forall \epsilon \in (0, M_{\mathcal{G}}]$, $d(\epsilon) \leqslant K_{\mathcal{G}} \epsilon^{-d_{\mathcal{G}}}$.

6. Final bound on the Rademacher complexity in terms of C and m:

$$R_m\left(\mathcal{F}_{\mathcal{G},\gamma}\right) \leqslant \underbrace{K\left(\gamma, d_{\mathcal{G}}, M_{\mathcal{G}}, K_{\mathcal{G}}\right)}_{\text{constant w.r.t. } m,C} \sqrt{C/m} \cdot F\left(m, C, d_{\mathcal{G}}\right)$$

Degree of polynomial	$F(m, C, d_{\mathcal{G}})$		
	[4], uses (1)	[5], uses (2)	this work, uses (3)
$0 < d_{\mathcal{G}} < 2$ (Donsker classes [10])	$C^{\frac{d_{\mathcal{G}}}{4}} \sqrt{\ln C}$	$\ln C$	$\ln m$
$d_{\mathcal{G}} = 2$ (e.g., M-SVMs)	$\sqrt{C} \ln^{\frac{3}{2}}\left(\frac{m}{\sqrt{C}}\right)$	$\ln(m) \ln(Cm)$	$\ln^2 m$
$d_{\mathcal{G}} > 2$ (e.g., Neural Networks)	$C^{\frac{1}{d_{\mathcal{G}}}} m^{\frac{1}{2} - \frac{1}{d_{\mathcal{G}}}} \sqrt{\ln \frac{m}{C}}$	$m^{\frac{1}{2} - \frac{1}{d_{\mathcal{G}}}} \ln(Cm)$	$m^{\frac{1}{2} - \frac{1}{d_{\mathcal{G}}}} \ln(m)$

Conclusions

- Better dependency on C for $d_{\mathcal{G}} \geqslant 2$ using a metric entropy bound that depends on the sample-size
- This dependency does not change with the complexity of the function class (it is independent of $d_{\mathcal{G}}$)
- Dependency on m is no worse (except for Donsker classes) than that in [5] which uses a dimension-free Sauer-Shelah lemma
- There is a trade-off between the dependencies on C and m

Ongoing work

Can the dependencies on C and m of the current bound be improved under stronger assumptions about the function classes?

1. Extend metric entropy bound of linear function classes [11] to reproducing kernel Hilbert spaces (RKHS)
2. Consider metric entropy bound of balls in Gaussian RKHS [9]

References

[1] Alon, N., Ben-David, S., Cesa-Bianchi, N., and Haussler, D. Scale-sensitive dimensions, uniform convergence, and learnability. *Journal of the ACM*, 44(4):615–631, 1997.

[2] Dudley, R.M. The sizes of compact subsets of Hilbert space and continuity of Gaussian processes. *Journal of Functional Analysis*, 1(3):290–330, 1967.

[3] Dudley, R.M., Giné, E. and Zinn, J. Uniform and universal Glivenko-Cantelli classes. *Journal of Theoretical Probability*, 4(3):485–510, 1991.

[4] Guermeur, Y. L_p-norm Sauer-Shelah lemma for margin multi-category classifiers. *Journal of Computer and System Sciences (JCSS)*, 89:450–473, 2017.

[5] Guermeur, Y. Rademacher complexity of margin multi-category classifiers. *WSOM+ 17.*

[6] Mendelson, S. Rademacher averages and phase transitions in Glivenko-Cantelli classes. *IEEE Transactions on Information Theory*, 48(1):251–263, 2002.

[7] Mendelson, S. and Vershynin, R. Entropy and the combinatorial dimension. *Inventiones mathematicae*, 152:37–55, 2003.

[8] Mohri, M., Rostamizadeh, A. and Talwalkar, A. Foundations of Machine Learning. *The MIT Press, Cambridge, MA, 2012.*

[9] Steinwart, I. and Scovel, C. Fast rates for support vector machines using Gaussian kernels. *The annals of statistics*, 35(2):575–607, 2007.

[10] van der Vaart, A.W. and Wellner, J.A. Weak Convergence and Empirical Processes, With Applications to Statistics. *Springer Series in Statistics. Springer-Verlag, New York, 1996.*

[11] Zhang, T. (2002). Covering number bounds for certain regularized linear function classes. *Journal of Machine Learning Research*, 2:527–550, 2002.

ECOLE DOCTORALE IAEM LORAINE

DYNAMIC GROUPING MAINTENANCE FOR MULTI-DEPENDENT COMPONENT-BASED MANUFACTURING SYSTEMS

Sustainable Systems Engineering Department (ISET)/CRAN

PhD student: Ho Si Hung NGUYEN (ho-si-hung.nguyen@univ-lorraine.fr)

Supervisors: Benoit IUNG & Phuc DO

Financial support: Grant from Vietnamese education ministry + Lab funds

Beginning of PhD works: April 2016

CONTEXT

- Manufacturing system has become more and more complex: multi-component, multi-dependence, multi-function, decentralized configuration, etc.
- Support system plays a key role to keep the target (manufacturing) system in its nominal operation space by means of preventive maintenance actions.
- Complex dependences in target system and support system have important impacts on **maintenance optimization and planning**, especially when the target system operates in dynamic contexts (e.g., multi-operating modes, time-dependent constraints, etc).
- *Research question: How to integrate these dependences into maintenance models and optimization process ?*

SCIENTIFIC ISSUES

- Identifying and modeling different kinds of dependences on both target and support systems.
- Integrating these dependences in integrated maintenance models.
- Finding the optimal logistic support and preventive maintenance planning from the integrated maintenance models.
- Updating logistic support and preventive maintenance planning in presence of a dynamic context.

SCIENTIFIC CONTRIBUTIONS

a) Proposal and formulation of dependence models incorporating both target system and support systems.

b) Development of integrated maintenance models taking into account different above kinds of dependences.

c) Development of joint optimization algorithms to find optimal logistic support and maintenance grouped planning.

d) Proposal of adaptive grouping maintenance decision rules allowing updating the maintenance planning in dynamic contexts.

METHODOLOGY

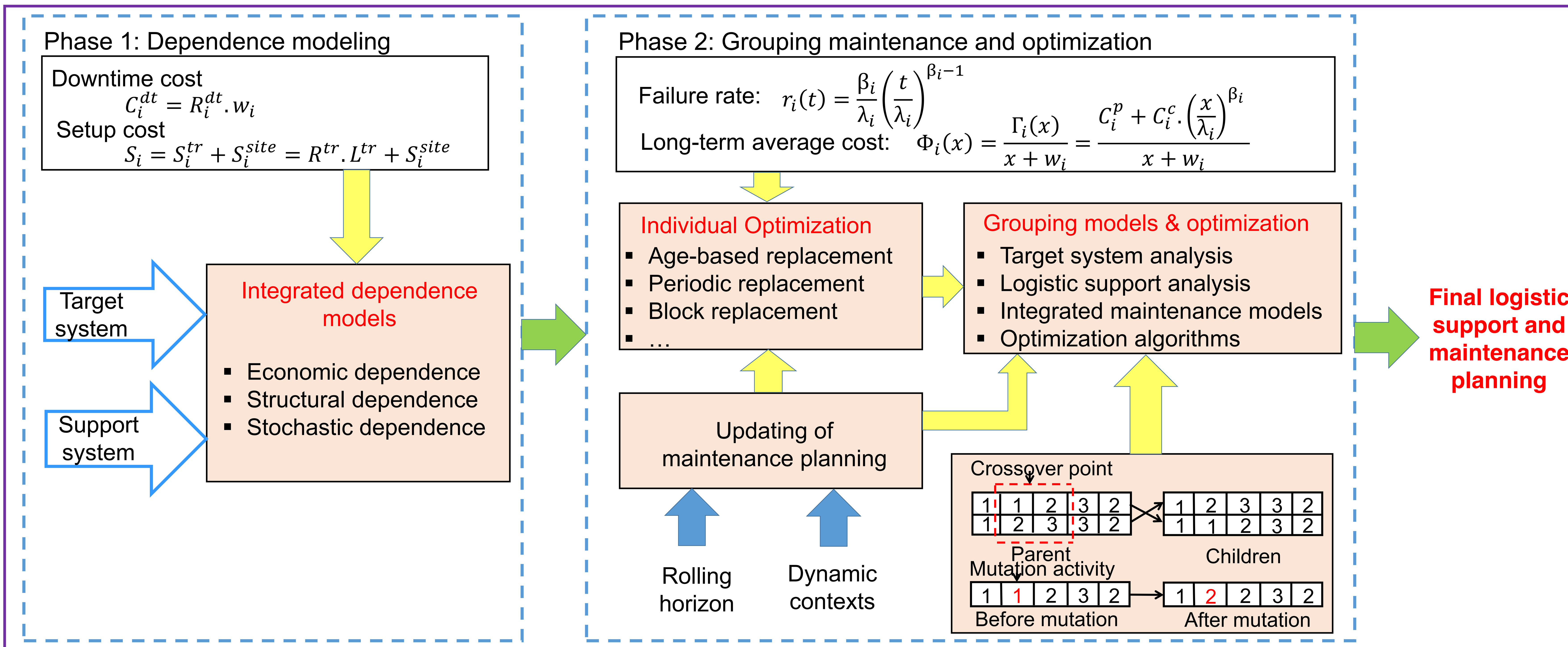

- **Mathematical tools**: Markov process, Weibull distribution, Stochastic processes.
- **Optimization algorithm**: Genetic algorithms, Traveling salesman problem (TSP), the best-first research.
- **Computing tools**: Matlab.

ACHIEVED WORKS

Developing a dynamic grouping maintenance for geographically dispersed production systems with consideration of both economic and structural dependence (contributions a & b).

PLANNED WORKS

- Incorporating optimization algorithms to optimize logistic support and maintenance grouped planning simultaneously (contribution c).
- Developing a grouping maintenance strategy in presence of dependencies and dynamic context (contribution d).

PRELIMINARY PUBLICATIONS

[1] **Nguyen, H. S. H.**, Do Van, P., Iung, B., & Vu, H. C. (2017, July). **A dynamic grouping maintenance strategy for geographically dispersed production systems**. In *10th International Conference on Mathematical Methods in Reliability*, MMR 2017.

[2] **Nguyen, H. S. H.**, Do Van, P., Iung, B., & Vu, H. C. **Dynamic grouping maintenance for geographically dispersed production systems**. *Reliability engineering and system safety, Submitted in Septembe 2017.*

An optimized domain decomposition method between interior and exterior domains for harmonic penetrable scattering problems

Boris Caudron, Christophe Geuzaine, Xavier Antoine

Institut Elie Cartan de Lorraine, Montefiore Institute (University of Liège), Thales Systèmes Aéroportés

Introduction

The study of harmonic scattering problems, should it be in acoustics or in electromagnetics, is central in fields of application such as sonars and radars.

The way these devices work is very simple. They send an incident wave in a particular direction and if there is an object in this direction, the incident wave hits the object and is reflected back to the source. Finally, measuring the intensity of the reflected signal allows to detect the presence of the object.

For conciseness, we will focus on acoustics, and therefore sonars, but electromagnetics, and therefore radars, can and have been dealt with the exact same way.

The Helmholtz equation is central in this work. This partial differential equation naturally appears when looking for harmonic solutions of the wave equation:

$$\Delta\tilde{\mathbf{u}} + \omega^2 \mathbf{c}^{-2}\tilde{\mathbf{u}} = 0 \quad \Rightarrow \quad \begin{cases} \mathbf{u} = \mathcal{R}\left(\tilde{\mathbf{u}}(\mathbf{x})e^{-i\omega t}\right) \\ \partial_t^2 \mathbf{u} - \mathbf{c}^2\Delta\mathbf{u} = 0 \end{cases}.$$

$\mathbf{c}$ is the wave velocity within the medium of interest, ω is the pulsation of the wave and the quantity $\omega\mathbf{c}^{-1}$ is known as the wave number.

The acoustic transmission problem

We denote by $\mathbf{\Omega}_-$ the scatterer, by $\mathbf{\Omega}_+$ the exterior domain $\mathbb{R}^3\backslash\overline{\mathbf{\Omega}}_-$, by $\mathbf{\Gamma}$ the surface of the scatterer and by $\mathbf{n}$ the unit normal vector on $\mathbf{\Gamma}$ which is outgoing for $\mathbf{\Omega}_-$.

The solution of the scattering problem should satisfy the Helmholtz equation in $\mathbf{\Omega}_- \cup \mathbf{\Omega}_+$ as well as the Sommerfeld radiation condition which encodes the fact that the scattered wave moves away from the scatterer:

$$\Delta\mathbf{u}_\pm + \mathbf{k}_\pm^2\mathbf{u}_\pm = \mathbf{0} \text{ in } \mathbf{\Omega}_\pm \quad , \quad \partial_r\mathbf{u}_+ - i\mathbf{k}_+\mathbf{u}_+ = \underset{r\to+\infty}{\mathcal{O}}\left(\mathbf{r}^{-2}\right).$$

$\mathbf{k}_+$, the exterior wave number, is assumed to be constant since the exterior domain is typically air or water but $\mathbf{k}_-$, the interior wave number, can be a function on $\mathbf{\Omega}_-$ thus allowing to handle inhomogeneous scatterers.

Finally, interface conditions should be imposed on $\mathbf{\Gamma}$:

$$\mathbf{u}_+ + \mathbf{u}_i = \mathbf{u}_- \text{ on } \mathbf{\Gamma} \quad , \quad \partial_n\mathbf{u}_+ + \partial_n\mathbf{u}_i = \rho\partial_n\mathbf{u}_- \text{ on } \mathbf{\Gamma}.$$

ρ, the transmission coefficient, can also be a function on $\mathbf{\Gamma}$.

$\mathbf{u}_i$, the incident wave, is supposed to be a plane wave and therefore satisfies the Helmholtz equation in $\mathbf{\Omega}_+$:

$$\mathbf{u}_i = e^{-i\mathbf{k}_+\mathbf{e}_r.\mathbf{x}} \quad , \quad \Delta\mathbf{u}_i + \mathbf{k}_+^2\mathbf{u}_i = \mathbf{0} \text{ in } \mathbf{\Omega}_+.$$

On a physical standpoint, $\mathbf{u}_-$ is the total pressure field in $\mathbf{\Omega}_-$. However, $\mathbf{u}_+$ is not the total pressure field in $\mathbf{\Omega}_+$. It is only the scattered pressure field in $\mathbf{\Omega}_+$, the total pressure field in $\mathbf{\Omega}_+$ being:

$$\mathbf{u}_{tot} = \mathbf{u}_i + \mathbf{u}_+.$$

As a result, the Dirichlet interface condition expresses the continuity of the total pressure field across $\mathbf{\Gamma}$. On the other hand, the Neumann interface condition is equivalent to the continuity of the normal velocity across $\mathbf{\Gamma}$.

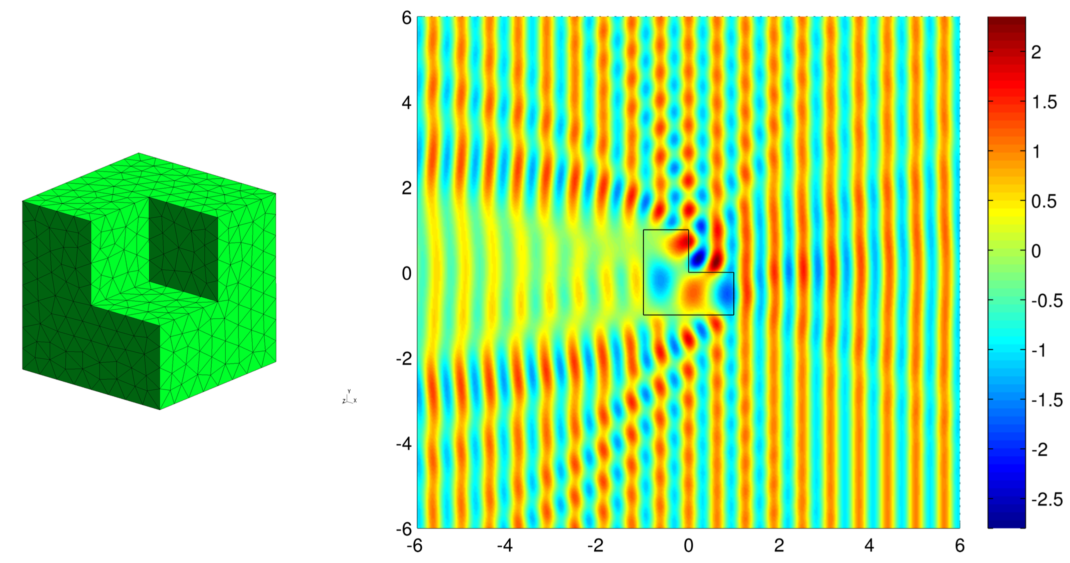

Acoustic scattering by a modified cube. The length of the longest edges is $\mathbf{2}$ whereas the one of the smallest edges is $\mathbf{1}$. The physical parameters are the following: $\mathbf{k}_- = \mathbf{5}$, $\mathbf{k}_+ = \mathbf{10}$ and $\rho = \mathbf{1}$.

Integral representation

$\mathbf{u}_+$ can be represented using volume integral operators:

$$\mathbf{u}_+ = -\mathcal{S}_{\mathbf{k}_+}\partial_n\mathbf{u}_+ + \mathcal{D}_{\mathbf{k}_+}\mathbf{u}_+ \text{ in } \mathbf{\Omega}_+.$$

$\mathcal{S}_{\mathbf{k}_+}$ and $\mathcal{D}_{\mathbf{k}_+}$ are respectively called the single and the double layer volume operators and they are defined for $\mathbf{x} \notin \mathbf{\Gamma}$ by:

$$\mathcal{S}_{\mathbf{k}_+}\partial_n\mathbf{u}_+(\mathbf{x}) = \int_\Gamma \mathbf{G}_{\mathbf{k}_+}(\mathbf{x}-\mathbf{y})\partial_n\mathbf{u}_+(\mathbf{y})d\mathbf{y},$$

$$\mathcal{D}_{\mathbf{k}_+}\mathbf{u}_+(\mathbf{x}) = \int_\Gamma \partial_{n(\mathbf{y})}\mathbf{G}_{\mathbf{k}_+}(\mathbf{x}-\mathbf{y})\mathbf{u}_+(\mathbf{y})d\mathbf{y}.$$

Green function for the Helmholtz equation:

$$\mathbf{G}_{\mathbf{k}_+}(\mathbf{x}) = \frac{e^{i\mathbf{k}_+||\mathbf{x}||}}{4\pi||\mathbf{x}||}$$

Classical resolution method and motivation

It is possible to define surface integral operators on $\mathbf{\Gamma}$, $\mathbf{S}_{\mathbf{k}_+}$ and $\mathbf{D}_{\mathbf{k}_+}$, using the same formulas as for $\mathcal{S}_{\mathbf{k}_+}$ and $\mathcal{D}_{\mathbf{k}_+}$. Using these operators, we can obtain an expression for the Dirichlet trace of $\mathbf{u}_+$ on $\mathbf{\Gamma}$, which, in the end, leads to the following integral equation:

$$\frac{1}{2}\mathbf{u}_+ - \mathbf{D}_{\mathbf{k}_+}\mathbf{u}_+ + \mathbf{S}_{\mathbf{k}_+}\partial_n\mathbf{u}_+ = \mathbf{0} \text{ on } \mathbf{\Gamma}.$$

A classical method to solve the transmission problem consists in coupling a classical variational formulation for the interior domain and the variational formulation of the previous integral equation. With this approach, the finite element method (FEM) and the boundary element method (BEM) are strongly coupled in one unique formulation:

$$\int_{\Omega_-}\nabla\mathbf{u}_-.\nabla\bar{\mathbf{v}} - \int_{\Omega_-}\mathbf{k}_-^2\mathbf{u}_-\bar{\mathbf{v}} - \int_\Gamma \rho^{-1}\partial_n\mathbf{u}_+\bar{\mathbf{v}} = \int_\Gamma \rho^{-1}\partial_n\mathbf{u}_i\bar{\mathbf{v}},$$

$$\frac{1}{2}\int_\Gamma \mathbf{u}_-\bar{\mathbf{v}} - \int_\Gamma(\mathbf{D}_{\mathbf{k}_+}\mathbf{u}_-)\bar{\mathbf{v}} + \int_\Gamma(\mathbf{S}_{\mathbf{k}_+}\partial_n\mathbf{u}_+)\bar{\mathbf{v}} = \frac{1}{2}\int_\Gamma \mathbf{u}_i\bar{\mathbf{v}} - \int_\Gamma(\mathbf{D}_{\mathbf{k}_+}\mathbf{u}_i)\bar{\mathbf{v}}.$$

However, there is a drawback to this approach. Let us suppose that we dispose of two pre-existing solvers: one BEM solver for exterior problems as a whole and one FEM solver for interior problems as a whole. Implementing this strong FEM/BEM coupling using the two pre-existing solvers will require serious modifications of their source code. Hence the following question. Would it be possible to solve the transmission problem by coupling the two pre-existing solvers without modifying them at all ?

The weak FEM/BEM coupling

It is indeed possible to reach the previous goal using the following equivalent reformulation of the transmission problem:

$$(\mathbf{Id} - \mathbf{S}_\pi)\begin{pmatrix}\mathbf{g}_- \\ \mathbf{g}_+\end{pmatrix} = \begin{pmatrix}\partial_n\mathbf{u}_i + \mathbf{T}_-\mathbf{u}_i \\ -\partial_n\mathbf{u}_i - \mathbf{T}_+\mathbf{u}_i\end{pmatrix}. \qquad (1)$$

The unknowns of this equation are defined through trace operators $\mathbf{B}_\pm$ on $\mathbf{\Gamma}$:

$$\mathbf{g}_\pm = \mathbf{B}_\pm\mathbf{u} \quad , \quad \mathbf{B}_- = \rho\gamma_N^- + \mathbf{T}_-\gamma_D^- \quad , \quad \mathbf{B}_+ = \gamma_N^+ + \mathbf{T}_+\gamma_D^+.$$

$\mathbf{S}_\pi$ involves continuous analogs of the pre-existing solvers $\mathbf{R}_\pm$:

$$\mathbf{S}_\pi = \begin{pmatrix}\mathbf{0} & \mathbf{S}_+ \\ \mathbf{S}_- & \mathbf{0}\end{pmatrix} \quad , \quad \mathbf{S}_\pm = \mathbf{Id}\pm(\mathbf{T}_- - \mathbf{T}_+)\mathbf{R}_\pm,$$

$$\mathbf{R}_\pm\mathbf{g} = \gamma_D^\pm\mathbf{u}_\pm \quad , \quad \Delta\mathbf{u}_\pm + \mathbf{k}_\pm^2\mathbf{u}_\pm = \mathbf{0} \text{ in } \mathbf{\Omega}_\pm \quad , \quad \mathbf{B}_\pm\mathbf{u}_\pm = \mathbf{g},$$

where $\mathbf{u}_+$ should of course satisfy the radiation condition. Equation (1) should therefore be solved iteratively, typically using the Generalized Minimal Residual (GMRES) method.

The approach adopted here is a domain decomposition method, with the transmission operators $\mathbf{T}_\pm$ transfering information from one domain to the other. The choice of these operators is crucial to ensure good GMRES convergence. Dirichlet-to-Neumann (DtN) operators, $\mathbf{\Lambda}_{\pm,\mathbf{k}_\pm}$, allow to build optimal transmission operators in the sense that they ensure $\mathbf{S}_\pi = \mathbf{0}$ rendering equation (1) trivial to solve:

$$\mathbf{T}_- = -\mathbf{\Lambda}_{+,\mathbf{k}_+} \quad , \quad \mathbf{T}_+ = -\rho\mathbf{\Lambda}_{-,\mathbf{k}_-}.$$

In pratice, DtN operators are unreasonnably costly to compute thus it is preferable to use some of their high or low order approximations:

$$\mathbf{\Lambda}_{\pm,\mathbf{k}_\pm} \simeq \pm i\mathbf{k}_\pm\sqrt{\mathbf{Id} + \frac{\Delta_\Gamma}{(\mathbf{k}_\pm + i\epsilon)^2}} \quad , \quad \mathbf{\Lambda}_{\pm,\mathbf{k}_\pm} \simeq \pm i\mathbf{k}_\pm\mathbf{Id}.$$

Numerical results

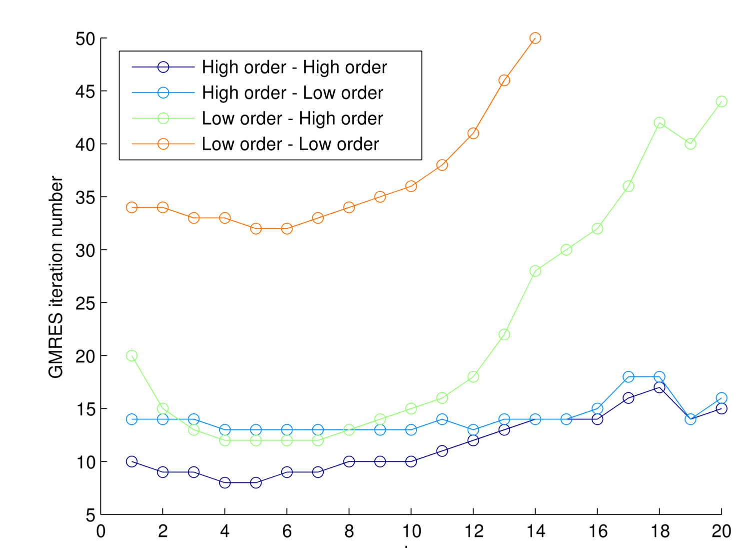

GMRES iteration number of the weak coupling for different pairs of transmission operators $(\mathbf{T}_-;\mathbf{T}_+)$. The scatterer is a sphere of radius $\mathbf{1}$, $\mathbf{k}_+ = \mathbf{10}$ and $\rho = \mathbf{1}$.

The weak FEM/BEM coupling appears to be a viable and interesting method, especially for high frequency problems.

- High order transmission operators allow for a low GMRES iteration number.
- High order transmission operators allow for an only slightly frequency-dependent GMRES iteration number.

Modeling and Classification of Network Scanning Traffic

Giulia De Santis, Abdelkader Lahmadi, Olivier Festor
INRIA - Nancy Grand Est
{giulia.de-santis, abdeklader.lahmadi, olivier.festor}@inria.fr

1. Motivation

- Internet-wide scanning techniques and services are heavily used for malicious activity: exploitation of vulnerabilities [1], control of hosts [2], first steps of Advanced Persistent Threats.
- Network scanning tools evolved over time gaining speed and stealthiness and differ around the world [2].

Is it possible to assess if and what scanning technique is faced by the hosted network?

2. Related work

- Tools used during scanning campaigns detected in [2], focusing on scanned ports.
- Authors in [3] focus on vertical scanning activities and find relationships between ports commonly scanned together.
- Hidden Markov Models (HMMs) applied to detect complex multi-stage network attacks [4], identifying various steps of elaborated attacks; to describe malicious traffic over port 22 [5] and model attackers' behavior.
- Work in [6] and current work provide models of scanning techniques that can be used by security experts to detect advanced attack during their early stages.

3. Proposed approach

Goal: assess if logs gathered by the network are originated by a scanner and what is the scanner.

Methods: Hidden Markov Models based on mixture of distribution models.

Approach:

- learn the models associated to each scanning technique;
- apply the inferred models to identify scanners in real traces.

Features: Intensity of scanners, differences of timestamps and of consecutive destination IP addresses

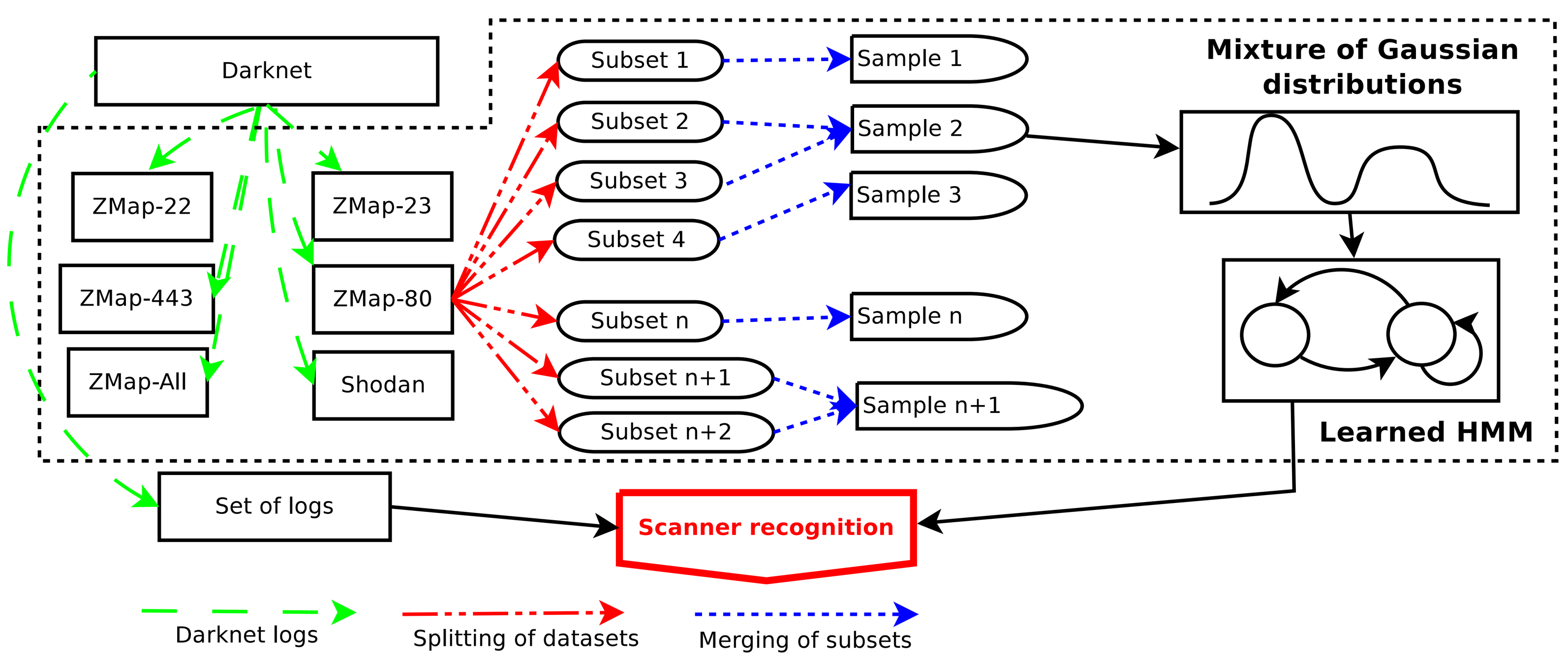

4. Models based on intensity of scanners [6]

- Dataset = {logs of probes received by a /20 darknet generated by Shodan and ZMap}.
- Intensity of the scanner = number of probes originated by the scanner and received in 10 minutes.
- Over-dispersion of datasets ⇒ Mixture of Poisson distributions.
- Mixture Poisson models ⇒ logs clustered in groups, each with:
  - its own Poisson distribution;
  - probability of the cluster.
- HMMs:
  - States of HMM = clusters generated by the mixture model
  - Minimum number of states of HMMs varies from 3 to 6.
  - Initial state of HMMs changing from each model to the other.

  Neither the Mixture distribution models nor the HMMs are comparable models ⇒ Intensity of ZMap and Shodan, respectively, are not comparable.

5. Temporal and spatial models

Datasets: Real logs of packets generated by ZMap-All and Shodan, respectively, collected by a /20 darknet, grouped in *learning* and *testing samples*.

Output: a HMM for each learning sample.

Goal 1: find and validate good candidate models for the considered feature of the scanner.

Phase 1: cluster HMMs according to log-likelihoods and select the *candidate model* from each cluster, labeled with "scanner-port" and "scanner".

Goal 2: Fingerprint scanning activities.

Phase 2: fit *candidate models* on test samples (each with *true label* "scanner-port"). HMM with highest log-likelihood ⇒ labeled with *predicted label*.

6. Classification results

Differences of destination IP addresses 91.3% of HMMs with 2 states. 95% of accuracy when detecting the scanner.

	zmap	shodan
zmap	368	4
shodan	17	50

Time gaps: HMMs with numbers of states between 1 and 7. 92.2% HMMs with less than 5 states. 98% of accuracy.

	zmap	shodan
zmap	362	10
shodan	0	67

Conclusions: Approach able to fingerprint scanning techniques, whose behavior is not related to the scanned port.

7. Future Work

- Leverage the models obtained here to early detection of cyber atacks and advanced persistent threats.

8. References

[1] Z. Durumeric, M. Bailey, and J. A. Halderman, "An Internet-Wide View of Internet-Wide Scanning," in *23rd USENIX Security Symposium (USENIX Security)*, pp. 65–78, 2014.

[2] V. Ghiette, N. Blenn, and C. Doerr, "Remote Identification of Port Scan Toolchains," in *8th IFIP International Conference on New Technologies, Mobility and Security (NTMS)*, pp. 1–5, IEEE, 2016.

[3] S. Lagraa and J. François, "Knowledge Discovery of Port Scans from Darknet," in *Symposium on Integrated Network and Service Management (IM), IFIP/IEEE*, pp. 935–940, IEEE, 2017.

[4] D. Ourston, S. Matzner, W. Stump, and B. Hopkins, "Applications of Hidden Markov Models to Detecting Multi-Stage Network Attacks," in *Proceedings of the 36th Annual Hawaii International Conference on System Sciences*, pp. 10–19, IEEE, 2003.

[5] A. Sperotto, R. Sadre, P.-T. de Boer, and A. Pras, "Hidden Markov Model Modeling of SSH Brute-Force Attacks," in *International Workshop on Distributed Systems: Operations and Management*, pp. 164–176, Springer, 2009.

[6] G. De Santis, A. Lahmadi, J. Francois, and O. Festor, "Modeling of IP Scanning Activities with Hidden Markov Models: Darknet Case Study," in *8th IFIP International Conference on New Technologies, Mobility and Security (NTMS)*, pp. 1–5, IEEE, 2016.

Acknowledgement

This work is partially funded by the HUMA project under the FUI-19 and the Region of Grand-Est.

Statistical parametric speech synthesis system for Arabic

Amal Houidhek, Vincent Colotte, Denis Jouvet, Zied Mnasri
Loria-Inria, Nancy, France
ENIT, Tunis, Tunisie

Introduction

- Statistical parametric speech synthesis system produces good quality speech and offers the possibility to change voice characteristics.
- Arabic speech synthesis and Arabic language particularities.
- For Arabic two particular phenomena: **consonant gemination** and **vowel lengthening.**
- The aim of this presentation is to answer the following question:

Is it better to consider geminated consonants (resp. long vowels) as fully-fledged phonemes ?

Statistical Parametric Speech Synthesis

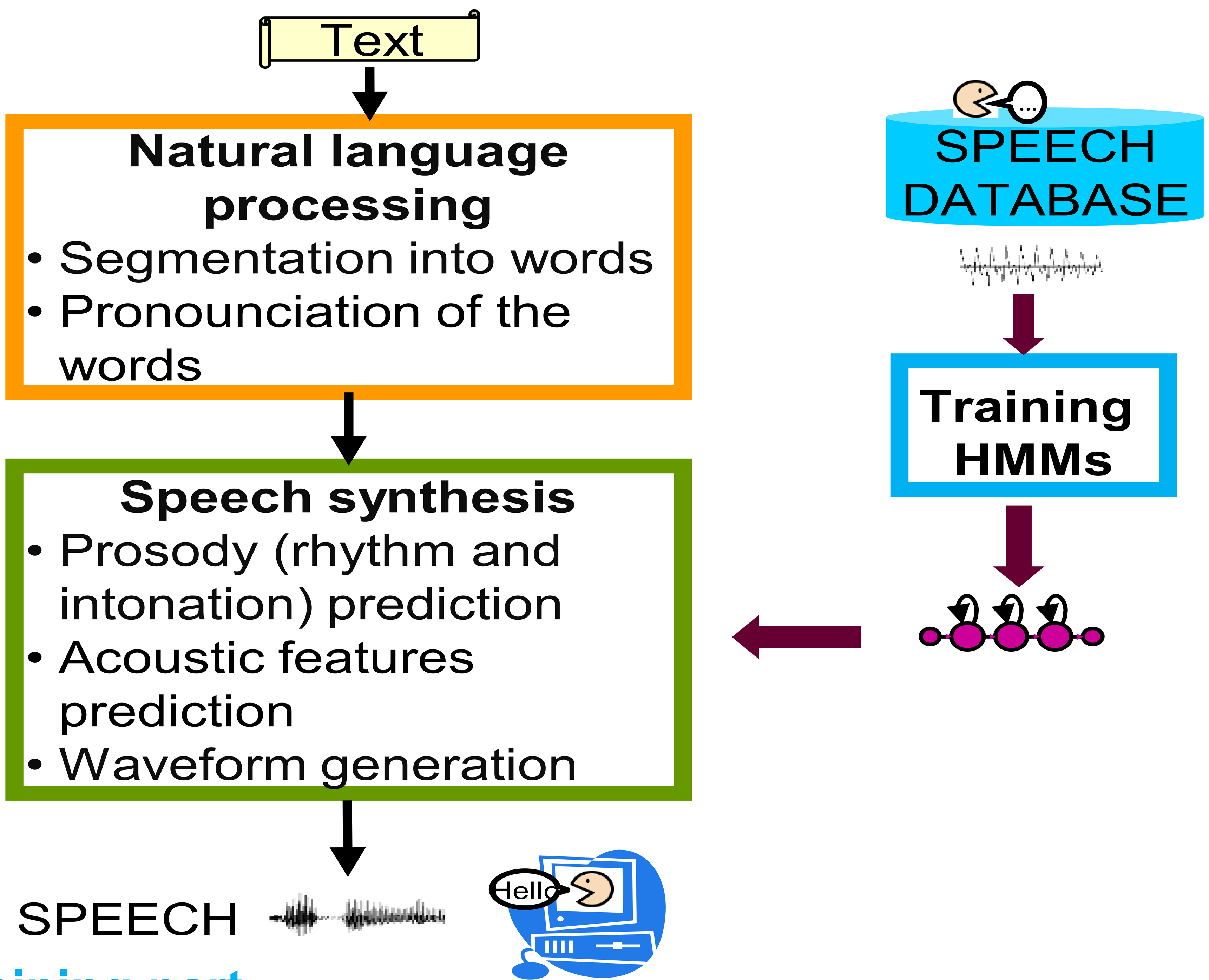

Training part

- Modelling spectrum and excitation features from a speech database.
- Linguistic and phonetic contexts are considered.

Synthesis part

- Prediction of acoustic and prosodic features based on linguistic informations.
- The waveform is generated based on predicted features.

Sound description

A speech unit is described by a set of linguistic and prosodic features such as phoneme identity (e.g., \b\), number of syllables in the current word…etc

Modelling

Four speech unit modelling approaches are proposed and then compared :

A. Differentiating simple vs. geminated consonants and short vs. long vowels.

B. Merging simple and geminated consonant and merging short and long vowels.

C. Differentiating short vs. long vowels.

D. Differentiating simple vs. geminated consonants.

- 1565 utterances for training
- 30 utterances for test
- Sample rate : 48 kHz

Evaluation

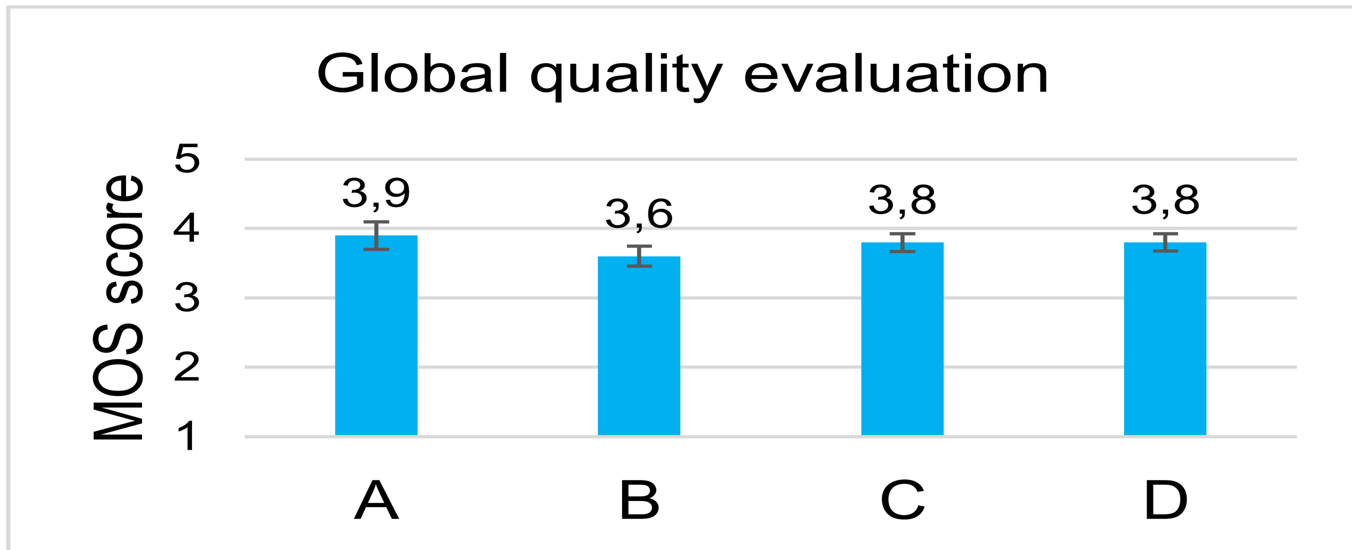

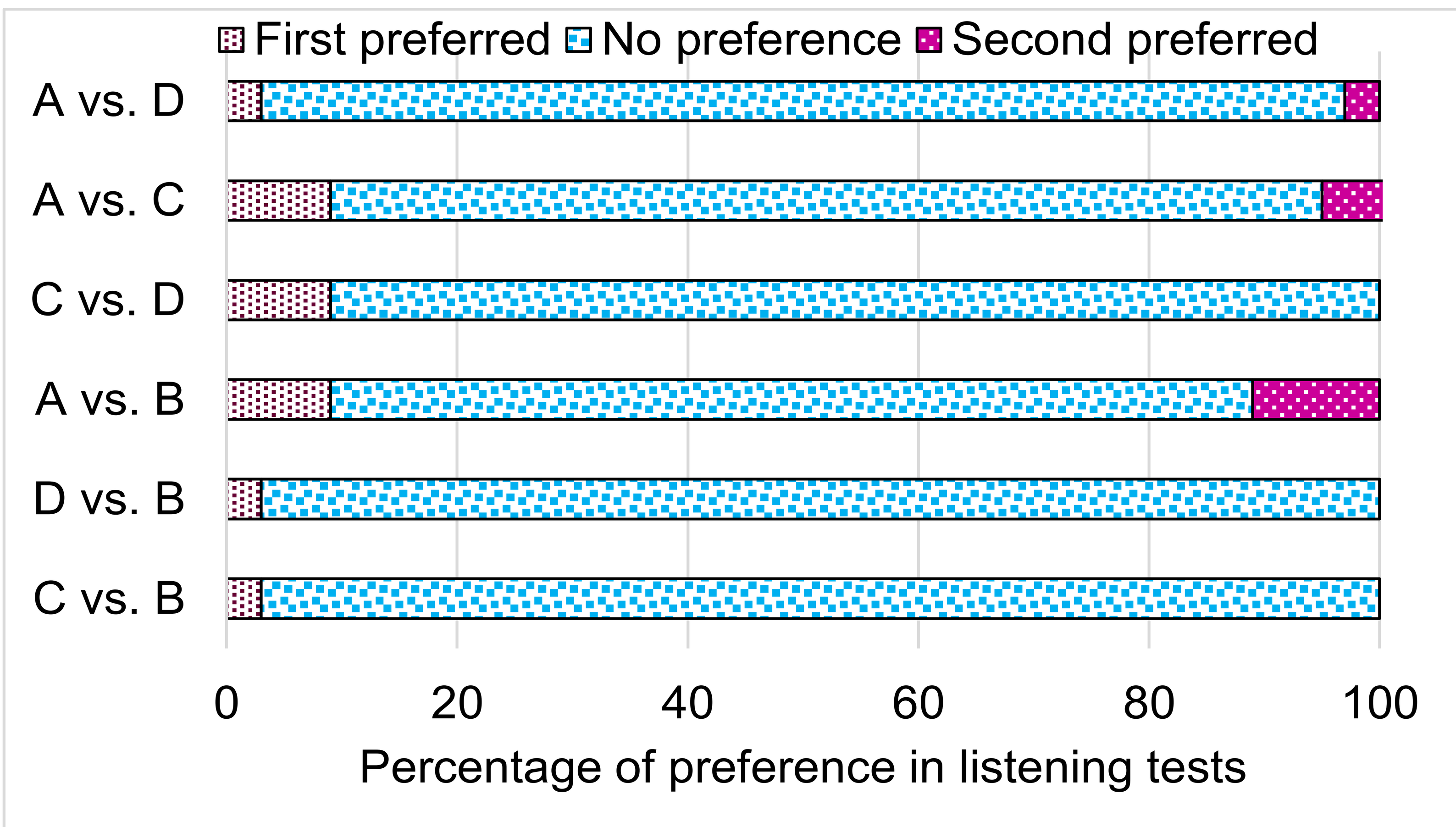

Perspective

- DNN are used in speech synthesis, they showed robustness and better quality compared to decision trees.
- Would neural network benefit from the explicit differentiation of geminated vs. simple consonants and long vs. short vowels ?

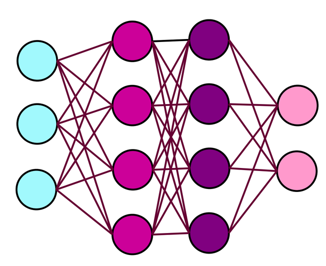

Point-counting on hyperelliptic curves over finite fields

Simon ABELARD

Advisors: Pierrick Gaudry and Pierre-Jean Spaenlehauer
Team Caramba, LORIA, Université de Lorraine

October 2017 — Journée d'Automne de l'École Doctorale IAEM — Nancy, France

Point counting: a toy example

Consider the following equation,

$$Y^2 \equiv X^5 - X^3 + 6X^2 + 4 \mod 23.$$

Problem: how many solutions modulo 23 ?
Naive method: test all the possible values.
(there are only $23^2 = 529$ possible pairs (x, y))

Our problem:

Count number of solutions of equation $Y^2 \equiv f(X) \bmod p$ with

- f monic square-free polynomial
- $\deg f = 2g+1$ where g can grow
- p a very large prime ($p > 2^{128}$)

$\Rightarrow$ Naive method no longer works.

Where is the link with curves?

The equation $Y^2 \equiv f(X) \bmod p$ can be seen as that of a hyperelliptic curve $\mathcal{C}$ over $\mathbb{F}_p$.

We consider f of degree $2g+1$ and say that g is the genus of the curve.

Each solution is a point on that curve, so counting them amounts to counting points on $\mathcal{C}$.

Advantage: we can now exploit powerful tools and results from Algebraic Geometry.

Discrete logarithm

Discrete logarithm problem (DLP): given G a cyclic group and γ a generator, for $a \in G$, find n such that $a = n\gamma$. Usually hard, depends on G.

The hardness of DLP in some groups is used in cryptography. A necessary condition for security is that $\#G$ must have a large prime factor.

Motivations for point-counting

Cryptography: each hyperelliptic curve $\mathcal{C}$ provides a group G in which there is no known subexponential algorithm for DLP, but we still need to compute $\#G$ to assess the security of $\mathcal{C}$.

Number theory: there are conjectures involving zeta functions or number of points on curves, e.g. genus 2 analogue Sato-Tate.

Point-counting on hyperelliptic curves

We actually compute the zeta function of the curve from which we deduce the number of points on the curve and in its Jacobian. By the Weil conjectures, it is of the form

$$\zeta(s) \stackrel{thm}{=} \frac{\Lambda(s)}{(1-s)(1-qs)},$$

where Λ is a polynomial of degree $2g$ with integer coefficients.

Two families of algorithms

What about their complexities ?

- p-adic: polynomial-time in g, exponential in $\log p$.
- ℓ-adic: polynomial-time in $\log p$, exponential in g.

The ℓ-adic methods consist in computing $\Lambda \bmod \ell$ for enough primes ℓ.

Our work: for ℓ-adic methods, study dependency in g of the complexity.

State of the art and contribution

Authors	Complexity
Pila'90	$(\log p)^{g^{O(g)}}$
Huang-Ierardi'98	$(\log p)^{g^{O(1)}}$
Adleman-Huang'01	$(\log p)^{O(g^2 \log g)}$
Our result	$O_g\left((\log p)^{cg}\right)$

Where c is a constant and O_g hides a factor depending on g only.

Group laws on (Jacobians of) curves

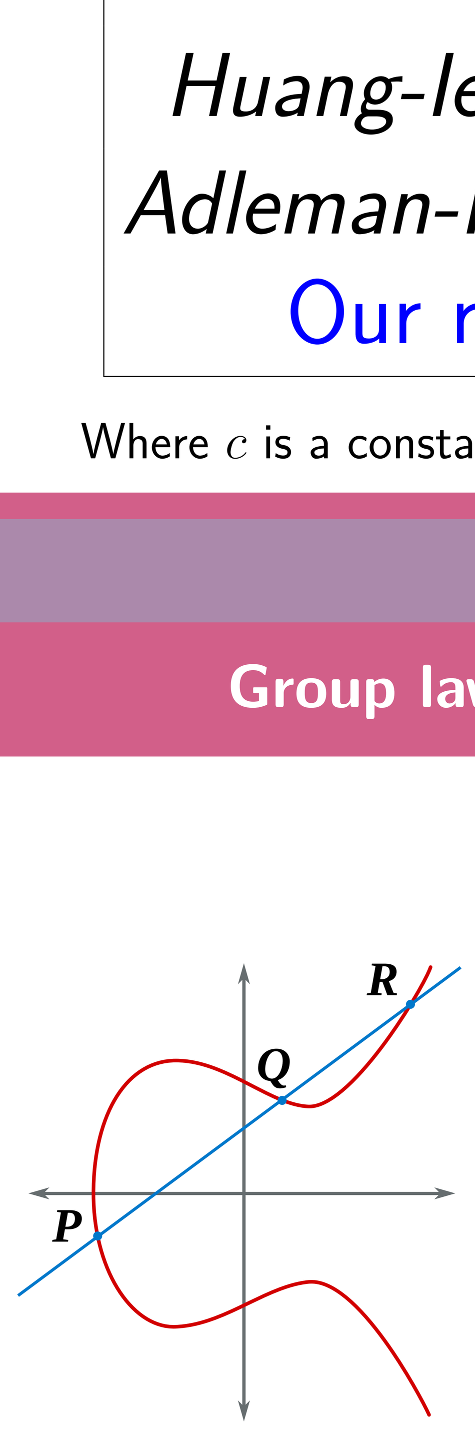

$P + Q + R = 0$

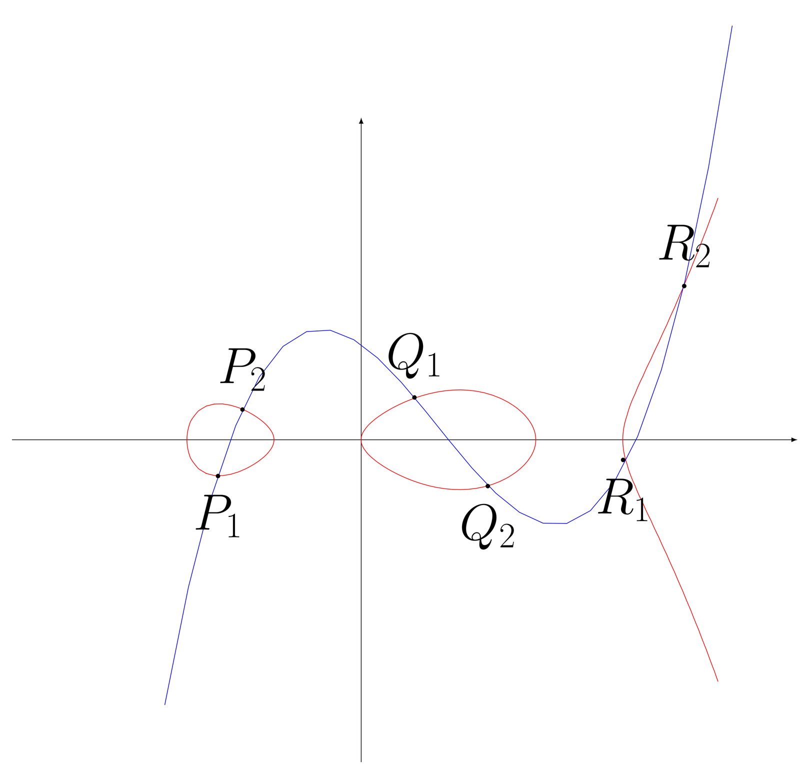

$P_1 + P_2 + Q_1 + Q_2 + R_1 + R_2 = 0$

Main steps towards our result

The ℓ-adic methods require many operations in some (torsion) subgroups. We need to represent them nicely to make these operations fast.

We propose a modelization using polynomial systems which we solve to compute a suitable representation for these subgroups.

Then bound the complexity of the solving step.

Bounding additional complexity

We expect the complexity of the solving step to depend on:

- the degrees of the input system
- the structure of the system
- the method we use to solve that system

The modelization is devised to be structured.
We use a solving method of the literature.
Bounding the degrees is essentially technical.

Future work

Applications and extensions of this work include:

- non-hyperelliptic point-counting
- practical point-counting in genus 3
- endomorphisms' kernels computation

And possibly anywhere we need a convenient description of the ℓ-torsion.

References

- L. Adleman, M.-D. Huang. Counting points on curves and Abelian Varieties over finite fields, 2001. Journal of Symbolic Computation, 32(3):171-189
- D.G. Cantor. On the analogue of the division polynomials, 1994. Journal für die reine und angewandte Mathematik, 447:91-146
- M. Giusti, G. Lecerf, B. Salvy. A Gröbner free alternative for polynomial systems solving, 2012. Journal of Symbolic Computation, 17(1):154-211
- J. Pila. Frobenius maps of Abelian Varieties and finding roots in finite fields, 1990. Mathematics of Computation, 55(192):745-763

ECOLE DOCTORALE IAEM LORRAINE

Acquisition IRM optimisée en vue du dépistage du cancer du sein

Maya DELBANY
Directeur de thèse : Jacques FELBLINGER
Co-directeur de thèse : Pierre-André VUISSOZ

Cancer du sein

- 1er cancer féminin en terme de fréquence
- 1ère cause de décès féminins par cancer

IRM

L'imagerie par résonance magnétique (IRM) est une technique d'imagerie médicale permettant d'obtenir des vues en deux ou en trois dimensions de l'intérieur du corps de façon **non invasive.**

IRM mammaire

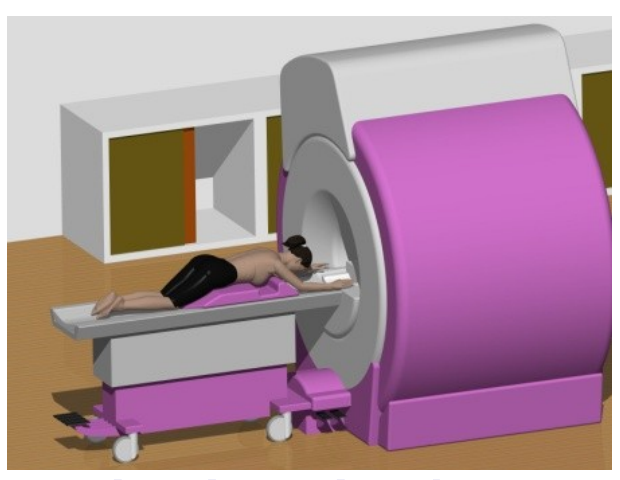

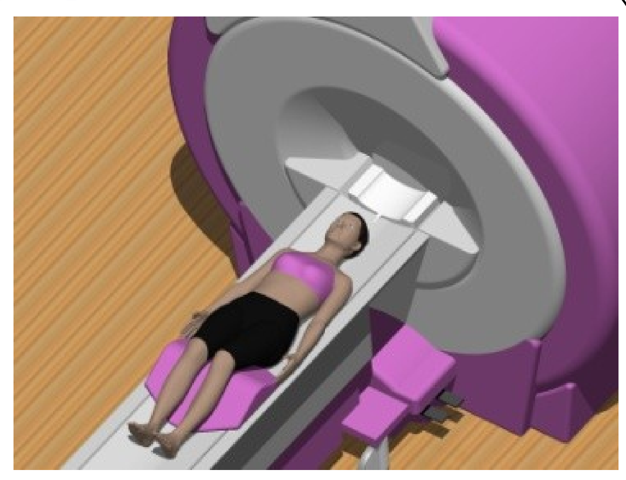

D'aujourd'hui:

- Acquisition décubitus ventral
- Inclut les séquences:
  - *Morphologiques.*
  - *Dynamiques: injection produit de contraste*
- Sensibilité excellente (>95%)
- Spécificité variable (37 => 86%)
- Examen + temps d'installation : 45 minutes

De demain:

- Acquisition décubitus dorsal
- **Séquences sans injection de produit de contraste**
- Excellente Sensibilité
- Meilleure spécificité
- Examen plus rapide

Super Résolution

Une meilleure résolution est nécessaire pour la détection de tumeur < 5 mm. Celle-ci ne peut se faire aujourd'hui sans perte de *SNR*. L'algorithme *SRR* résout le problème de la perte du *SNR* lorsqu'on diminue l'épaisseur de la coupe; c'est un post-traitement combiné avec une stratégie d'acquisition qui peut fournir des images avec des bonnes résolutions. Nous souhaitons obtenir une super résolution avec des techniques d'IRM de diffusion pour le dépistage du cancer du sein.

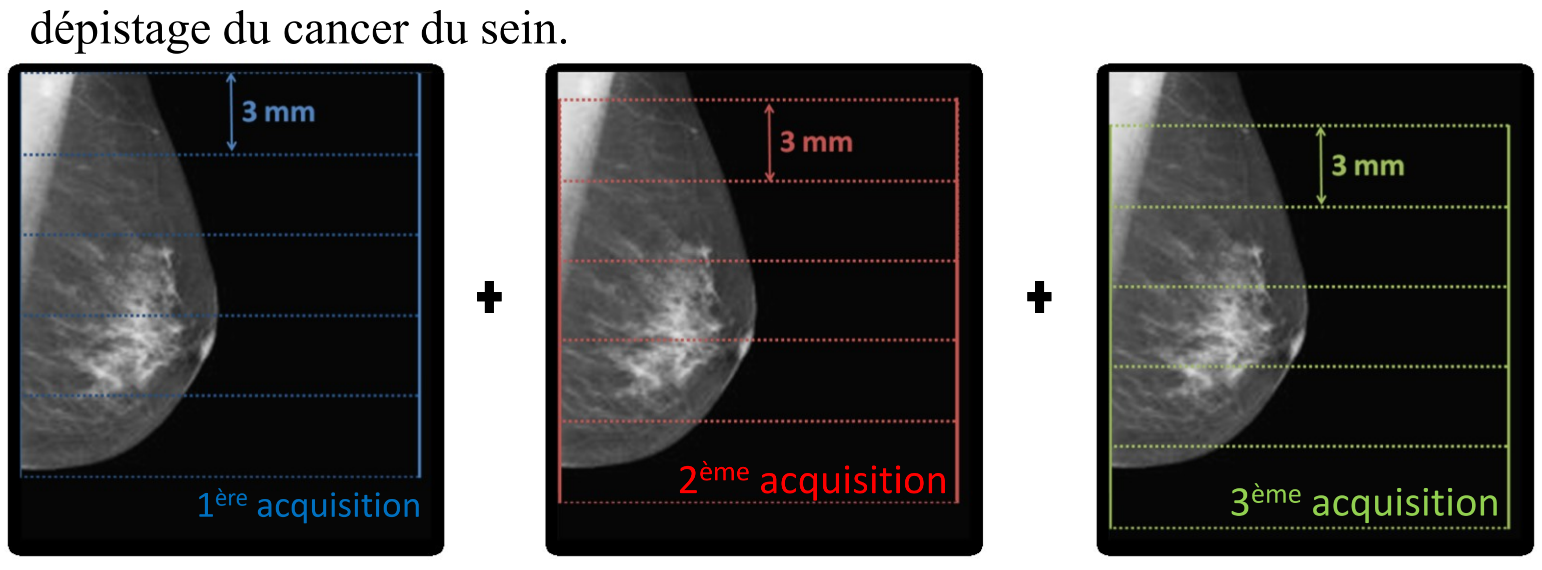

Faible résolution spatiale 1x1x3 mm³

+ SRR

↓

Grande résolution spatiale 1x1x1 mm³

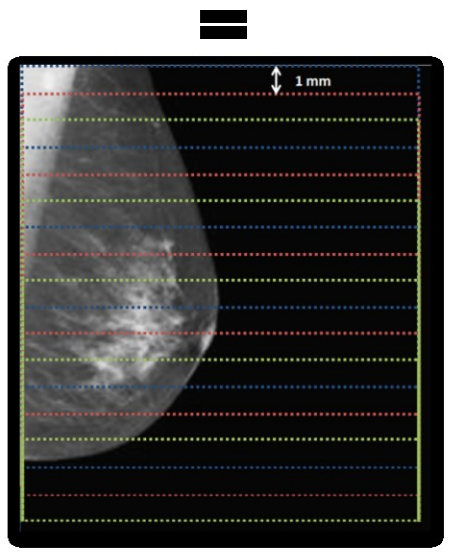

Pour construire un volume isotopique x à partir des images anisotropiques acquises ρ, il suffit de résoudre le problème de moindre carré linéaire suivant: (Odille et al)

$$\min_{x} \sum_{i=1}^{3} ||D_i B_i M_i x - \rho_i||^2 + \lambda C(x)$$

où M_i est l'opérateur linéaire qui décrit les transformations géométriques, $D_i B_i$ est l'opérateur de sélection de la coupe, décomposé d'un opérateur de lissage (*blurring*) et d'un autre facteur de sous échantillonnage D_i .

Dans cette étude, deux régularisations sont testées:

Tikonov est une régularisation qui contraint les intensités de l'image :

$$C(x) = ||x||^2$$

Beltrami est une régularisation qui contraint les gradients de l'image:

$$C(x) = (1 + \beta^2 |\nabla x|^2)^{1/2}.$$

Résultats qualitatifs

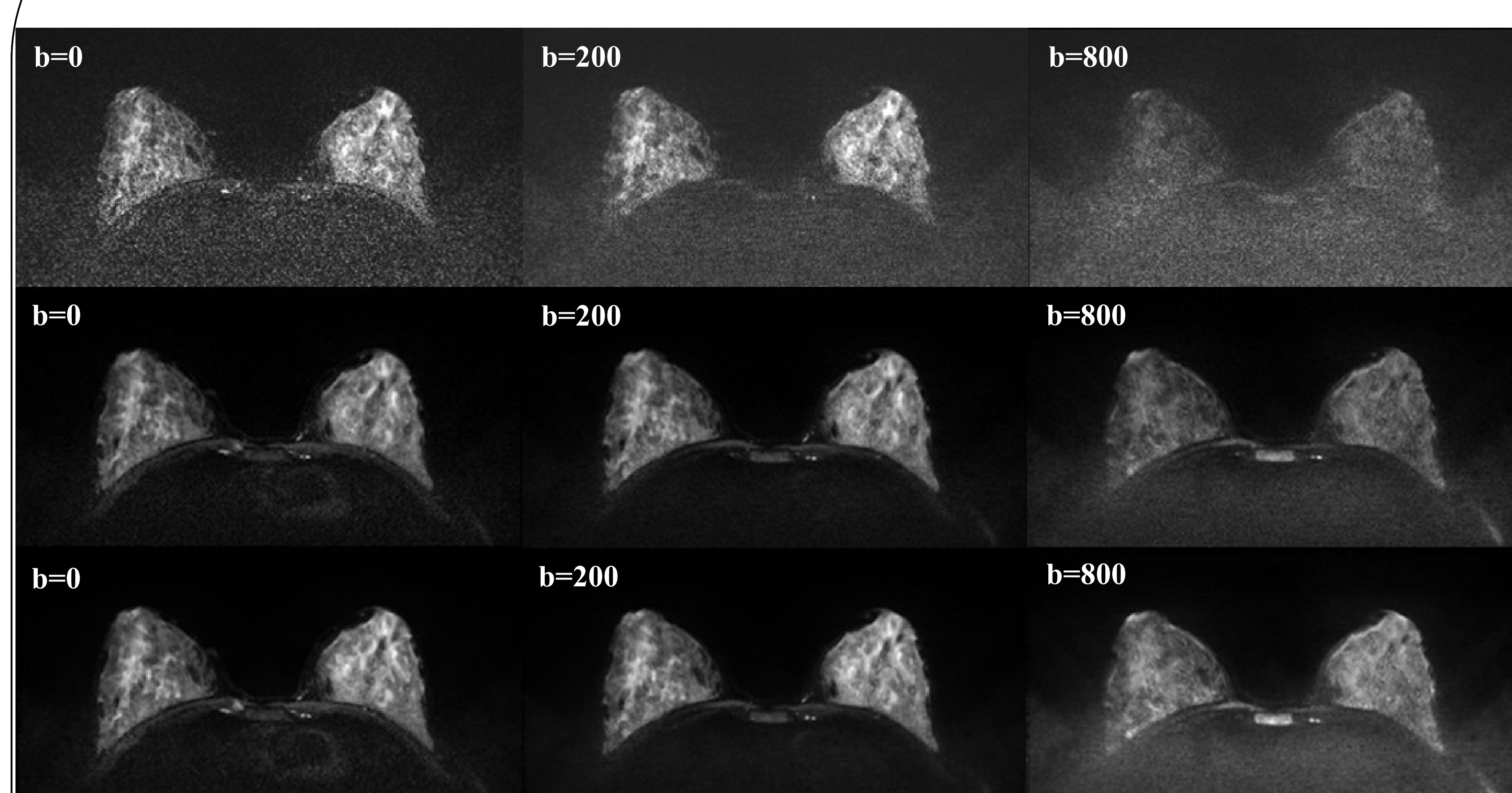

• Les images natives sont situées dans la première ligne, les reconstructions Tikonov dans la deuxième et les reconstructions Beltrami dans la troisième.
• Les natives sont des images de diffusions directement acquises avec une grande résolution 1x1x1 mm³ sur la machine d'IRM.

Résultats quantitatifs: *Sharpness Index (SI)*

	SRR			P		
	Native	Tikhonov	Beltrami	Tikhonov versus Native	Beltrami versus Native	Tikhonov versus Beltrami
b=0 (s/mm²)	430.6 (±48)	655.4 (±83)	914.0 (±146)	< 0.001	< 0.001	< 0.001
b=200 (s/mm²)	509.1 (±120)	617.9 (±112)	822.1 (±127)	0.0505	0.0011	< 0.001
b=800 (s/mm²)	230.5 (±20)	328.8 (±103)	465.6 (±130)	0.0441	0.0051	< 0.001

• Algorithme *SI* (Blanchet et Moisan) permet d'évaluer la qualité des images 2D sans référence. Le score de *SI* diminue avec le flou, le bruit, et les repliements.
• On montre que la méthode Beltrami est meilleure que la reconstruction Tikhonov sur 8 sujets sains et sur l'ensemble du volume.

ANNEXE:

SRR: super resolution-reconstruction, **SNR**: signal-to-noise ratio, **P**: paired t-test
b: Le degré de pondération en diffusion de la séquence, **SI** : Sharpness index

PERSPECTIVES:

- Validation de la SRR par des simulations Monte-Carlo pour comparer la sensibilité des images natives et les images reconstruites aux bruits.
- Validation de la SRR sur des patientes avec une lecture d'un expert radiologue.
- Publication de la méthode validée sur sujets sains est en cours de rédaction.

REFERENCES:

[1] Fondation de la Recherche Médicale : http://www.frm.org/cancer-du-sein/chiffres.html
[2] « Tips and techniques in breast MRI » I.Thomassin-Naggara.
[3] « Motion-Corrected, Super-Resolution Reconstruction for High-Resolution 3D Cardiac Cine MRI». ODILE et al. MICCAI 2015, MRM 2017.

Risk Analysis of Information-Leakage through Interest Packets in NDN

Daishi Kondo†,†† Thomas Silverston††† Hideki Tode†††† Tohru Asami††††† Olivier Perrin†,††

† University of Lorraine, LORIA (CNRS UMR 7503) †† Inria Nancy – Grand Est ††† NICT †††† Osaka Prefecture University ††††† ATR

1. Threat of Information-Leakage

- Many companies suffer from information-leakage through Targeted Attacks [1]
  - E.g., Retail chain "Target" spent more than $100 million to upgrade systems
- In Targeted Attacks,
  - Attacker infects PCs within target network with malware via email, etc.
  - Attacker probes the network and steals data such as customer information
- Countermeasure
  - Train employees not to access suspicious media
  Almost impossible to eliminate human error!!

[1] Understanding Targeted Attacks: The Impact of Targeted Attacks, http://www.trendmicro.com/vinfo/us/security/news/cyber-attacks/the-impact-of-targeted-attacks

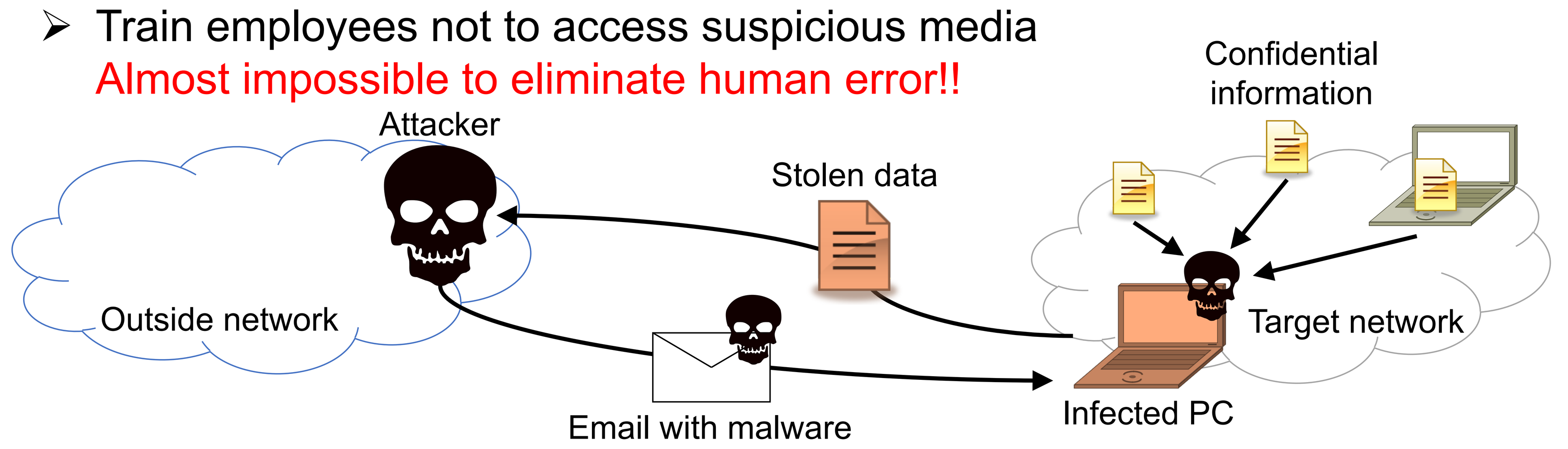

Important to investigate how to prevent information-leakage after infection

Main motivation of this work is to perform risk analysis of information-leakage in NDN for company network

2. Information-Leakage in NDN

- NDN is basically "Pull"-based architecture and there are two kinds of packets; *Interest* and *Data*
  - *Interest* includes content name, etc
  - *Data* includes content name, data, etc
- How about information-leakage through Data?
  - Users can reply with Data only if he/she has received the Interest packet for the content name
  - Information-leakage through Data packets can be prevented with properly configured firewall [2]
- How about information-leakage through Interest?
  - If PC is compromised by attacker's malware, the malware can use the PC to encode confidential information into names of Interest packets (i.e., *steganography embedded*)
  - The malware sends *steganography embedded* Interest packets out of the network toward the attacker

[2] D. Kondo, et al, "Name Anomaly Detection for ICN," in *IEEE LANMAN* 2016.

3. Information-Leakage through Interest packets

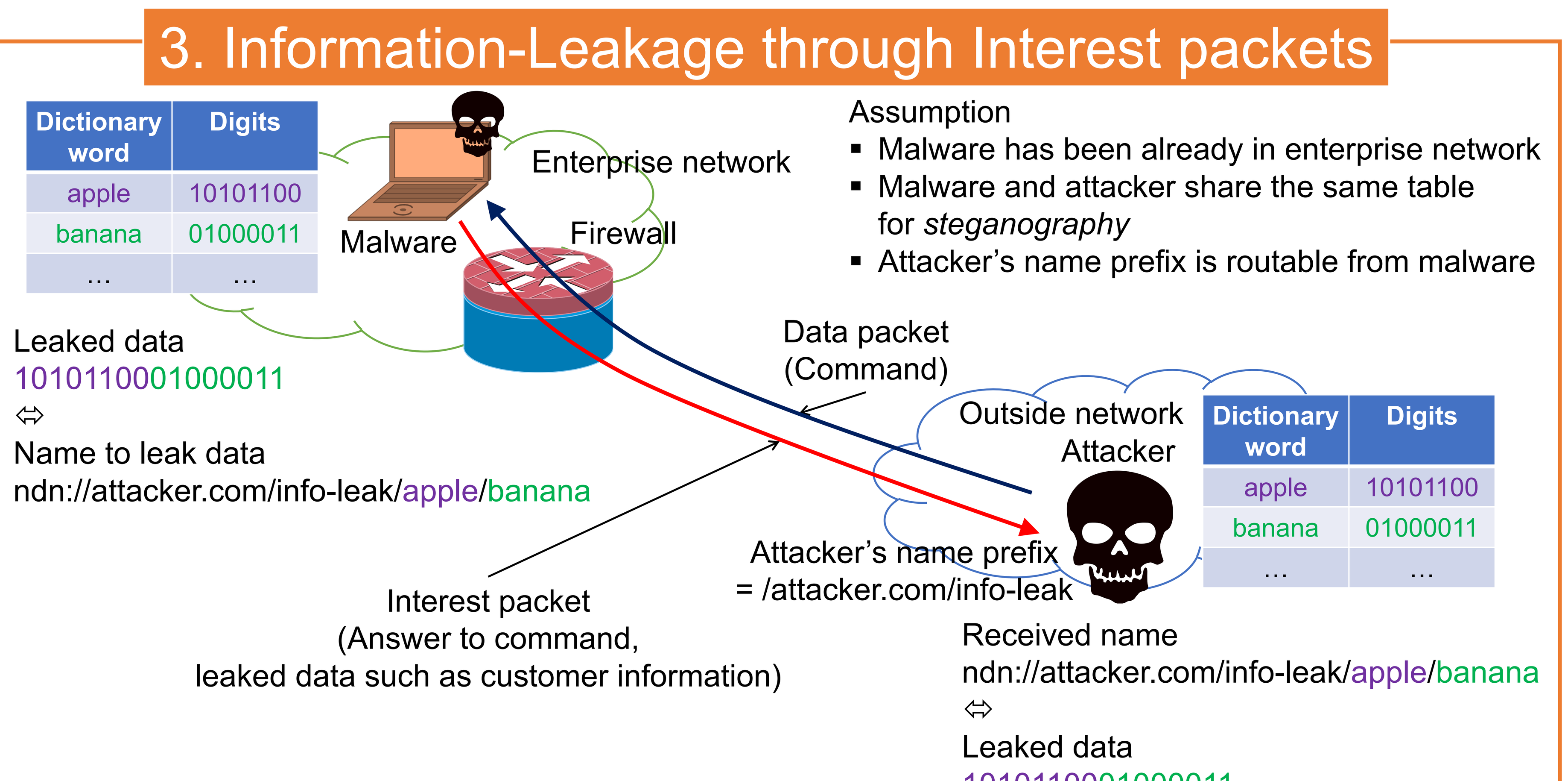

Assumption

- Malware has been already in enterprise network
- Malware and attacker share the same table for *steganography*
- Attacker's name prefix is routable from malware

Possible for *steganography embedded* Interest packet to perform information-leakage

4. Objective and Proposal

Objective

Performing risk analysis of information-leakage through content names in NDN Interest packets

Proposal

1. Name-based filter using search engine information

- Interest names are considered legitimate if highly ranked
- Search engine information should be useful against the attack but it covers only 4% of all contents (Surface Web)

2. Name-based filter using one-class SVM

- Interest names are judged legitimate or anomalous based on legitimate name attributes

➡ **Filters can choke drastically throughput of information-leakage**

5. NDN Name Dataset Extracted from URL

- Regarding NDN architecture, there are currently not anomalous traffic nor names available
  - Extracting URL properties as characteristics of legitimate names from dataset we made
- Legitimate URLs from Common Crawl [3]
  - Extracting 1M URLs for each TLD; "com", "net", "org", "info", "jp", "fr", and "uk"
- URL attributes and computed percentiles

[3] Common Crawl, http://commoncrawl.org/

Attributes	Percentiles 90%	95%	99%
Path Length (L_P)	81	98	147
Query Length (L_Q)	108	171	236
Directory Length (L_D)	19	34	72
File Name Length (L_{FN})	47	72	106
Number of "/" in Path ($N_/$)	4	5	7
Number of "=" in Query ($N_=$)	4	6	13
Number of "&" in Query ($N_\&$)	3	5	13

- Cosine similarity of averaged frequencies of alphabets in path and query compared to typical English text [4]

TLD	com	net	org	info	jp	fr	uk
Path	0.970	0.957	0.960	0.968	0.976	0.975	0.975
Query	0.930	0.889	0.936	0.928	0.922	0.944	0.947

[4] Frequency analysis, https://en.wikipedia.org/wiki/Frequency_analysis

  - High similarity with typical English text => Using WordNet [5] for *steganography embedded* Interest packet

[5] G. A. Miller, "WordNet: A Lexical Database for English," *Commun. ACM*, vol. 38, no. 11, pp. 39–41, Nov. 1995.

6. Protector Using One-Class SVM Filter

[5] B. Schölkopf, et al., "Estimating the Support of a High-Dimensional Distribution," *Neural Comput.*, vol. 13, no. 7, pp. 1443–1471, Jul. 2001.

- One-class SVM [5] is unsupervised model to perform anomaly detection
  - It can be used in the case that there are not enough anomalous samples
- Parameter setting for name-based filter using one-class SVM
  - Feature vector: 125 features (7 URL attributes ($L_P, L_Q, L_D, L_{FN}, N_/, N_=, N_\&$), frequencies of 26 alphabets in path and query, frequencies of 33 other printable characters in path and query)
  - Kernel parameter: RBF (Radial Basis Function kernel)
  - Parameter ν (upper bound of training error): 0.01, 0.05, 0.1, 0.2, 0.3, 0.4
  - Parameter γ (kernel coefficient): 1/125 (=1/number of features) (default value in scikit-learn [6])

[6] F. Pedregosa, et al., "Scikit-learn: Machine Learning in Python," *Machine Learning Research*, vol. 12, pp. 2825–2830, 2011.

7. Attacker Using Anomalous Names with $\nu = 0.4$

[7] ITU-T, http://www.itu.int/en/ITU-T/publications/Pages/latest.aspx

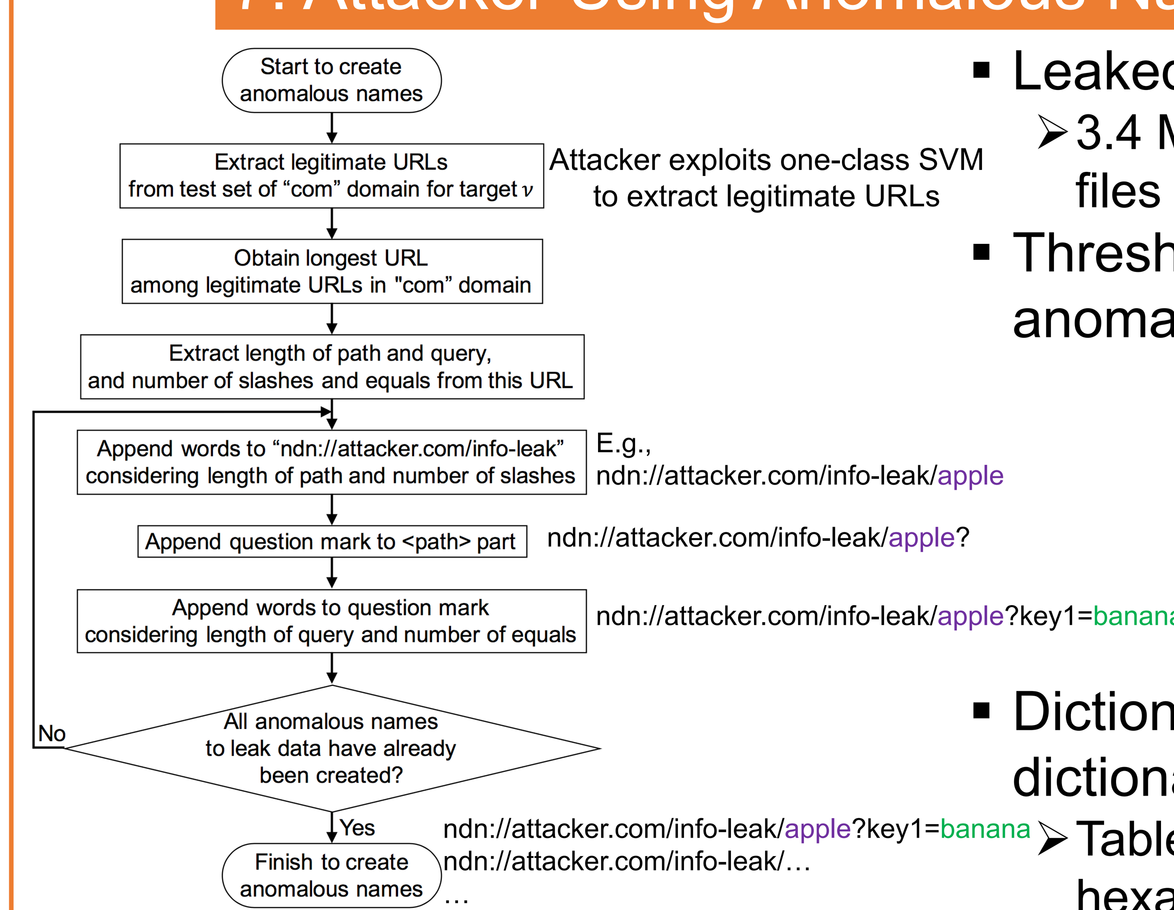

Flow to create anomalous names with dictionary coding (i.e., *steganography*) in "com" domain

- Leaked data
  - 3.4 MB Zip file compressing 3 PDF files from ITU-T recommendations [7]
- Threshold for each attribute in anomalous names with $\nu = 0.4$

	L_P ($\nu = 0.4$)	L_Q	$N_/$	$N_=$
com	15	112	2	4
net	20	76	2	3
org	17	98	2	4
info	16	80	2	1
jp	190	0	4	0
fr	26	178	3	14
uk	12	132	2	7

- Dictionary coding with 65,536 dictionary words from WordNet [5]
  - Table with each dictionary word and 4 hexadecimal digits to each word (one word is equal to 2 Bytes)

8. Per-Packet Throughput of Information-Leakage

- Throughput analysis
  - Without filter
    - ✓ Attacker can fill names with leaked data in hexadecimal digits
    - ✓ Selecting longest URL in dataset (4,127 characters excluding name prefix), throughput reaches 2.06 Kbytes/Interest_packet
      (Name example) ndn://attacker.com/info-leak/0ab7c9…
      4,127 characters ≒ 2.06 KB
  - With filter
    - ✓ Attacker has to encode 2 Bytes of leaked data into each word used in name template
    - ✓ When ν for name-based filter is set to less than 0.2, averaged throughput except "fr" can be choked off up to 7.79 Bytes/Interest_packet
      (Name example) ndn://attacker.com/info-leak/word1?key1=word2&key2=word3
      3 words = 6 Bytes

By using filter, malware has to send 264 times (2.06 KB/ 7.79B) more Interest packets to the attacker than without using filter

9. Future Work and Publications

- Future work
  - Propose per-flow filters against possible counter-attacks for per-packet filters
- Publications
  - D. Kondo, et al., "Name Anomaly Detection for ICN," in *IEEE LANMAN* 2016.
  - D. Kondo, et al., "Risk Analysis of Information-Leakage through Interest Packets in NDN," in *IEEE INFOCOM Workshop* 2017 (NOM)

Optimization models and methods for Network Functions Virtualization (NFV) architectures

Meihui Gao[1], Bernardetta Addis[1], Ye-qiong Song[1]
[1]*LORIA, University of Lorraine, Nancy, France*

I. Background

- **Network ossification issue**: Due to the exponential growth of service demands, deployment of large diverse proprietary network appliances increases both the capital and operational expense of service providers.
- **NFV approach**: NFV reduces appliances deployed in the networks by implementing network functions as software on commodity hardware.
- **Key problem in NFV**: virtual network functions (VNFs) chaining problem.

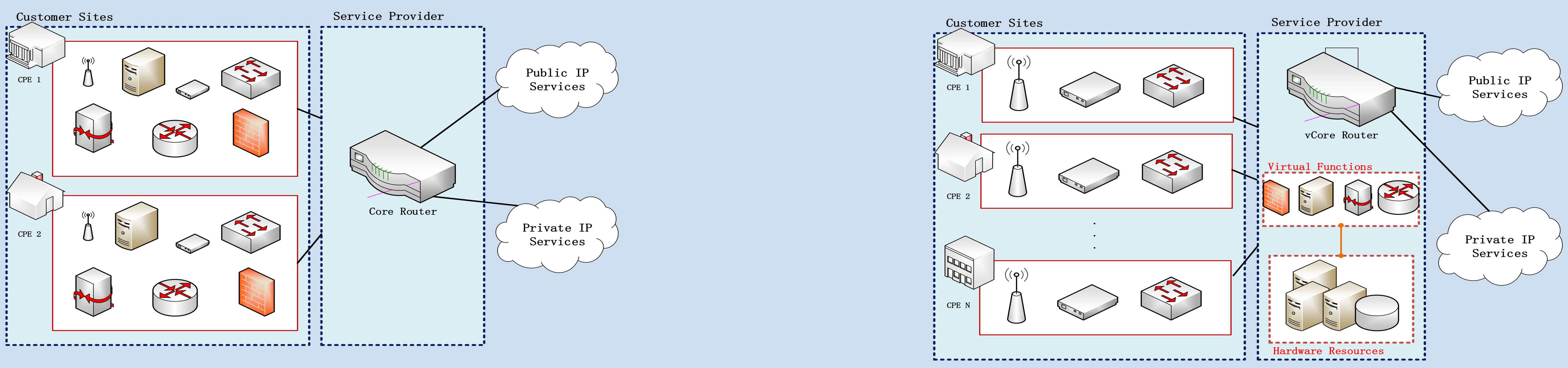

Figure 1. Left side: traditional CPE with ossification issues. Right side: possible CPE with NFV solution.

II. VNFs chaining problem and research objectives

Cost-efficient VNFs chaining: to reduce the capital and operational expense

- Place required VNFs on potential locations: **capacity, VNF affinity / anti-affinity, etc.**
- Route demands from source to destination: **latency, VNFs order, etc.**

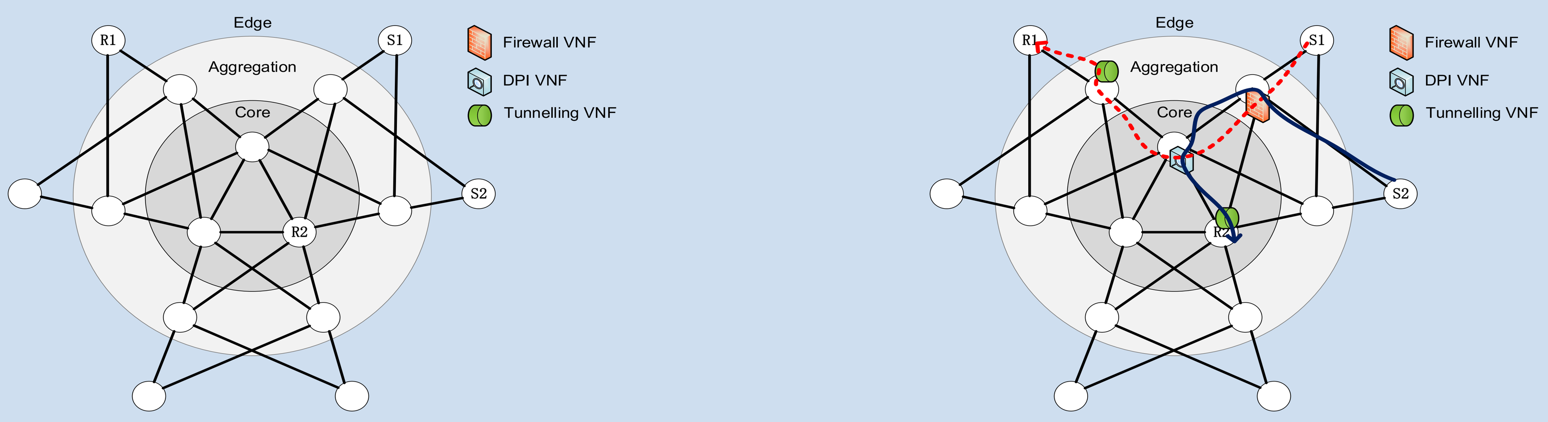

Figure 2. VNF chains deployment

Motivation: the VNFs chaining problem is out the scope of the optimization literature

- No computational complexity analysis nor detailed properties of the VNFs chaining problem has been investigated so far.
- No rigorous comparison of different formulation strategies has been proposed.
- Due to the fact that the VNFs chaining problem is not polynomially solvable, developing efficient exact optimization methods and heuristic methods represents big challenges.

III. Complexity analysis

1. Related optimization problems

- VNFs placement: Facility Location problems
- Demands routing: Network Design problems
- Placement and Routing ⇒ **New challenge**

2. Computational complexity: VNFs chaining problem is $\mathcal{NP}$-hard even with one single VNF type

- Considering only link capacity limit: problem $\mathcal{NP}$**-complete** (by reduction from the Unsplittable Multi-commodity Flow problem).
- Considering only VNF capacity limit: problem $\mathcal{NP}$**-complete** (by reduction from the Bin Packing problem).
- Considering general graphs without any capacity limits: problem $\mathcal{NP}$**-complete** (by reduction from the Set Covering problem).
- Considering the uncapacitated basic version of the VNFs chaining problem on full-mesh graphs, ring graphs or tree graphs: problem polynomially solvable.

IV. Optimization Models

Two popular Integer Linear Programming (ILP) Formulation strategies:

- Virtual Network Embedding (VNE) based model (as shown in Figure 3. (1))
- Virtual Network Function Placement and Routing (VNF-PR) model (as shown in Figure 3. (2))

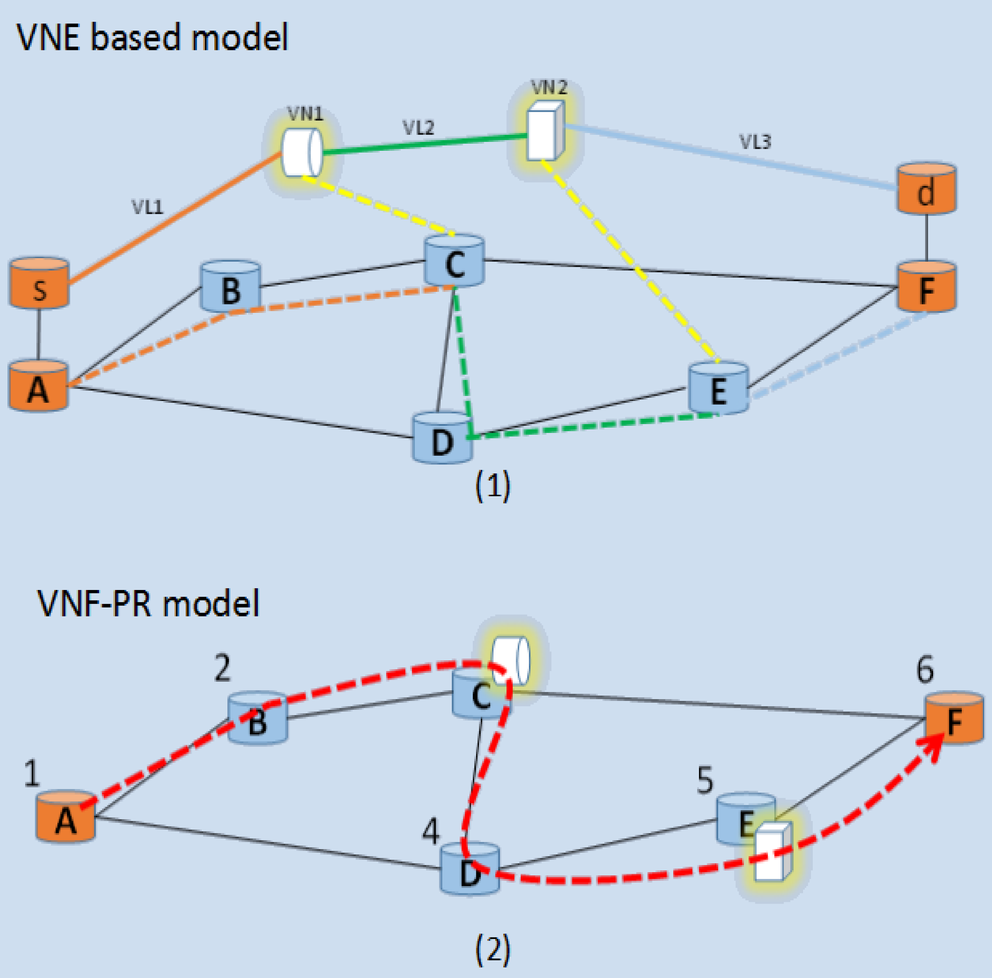

Figure 3. Formulation strategies

V. Evaluation of formulations

Computational results of a basic version of the VNFs chaining problem: tested on 16 network instances of SNDlib (the number of potential location nodes varies from 10 to 28, and the number of traffic demands varies from 22 to 702)

Figure 4. VNE based model vs. VNF-PR model

In the horizontal axis, h (high), m (medium) and l (low) represent different levels of capacity of VNF and link, e.g., h_m is the case of high VNF capacity and medium link capacity.

VI. Conclusion and future work

- ✓ The complexity of VNFs chaining problem is $\mathcal{NP}$-hard in general.
- ✓ The problem formulation has a fundamental impact on the computational performance.
- Efficient optimization methods are needed (e.g., to find closer feasible solutions to the optimality, to save computational runtime):
  - ✓ **Valid inequalities**: strengthen the formulations.
  - – **Column generation**: to cope with the large version of VNFs chaining problems, and for dealing with the case where the order is not fixed.

Augmented Dickey Fuller and Engle Granger Tests to Estimate Parameters Relationship of Photovoltaic Energy Output.

Mouhamadou Moustapha Ba, Harry Ramenah Camel Tanougast, Philippe Casin
University of Lorraine, 7 rue Marconi 57000 Metz, France.
{mouhamadou-moustapha.ba, harry.ramenah, camel,tanougast, philippe.casin} @univ-lorraine.fr

1. Introduction

This paper describes the statistical study and prediction of energy output of a photovoltaic system as a function of global solar radiation upon one year measurement for a particular site. We first expected a linear relationship explaining the variable power output as a function of variables such as solar radiation and temperature. For such study we first determine whether or not there is a stationarity character of each series, that is radiation series and temperature series because it conditions the statistical methods to be used. We applied the Augmented Dickey Fuller (ADF) and Engle Granger (EG) to propose a model of power output and thus energy output based on outdoor real conditions measurements (see Figure 3).

2. Augmented Dickey Fuller Test

Augmented Dickey Fuller (ADF) which is a unit root test for stationarity. The ADF test can handle more complex models than the Dickey-Fuller test, and is also more powerful as more explanatory variables are introduced such as variables lags. For example if X_{t-1} is the variable, the variables lags are $\Delta X_{t-2}, \ldots, \Delta X_{t-p}$. The Augmented Dickey Fuller adds lagged differences to following:

$$X_t = \rho X_{t-1} + \sum_{j=1}^{p} \Psi_j \Delta X_{t-j} + u_t \ or\ \Delta X_t = \pi X_{t-1} + \sum_{j=1}^{p} \Psi_j \Delta X_{t-j} + u_t$$

However when ADF test suffer from correlation between residuals a more rigorous method such as EG model is applied so that residuals in the regression appear serially uncorrelated.

3. Augmented Dickey Fuller Irradiance Test Equation

Eye examination of solar radiation series to determine the appropriate model.

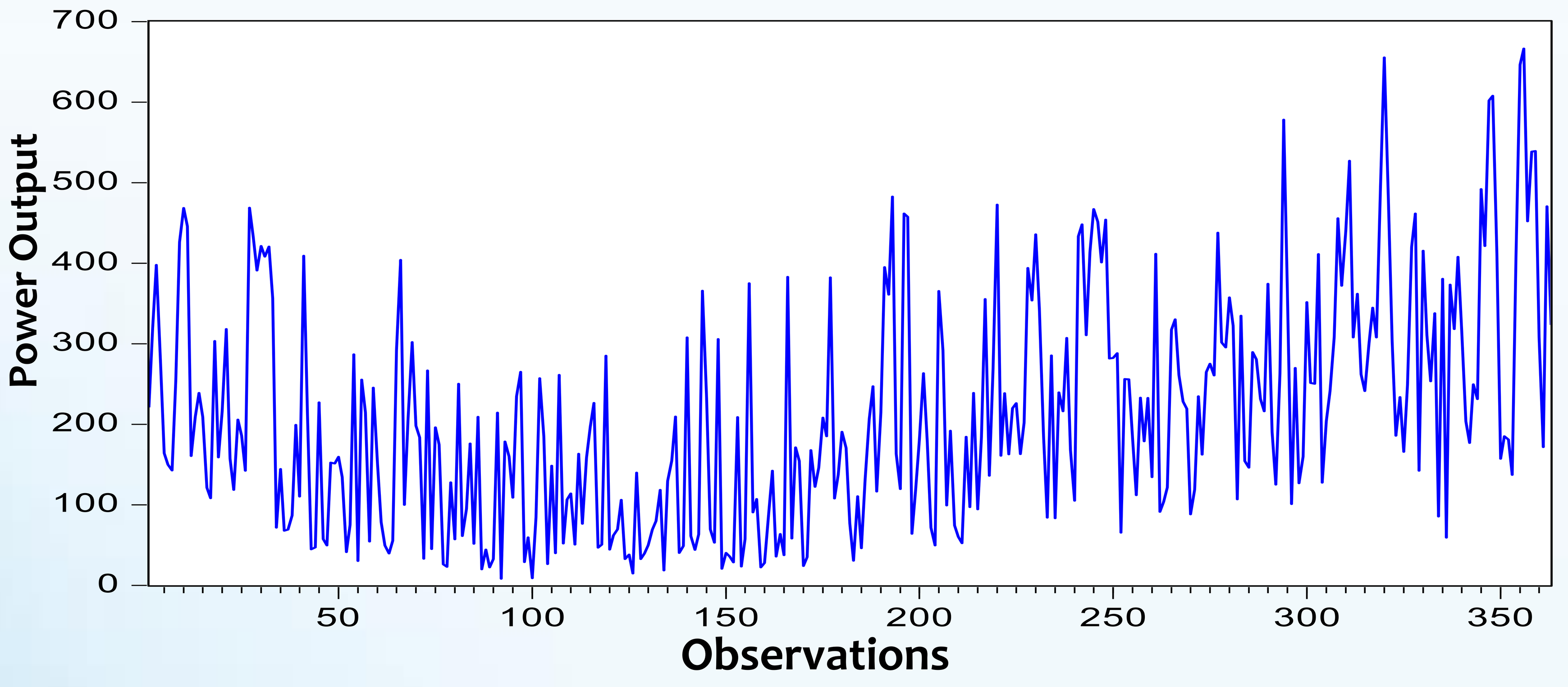

Figure 1: Irradiance evolution for one year observation.

4. Difference Regression Equation

$$\Delta P = 0.969 \Delta E + 0.5 \Delta T - 0.01$$

Dependent Variable: DELTA P				
Method: Least Squares				
Sample (adjusted 363)				
Included observations 362 after adjustments				
Variable	Coefficient	Std.Error	t-Statistic	Prob.
DELTA E	0.969868	0.027980	34.66231	0.0000
DELTA T	0.500517	0.603774	0.828980	0.4077
C	-0.010523	1.778432	-0.005917	0.9953

Table 1: Regression difference data.

Figure 2 represents the residual graph delta P with outliers, where the blue curve is the residuals from the regression, provided by a residual table (not shown here). The green and red curves are the real and fitted curves.

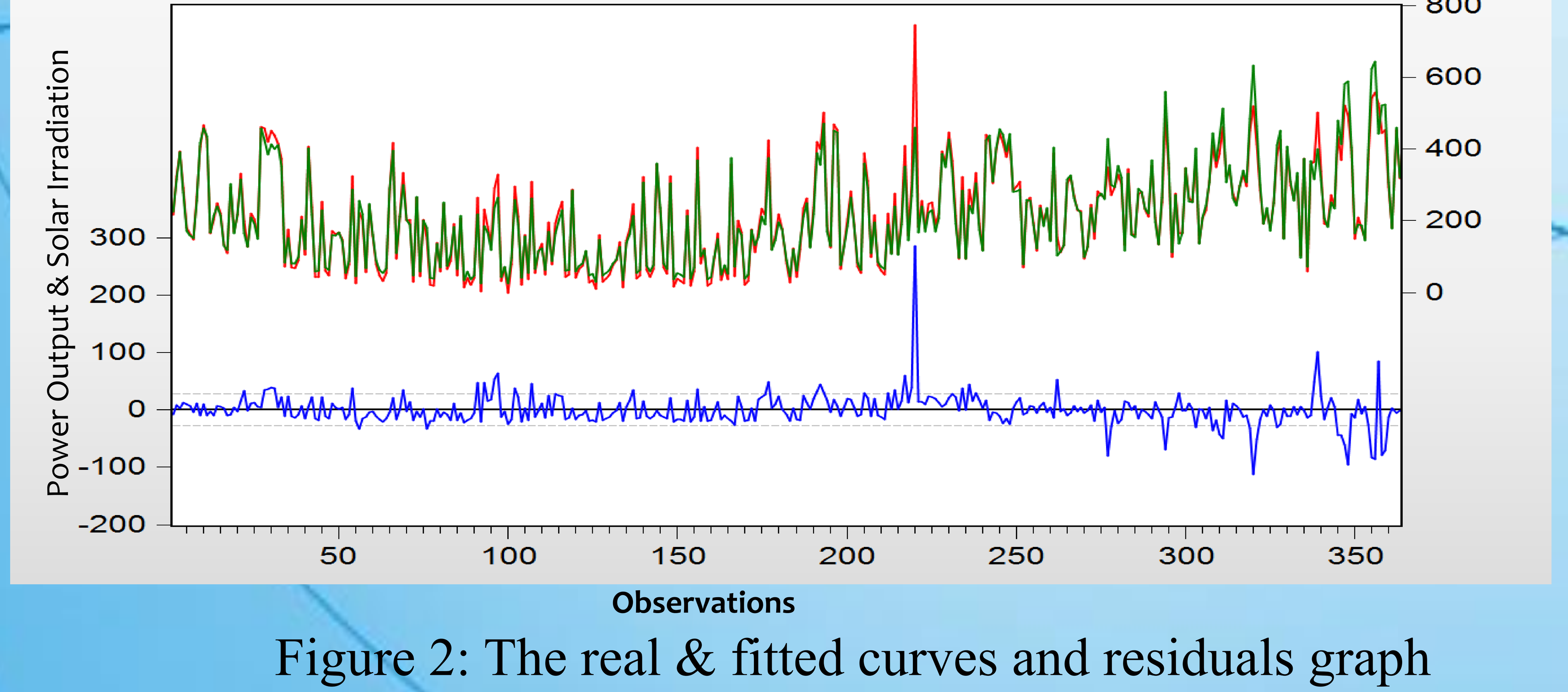

Figure 2: The real & fitted curves and residuals graph

Figure 3: Photovoltaic (PV) Polycrystalline modules.

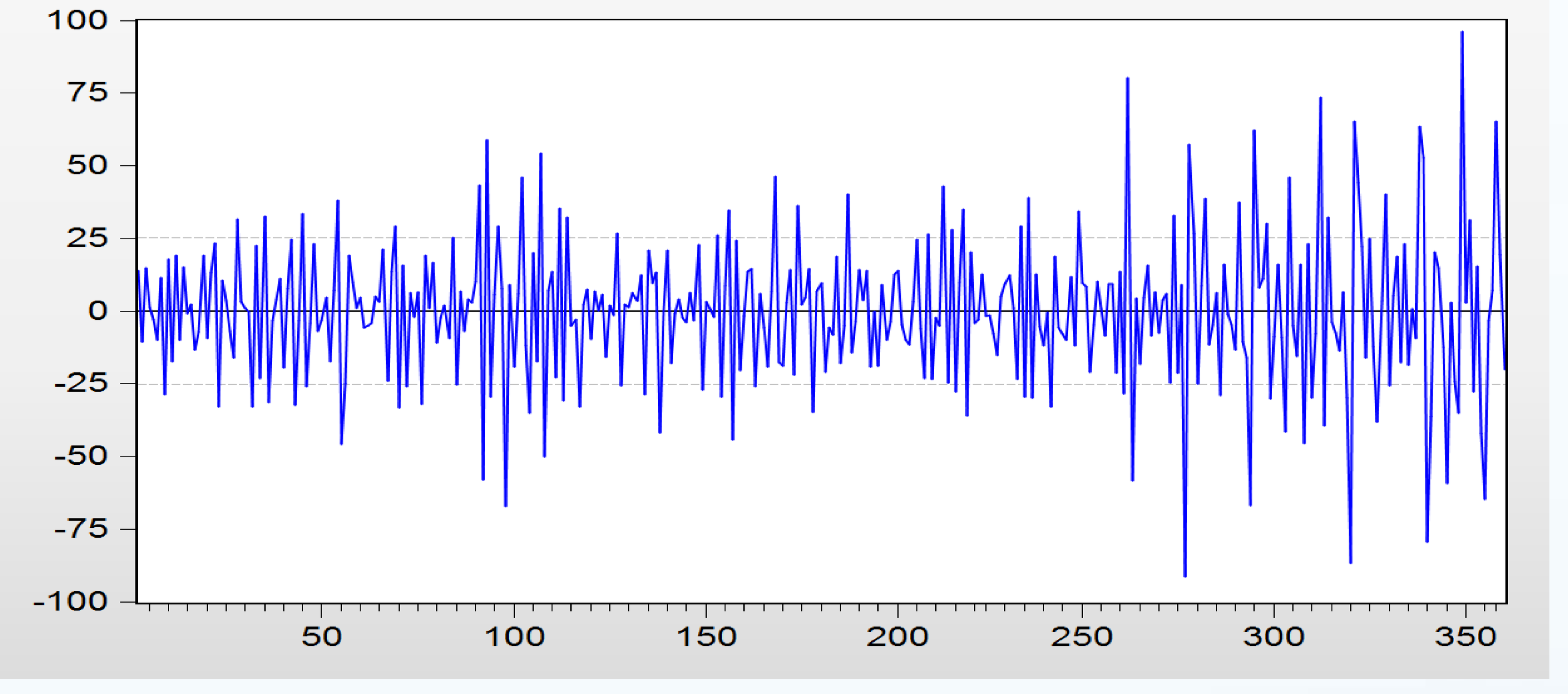

Figure 4: The residual graph of ΔP.

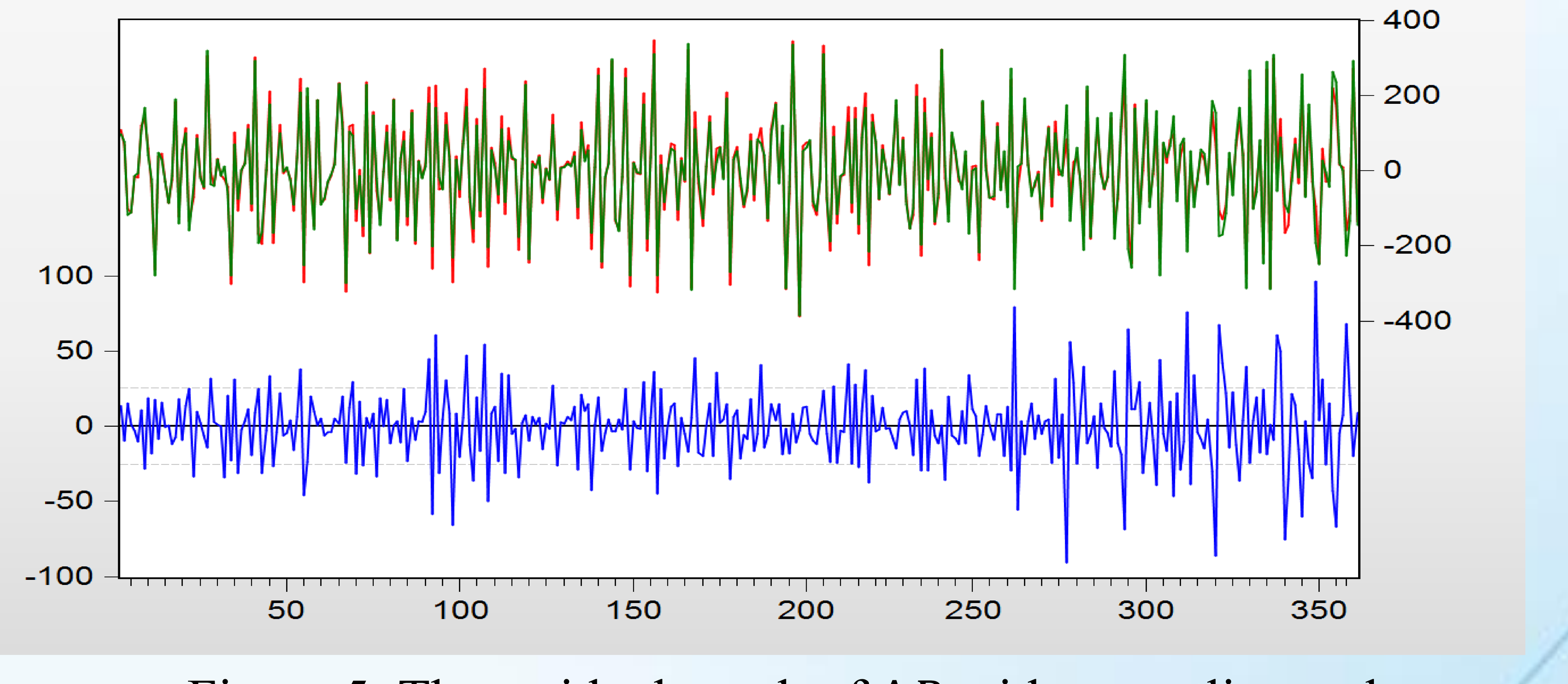

Figure 5: The residual graph of ΔP with no outliers values.

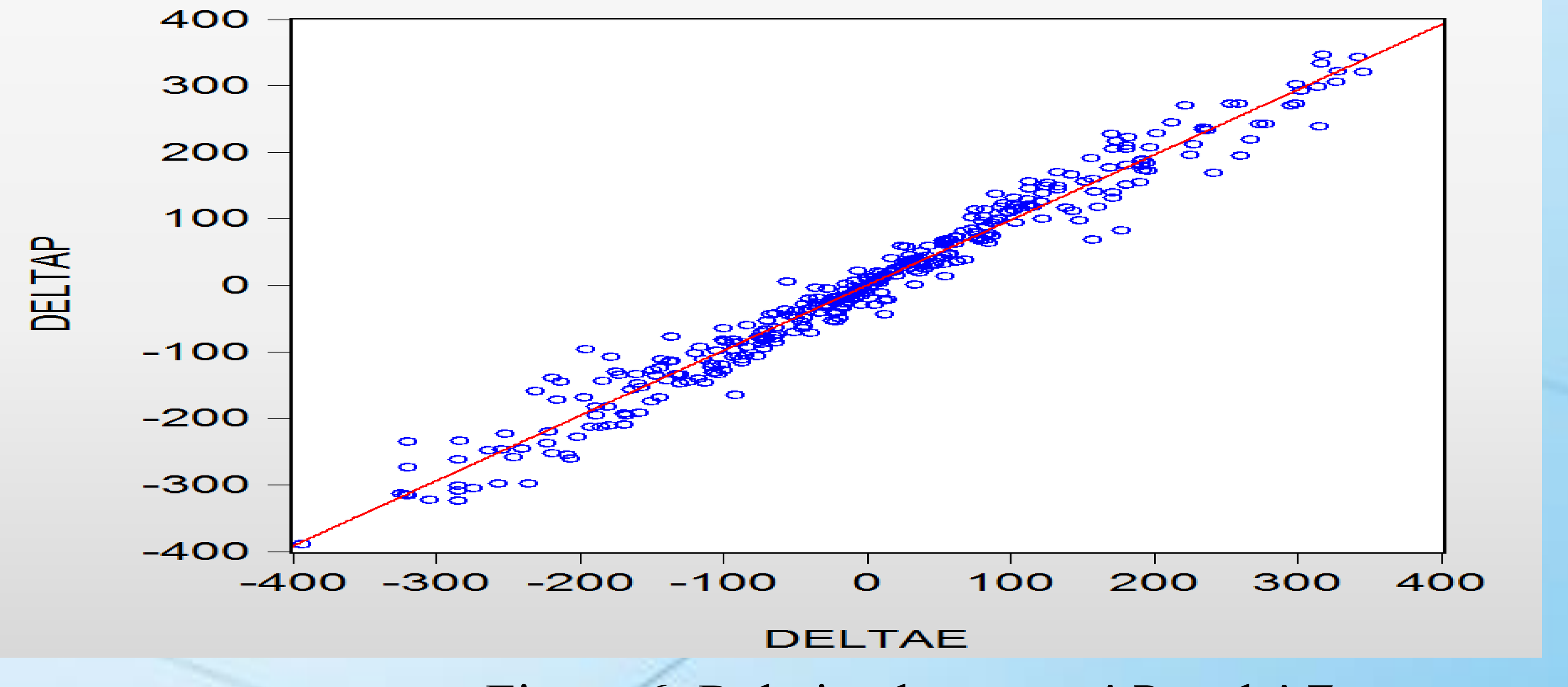

Figure 6: Relation between ΔP and ΔE .

The EG test for cointegration is a two step residual based test, is given as follow:

$$\Delta P = 0.99\ \Delta E$$

5. Conclusions

The regression relationship between first difference of Photvoltaic parameters is validated without outliers and heteroscedasticity.

Construction and analysis of exact algorithms: Enumeration and Counting

Mohamed Yosri Sayadi

Laboratoire d'Informatique Theorique et Appliquee (LITA)
yosri.sayadi@univ-lorraine.fr
Directors of thesis: Prof. Dieter Kratsch and Mathieu Liedloff

Abstract

We are interested in **exponential time algorithms** because many problems most likely cannot be solved by polynomial time algorithms. The most famous **hard problems** is the family of **NP-complete** problems and the exponential running time seems be unavoidable.

Enumeration

An **enumeration problem** asks to list all **feasible solutions**. While optimization is ubiquitous in algorithms, in some applications finding one or even all optimal solutions is not always satisfactory. Optimization might simply not be the goal. To give an example, experts of the domain of origin of the problem to solve it in an algorithmic way, for example biologists, may prefer to have a large set of feasible solutions that under their hard-to-formalize-objectives is used to find the " good solution(s)" in a non-algorithmic way. Another motivation for the study of enumeration algorithms is the fact that for many problems, even well-studied ones, we cannot exclude that the essentially best algorithm is one solving a corresponding enumeration problem.

Our Contributions

Graph	Lower bound	Upper bound
Chordal	1.4961^n	2^n
Split	1.4766^n	1.6042^n
Cobipartite	$3^{n/3}$	$n^2.3^{n/3} + n^2$
Interval	$3^{n/3}$	1.8613^n
Block	$3^{n/3}$	$3^{n/3}$

Table 1: Enumeration of Minimal Tropical Connected Sets [5]

Input-sensitive

The classical algorithmic approach to enumeration (sometimes called output-sensitive) has been studied since more than 50 years with an ever growing interest in the last years. The holy grail of **output-sensitive** algorithms are those of polynomial (or even linear) **delay**. Recently classical worst-case running time analysis has been applied successfully to enumeration. Those algorithms typically have exponential running times due to the fact that, contrary to optimization, the output-size is exponential in the input-size. Often these (**input-sensitive**) enumeration algorithms are **branching** ones and a sophisticated time analysis like **Measure & Conquer** is needed. The running time of an enumeration algorithm implies in a trivial way a combinatorial upper bound on the output-size, i.e. the (maximum) number of objects to be enumerated in an input of size n, called an **upper bound**. The ultimate aim of input-sensitive enumeration are algorithms of best possible (worst case) running times, i.e. there are inputs that indeed show optimality of the established running time. This motivates the search for lower bounds as a measure for optimality which are typically achieved via the explicit construction of families of inputs having a certain number of objects which is called a **lower bound**. Thus one aims at so-called matching upper and lower bounds.

Our Contributions

Graph	Lower bound	Upper bound
Claw-Free	1.5848^n [4]	$O(1.9341^n)$ [4]
Chordal	1.5292^n [2]	1.7549^n [2]
Interval	1.5292^n [2]	1.6957^n [2]
Forest	1.5292^n [2]	1.6181^n [2]
Path	$\Theta(1.4696\ldots^n)$ [1]	$\Theta(1.4696\ldots^n)$ [1]

Table 2: Enumeration of Maximal Irredundant Sets

Studied problems

- **Maximal irredundant sets:**
  A set of vertices D of a graph is **irredundant** if each vertex $u \in D$ has a **private vertex** v in the closed neighborhood of u that is not dominated by any other vertex of D except u. An irredundant set D is **(inclusion) maximal** if D is irredundant but any proper superset of D has not this property.
- **Minimal dominating sets:**
  A set D is **dominating set** of G if $V(G) = N_G[D]$. A dominating set D is **(inclusion) minimal** if D is a dominating set but any proper subset of D has no this property. It is folklore that every minimal dominating set is an (inclusion) maximal irredundant set.
- **Minimal connected dominating sets:**
  A set D is connected dominating set of G if D is a dominating set and $G[D]$ is **connected** graph. A connected dominating set is minimal if no proper subset of it is a connected dominating set.
- **Minimal Tropical Connected Sets:**
  A set X is a minimal **tropical** connected set if every **colour** of the graph appears at least once in the set X, the graph induced by X , denoted by $G[X]$, is connected, and no proper subset of X being tropical connected.

Our Contributions

Graph	Lower bound	Upper bound
Chordal	1.4422^n	1.5048^n [3]

Table 3: Enumeration of minimal dominating sets

Graph	Lower bound	Upper bound
Outerplanar	$2^{\frac{n}{3}}$	$O^*(3^{\frac{n}{3}})$

Table 4: Enumeration of minimal connected dominating sets

Publications

[1] Petr A. Golovach, Dieter Kratsch, Mathieu Liedloff, Michaël Rao, and Mohamed Yosri Sayadi.
On maximal irredundant sets and (σ, ϱ)-dominating sets in paths.
WEPA 2016 : First Workshop on Enumeration Problems and Applications 21-22 Nov 2016 Aubiere (France).

[2] Petr A. Golovach, Dieter Kratsch, Mathieu Liedloff, and Mohamed Yosri Sayadi.
Enumeration and maximum number of maximal irredundant sets for chordal graphs.
In *Graph-Theoretic Concepts in Computer Science - 43nd International Workshop, WG 2017, Eindhoven, The Netherlands, June 21-23, 2017.*

[3] Petr A. Golovach, Dieter Kratsch, Mathieu Liedloff, and Mohamed Yosri Sayadi.
Enumeration and maximum number of minimal dominating sets for chordal graphs.
submitted to Journal of Discrete Algorithms.

[4] Petr A. Golovach, Dieter Kratsch, and Mohamed Yosri Sayadi.
Enumeration of maximal irredundant sets for claw-free graphs.
In *Algorithms and Complexity - 10th International Conference, CIAC 2017, Athens, Greece, May 24-26, 2017, Proceedings*, pages 297–309, 2017.

[5] Dieter Kratsch, Mathieu Liedloff, and Mohamed Yosri Sayadi.
Enumerating minimal tropical connected sets.
In *SOFSEM 2017: Theory and Practice of Computer Science - 43rd International Conference on Current Trends in Theory and Practice of Computer Science, Limerick, Ireland, January 16-20, 2017, Proceedings*, pages 217–228, 2017.

ECOLE DOCTORALE IAEM LORRAINE

Diagnostic de systèmes non linéaires par méthodes à noyau

Prénom Nom : Kwami Anani

Directeur de thèse : Didier Maquin

Co - directrice de thèse : Maya Kallas

Contexte et objectifs

- Le diagnostic d'un système consiste à détecter des défauts, à les localiser et à estimer l'amplitude du défaut détecté.
- **Méthode utilisée**
  — Analyse en Composantes Principales (ACP) à noyau
- **Principales difficultés :** estimation de l'amplitude des défauts détectés, choix des paramètres du noyau choisi, dimension des données, ...

ACP à noyau

Principes de l'ACP à noyau

- ACP : recherche d'axes principaux qui maximisent la variance entre les données
- Projection des données dans un espace fonctionnel et application de l'ACP
- Cette transformation n'est pas explicite puisqu'une fonction noyau permet d'évaluer le produit scalaire : $k(\boldsymbol{x}_i, \boldsymbol{x}_j) = \varphi^\top(\boldsymbol{x}_i)\varphi(\boldsymbol{x}_j)$, $(\boldsymbol{x}_i \in \mathbb{R}^m)$, m : nombre de variables

Espace principal et espace résiduel

- Recherche des valeurs propres et vecteurs propres de la matrice de Gram $\boldsymbol{K}$ (qui a pour éléments $k(\boldsymbol{x}_i, \boldsymbol{x}_j)$), $\boldsymbol{K} \in \mathbb{R}^{N \times N}$, N : nombre d'observations
- Détermination du nombre ℓ de Composantes Principales (CPs) correspondant aux axes principaux
- Espace principal : associé aux ℓ plus grandes valeurs propres
- Espace résiduel : associé aux dernières valeurs propres (détermination d'un seuil de détection δ^2)

Détection de défaut

- Nouvelle observation : $\boldsymbol{x}$, projection de $\boldsymbol{x}$ sur les espaces principal et résiduel
- Erreur quadratique d'estimation $SPE(\boldsymbol{x}) = \|\varphi(\boldsymbol{x}) - \hat{\varphi}(\boldsymbol{x})\|^2 = k(\boldsymbol{x}, \boldsymbol{x}) - \boldsymbol{k}^\top(\boldsymbol{x})\, \boldsymbol{C}\, \boldsymbol{k}(\boldsymbol{x})$
- Cas du noyau Gaussien : $k(\boldsymbol{x}_i, \boldsymbol{x}_j) = \exp\left(-\frac{(\boldsymbol{x}_i - \boldsymbol{x}_j)^\top(\boldsymbol{x}_i - \boldsymbol{x}_j)}{2\sigma^2}\right)$
- $\begin{cases} \boldsymbol{k}(\boldsymbol{x}) = \left[k(\boldsymbol{x}_1, \boldsymbol{x}) \quad \cdots \quad k(\boldsymbol{x}_N, \boldsymbol{x})\right]^\top \\ \boldsymbol{C} = \frac{1}{N-1} \widehat{\boldsymbol{P}}\, \widehat{\boldsymbol{\Lambda}}^{-1}\, \widehat{\boldsymbol{P}}^\top \end{cases}$

$\widehat{\boldsymbol{\Lambda}}$ et $\widehat{\boldsymbol{P}}$ sont respectivement les matrices des ℓ plus grandes valeurs propres de $\boldsymbol{K}$ et leurs vecteurs propres correspondants.

Détection du défaut : si $SPE(\boldsymbol{x}) > \delta^2 \Rightarrow$ un défaut est détecté sur cette observation

Localisation et estimation de l'amplitude du défaut

Objectif : Trouver la direction $\boldsymbol{\xi}_i$ et l'amplitude f_i qui permettent de minimiser le SPE : $\hat{f}_i = \arg\min_{\boldsymbol{\xi}_i, f_i} SPE(\boldsymbol{z}_i)$

- Solution $\hat{f}_i$ donnée par l'algorithme itératif du point fixe
- Variable liée à la direction $\hat{\boldsymbol{\xi}}_i$ est peut-être affectée par un défaut si après reconstruction, pour le couple $(\hat{\boldsymbol{\xi}}_i, \hat{f}_i)$, le $SPE < \delta^2$
- **Problème :** $\hat{f}_i = \arg\min_{\boldsymbol{\xi}_i, f_i} SPE(\boldsymbol{z}_i) \Rightarrow \hat{f}_i = g(\hat{f}_i)$, **Solution :** Il faut faire une initialisation
- Nous avons ainsi développé différentes techniques d'initialisation. Les méthodes et résultats de deux techniques sont présentés ci-dessous.

Technique de l'observation la plus proche

- $t^* = \arg\min_t |(\boldsymbol{x} - \boldsymbol{x}_t)^\top \boldsymbol{\xi}_i|$, t^* est le numéro de l'observation retenue
- $\widehat{f_i^0} = -(\boldsymbol{x} - \boldsymbol{x}_{t^*})^\top \boldsymbol{\xi}_i$ est considéré le point initial pour le début de l'algorithme

Données simulées (objectif : corriger l'observation en défaut)

- Système de données

$$\begin{aligned} \boldsymbol{x}_1 &= \boldsymbol{u}_1 + \boldsymbol{\varepsilon}_1 \\ \boldsymbol{x}_2 &= \boldsymbol{u}_1^2 + \boldsymbol{\varepsilon}_2 \end{aligned}$$

- $\sigma = 0.35$ (noyau Gaussien)
- $\ell = 18$ (correspond à 98% de la somme totale des valeurs propres)

Simulation sur la technique de l'observation la plus proche - observation en défaut reconstruite (solution) est toujours affectée par le défaut

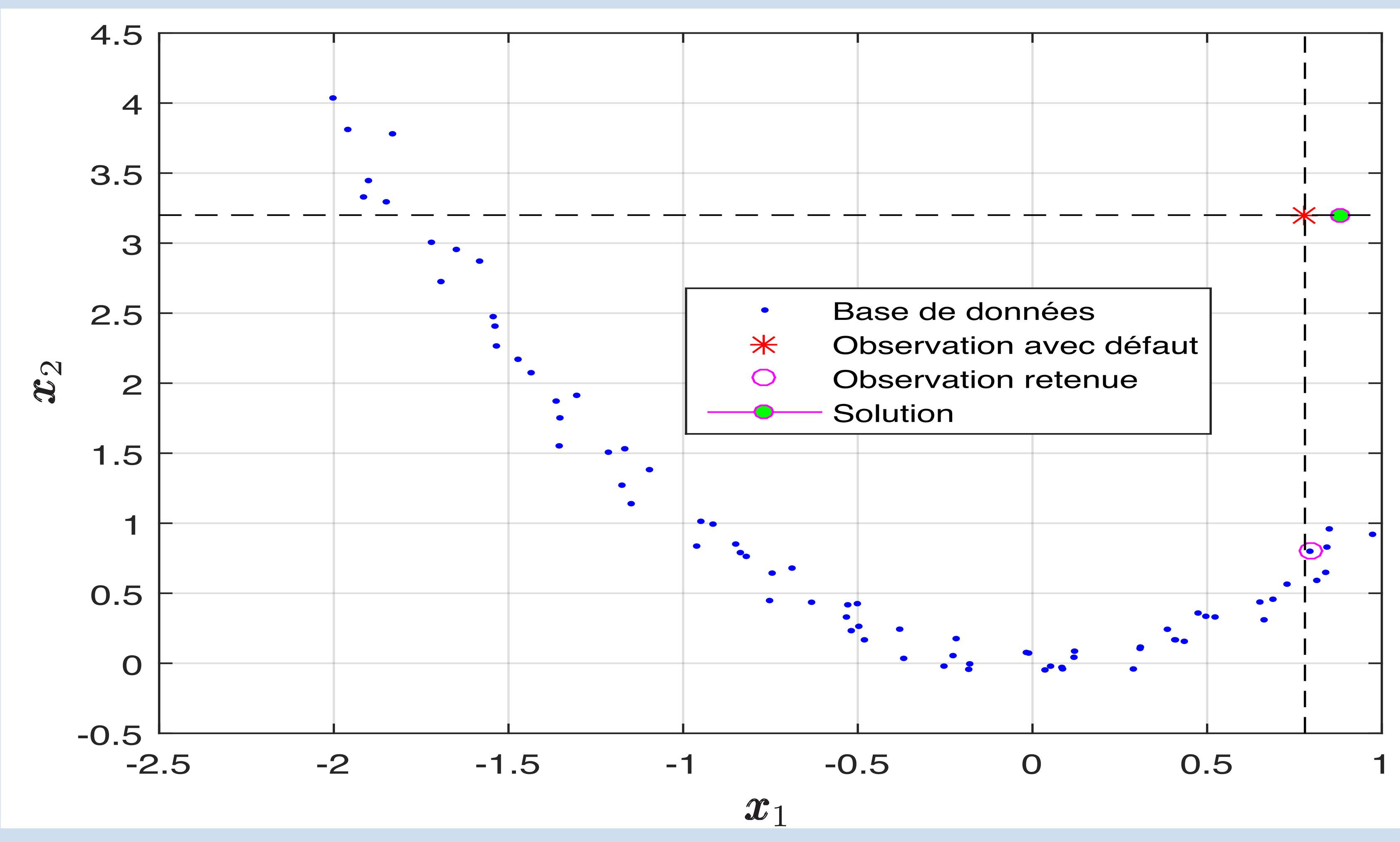

Technique de la limite de détection

- Recherche de l'observation dont le SPE est à la limite du seuil fixé (δ^2) et dans la direction de reconstruction
- Recherche de l'amplitude minimum f_i pour lequel $SPE(\boldsymbol{z}_i) \geq \delta^2$
- Par la minimisation du SPE nous retenons une observation : $\boldsymbol{x}_{t^*}$
- La résolution de : $SPE(\boldsymbol{z}_i) \geq \delta^2$ donne : $\widehat{f_{i1,2}^0} = d_i \pm \sqrt{a}$ avec $d_i = (\boldsymbol{x} - \boldsymbol{x}_{t^*})^\top \boldsymbol{\xi}_i$, $a = c - \sum_{j=1, j \neq i}^{m} ([\boldsymbol{x}]_j - [\boldsymbol{x}_{t^*}]_j)^2$ et c est une constante
- L'amplitude minimum de ces deux solutions est considérée comme le point de départ de l'algorithme

Simulation sur la technique de la limite de détection - Observation en défaut reconstruite (solution) est bien ramenée dans la base de données

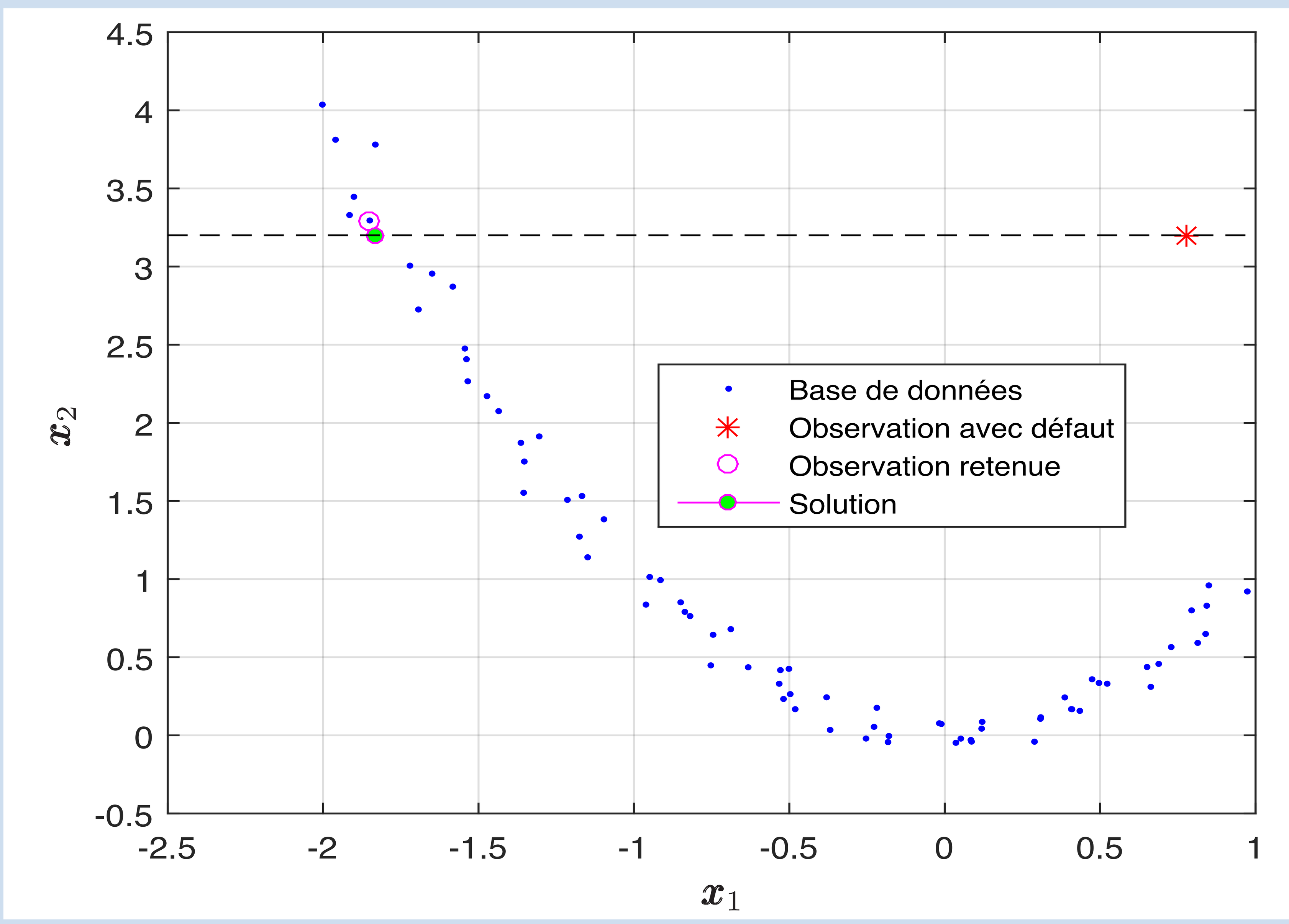

Power Electronics Converter With High Efficiency And High Power Density For Embedded Systems

Davide DELL'ISOLA[1]

Supervisors: Pr. Farid MEIBODY-TABAR[1] and Dr. Matthieu URBAIN[1]

[1]GREEN-ENSEM, University of Lorraine, Nancy, France

Embedded Systems

In the field of electric or hybrid vehicles, **autonomy** and **power density** are of prime importance. The criteria for the design of a switched power converter for embedded applications are focused basically into the need of a lightweight and small sized solution, with a high energy efficiency. The optimization of a power converter involves all the main system sub-parts, namely **the active components, the driver circuit** and **the passive components.**

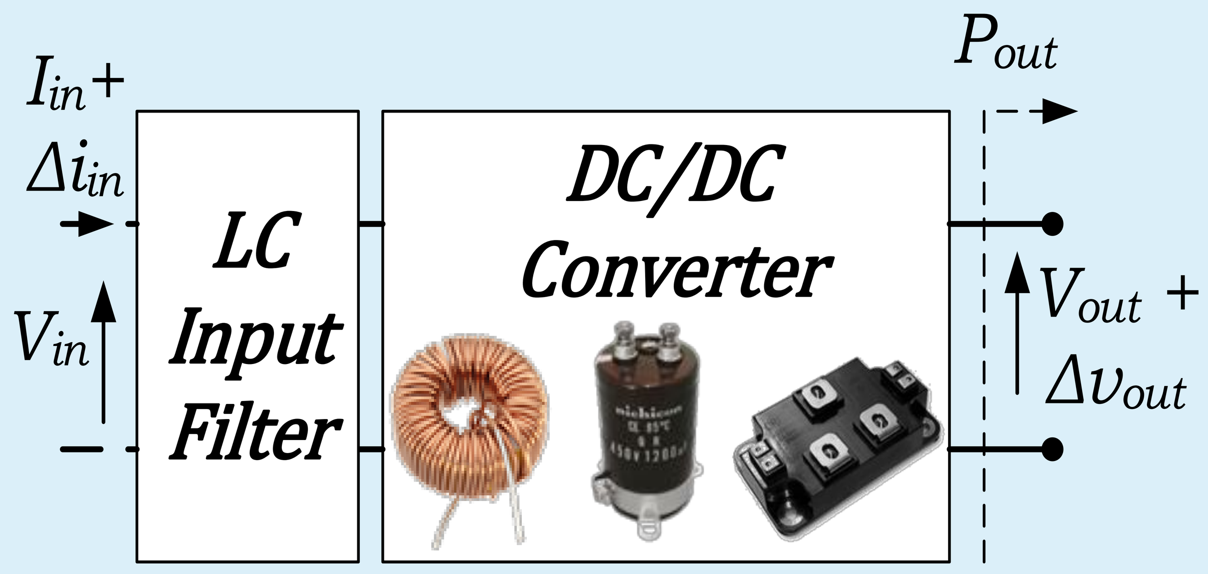

System
- ❑Power devices (SiC MOSFETs)
- ❑Driver circuit
- ❑Passive Components (input and output filter)

Objectives
- ❑Efficiency
- ❑Compactness

Constraints
- ❑Operating point and I/V ripples
- ❑EMI Standards
- ❑Stability

SiC Technology

In recent years, new SiC (silicon carbide) technology offers a clear opportunity for improving compactness and efficiency of the power switching converters. Wide band-gap semiconductor (SiC, H-SiC, 4H-SiC) transistors exhibit several advantages compared to the Si ones:

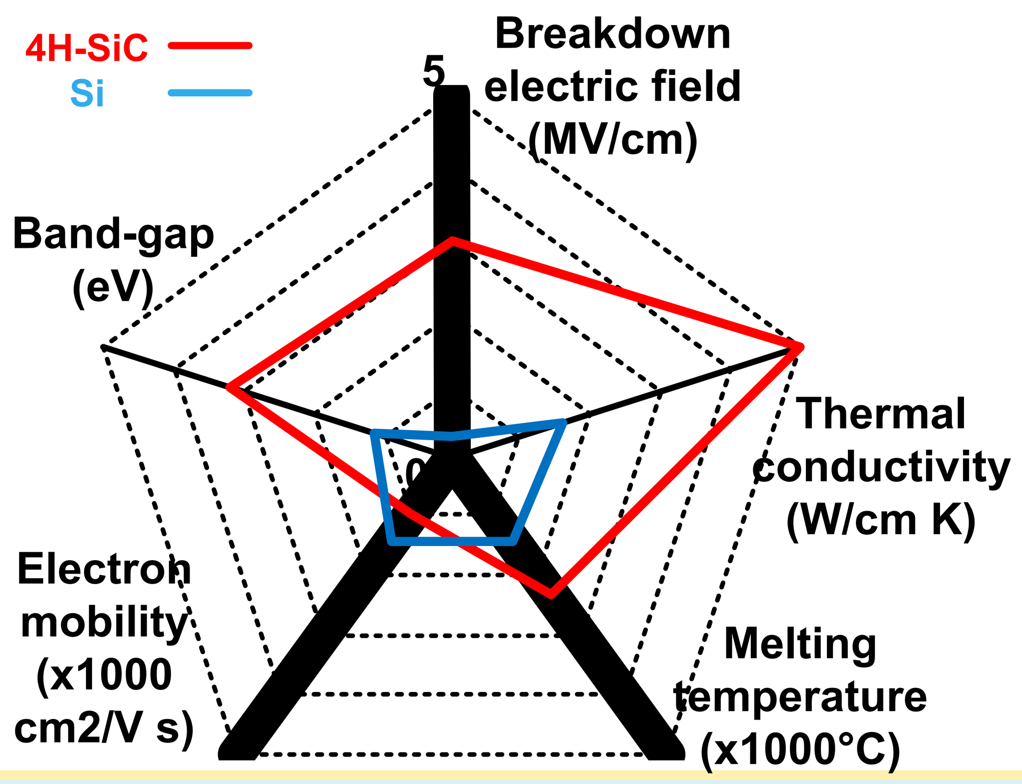

- ❑ Higher operating Temperature
- ❑ Higher Blocking Voltage
- ❑ Lower on-resistivity
- ❑ Higher $\frac{dv}{dt}$, $\frac{di}{dt}$
- ❑ Higher switching frequency

Driver Improvement

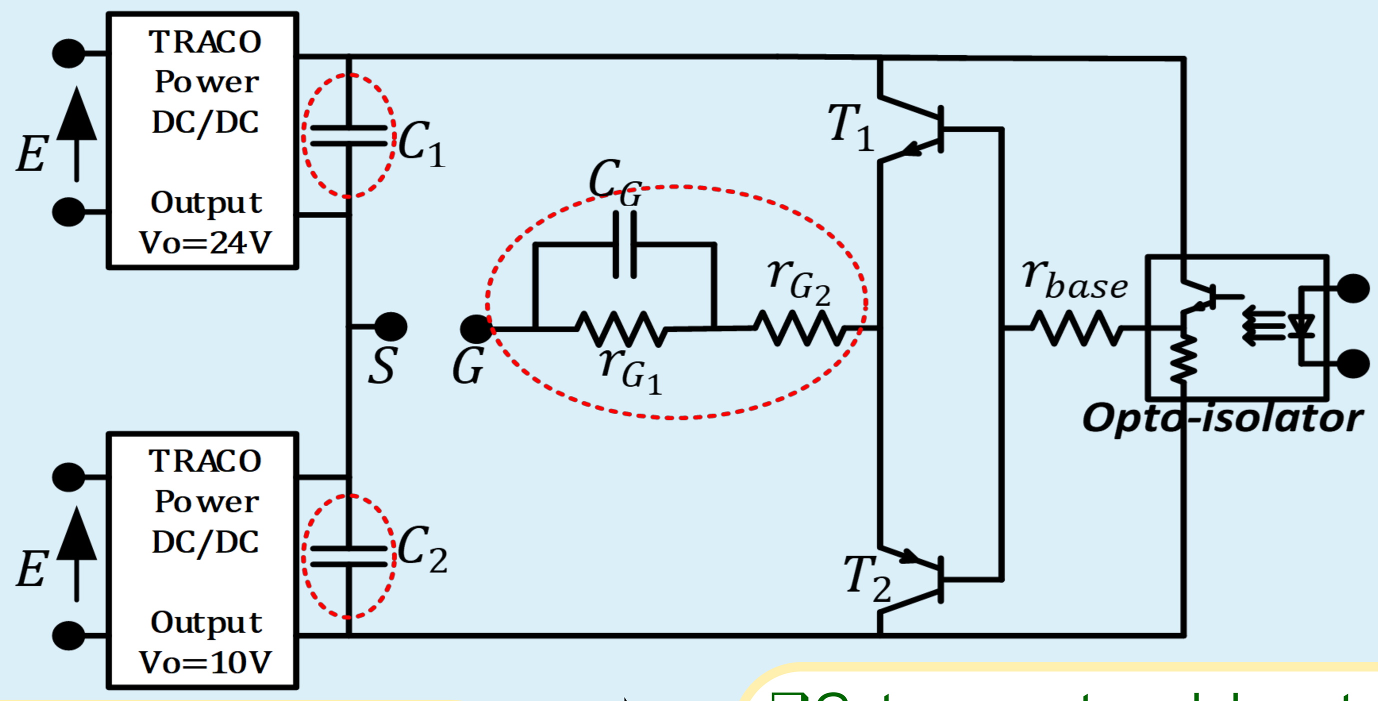

- ➢C_1 and C_2 augmented
- ➢Gate resistance splitted
- ➢C_G bypass capacitor

- ❑Gate current peak boosted
- ❑Less energy losses through the switch
- ❑Less energy provided by the Driver
- ❑Higher i_{DS} overshoot

Parameters Influence on the System: Example

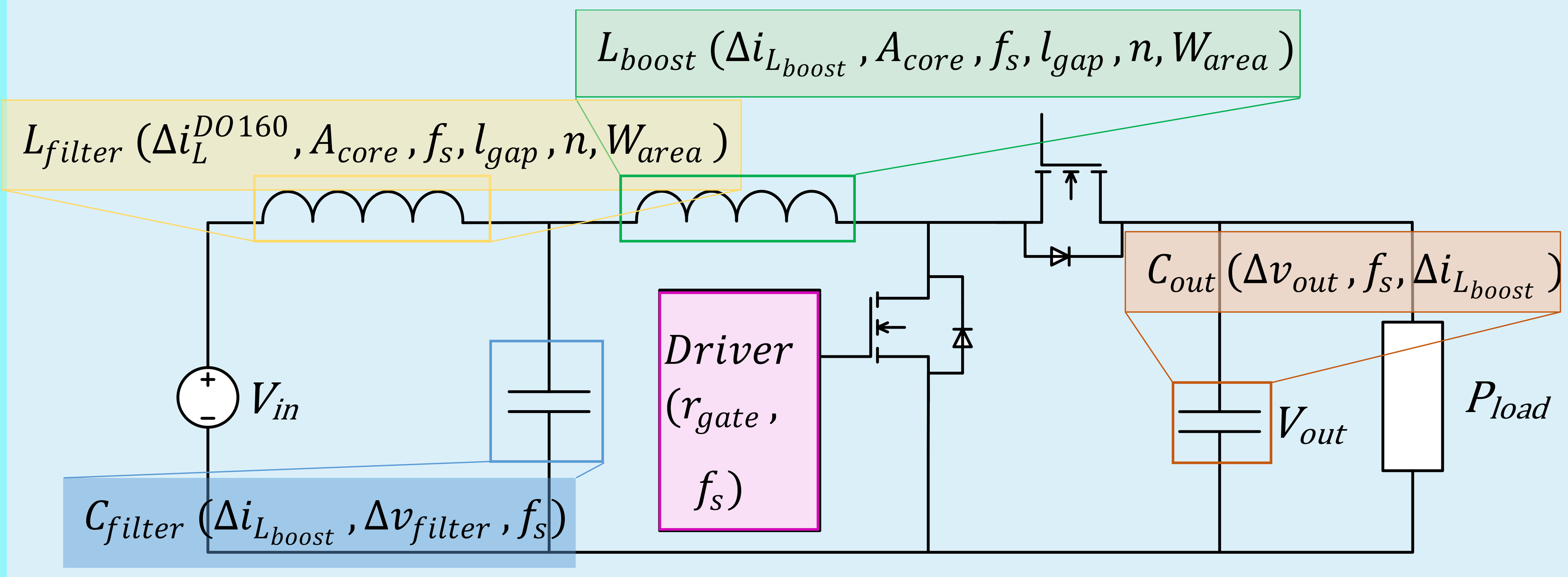

In the power converter design, a great number of parameters needs to be considered. Each parameter influences, directly or not, the converter behavior, the **power losses**, the passive components **size** and the **Electromagnetic interferences**.

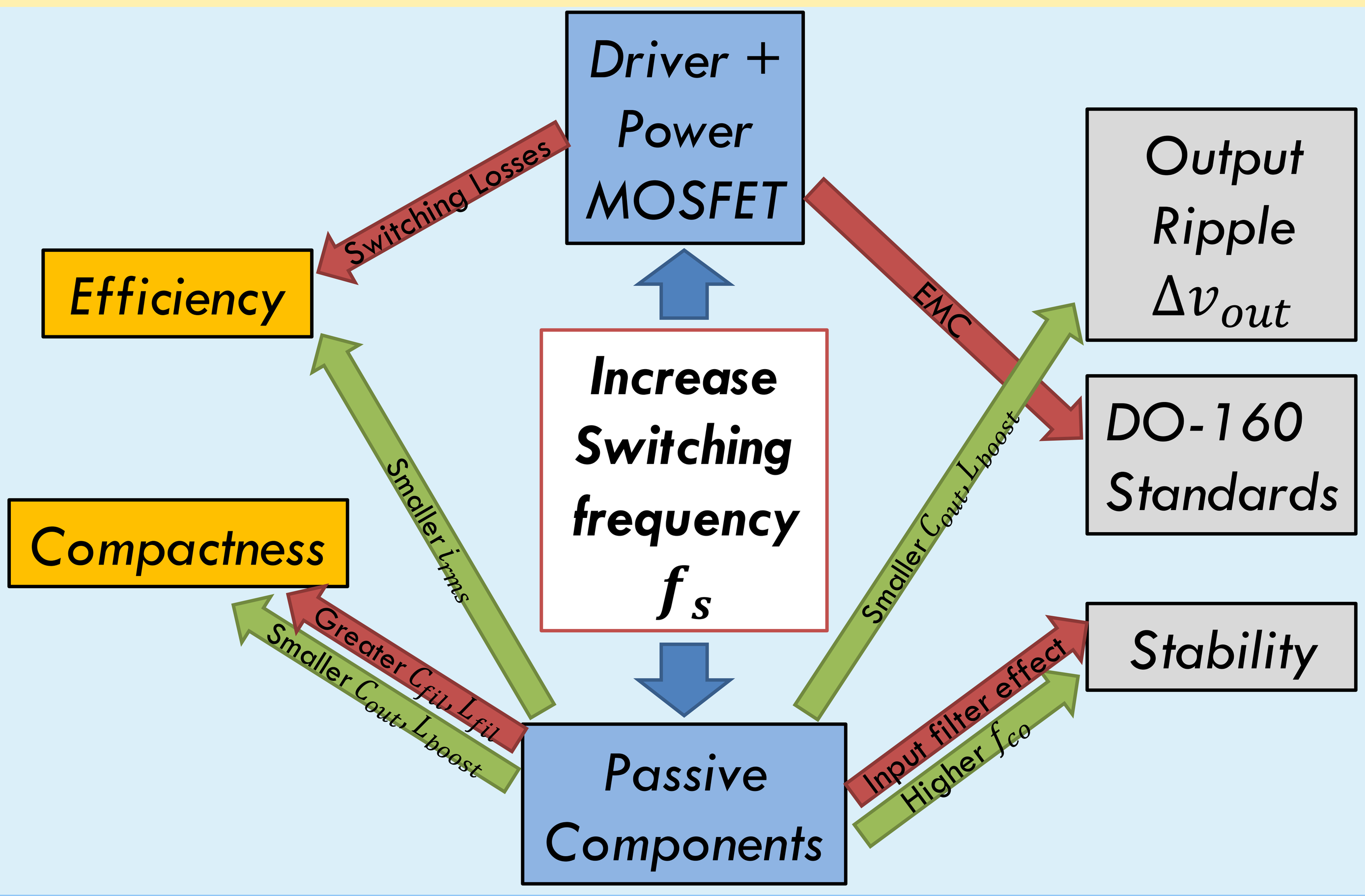

Optimization Problem Description

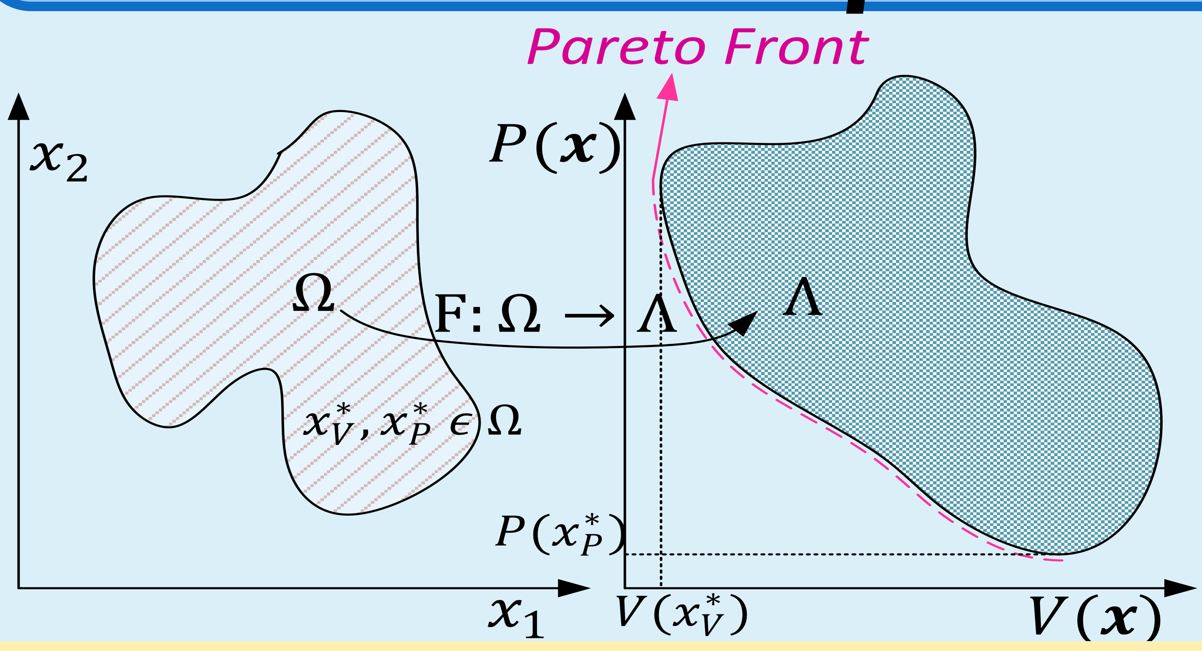

Objective Functions
- $\boldsymbol{F}(\boldsymbol{x}) = [V(\boldsymbol{x}), P(\boldsymbol{x})]$

System Parameters
- $\boldsymbol{x} = [x_1, x_2]$

*It does **NOT** exist a single optimum point $\boldsymbol{x}^*$ which minimizes both the objective functions: $\boldsymbol{x}_V^* \neq \boldsymbol{x}_P^*$*

Preliminary Results

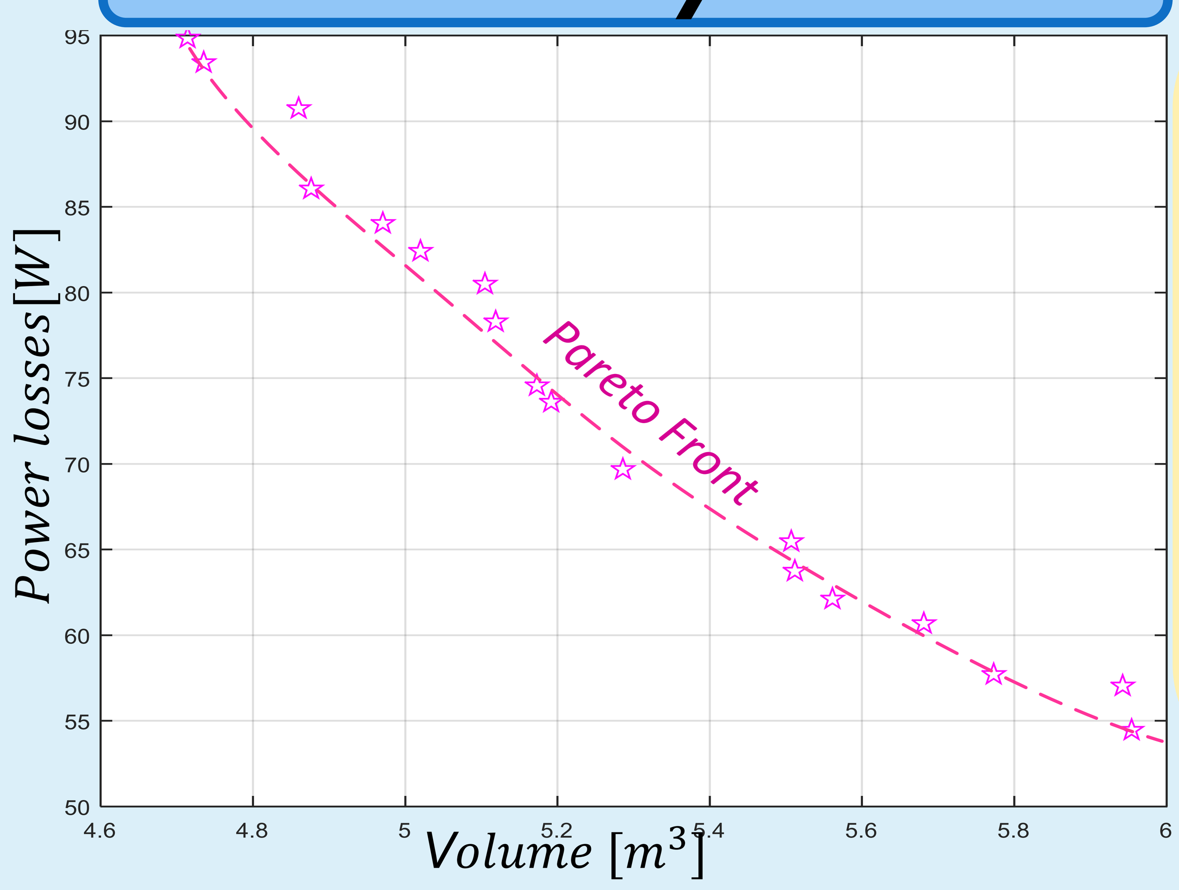

Objective functions
- *Volume*: L_{boost}, C_{out};
- *Power Losses*.

Parameters :

$\boldsymbol{x} = [L\_boost, A_{core}, f_s]$

Contraints:
- *Core Saturation* B_{sat}
- *Output ripple* Δv_{out}

Contacts

Davide DELL'ISOLA
Université de Lorraine, G.R.E.E.N., ENSEM
Email: davide.dell-isola@univ-lorraine.fr

ECOLE DOCTORALE IAEM Lorraine

Backward stochastic differential equations

Habiba KNANI

Lorraine University and Sousse University

habiba.knani@univ-lorraine.fr

1 Introduction

We introduce backward stochastic differential equations (BSDE) in a general way. Contrary to classical differential equations which start with an initial condition, usually at time $t = 0$, the BSDE have to respect a terminal condition at a certain time $T > 0$.

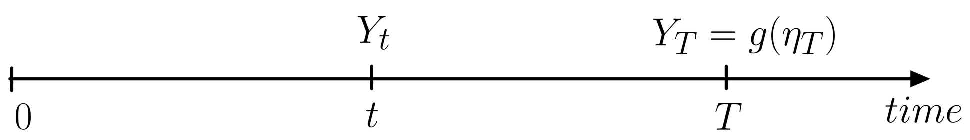

In mathematical terms a BSDE for a pair of processes $((Y_t, Z_t), t \in [0,T])$ is given by

$$Y_t = g(\eta_T) + \int_t^T f(s, \eta_s, Y_s, Z_s)ds + \int_t^T Z_s \delta B_t^h. \quad (1)$$

The meaning of (Y, Z) depends on the framework in which the equation is studied. In finance for example Y_t is the value at time t of the replicating portfolio, Z_t is the composition of the hedging portfolio (the investment strategy) and η_t is the value of the underlying asset at time t. The problem in this case is to determine Y such that Y_T is equal to a contingent claim $g(\eta_T)$ at maturity T. The second integral in (1) models the randomness of the time evolution. We have chosen a multi-fractional Brownian motion $B^h = (B_t^{h(t)}, t \geqslant 0)$ with Hurst function $h : \mathbb{R}_+ \to (\frac{1}{2}, 1)$. Contrary to the classical case of Brownian motion, i.e. the case of $H = \frac{1}{2}$, multi-fractional Brownian motion induces a memory into the time evolution and is able to reproduce certain aspects of the behaviour of the system (i.e. of the financial market in our example).
In mathematical terms B^h is given by

$$B_t^{h(t)} = \int_0^t K_{h(t)}(t,s)dW_s.$$

Here W is a standard brownian motion and $K_{h(t)}(t,s) = s^{1/2-h(t)} \int_s^t (y-s)^{h(t)-3/2} y^{h(t)-1/2} dy.$

Our model for η_t is given by $\eta_t := \eta_0 + \int_0^t \sigma(s)\delta B_s^h + b(t)$ with η_0 being a constant, $b(t)$ and $\sigma(t)$, $0 \le t \le T$, being deterministic functions.
Equation (1) generalizes the classical model of BSDE with $K = \sigma = 1$.
We show that the solution of (1) is directly connected to the following partial differential equation

$$\begin{cases} \partial_t u(t,x) = -\frac{1}{2}\frac{d}{dt}R(\sigma)_t \partial_{xx} u(t,x) - b'(t)\partial_x u(t,x) + f(t,x,u(t,x), -\sigma(t)\partial_x u(t,x)); & (t,x) \in [0,T] \times \mathbb{R} \\ u(T,x) = g(x), \quad x \in \mathbb{R} \end{cases} \quad (2)$$

Here,

$$R(\sigma)_s := Var \int_0^s \sigma(r)\delta B_r^h = \int_0^s (K_s^* \sigma)_r^2 dr \text{ and } (K_s^*\sigma)_r := \int_r^s \sigma(\theta)\frac{\partial}{\partial \theta}K_{h(\theta)}(\theta, s)d\theta. \quad (3)$$

The explicit solution of (1) has been determined in [5] in the case when f is a linear function.
In this paper, we show the existence and uniqueness of the solution in the nonlinear case of (1), without using the partial differential equations and we state some results which are an important to prove the existence and uniqueness by means of probabilistic and potential theoretic methods.

2 Existence and uniqueness of the solution in the nonlinear case

We need a stochastic Taylor formula (**Itô formula**) for $\eta_t := \eta_0 + \int_0^t \sigma(s)\delta B_s^h + b(t)$.
Let $F \in \mathcal{C}^{1,2}([0,T] \times \mathbb{R})$ satisfy the growth condition

$$\max_t \{| F(t,x) |, | \frac{\partial F}{\partial x}(t,x) |, | \frac{\partial F}{\partial t}(t,x) |, | \frac{\partial^2 F}{\partial x^2}(t,x) |\} \leqq ce^{\lambda x^2} \text{ for some constants } c, \lambda > 0. \quad (4)$$

Then

$$F(t,\eta_t) = F(0,0) + \int_0^t \frac{\partial F}{\partial s}(s,\eta_s)ds + \int_0^t \frac{\partial F}{\partial x}(s,\eta_s)\sigma(s)\delta B_s^h + \frac{1}{2}\int_0^t \frac{\partial^2 F}{\partial^2 x}(s,\eta_s)\frac{d}{ds}R(\sigma)_s ds + \int_0^t b'(t)\frac{\partial F}{\partial x}(s,\eta_s)ds. \quad (5)$$

2.1 Connection with partial differential equations

Theorem 1 If (2) has a solution $(u(t,x), (t,x) \in [0,T] \times \mathbb{R})$ which satisfies (4), then $(Y_t, Z_t) := (u(t,\eta_t), -\sigma_t \frac{\partial u}{\partial x}(t,\eta_t))$, $t \in (0,T)$, satisfies (1).

In order to show the uniqueness of the solution we require the following result:

Proposition Suppose that (1) has a solution $(Y_t, Z_t) := (u(t,\eta_t), v(t,\eta_t))$, $t \in (0,T)$, where u is as in Theorem 1 and $v \in \mathcal{C}^{1,2}([0,T] \times \mathbb{R})$ satisfies (4). Then $v(t,x) = -\sigma_t \frac{\partial u}{\partial x}(t,x)$, $t \in (0,T)$.

Corollary If (2) has a unique solution which satisfies (4), (1) has a unique solution in the class of functions $Y_t = u(t,\eta_t)$, $u \in \mathcal{C}^{1,2}([0,T] \times \mathbb{R})$.

If h is a constant, we recover the result in [4].

2.2 Existence and uniqueness of a class of nonlinear BSDE

The aim of this section is to present another method to show the existence and uniqueness of the solution of (1), without using the partial differential equations, but by means of probabilistic and potential theoretic methods.

Hypotheses

(H1): The function $f : [0,T] \times \mathbb{R}^3 \longrightarrow \mathbb{R}$ belongs to the space $\mathcal{C}_{pol}^{0,1}([0,T] \times \mathbb{R} \times \mathbb{R}^2)$, and there exists a constant L such that, for all $t \in [0,T]$, $x, y_1, y_2, z_1, z_2 \in \mathbb{R}$,

$$| f(t,x,y_1,z_1) - f(t,x,y_2,z_2) | \leqslant L(| y_1 - y_2 | + | z_1 - z_2 |).$$

Here, $\mathcal{C}_{pol}^{k,l}([0,T] \times \mathbb{R}^m)$ is the space of all $\mathcal{C}^{k,l}$-functions over $[0,T] \times \mathbb{R}^m$, which together with their derivatives, are of polynomial growth.
(H2): $g : \mathbb{R} \longrightarrow \mathbb{R}$ is a differentiable function with polynomial growth.

Existence and uniqueness

We introduce the following space of stochastic processes

$$\mathcal{V}_T = \{Y_. = \phi(., \eta_.); \phi \in \mathcal{C}_{pol}^{1,3}([0,T] \times \mathbb{R}) \text{ with } \frac{\partial \phi}{\partial t} \in \mathcal{C}_{pol}^{0,1}([0,T] \times \mathbb{R})\},$$

and solve in $\mathcal{V}_T$ the equation

$$Y_t = g(\eta_T) + \int_t^T f(s, \eta(s), \chi(s,\eta(s)), \psi(s,\eta(s)))ds + \int_t^T Z_s \delta B_s^h, \quad 0 \le t \le T, \quad (6)$$

where $\chi, \psi \in \mathcal{C}_{pol}^{1,3}([0,T] \times \mathbb{R})$ with $\frac{\partial \chi}{\partial t}, \frac{\partial \psi}{\partial t} \in \mathcal{C}_{pol}^{0,1}([0,T] \times \mathbb{R})$.

The following proposition is an important step to prove the existence and uniquenss of the solution of (1).

Proposition Under the assumptions (H1)-(H2), (6) has a unique solution $(Y, Z) \in \mathcal{V}_T \times \mathcal{V}_T$. This solution has the form: $Y(t) = u(t,\eta(t)), Z(t) = v(t,\eta(t))$, where $v(t,x) = -\sigma(t)\frac{\partial}{\partial x}u(t,x)$ and $u, v \in \mathcal{C}_{pol}^{1,3}([0,T] \times \mathbb{R})$ with $\frac{\partial u}{\partial t}, \frac{\partial v}{\partial t} \in \mathcal{C}_{pol}^{0,1}([0,T] \times \mathbb{R})$

We state some notations and results which are crucial for the proof of this proposition.

A- Wiener chaos

For any $n \geqslant 1$ let $\mathcal{H}^{\otimes n}$ be the set of all real symmetric Borel functions f_n for n variables such that,

$$\|f_n\|_{\mathcal{H}^{\otimes n}}^2 := \int_{[0,T]^{2n}} \prod_{i=1}^n \phi(s_i,t_i) f_n(s_1,..,s_n) f_n(t_1,..,t_n) ds_1....ds_n dt_1....dt_n < \infty,$$

where

$$\phi(s_i,t_i) := \frac{\partial^2 R_h}{ds_i dt_i}(s_i,t_i) = \int_0^{inf(s_i,t_i)} \frac{\partial K_{h(s_i)}}{\partial s_i}(s_i,v_i)\frac{\partial K_{h(t_i)}}{\partial t_i}(t_i,v_i)dv_i.$$

Moreover, for $f_n \in \mathcal{H}^{\otimes n}$; let

$$I_n^h(f_n) = \int_0^T \int_0^{t_n} ... \int_0^{t_2} f_n(t_1,...,t_n)\delta B_{t_1}^{h(t_1)} ... \delta B_{t_n}^{h(t_n)}.$$

B- Isometry property

Theorem [7] Let $F \in L^2(\Omega, \mathcal{F}, \mathbb{P})$. Then there exist $f_n \in \mathcal{H}^{\otimes n}$, $n \geqslant 0$, such that $F = \sum_{n=0}^\infty I_n^h(f_n)$.
Moreover,

$$\mathbb{E} \mid F \mid^2 = \sum_{m=0}^\infty n! \parallel f_n \parallel_{\mathcal{H}^{\otimes n}}^2 .$$

The convergence in this chaos expansion of F is understood in the sense of $L^2(\Omega, \mathcal{F}, \mathbb{P})$.

C- Quasi-conditional expectation

For $F \in L^2(\Omega, \mathcal{F}, \mathbb{P})$, the quasi-conditional expectation is defined as

$$\widehat{\mathbb{E}}\Big[F \mid \mathcal{F}_t\Big] = \sum_{n=0}^\infty I_n^h(f_n 1_{[0,t]}^{\otimes n}), \quad (7)$$

if the series on the right side converges in $L^2(\Omega, \mathcal{F}, \mathbb{P})$. Here

$$1_{[0,t]}^{\otimes n}(t_1,...,t_n) := 1_{[0,t]}(t_1)...1_{[0,t]}(t_n).$$

Lemma Let $F = k(\eta(T))$, where $k : \mathbb{R} \longrightarrow \mathbb{R}$ is a continuous function of polynomial growth and we suppose that R is increasing or decreasing. Then $F \in L^2(\Omega, \mathcal{F}, \mathbb{P})$ and

$$\widehat{\mathbb{E}}[F|\mathcal{F}_t] = P_{|R(\sigma)_T - R(\sigma)_t|}k(\eta(t)), \quad t \in [0,T], \quad (8)$$

where P is the heat kernel evaluated in the scale of $R(\sigma)$.

3 Conclusions

In this paper, we generalize to multi-fractional brownian motion the existence and uniqueness of solutions for a class of nonlinear backward stochastic differential equations (BSDE), known for fractional brownian motion. The stochastic calculus applied to show these results is the Malliavin calculus [1]. In the second section, we show the existence and uniqueness of solutions of BSDE by an associated partial differential equation and by probabilistic and potential theoretic methods. Finally, we recall that in the linear case, (1) is solved explicitly in terms of the solution of the associated partial differential equation in [5].

Acknowledgments

I would like to thank Prof. Marco DOZZI for all of this encouragement, knowledge and advice.

References

[1] E. Alòs, O. Mazet, D. Nualart. Stochastic calculus with respect to gausssian processes. Annls Probab. 29 (2001), 766 - 801.

[2] C. Bender. Explicit solutions of a class of linear fractional BSDE's. Systems Control Letters 54 (2005), 671 - 680.

[3] B. Boufoussi, M. Dozzi, R. Marty. Local time and Tanaka formula for a Volterra-type multifractional Gaussian process. Bernoulli 16 (2010), 1294-1311.

[4] Y. Hu, S. Peng. Backward stochastic differential equation driven by fractional brownian motion. SIAM J. Control Optim. 48 (2009), 1675 - 1700.

[5] M. Dozzi, H. Knani. Backward stochastic differential equations and their applications to finance (in french). Lorraine University and Sousse University, 2014.

[6] L. Maticiuc, T. Nie, Fractional backward stochastic differential equations and fractional backward variational inequalities, J Theor Probab (2015)28:337-395.

[7] I. Nourdin and G. Peccati, Normal approximations with malliavin calculus, Cambridge University Press, 2012.

ON THE HARDY-SCHRÖDINGER OPERATOR FOR SINGULARITIES ON A NON-SMOOTH BOUNDARY

Hussein CHEIKH ALI

Université de Lorraine (France)

Université Libre de Bruxelles (Belgique)

Hussein.cheikh-ali@univ-lorraine.fr; Hussein.cheikh-ali@ulb.ac.be

Abstract

Let Ω be a domain of $\mathbb{R}^n$, $(n \geq 3)$, and fix $\gamma \in \mathbb{R}$. In this note, we investigate minimizing solutions $u : \Omega \to \mathbb{R}_+$ to the equation $L_\gamma u = \frac{u^{2^*(s)-1}}{|x|^s}$ (H) with Dirichlet boundary condition, where $L_\gamma := -\Delta - \frac{\gamma}{|x|^2}$ is the Hardy-Schrödinger operator. Equation (H) is the Euler-Lagrange equation associated to the Hardy-Sobolev inequality. When $0 \in \Omega$, the problem makes sense when $\gamma < (n-2)^2/4$, the classical Hardy constant. When $0 \in \partial\Omega$, one can tolerate larger values that depend on the structure of the tangent cone of Ω at 0. When the domain is smooth, the question was studied by Ghoussoub-Robert [3]. In this note, we consider nonsmooth domain modeled on some regular cones (we refer them as "model singularities"). We show how the geometry of the model cone influences the value of the Hardy constant on Ω. When γ is small, we introduce "mean curvatures" at the conical singularity to get extremals for the inequality. When γ is large, we introduce a "mass" in the spirit of Schoen-Yau [4] to recover the existence of extremals.

1. Introduction

We classical Hardy-Sobolev inequality writes as follows: let Ω be a domain of $\mathbb{R}^n$, $n \geq 3$, $s \in [0,2)$ and $\gamma < \frac{(n-2)^2}{4}$, there exists $K > 0$ such that

$$\left(\int_\Omega \frac{|u|^{2^*(s)}}{|x|^s}dx\right)^{\frac{2}{2^*(s)}} \leq K\int_\Omega \left(|\nabla u|^2 - \gamma\frac{u^2}{|x|^2}\right)dx, \quad (1)$$

$\forall u \in C_0^\infty(\Omega)$, where $2^*(s) := \frac{2(n-s)}{n-2}$ is the critical Hardy-Sobolev exponent.

Indeed, this inequality can be seen as a direct consequence of the Caffarelli-Kohn-Nirenberg inequality. This inequality makes sense for $u \in D^{1,2}(\Omega)$, that is the completion of $C_0^\infty(\Omega)$ with respect to the norm $u \mapsto \|u\| := \sqrt{\int_\Omega |\nabla u|^2 dx}$.

More generally, for any $0 \leq s < 2$ and any $\gamma \in \mathbb{R}$, we set the ratio

$$J^\Omega_{\gamma,s}(u) := \frac{\int_\Omega |\nabla u|^2 dx - \gamma\int_\Omega \frac{u^2}{|x|^2}dx}{\left(\int_\Omega \frac{|u|^{2^*(s)}}{|x|^s}dx\right)^{\frac{2}{2^*(s)}}}, \quad (2)$$

for $u \in D^{1,2}(\Omega) \setminus \{0\}$, and we define

$$\mu_{\gamma,s}(\Omega) = \inf_{u \in D^{1,2}(\Omega)\setminus\{0\}} J^\Omega_{\gamma,s}(u). \quad (3)$$

We address the following questions:

1. For which values of $\gamma \in \mathbb{R}$ does (1) hold for some $K > 0$ and all $u \in D^{1,2}(\Omega)$? In other words, when do we have $\mu_{\gamma,s}(\Omega) > 0$?
2. Is the best constant achieved? In other words, is $\mu_{\gamma,s}(\Omega)$ achieved by some $u \in D^{1,2}(\Omega)$? The answer to the first question depends on the Hardy constant.

Define

$$\gamma_H(\Omega) := \inf\left\{\frac{\int_\Omega |\nabla u|^2 dx}{\int_\Omega \frac{u^2}{|x|^2}dx};\, u \in C_0^\infty(\Omega)\backslash\{0\}\right\}.$$

The classical Hardy inequality reads $\gamma_H(\mathbb{R}^n) = \frac{(n-2)^2}{4}$, and therefore, we have that $\gamma_H(\Omega) \geq \frac{(n-2)^2}{4}$. As a consequence, interpolating the Hardy and Sobolev inequalities, we get that

$$\mu_{\gamma,s}(\Omega) > 0 \;\Leftrightarrow\; \gamma < \gamma_H(\Omega).$$

When $0 \in \Omega$ is an interior point, it is classical that $\gamma_H(\Omega) = \gamma_H(\mathbb{R}^n) = \frac{(n-2)^2}{4}$.

We consider the case $0 \in \partial\Omega$. When Ω is a smooth domain, the problem was studied by Ghoussoub-Robert [3].

In this work, we tackle the more intricate case of a nonsmooth domain. We restrict ourselves to domains modeled locally on $\mathbb{R}^k_+ \times \mathbb{R}^{n-k}$. We define the *model cone* at $P \in \Omega$ as

$$C_P(\Omega) := \{\lim_{t\to 0}\frac{1}{t}\overrightarrow{PM_t} /\ t \mapsto M_t \text{ is a curve of } \Omega \text{ and the limit exists}\}.$$

Note that if Ω is smooth, $C_{x_0}(\Omega) = \mathbb{R}^n$ if $x_0 \in \Omega$ and $C_{x_0}(\Omega)$ is a half-space bounded by the tangent space at x_0 if $x_0 \in \partial\Omega$.

Moreover, when $x_0 \in \partial\Omega$, then $\partial C_{x_0}(\Omega)$ is exactly the tangent space at x_0.

Definition 1 *We fix $1 \leq k \leq n$. Let Ω be a domain of $\mathbb{R}^n$. We say that $x_0 \in \partial\Omega$ is a singularity of type $(k, n-k)$ if there exist U, V open subsets of $\mathbb{R}^n$ such that $0 \in U$, $0 \in V$ and there exists $\phi \in C^\infty(U,V)$ a diffeomorphism such that $\phi(0) = x_0$ and*

$$\phi(U \cap (\mathbb{R}^k_+ \times \mathbb{R}^{n-k})) = \phi(U) \cap \Omega$$
$$\phi(U \cap \partial(\mathbb{R}^k_+ \times \mathbb{R}^{n-k})) = \phi(U) \cap \partial\Omega,$$

and $C_{x_0}(\Omega)$ is isometric to $\mathbb{R}^k_+ \times \mathbb{R}^{n-k}$.

For example:

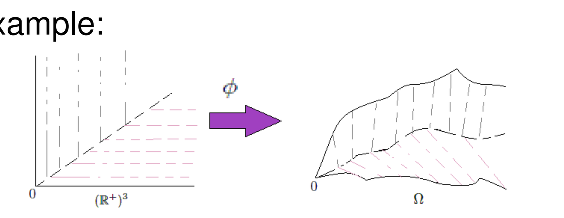

Figure 1: *Case:* $k = 3$, $n - k = 0$.

2. The best Hardy constant

Definition 2 *We can write $\Omega \cap B_\delta(0) = \bigcap_{i=1}^k \Omega_i \cap B_\delta(0)$ where the Ω_i are smooth domains. In other words (see picture below), Ω can be written locally as an intersection of smooth domain. A decomposition as k domains is unique (at least in the local sense).*

For example:

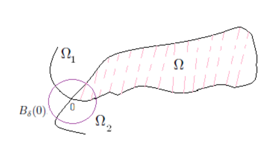

Figure 2: *Case:* $k = 2$, $n - k = 0$.

For any sub-domain D of the n-dimensional sphere S^{n-1}, we associate a conical domain $C \subset \mathbb{R}^n$ having 0 as a vertex,

$$C := \{r\sigma; r > 0 \text{ et } \sigma \in D\}.$$

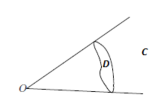

Figure 3: *The cone* C.

In particular, if D is the sphere S^{n-1}, then $C = \mathbb{R}^n\backslash\{0\}$ and if $D = S^{n-1} \cap (\mathbb{R}^k_+ \times \mathbb{R}^{n-k})$, then $C = \mathbb{R}^k_+ \times \mathbb{R}^{n-k}$ for all $k \in \{1, ..., n\}$.

The best constant for such cone is known. As it is noted in the book of Ghoussoub-Moradifam [2]

$$\gamma_H(C) = \frac{(n-2)^2}{4} + \lambda_1(D),$$

such that $\lambda_1(D)$ is the first eigenvalue of Laplacien on $D \subset S^{n-1}$ with Dirichlet boundary condition.

In particular, for all $k \in \{1, ..., n\}$ we have that

$$\gamma_H(\mathbb{R}^k_+ \times \mathbb{R}^{n-k}) = \frac{(n+2k-2)^2}{4}.$$

3. Existence of extremals

We now tackle the second question, that is the existence of extremals for (3). In this framework, it is classical that the infimum must be below a critical threshold:

Theorem 3.1 *Let $\Omega \subset \mathbb{R}^n$ be a domain such that $0 \in \partial\Omega$ is a singularity of type $(k, n-k)$. Assume that $\gamma < \gamma_H(\mathbb{R}^k_+ \times \mathbb{R}^{n-k})$, $0 \leq s \leq 2$, et $\mu_{\gamma,s}(\Omega) < \mu_{\gamma,s}(\mathbb{R}^k_+ \times \mathbb{R}^{n-k})$. Then there are extremals for $\mu_{\gamma,s}(\Omega)$. In particular, there exists a minimizer u in $D^{1,2}(\Omega)\backslash\{0\}$ that is a positive solution to the equation*

$$(E)\begin{cases} -\Delta u - \frac{\gamma}{|x|^2}u = \mu_{\gamma,s}(\Omega)\frac{u^{2^*(s)-1}}{|x|^s} & \text{in } \Omega, \\ u > 0 & \text{in } \Omega, \\ u = 0 & \text{on } \partial\Omega. \end{cases}$$

4. Regularity and approximate solutions

Let $\alpha \in \mathbb{R}$ be an arbitrary real number and fix $\gamma < \gamma_H(\mathbb{R}^k_+ \times \mathbb{R}^{n-k})$. Then

$$\left(-\Delta - \frac{\gamma}{|x|^2}\right)\frac{\prod_{i=1}^k x_i}{|x|^{\alpha+k}} = 0 \quad \Leftrightarrow \quad \alpha \in \{\alpha_-(k), \alpha_+(k)\},$$

where

$$\alpha_\pm = \alpha_\pm(\gamma, n, k) := \frac{n-2}{2} \pm \sqrt{\gamma_H(\mathbb{R}^k_+ \times \mathbb{R}^{n-k}) - \gamma}.$$

We must think of $\frac{\prod_{i=1}^k x_i}{|x|^{\alpha+k}}$ as the prototype of solution to the above equation vanishing on the boundary of $\mathbb{R}^k_+ \times \mathbb{R}^{n-k}$. The behavior of solutions to equations like (E) is governed by the prototypes. Indeed, there exists $K > 0$ such that

$$\lim_{x\to 0}\frac{u(x)|x|^{k+\alpha_-}}{\prod_{i=1}^k d(x, \partial\Omega_i)} = K.$$

Such a result can be adapted to more general nonlinearities and sign-changing solutions. This result is essentially in Felli-Ferrero [1], and the proof goes by super-sub solutions.

Proposition 4.1 *Let $\gamma < \gamma_H(\mathbb{R}^k_+ \times \mathbb{R}^{n-k})$ and $\alpha \in \{\alpha_-(\gamma), \alpha_+(\gamma)\}$. Let $0 < \tau \leq 1$ and $\beta \in \mathbb{R}$ such that $\alpha - \tau < \beta < \alpha$ and $\beta \neq \{\alpha_-(\gamma), \alpha_+(\gamma)\}$. Then, there exist $r > 0$, $u_{\alpha,+}, u_{\alpha,-} \in C^2(\overline{\Omega}\backslash\{0\})$ such that*

$$\begin{cases} u_{\alpha,+}, u_{\alpha,-} > 0 & \text{in } \Omega \cap B_r(0), \\ u_{\alpha,+}, u_{\alpha,-} = 0 & \text{on } \partial\Omega \cap B_r(0), \\ -\Delta u_{\alpha,+} - \frac{\gamma}{|x|^2}u_{\alpha,+} > 0 & \text{in } \Omega \cap B_r(0), \\ -\Delta u_{\alpha,-} - \frac{\gamma}{|x|^2}u_{\alpha,-} < 0 & \text{in } \Omega \cap B_r(0). \end{cases}$$

Moreover, asymptotically, we have that

$$u_{\alpha,+}(x) \simeq_{x\to 0} u_{\alpha,-}(x) \simeq_{x\to 0} \frac{\prod_{i=1}^k d(x, \Omega_i)}{|x|^{k+\alpha}}.$$

Corollary 4.1 *Suppose $u \in D^{1,2}(\mathbb{R}^k_+ \times \mathbb{R}^{n-k})$, $u \geq 0$, $u \neq 0$ is a weak solution of*

$$-\Delta u - \frac{\gamma}{|x|^2}u = \frac{u^{2^*(s)-1}}{|x|^s} \text{ in } \mathbb{R}^k_+ \times \mathbb{R}^{n-k}. \quad (4)$$

Then, there exists $K_1, K_2 > 0$ such that

$$u(x) \sim_{x\to 0} K_1\frac{\prod_{i=1}^k x_i}{|x|^{k+\alpha_-}},$$

and

$$u(x) \sim_{|x|\to+\infty} K_2\frac{\prod_{i=1}^k x_i}{|x|^{k+\alpha_+}}.$$

5. Existence of extremals: the case of small values of γ

Here, we estimate the functional J at some natural test-functions. We let $W \in D^{1,2}(\mathbb{R}^k_+ \times \mathbb{R}^{n-k})$ be a positive extremal for $\mu_{\gamma,s}(\mathbb{R}^k_+ \times \mathbb{R}^{n-k})$.

They exists under the assumption that $s > 0$ or $\{s = 0$ and $\gamma > 0\}$ (see Ghoussoub-Robert [3]). We keep the chart (ϕ, U) given in Definition 1 and for all $x \in \Omega$ we define:

$$W_\epsilon(x) := \eta(x)\epsilon^{-n-2}W\left(\epsilon^{-1}\varphi^{-1}(x)\right),$$

where $\eta \in C_c^\infty(\mathbb{R}^n)$ is such that $\eta(x) \equiv 1$ around 0, and Supp $\eta \subset \phi(U)$. Computations yield the following:

Proposition 5.1 *Let $\gamma < \gamma_H(\mathbb{R}^k_+ \times \mathbb{R}^{n-k}) = \frac{(n+2k-2)^2}{4}$, and assume that there are extremals for $\mu_{\gamma,s}(\mathbb{R}^k_+ \times \mathbb{R}^{n-k})$. Then there exists k positives constantes $c^i_{\gamma,s}$ for all $i \in \{1, ..., k\}; k \in \{1, ..., n\}$ such that:*

1. *For $\gamma < \gamma_H(\mathbb{R}^k_+ \times \mathbb{R}^{n-k}) - \frac{1}{4}$, we have that*

$$J(W_\epsilon) = \mu_{\gamma,s}(\mathbb{R}^k_+ \times \mathbb{R}^{n-k})(1 + \sum_{i=1}^k c^i_{\gamma,s} \cdot h_{\Omega_i}(0) \cdot \epsilon + o(\epsilon)).$$

2. *For $\gamma = \gamma_H(\mathbb{R}^k_+ \times \mathbb{R}^{n-k}) - \frac{1}{4}$, we have that*

$$J(W_\epsilon) = \mu_{\gamma,s}(\mathbb{R}^k_+ \times \mathbb{R}^{n-k})[1 + \sum_{i=1}^k c^i_{\gamma,s} \cdot h_{\Omega_i}(0) \cdot \epsilon\ln\left(\frac{1}{\epsilon}\right) + o\left(\epsilon\ln\left(\frac{1}{\epsilon}\right)\right)],$$

as $\epsilon \to 0$, and where $h_{\Omega_i}(0)$ denotes the mean curvature of Ω_i at 0.

Theorem 5.1 *Let Ω be a bounded domain in $\mathbb{R}^n$ be a singularity of type $(k, n-k)$ at 0 for some $k \in \{1, ..., n\}$. We fix $0 \leq s < 2$ and $\gamma < \gamma_H(\Omega)$. Assume that either $s > 0$, or that $\{s = 0, n \geq 4$ and $\gamma > 0\}$. We assume that*

$$\gamma \leq \gamma_H(\mathbb{R}^k_+ \times \mathbb{R}^{n-k}) - \frac{1}{4}.$$

Then there are extremals for $\mu_{\gamma,s}(\Omega)$ if the mean curvatures of $\partial\Omega_i$ at 0 are all negative.

6. Existence of extremals: the case of large values of γ

Theorem 6.1 *Let Ω be a singularity of type $(k, n-k)$ at 0, such that $0 \in \partial\Omega$, and assume that $\gamma < \gamma_H(\Omega)$. Then, up to multiplication by a positive constant, there exists a unique function $H \in C^2(\bar{\Omega}\backslash\{0\})$ such that*

$$\begin{cases} -\Delta H - \frac{\gamma}{|x|^2}H = 0 & \text{in } \Omega, \\ H > 0 & \text{in } \Omega, \\ H = 0 & \text{on } \partial\Omega\backslash\{0\}. \end{cases} \quad (5)$$

Assume in addition that $\gamma_H(\mathbb{R}^k_+ \times \mathbb{R}^{n-k}) - \frac{1}{4} < \gamma$. There there exists $c_1 > 0$ and $c_2 \in \mathbb{R}$ such that

$$H(x) = c_1\frac{\prod_{i=1}^k d(x, \Omega_i)}{|x|^{k+\alpha_-}} + c_2\frac{\prod_{i=1}^k d(x, \Omega_i)}{|x|^{k+\alpha_+}} + o\left(\frac{\prod_{i=1}^k d(x, \Omega_i)}{|x|^{k+\alpha_-}}\right) \text{ as } x \to 0.$$

The quantity

$$m_\gamma(\Omega) := \frac{c_2}{c_1} \in \mathbb{R},$$

which is independent of the choice of H satisfing (5), will be called the " Hardy b-mass" of Ω associated to L_γ.

Theorem 6.2 *Let Ω be a bounded domain in $\mathbb{R}^n$ be a singularity of type $(k, n-k)$ at 0 for some $k \in \{1, ..., n\}$. We fix $0 \leq s < 2$ and $\gamma < \gamma_H(\Omega)$. Assume that either $s > 0$, or that $\{s = 0, n \geq 4$ and $\gamma > 0\}$. We assume that*

$$\gamma > \gamma_H(\mathbb{R}^k_+ \times \mathbb{R}^{n-k}) - \frac{1}{4}.$$

Then there are extremals for $\mu_{\gamma,s}(\Omega)$ if $m_\gamma(\Omega) > 0$.

References

[1] Veronica Felli and Alberto Ferrero, Almgren-type monotonicity methods for the classification of behaviour at corners of solutions to semilinear elliptic equations, Proc. Roy. Soc. Edinburgh Sect. A, 143, 2013, 5, 957–1019.

[2] Nassif Ghoussoub and Amir Moradifam, Functional inequalities: new perspectives and new applications, Mathematical Surveys and Monographs, 187, American Mathematical Society, Providence, RI, 2013, xxiv+299.

[3] Nassif Ghoussoub and Frédéric Robert, Hardy-singular boundary mass and Sobolev-critical variational problems, Anal. PDE, 10, 2017, 5, 1017–1079.

[4] Richard Schoen and Shing-Tung Yau , Conformally flat manifolds, Kleinian groups and scalar curvature, Invent. Math. 92, 1988, 1,47–71.

ECOLE DOCTORALE IAEM LORRAINE

Unification des stratégies de contrôle d'un réseau embarqué temps-réel reconfigurable

Dorine Petit {dorine.petit@univ-lorraine.fr}

Directeur de thèse : **Thierry Divoux**

Co-directeur de thèse : **Jean-Philippe Georges**

Contexte

De nos jours, beaucoup de systèmes embarqués utilisent des bus de communication pour garantir l'échange des données. Les nouvelles générations d'**applications spatiales** s'orientent vers l'utilisation de composants sur étagère tel que des réseaux **Ethernet commutés** dans le but de réduire le coût financier, le poids et de s'orienter vers une standardisation effective. Les problèmes liés à ce type d'architecture sont :

- Le respect d'une qualité de service comme la garantie d'acheminement **temps réel.**
- La sûreté de fonctionnement, comme la maitrise du temps de **reconfiguration** lors d'une défaillance ou d'une séparation d'étage.
- L'**observabilité**, qui regroupe la traçabilité et la testabilité de tous les échanges qui doivent pouvoir être rejoués au sol.

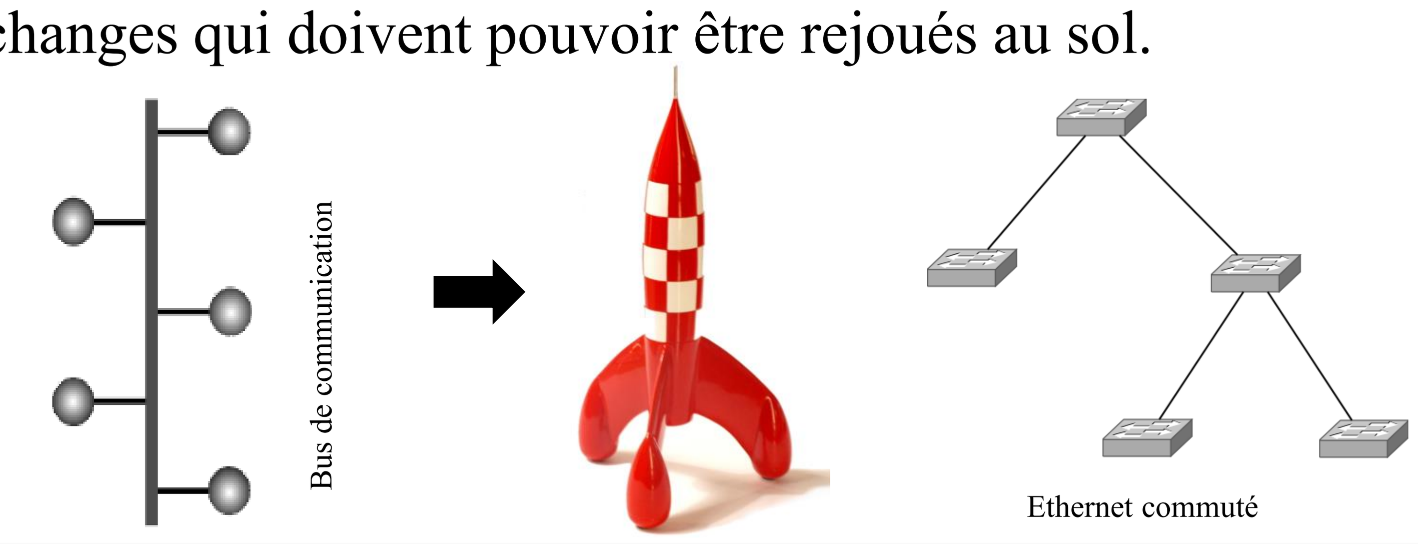

Objectifs

Dans le cadre d'une collaboration pérenne avec le CNES (Centre National d'Etudes Spatiales), les travaux menés jusqu'à présent (Robert, 2012) ont traité les problèmes ci-dessus de manière unitaire. Le but est de compléter et d'**unifier** les différentes stratégies de contrôle déjà existantes en proposant une **automatisation** du réseau utilisant l'architecture **Software-Defined Networking** (SDN).

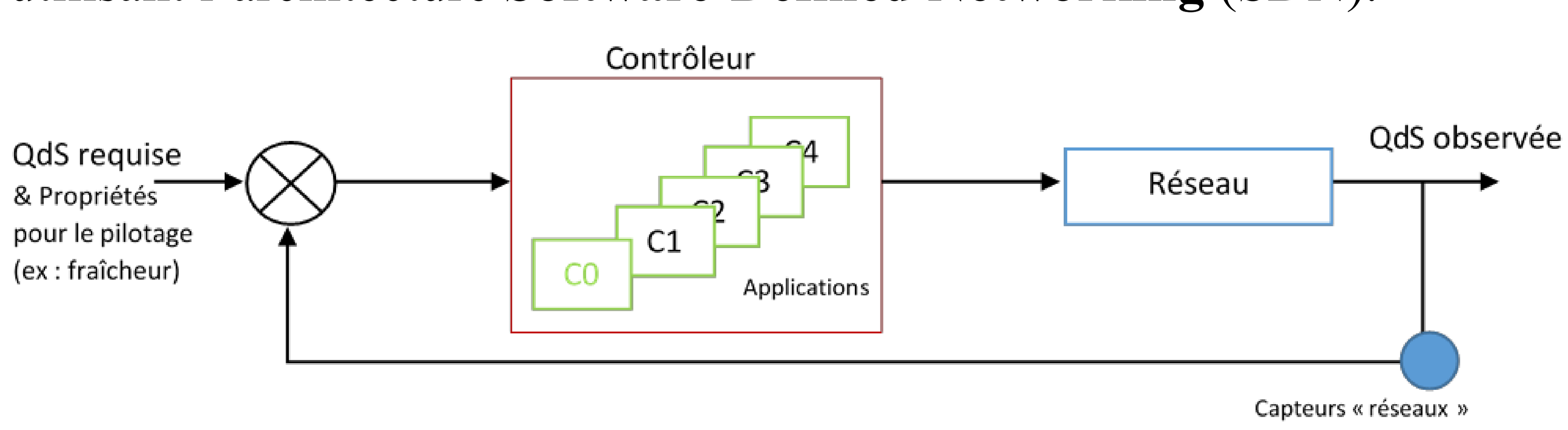

Robert, J., 2012. De l'usage d'architectures Ethernet commutées embarquées dans les lanceurs spatiaux. Thèse, Université de Lorraine, CRAN.

Une nouvelle problématique d'observabilité :

❖ Identification des conditions d'observation de la fraîcheur à partir de traces

Observation de la fraîcheur d'information de commande

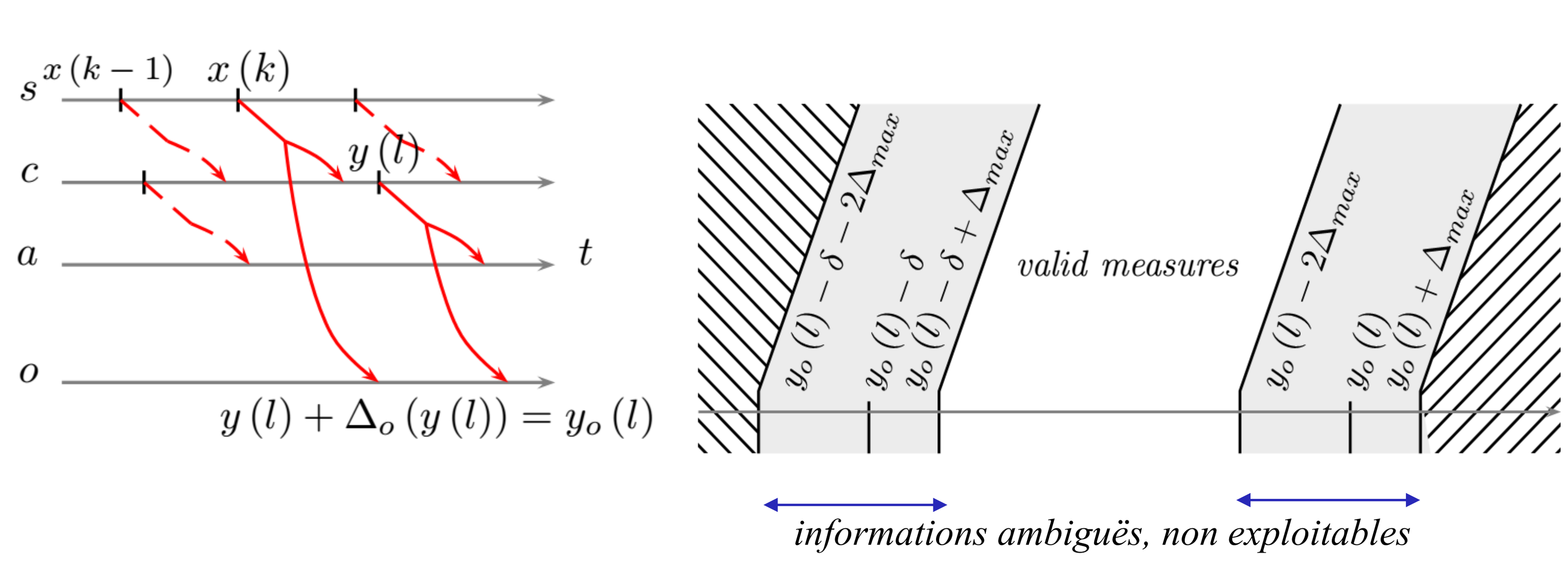

$$\exists k \in \mathbb{N} \mid y_o(l) - \delta + \Delta_{max} \leq x_o(k) \leq y_o(l) - 2\Delta_{max}$$

C0 Fonction d'observabilité

```
Algorithm 1: Parsing trace
Data: The frames captured F = (T|D|K) and the
      sequences specifications S = (C|R)
Result: V the successful frames collections
forall S_j ∈ S do
    F' ⟵ {F_i ∈ F | T_i ∈ C_j};
    l ⟵ |C_j|;
    foreach F'_i | T_i = C_{j,l} do
        P ⟵ {F'_i};
        forall P_z ∈ P | P_z NEq C_j do
            k ⟵ |P_z|;
            p ⟵ x | F'_x = P_{z,k};
            V ← FindInputs(F', p, C_{j,l−k}, R_{j,l−k+1});
            P ⟵ P ∪ {P_z × V};
            P ⟵ P\P_z;
        if P ≠ ∅ then
            V_j ⟵ V_j ∪ P;
```

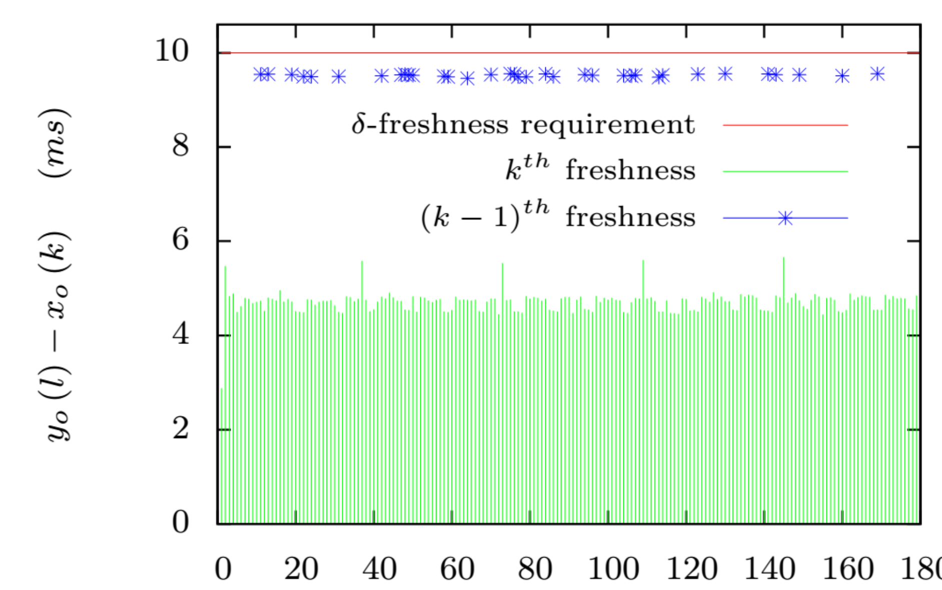

❖ Modélisation de l'activité générée par la commande

Vérifier la commande de pilotage lors d'un vol ne peut se faire pour le CNES que par l'image de son activité sur le réseau. Une trace unique collectant l'ensemble des trames du réseau doit permettre, à elle seule, d'établir que l'ensemble des séquences de commandes se sont conformément (ou non) déroulées. Comme montré précédemment, l'unique observateur n'a pas une vue omnisciente et crée de l'ambiguïté sur l'interprétation de la trace. Nous proposons alors de confronter la trace d'un vol à un modèle de comportement - réseau - dynamique attendu sous la forme d'automates communicants et en rejetant à la volée les trames ambiguës. Par la suite, cette observation permettra de paramétrer le réseau (priorités des trames, fréquences d'échantillonnage, …) non plus simplement vis à vis de contraintes temps réel, mais aussi en réduisant l'incertitude d'observation.

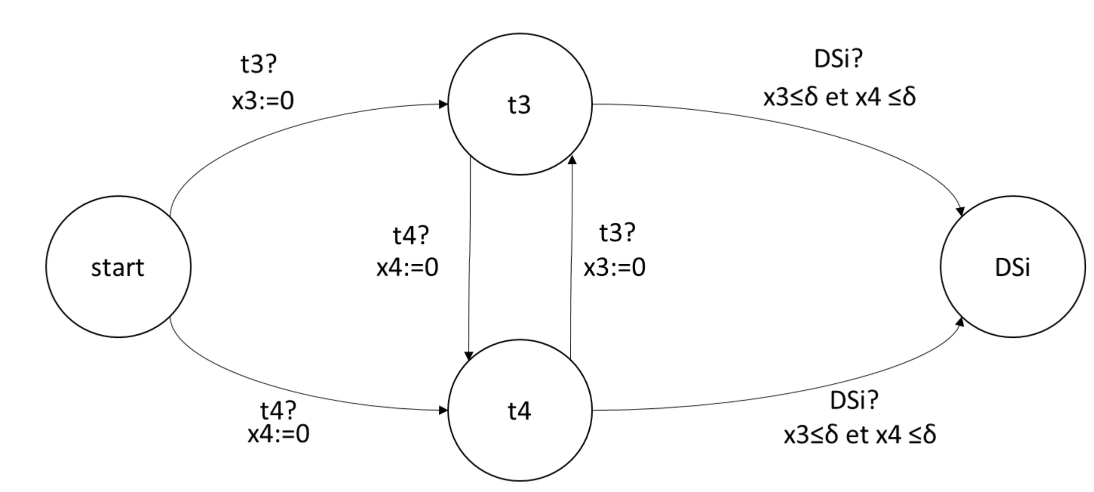

Vers une automatisation unifiée

Les différentes commandes de réseau peuvent induire des conséquences orthogonales. Par exemple, une reconfiguration du réseau peut conduire à une augmentation du délai d'acheminement.

Il est alors envisagé d'automatiser la commande du réseau en s'appuyant sur une architecture SDN. La responsabilité du contrôleur est de garantir des délais bornés et une reconfiguration temps réel en ajustant les priorités des messages de contrôle applicatif et de gestion de la reconfiguration.

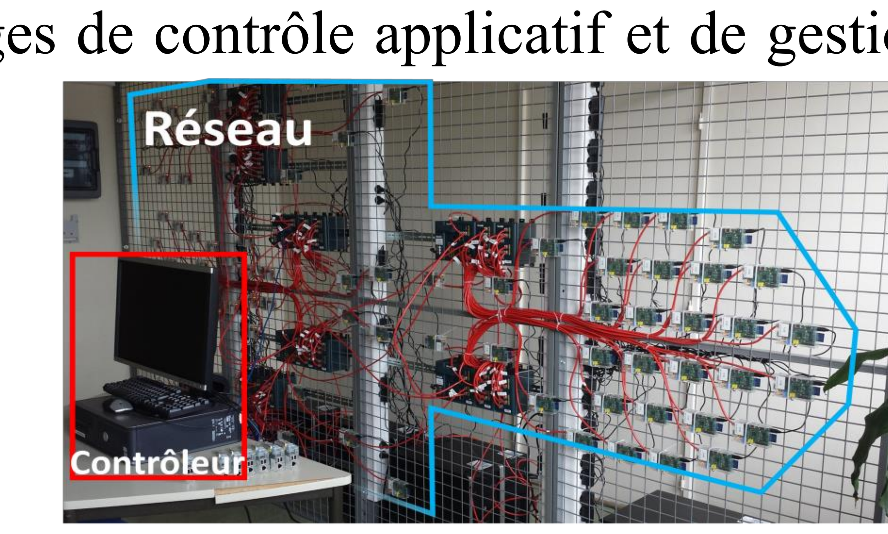

Nos travaux sont validés expérimentalement sur une plateforme conçue avec le CNES qui reproduit fidèlement l'avionique embarquée.

Publications

- Dorine Petit, Jean-Philippe Georges, Thierry Divoux, Bruno Regnier, Philippe Miramont, Freshness analysis of functional sequences in launchers. Telematics Applications 2016, IFAC Symposium, Porto Alegre, Brazil.
- Dorine Petit, Jean-Philippe Georges, Thierry Divoux, Bruno Regnier, Philippe Miramont, A demonstrator of an Ethernet based embedded network in space launchers, 20th IFAC World Congress, IFAC 2017, Toulouse, France.

Trial and Error Learning for Robot Damage Recovery

■ **Project:** ERC "ResiBots", **Supervisor:** Jean-Baptiste Mouret

APIL 2017 — Annual PhD students conference IAEM Lorraine 2017

Konstantinos Chatzilygeroudis — konstantinos.chatzilygeroudis@inria.fr

- The recently introduced **Intelligent Trial-and-Error algorithm (IT&E)**, by *Cully et al.* [1], is a first step towards fast and autonomous robot damage adaptation.

Main challenges

- As little interaction time between the robot and the environment as possible (data-efficiency).
- Take into account the environment as to not further damage the robot.
- No reset between episodes in order to be applied in real-world scenarios.
- Take into account safety constraints in order to be applied in humanoid/fragile robots.
- Scale well with regards to the dimensionality of the state and action space of robot.

Main ideas

- Formulate the problem as a Reinforcement Learning problem
- Use models (either full transition models, or reward surrogates) to increase data-efficiency.
- Pre-compute off-line behaviors with corresponding controllers, performances and other information (like constraints/forces data).
- Take advantage of all state of the art algorithms regarding optimization and probabilistic planning (e.g. Bayesian optimization, Monte Carlo Tree Search, QP programming, etc).

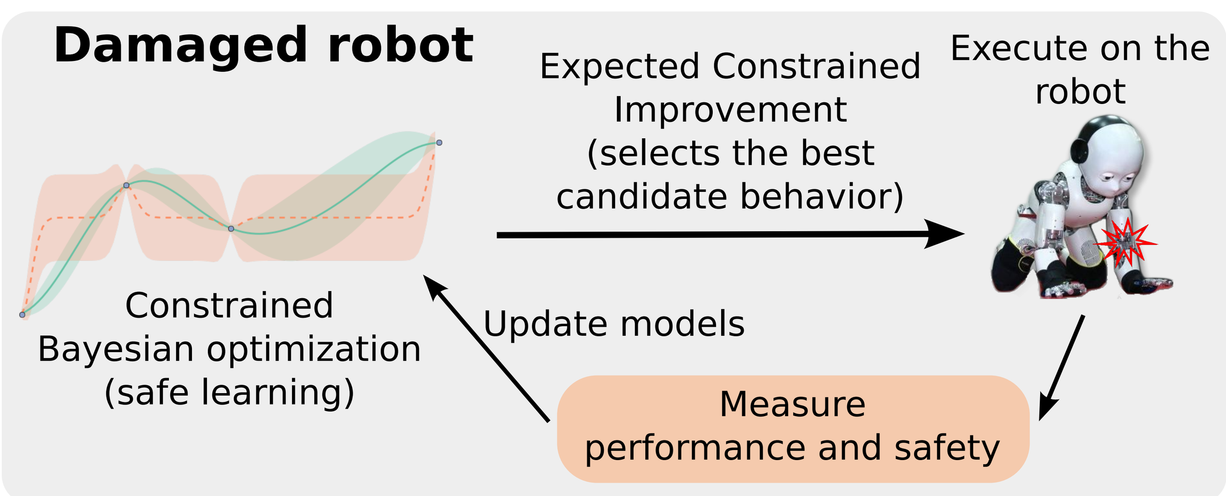

sITE: Safety-aware damage recovery with a crawling humanoid [2]

- Pre-compute a "behavior-performance" map with additional diversity and priors over user-defined safety constraints.
- The behavior space is 5D: 4 dimensions for crawling diversity and 1 dimension for the sum of contact point forces.
- We use Gaussian Processes to model the difference between the performance of the intact and the damaged robot, and to model each safety constraint.
- After damage, the robot (1) selects the most promising behavior in terms of performance but within the safe region defined by the constraints (using constrained Bayesian optimization), (2) executes it, and (3) updates the Gaussian processes.

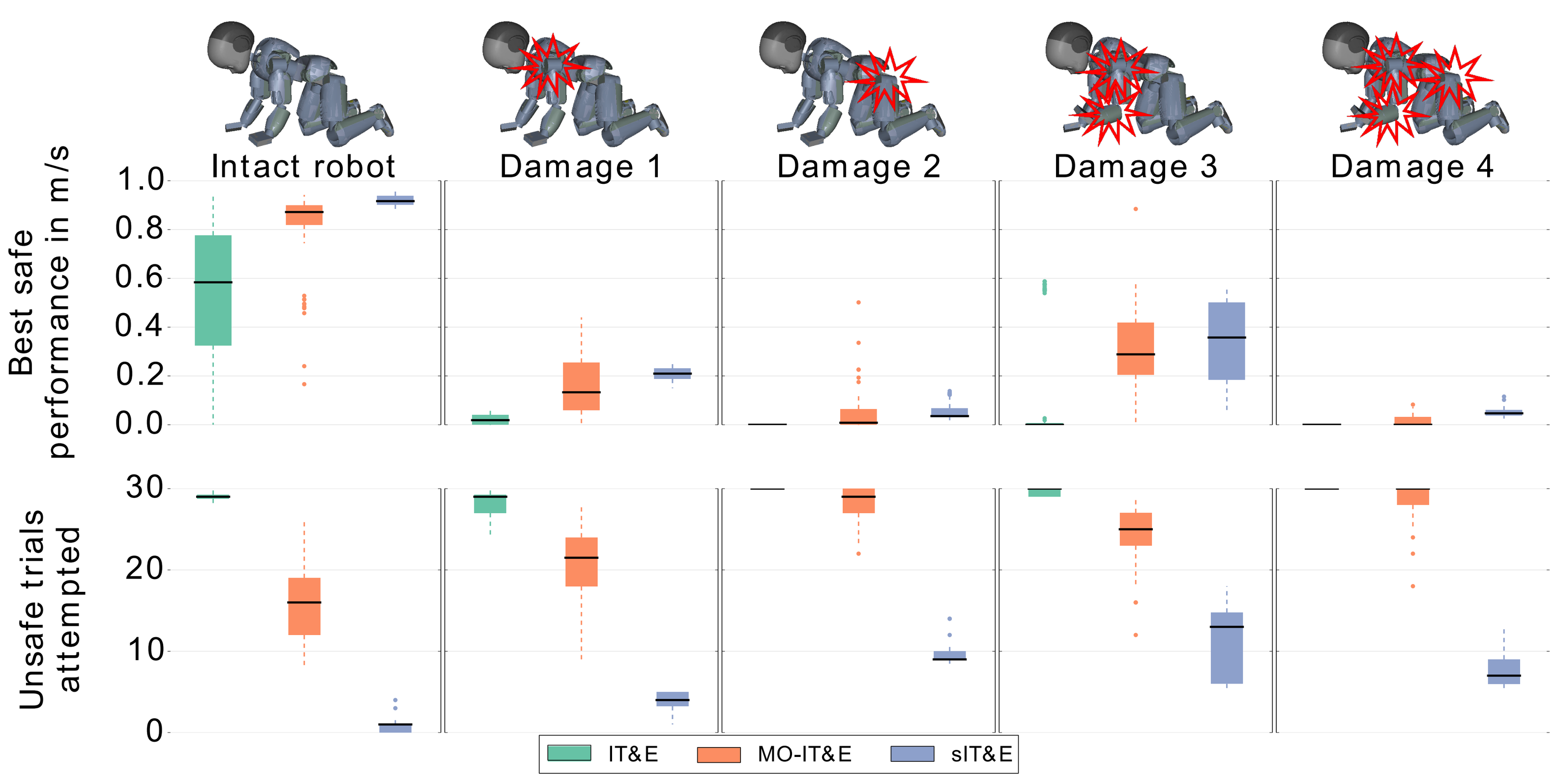

RTE: Reset-free Trial and Error learning with a damaged hexapod [3]

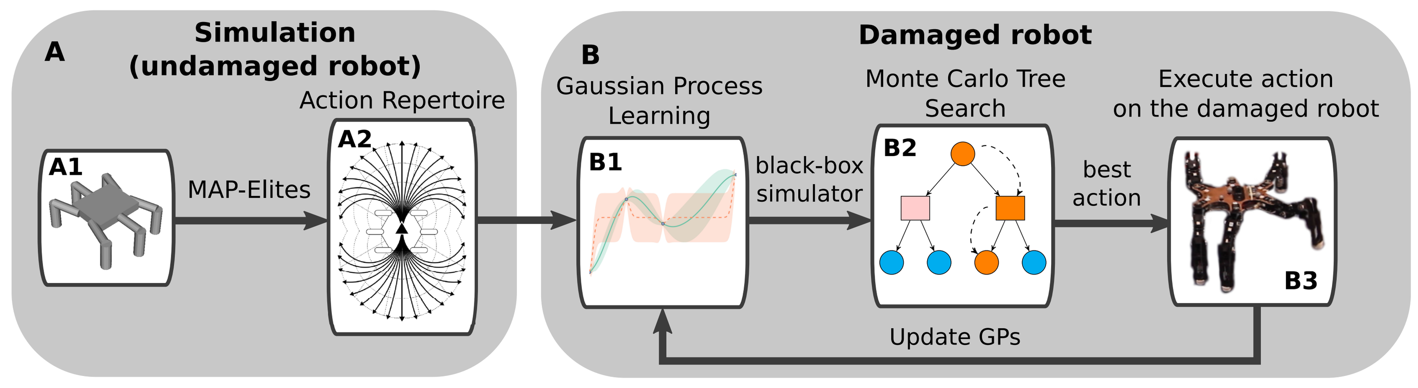

- Pre-compute diverse and locally high performing "action" repertoire with corresponding relative action outcomes.
- Correct the relative outcomes with Gaussian processes on the damaged robot.
- Use Monte Carlo Tree Search to re-plan at every episode taking into account the model uncertainties and the environment.
- No need for reset and the algorithm applies the same from simple navigation robots (e.g. Roomba like) to hexapod ones (i.e. we break the complexity with the action repertoire).

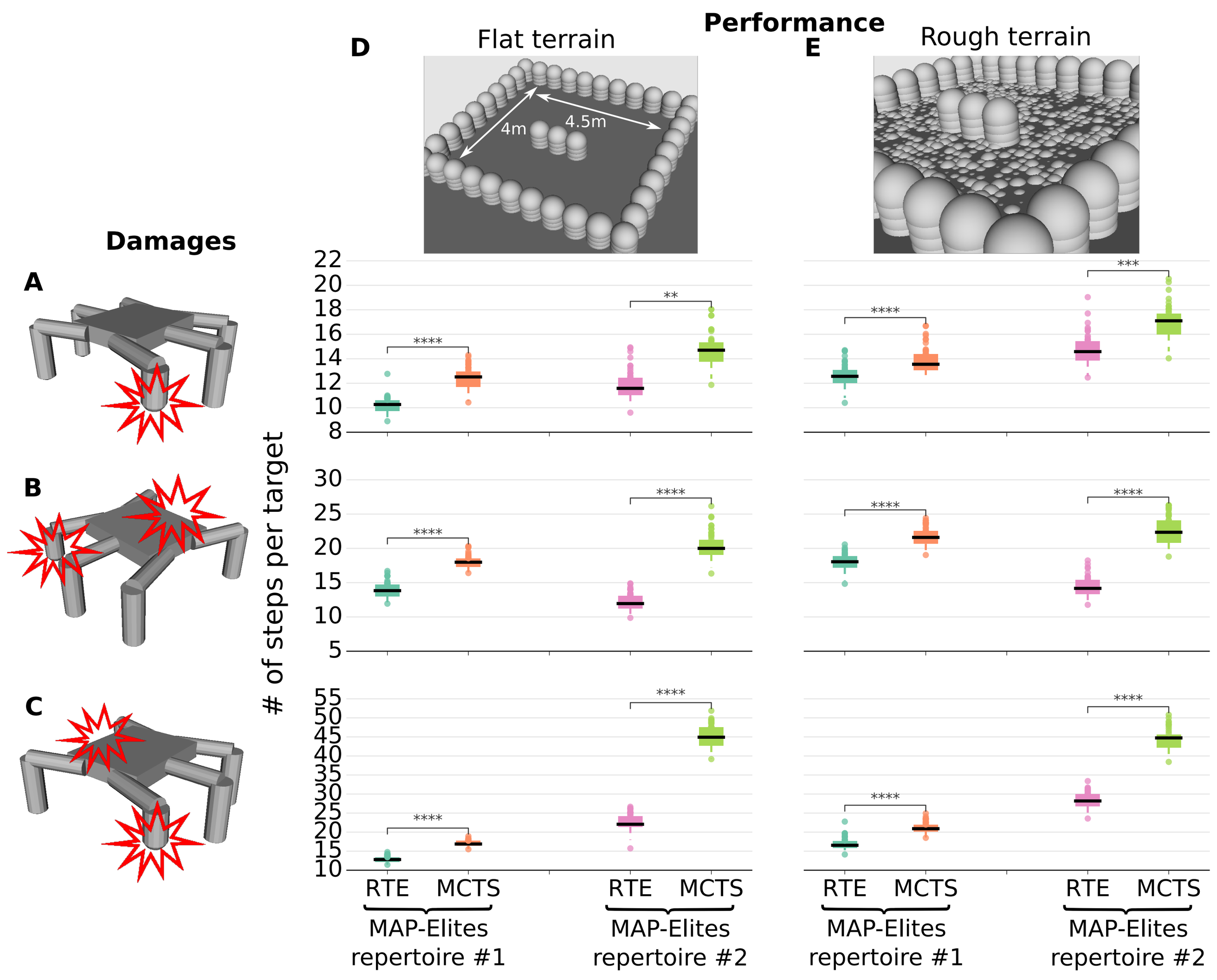

Black-DROPS: Black-box Data-efficient RObot Policy Search [4]

- Model-based (indirect) policy search.
- Exploit multiple cores to speed-up black-box optimizers.
- Use model uncertainty to increase data-efficiency.
- Remove constraints on type of policies and rewards.

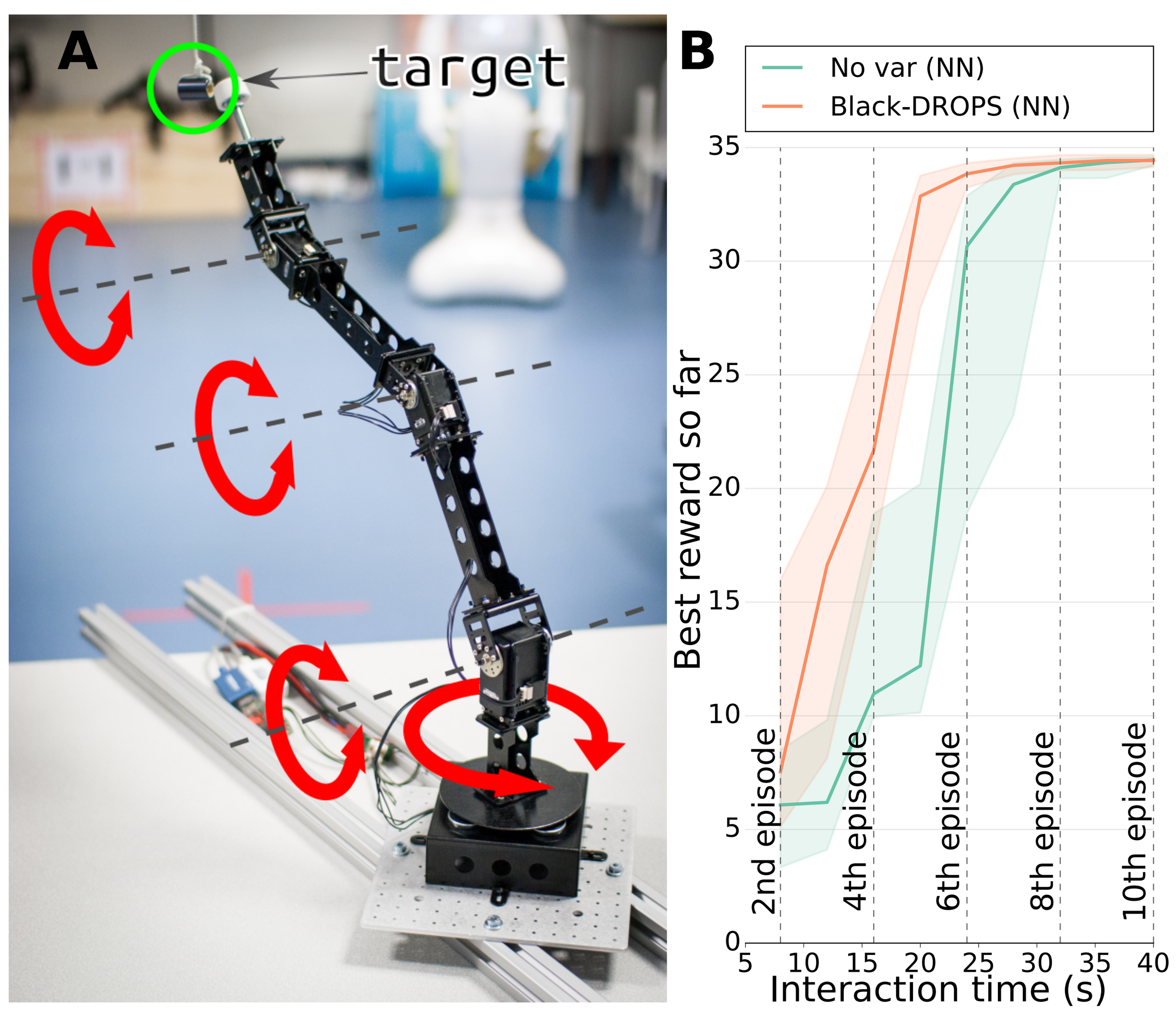

[1] A. Cully, J. Clune, D. Tarapore, and J.B. Mouret, "Robots that can adapt like animals", Nature, vol. 521, no. 7553, pp. 503–507, 2015.

[2] V. Papaspyros, K. Chatzilygeroudis, V. Vassiliades and J.B. Mouret, "Safety-Aware Robot Damage Recovery Using Constrained Bayesian Optimization and Simulated Priors". BayesOpt Workshop. NIPS 2016.

[3] K. Chatzilygeroudis, V. Vassiliades and J.B. Mouret, 2016. "Reset-free Trial-and-Error Learning for Data-Efficient Robot Damage Recovery". arXiv preprint arXiv:1610.04213.

[4] K. Chatzilygeroudis, R. Rama, R. Kaushik, D. Goepp, V. Vassiliades and J.B. Mouret, 2016. "Black-Box Data-efficient Policy Search for Robotics ". Submitted to IROS 2017.

APRIL 2017

Articulatory Speech Synthesis from Static Context-Aware Articulatory Targets

Anastasiia Tsukanova, Benjamin Elie, Yves Laprie

THE AIM is to develop an algorithm for controlling the articulators (the jaw, the tongue, the lips, the velum, the larynx and the epiglottis) to produce given speech sounds, syllables and phrases. This control has to take into account coarticulation and be flexible enough to be able to vary strategies for speech production.

THE SETUP a statistical vocal tract model with target-driven dynamics for articulatory synthesis and an acoustic simulation model.

THE DATA for the algorithm are 97 static MRI images capturing the articulation of French vowels and blocked consonant-vowel syllables.

EVALUATION is visual, acoustic and perceptual.

ARTICULATORY SPEECH SYNTHESIS

is a method of synthesizing speech by managing the vocal tract shape on the level of the speech organs – in contrast to the state-of-the-art speech synthesis methods that do not usually incorporate any articulatory information.

- It can provide insights into speech production.
- It can be used in language learning and language therapy.

The vocal tract can be modeled with geometric, biomechanical and statistical models. Statistical models may use very few parameters and hence speed up the computation time. On the other hand, having no guidance on what is realistic or physically possible, they are prone to mistakes.

THE ARTICULATORY SYNTHESIZER

has three components:

- the database with the "building blocks" for articulating utterances,
- the joint control algorithm for the vocal tract and the glottal source,
- an acoustic simulation system.

THE DATABASE

is inspired by the work of Birkholz (2013): it is 97 manually annotated MRI midsagittal images that capture articulation without phonation. In the consonant-vowel case (CV), the subject was tasked to take such a position as if he were about to start pronouncing the syllable, and in the case of a single vowel (V), as if he were in the middle of pronouncing it. There were 13 vowels, 72 CV syllables and 2 semi-vowels in the final dataset.

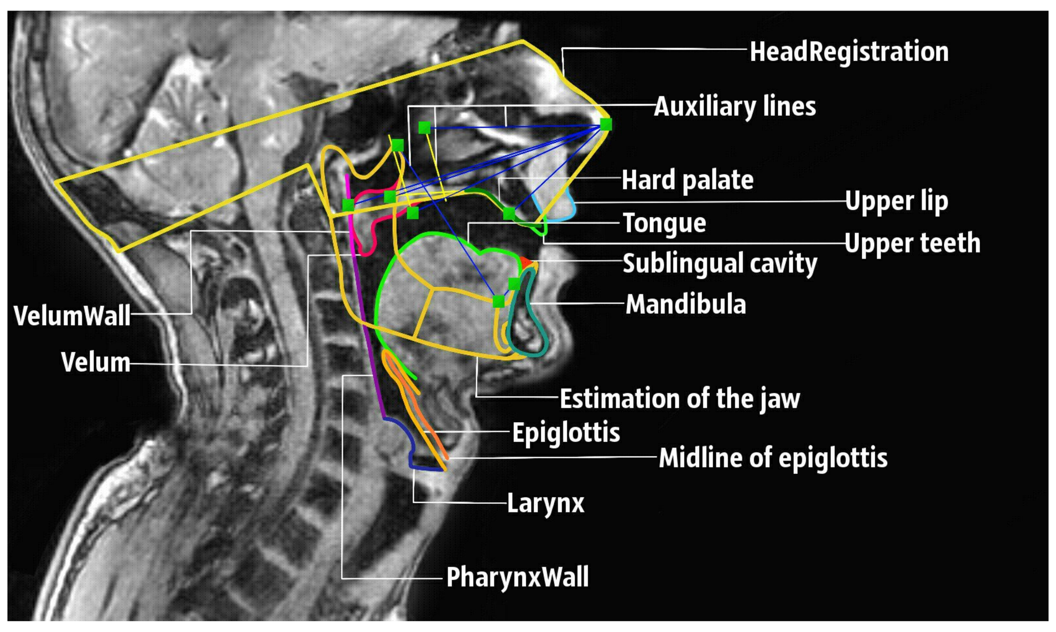

An example of annotating the data

THE ARTICULATORY MODEL

is principal-component-analysis-based (Laprie and Busset, 2011). Each articulator position is encoded in several parameters.

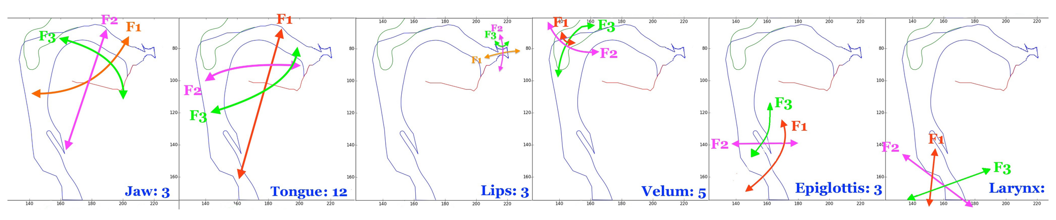

The first three principal components for each articulator

TO EXPAND THE DATASET

we derived the relationship between the cardinal vowels /a/, /i/ and /u/ and all other ones: the articulatory vectors of all other vowels were projected onto the convex hull of the vectors for /a/, /i/ and /u/.
Then we assumed that the relationship between the vectors /a/, /i/ and /u/ and, for example, /y/ must be the same as the one between /ba/, /bi/ and /bu/ and /by/, and derived, and derived the vectors for the missing CV-syllables in that way.

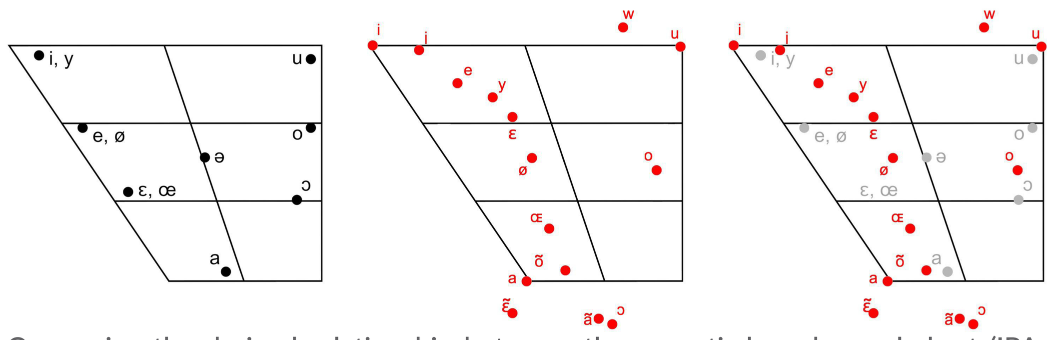

Comparing the derived relationship between the acoustic-based vowel chart (IPA, black and gray) and the articulatory-based one (red)

TO CHOOSE ARTICULATORY TARGETS

the algorithm assumes that there are several restrictions:

- Temporal: no coarticulatory effect if the anticipated phoneme is more than 200 ms ahead;
- Spatial: if there is any movement scheduled between the anticipated vowel and the phoneme in question, that negates the effect. For example, consider such sequence as /lki/: after /l/, the tongue needs to move backward to produce /k/ before coming back forward for /i/. In this situation, our algorithm does not allow the /l/ to anticipate the coming /i/;
- Segmental: it is not possible to anticipate a vowel more than 5 phonemes ahead, and this restriction becomes stricter if it applies across syllable boundaries.

TO TRANSITION BETWEEN THE TARGETS

- Linear / cosine approach: linear / cosine interpolation between the target vectors;
- Complex: cosine transitions vary by the articulators:
  - The heavy articulators move slower
  - The critical ones with a determinative contribution to the final sound intelligibility move to their target faster
  - If there is not enough time, at some point the target stops being pursued (target undershoot).

TO SIMULATE THE SOUND

the vocal tract shape was represented through area functions as follows: the acoustic simulation unit, the glottal chink model, was brought by Elie and Laprie (2016). It required coordinating the articulatory movements with the glottal control, which was modeled by using external lighting and sensing photo-glottography (ePGG) data. The glottis was modeled to be at its most closed position when producing vowels.

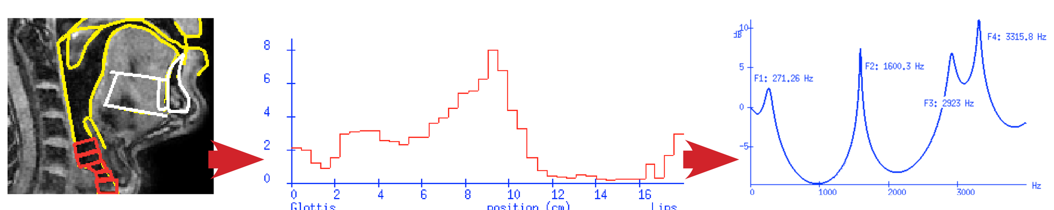

Representing the vocal tract through area functions and obtaining the sound

1. Birkholz, Peter (2013). "Modeling consonant-vowel coarticulation for articulatory speech synthesis". PloS one 8.4, e60603.
2. Elie, Benjamin and Yves Laprie (2016). "Extension of the single-matrix formulation of the vocal tract: Consideration of bilateral channels and connection of self-oscillating models of the vocal folds with a glottal chink". Speech Communication 82, pp. 85–96.
3. Laprie, Yves and Julie Busset (2011). "Construction and evaluation of an articulatory model of the vocal tract". EUSIPCO-2011.

EVALUATION

The articulatory model captured vocal tract positions correctly or with no critical errors, and some adjustments could be necessary only at the points of constriction, since the model was not guided by their acoustic impact. The movements were reasonable enough to produce a particular utterance. However, the rule-based timing strategy seems to be very rigid for the dynamic nature of speech; it would be more natural to follow speech production processes in humans and to guide the synthesis with the elicited sound or the speaker's expectation – based on their experience – on what this sound will be.

The glottal source control differentiates well between consonants and vowels; however, distinguishing between voiced consonants and their voiceless counterparts stays a point for improvement.
Vowels and voiced stops were the most identifiable and correct. The most notable difference is the timing of formant transitions; this highlights the utmost importance of realistic timing strategies.

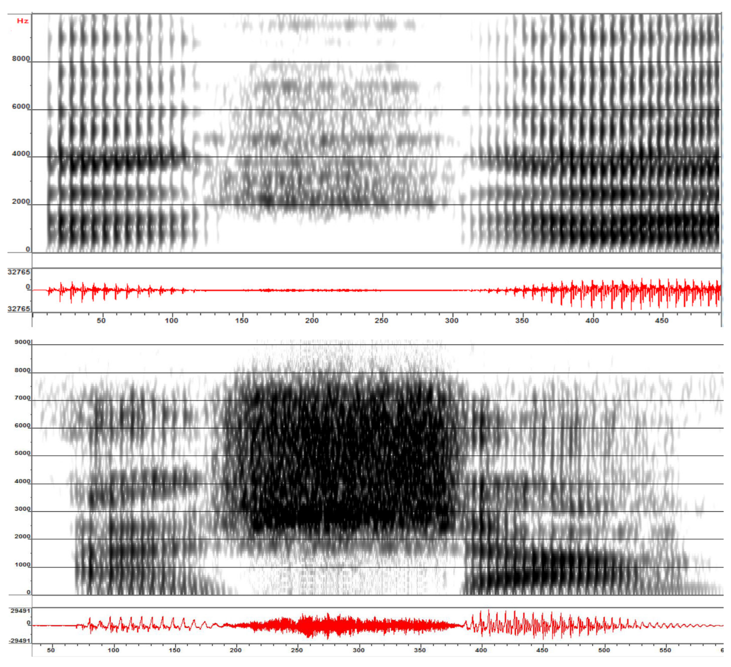

An example of synthesis of /aʃa/, not guided by the timing information (above), and the same utterance by a human (below).

CONCLUSION

Regarding speech as a process of transitioning between context-aware targets can be connected with the mental processes of speech production. However, the algorithm solves a static problem, laid out in full; it needs to hit particular targets in a given order, whereas humans solve a dynamic problem, where coarticulation is a means to make the problem of reaching too many targets in a too short period of time solvable.

The statistically derived articulatory model encodes complicated shapes of the articulators in only 29 parameters, sometimes struggling at the constrictions because of the inherent – and intentional – lack of control over the resulting geometry of the vocal tract.
Theoretically, the trajectory transitions are phonetically sound. Whether there are any important differences between those movements and articulation in real speech, needs to be verified with actual dynamic data. The timing strategies, currently rule-based, apparently need to be extracted from dynamic data.

A closer, intertwined interaction with the acoustic simulation unit – such as guidance on how to navigate between the area functions at the level of separate acoustic tubes and improved control over the glottal opening – could improve the results for consonants.

anastasiia.tsukanova@inria.fr benjamin.elie@inria.fr yves.laprie@loria.fr LORIA, INRIA / CNRS / Université de Lorraine, Nancy, France

MULTISPEECH Speech Modeling for Facilitating Oral-Based Communication · Loria · Inria · CNRS · UNIVERSITÉ DE LORRAINE · IAEM

Analyse sur les espaces singuliers et algèbres d'opérateurs.

Problème à N-corps et C^*-algèbres

Jérémy Mougel.
Directeur de thèse : Victor Nistor.
Université de Lorraine, IECL.
E-mail: jeremy.mougel@univ-lorraine.fr

Introduction

Motivation

L'opérateur de Hamilton ou Hamiltonnien H est un opérateur lié à l'énergie du système et permettant de décrire en partie son évolution. Par exemple, en mécanique quantique il permet de construire l'opérateur d'évolution $U(t,t_0)$ entre un temps de départ t_0 et t. Pour un état f, on a (à constante près)

$$U(t,t_0)(f) = \exp(iH(t-t_0))(f).$$

Plus précisément, si on part d'un état f au temps t_0, la mesure d'un observable A (comme la vitesse ou la position) après un t est lié à la densité de probabilité induit par A et $U(t,t_0)f$.
L'étude du spectre du spectre de H permet de trouver les états stables (liés aux valeur propres) et les états libres du systèmes (liés aux spectre essentiel).

Contexte

Un des objectifs de ma thèse est d'étudier un opérateur H_0 modélisant après quelques simplifications physique (comme le fait qu'on néglige les champs magnétiques) l'énergie du problème à N-corps. Pour une fonction $f : X \to \mathbb{C}$ où $X = \mathbb{R}^{3N}$ et $x = (x_i)_{i=1,...,N} \in X$, l'opérateur H_0 est défini par :

$$H_0 f(x) = -\Delta f(x) + \left(\sum_{1\le i\le n} \frac{1}{||x_i||} + \sum_{1\le i<jn} \frac{1}{||x_i - x_j||} \right) \times f(x) \quad (1)$$

Résultat principal :

En poursuivant les travaux de Georgescu et Nistor dans [2] , nous avons obtenu dans [3] la décomposition du spectre essentiel suivante :

$$Sp_{ess}(H_0) = \bigcup_{\alpha\in\mathbb{S}_X} Sp(\tau_\alpha \rtimes X(H_0)) \quad (2)$$

où les $\tau_\alpha \rtimes X$ peuvent être pensées comme des limites le long des demi-droites de la compactification sphérique.

Déroulement du raisonnement

Approche par les C^*-algèbres

Principe

On peut résumer l'écriture de H_0 par :

$$H_0 = -\Delta + \sum_{1\le i\le n} \frac{1}{||x_i||} + \sum_{1\le i<jn} \frac{1}{||x_i - x_j||} \quad (3)$$

Plus généralement, les Hamiltoniens avec potentiel (la fonction V) sont de la forme :

$$H = -\Delta + V \quad (4)$$

Une approche du à Georgescu et Damak dans [1] est de construire un espace de fonctions A tel que :

- L'ensemble des Hamiltoniens $H = -\Delta + V$ avec $V \in A$ contient l'opérateur H_0.
- L'espace A est une C^*-algèbre.

Construction de la C^*-algèbre : $\mathcal{E}_\mathcal{S}(X)$

On considère une famille $\mathcal{S}$ de sous-espaces vectoriels de l'espace X. On définit alors $\mathcal{E}_\mathcal{S}(X)$ par :

$$\mathcal{E}_\mathcal{S}(X) =< \mathcal{C}(\overline{X/Y}), Y \in \mathcal{S} > \quad (5)$$

En d'autres termes, $\mathcal{E}_\mathcal{S}(X)$ est la C^*-algèbre des fonctions continues sur la compactification sphérique des espaces quotients de X par tous les $Y \in \mathcal{S}$. Dis plus simplement, $\mathcal{E}_\mathcal{S}(X)$ est un espace de fonctions regroupant toutes les fonctions continues sur les quotients X/Y et possédant des limites le long de chaque demi-droite partant de l'origine. En particulier, $\mathcal{E}_\mathcal{S}(X)$ contient le potentiel de H_0.

Utilisation d'une famille exhaustive

Propriété de décomposition spectrale des familles exhaustives

Dans [4], les auteurs ont introduit le concept de famille exhaustive et on montré la propriété de décomposition spectrale suivante : Si $(\phi_i)_{i\in I}$ est une famille exhaustive de la C^*-algèbre A alors :

$$\forall a \in A, \quad Sp(a) = \bigcup_{i\in I} Sp(\phi_i(a)) \quad (6)$$

Construction d'une famille exhaustive

Pour chaque $\alpha \in \mathbb{S}_X$ qui correspond au point $a \in S^{n-1}$, on considère la translation par a des éléments de A :

$$\tau_a(f)(x) = f(x+a) \quad (7)$$

On translate de la fonction f dans la direction de a pour une distance de 1. La famille exhaustive agira sur les fonctions également par translation mais cette fois par une distance infinie. On définit cette translation à l'infini par

$$\tau_\alpha(f)(x) = \lim_{r\to+\infty} \tau_{ra}(f(x)) = \lim_{r\to+\infty} f(x+ra) \quad (8)$$

Extension au produit croisé

Afin de pouvoir étudier directement l'opérateur H_0 et non pas simplement son potentiel, il faut enrichir l'algèbre $\mathcal{E}_\mathcal{S}(X)$ en prenant son produit croisé : $\mathcal{E}_\mathcal{S}(X) \rtimes X$. Puis on étend τ_α de manière naturelle à $\mathcal{E}_\mathcal{S}(X) \rtimes X$ et cette extension sera notée $\tau_\alpha \rtimes X$.

Quotient par les compacts

On peut montrer que la famille $(\tau_\alpha \rtimes X)_{\alpha\in\mathbb{S}_X}$ est exhaustive pour la C^*-algèbre :

$$(\mathcal{E}_\mathcal{S}(X) \rtimes X)/(\text{Opérateurs compact}). \quad (9)$$

Le fait de quotienter par les opérateurs compacts revient à enlever les valeurs propres des opérateurs, c'est pour cela qu'on a un résultat sur le spectre essentiel.

Conclusion

Pour finir, on applique ensuite la propriété de décomposition spectrales des familles exhaustives (6) à la C^*-algèbre (9) qui contient (dans un certains sens) H_0 et on a le résultat annoncé :

$$Sp_{ess}(H) = \bigcup_{\alpha\in\mathbb{S}_X} Sp(\tau_\alpha \rtimes X(H_0))$$

Travaux en cours:

- Par soucis de clarté, je n'ai pas donné les conditions qu'on imposait sur la famille $\mathcal{S}$ de sous-espaces vectoriels. Cependant, un de mes projets est de comprendre l'algèbre $\mathcal{E}_\mathcal{S}(X)$ pour n'importe quelle famille $\mathcal{S}$.
- Remplacer l'espace euclidien X par un groupe et la famille $\mathcal{S}$ par une famille de sous-groupe et essayer d'obtenir le même genre de résultat.
- Mieux comprendre les algèbres $\mathcal{E}_\mathcal{S}(X)$ et $\mathcal{E}_\mathcal{S}(X) \rtimes X$ afin de remplacer le $-\Delta$ du H_0 par des opérateurs de dérivations plus exotiques.

Objets et constructions utilisés:

1. C^*-algèbres: Une C^*-algèbre est une algèbre de Banach munie d'une involution "$*$" qui est compatible avec la norme et la structure d'algèbre:
$$\forall a,b \in A, \lambda \in \mathbb{C}, \quad (ab)^* = b^*a^*, (\lambda a)^* = \overline{\lambda}a^* \text{ et } ||aa^*|| = ||a||^2$$
Exemple : $\mathcal{C}(X)$, les fonctions continues sur un espace compact muni de la norme infinie et de l'involution est définie par la conjugaison complexe point par point.
2. Spectre d'un opérateur. Pour un opérateur H, son spectre $Sp(H)$ est défini par :
$$Sp(H) := \{\lambda \in \mathbb{C} \text{ tel que } H - \lambda \text{ n'est pas inversible } \} \quad (10)$$
Dans le cas où l'opérateur est une matrice carrée sur $\mathbb{R}$ ou $\mathbb{C}$, le spectre correspond à l'ensemble des valeurs propres. Quant au spectre essentiel Sp_{ess}, il est justement défini comme le spectre privé des valeurs propres.
3. Compactification sphérique : Prenons le cas du plan $\mathbb{R}^2$:
A chaque demi-droite partant de l'origine, on associe un point à l'infini qui est "l'extrémité infinie" de la demi-droite. Chaque demi-droite coupe en un point unique le cercle unité, on peut donc indexer l'ensemble des points à l'infini par le cercle unité S^1.
On peut généraliser cette construction à n'importe quel espace vectoriel réel de dimension finie X. Si on note $\overline{X}$ la compactification sphérique de X, en tant qu'ensemble on obtiendra $\overline{X} = X \cup \mathbb{S}_X$ avec $\mathbb{S}_X \simeq S^{n-1}$ où n est la dimension de X.
4. Famille exhaustive : Soit Ω un espace compact et $(\phi_i)_{i\in I}$ une famille de morphisme de $C(\Omega) \to \mathbb{C}$. Une telle famille est dite exhaustive si elle vérifie la propriété suivante :
$$\forall \omega \in \Omega, \exists i \in I \text{ tel que } \{f \in \mathcal{C}(\Omega), f(\omega) = 0\} \subset Ker(\phi_i) \quad (11)$$
Un exemple simple est de prendre la famille des évaluations en chaque point : $(ev_\omega)_{\omega\in\Omega}$ définit par $ev_\omega(f) = f(\omega)$.
5. Produit croisé : La notion de produit croisé est assez technique. Dans notre cas, elle permet d'ajouter des opérateurs de dérivations en plus des opérateurs de multiplication par des potentiels déjà présents dans l'algèbre $\mathcal{E}_\mathcal{S}(X)$.

References

[1] M. Damak and V. Georgescu. Self-adjoint operators affiliated to C^*-algebras. *Rev. Math. Phys.*, 16(2):257–280, 2004.

[2] V. Georgescu and V. Nistor. The essential spectrum of N-body systems with asymptotically homogeneous order-zero interactions. *C. R. Math. Acad. Sci. Paris*, 352(12):1023–1027, 2014.

[3] V. Nistor J. Mougel and N. Prudhon. A refined hvz theorem for asymptotically homogeneous interactions : the finite lattice case. à paraître dans revue roumaine de mathématiques pures et appliqués, Simion Stoilow Institute of Mathematics.

[4] V. Nistor and N. Prudhon. Exhausting families of representations and spectra of pseudodifferential operators. preprint [math.OA], http://arxiv.org/abs/1411.7921, to appear in J. Oper. Theory.

ECOLE DOCTORALE IAEM LORRAINE

Analyse spatiale multi-échelle : Relations entre signaux issus de micro et macro-électrodes

TRAN Harry

Directeurs de thèse : Valérie LOUIS-DORR, Radu RANTA

Encadrant de thèse : Steven LE CAM

OBJECTIF :
Séparation des composantes locales, propagées et des potentiels d'action (AP)

Validation mutuelle

OBJECTIF :
Validation des méthodes d'analyse sur des signaux simulés

La *local field potential (LFP)* est un signal basse fréquence (0-400Hz) traduisant l'activité synaptique des neurones. Son étude permet de mieux comprendre le fonctionnement les maladies neuronales.

Problématique

- Deux signaux enregistrés à différentes échelles par deux types d'électrodes : x_{micro} (micro-électrode) et x_{seeg} (macro-électrode)
- **Pourquoi les séparer ? Pour étudier une causalité entre les potentiels d'action et la LFP.**

Modèle :

$$x_{micro} = LFP_{macro} + LFP_{micro} + APs + \varepsilon$$
$$x_{seeg} = LFP_{seeg} + \varepsilon$$

Avec

LFP_{macro}	Activité de neurones (propagée venant des synapses)		
LFP_{micro}	Activité de neurones (locale)	APs	Potentiels d'action (locaux)
x_{micro}	Signal provenant des micro-électrodes	ε	Bruit
x_{seeg}	Signal provenant des macro-électrodes		

Objectifs :

1. Identifier LFP_{macro} à l'aide de LFP_{seeg}
2. Détecter, extraire et classifier les APs
3. Identifier les relations APs ⟷ LFP_{macro}

Lors de la 2ème année, notre travail s'est porté sur l'amélioration de la détection des APs.

Pré-traitement des signaux : méthode de débruitage

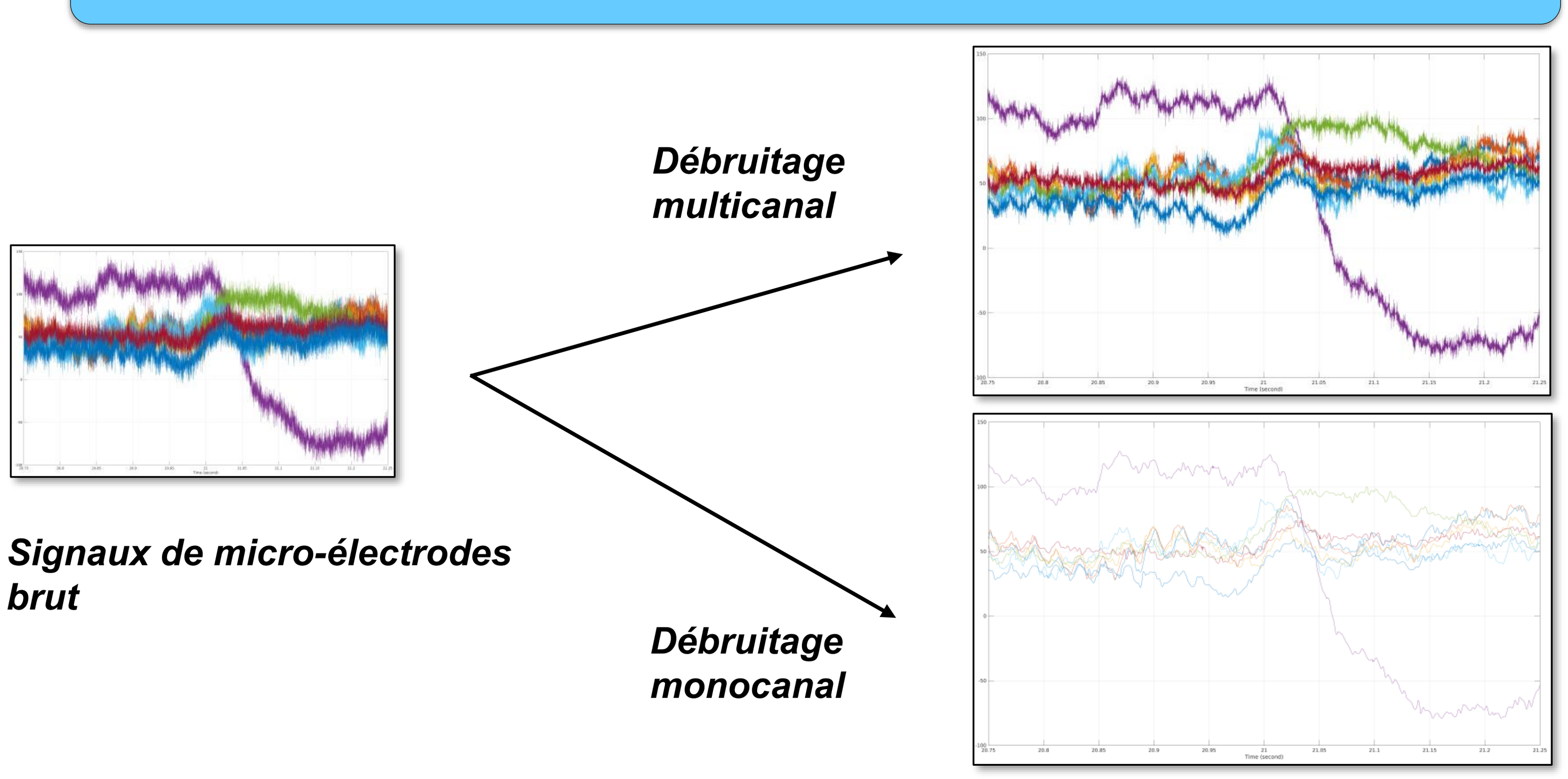

- Pourquoi le débruitage multicanal ? [Oweiss2001]

Cela permet de conserver de l'information au niveau des APs.

Potentiels d'action : Détection, analyse et classification

- Analyses des APs : plusieurs types d'APs présents sur un seul canal de micro-életrodes

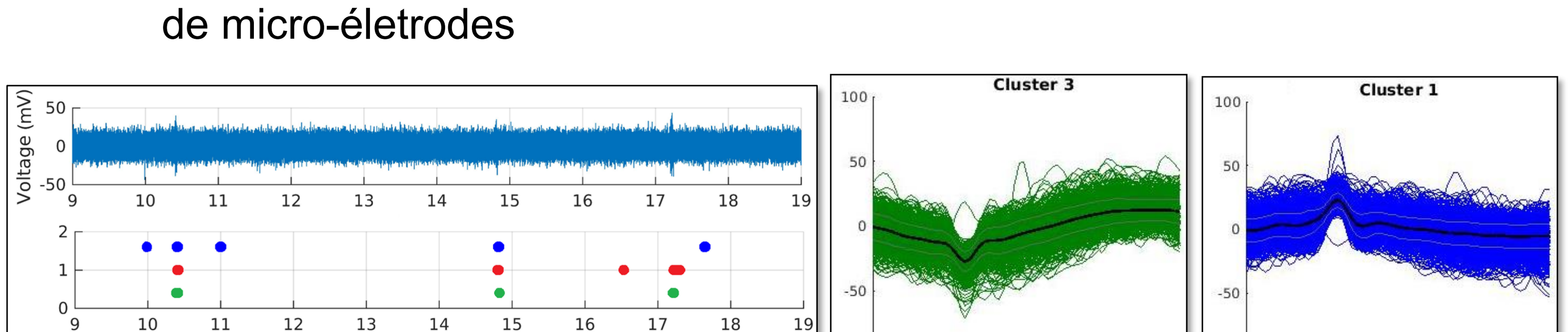

Equation de la *local field potential* : $\phi_{LFP} = \frac{1}{4\pi\sigma} \sum_{n=1}^{Sources} \frac{I_n(t)}{r_n}$

Avec

I_n	Courant généré par la source (neurone)
r_n	Distance entre le neurone et l'électrode
σ	Conductivité du milieu

Simulation de signaux réalistes

- Outil de simulation : VERTEX [Tomsett2014]
- Activité d'une grande population de neurone possible (>100.000)
- Modélisation compartimentale des neurones
- Dynamique implémentée : modèle AdEX (*Adaptative exponential integrate-and-fire*)
- Inconvénient : forme d'onde des APs non simulée !

Figure : Géométrie d'un neurone pyramidal

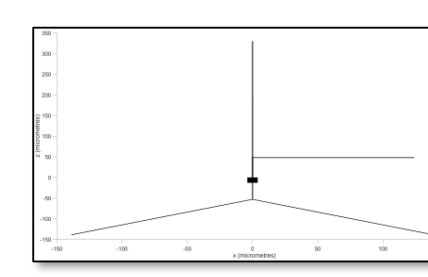

- Lors de la 2ème année, nous nous sommes familiarisés avec l'outil et nous sommes en train de le patcher en intégrant la dynamique de Hodgkin-Huxley dans VERTEX.
- Pourquoi ? Pour obtenir des signaux x_{micro} avec des APs réalistes

Figure : Configuration des micro et macro-électrodes

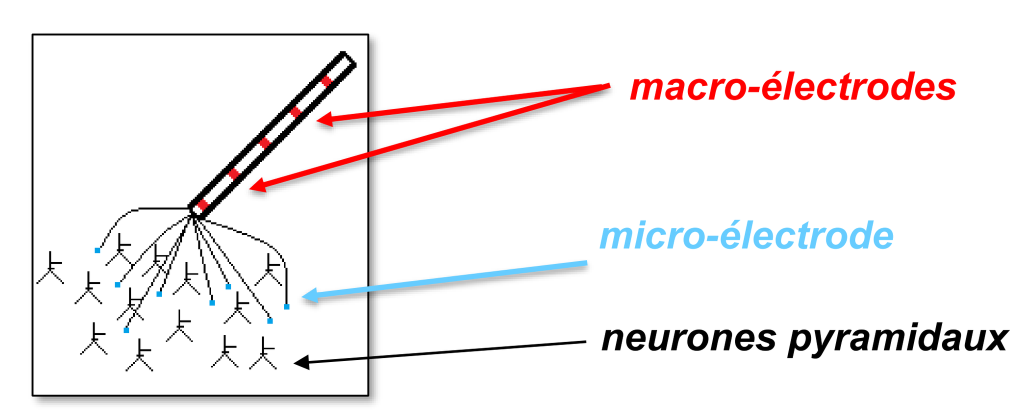

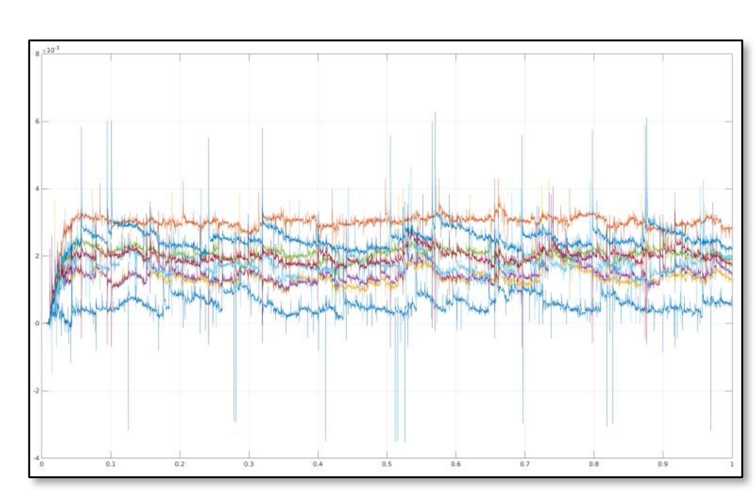

Figure : Signaux de micro-électrodes
Unités : abscisse (seconde)
ordonnée (mV)

Perspectives

- Application des méthodes de séparation multicanale entre composantes locales et propagées sur signaux simulés
- Evaluation des relations entre *spikes* et LFP_{micro} (extension de la *spike-triggered average* [zanos2011])

Références

Oweiss, K. G. et al. (2001). Noise reduction in multichannel neural recordings using a new array wavelet denoising algorithm. *Neurocomputing*, *38*,

Tomsett, R. J., et al.. (2015). Virtual Electrode Recording Tool for EXtracellular potentials (VERTEX): comparing multi-electrode recordings from simulated and biological mammalian cortical tissue. *Brain Structure and Function*, *220*(4), 2333-2353.

Zanos, T. P. et al. (2011). Removal of spurious correlations between spikes and local field potentials. *Journal of neurophysiology*, *105*(1), 474-486.

MongoDB I/O access patterns are under the microscope

Abdulqawi Saif[1,2,3,4], Lucas Nussbaum[1,2,3] and Ye-Qiong Song[1,2,3]
{first name.last name}@loria.fr
[1] Université de Lorraine [2] Inria Nancy Grand Est [3] CNRS, LORIA - UMR 7503 [4] Xilopix SAS

I. Context

- *MongoDB* is a **document-based *NoSQL*** database
- *NoSQL* databases store **semi-structured and/or unstructured data**
- We need to **create indexes** to optimize querying data
- Based on certain industry reports, ***MongoDB* takes unjustified time to create indexes over a pre-stored data**
- Benchmarks report **high-level results** in general, they also use synthetic data ($\neq$ in-production data)

II. Objectives

- **Investigation on creating indexes** by *MongoDB*
- Introducing **new experimental methods** that could go beyond benchmarking high-level results

III. Experimental settings

- A data set of **20 million doc.** is created; about 71 *GB*

- Experiments are performed on **Grid'5000 testbed**
- Ubuntu 14.04, Linux 4.9.13
- Tests are performed on **one HDD per machine**
- *MongoDB V3.4*, replicas are disabled, hash sharding, sharding on $\_id_s$
- *MongoDB* storage engine (WT) stores each collection on a **separate file**

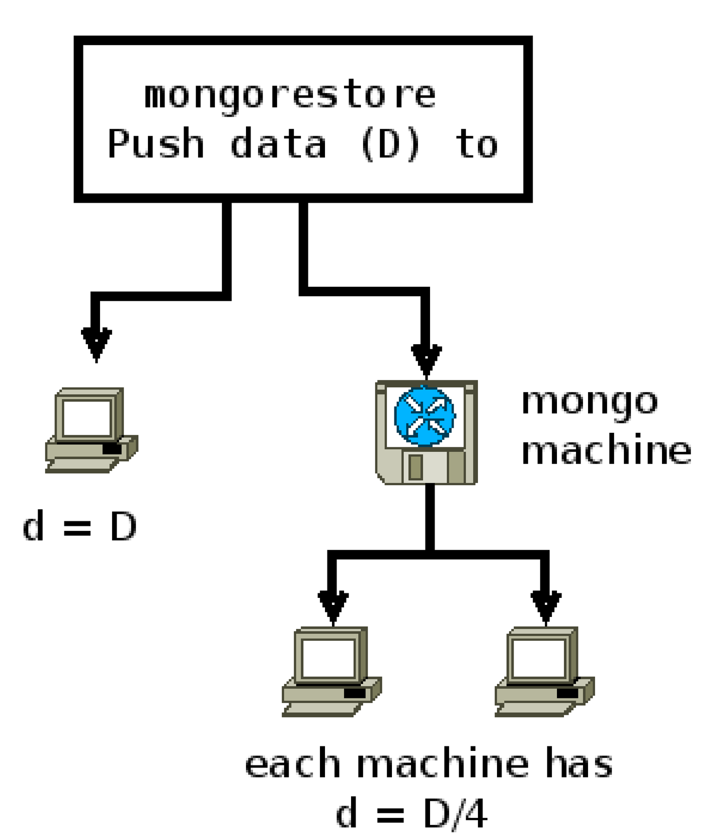

Worklaod: try to index a simple field (int)
Experimental scenarios

IV. Performance results

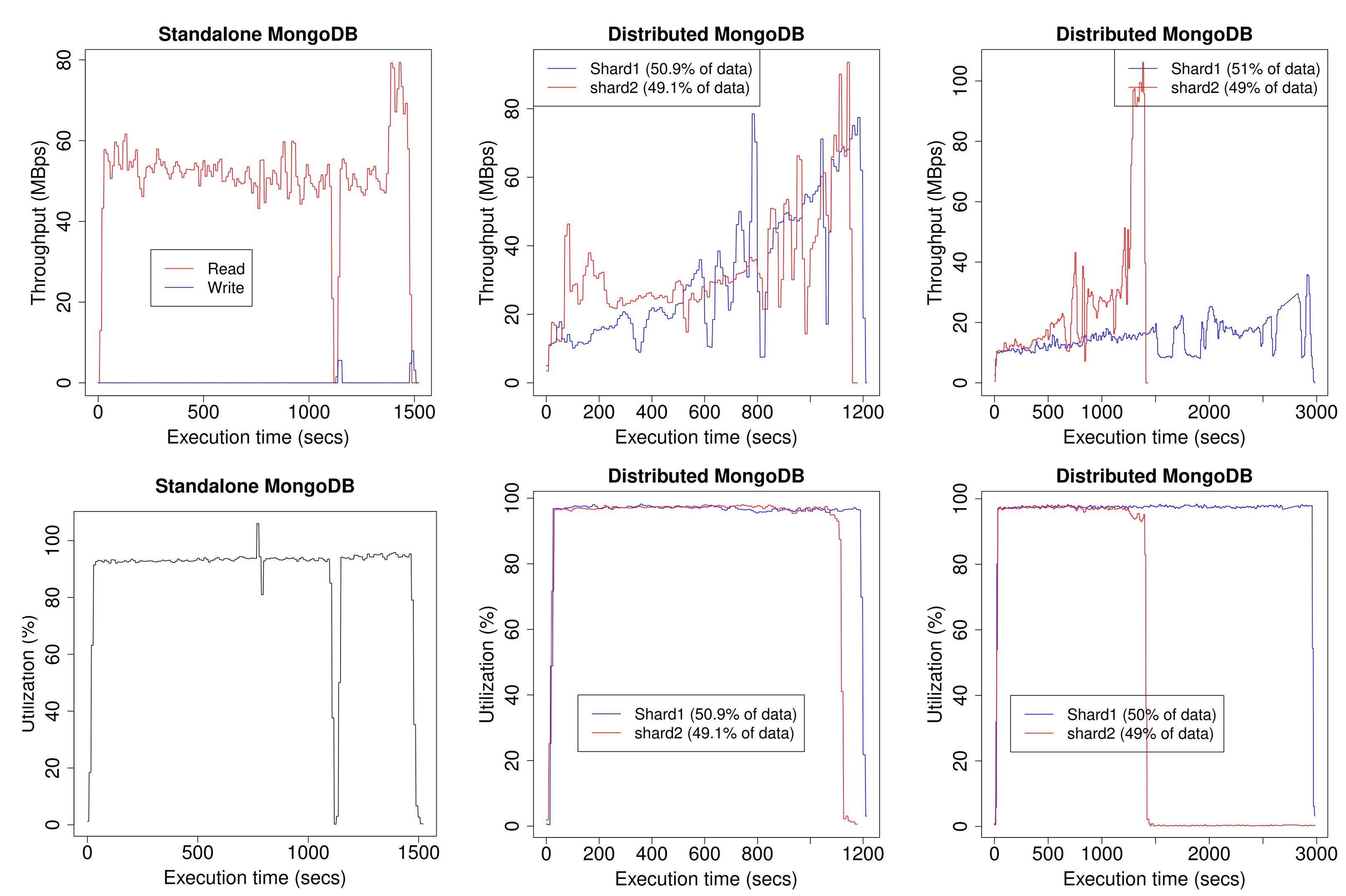

Standalone throughput & disk util. Two shards throughput & disk util. Two shards (another execution)

- **Data distribution is poorly done** by *MongoDB*
- Every Shard uses a **different plan** for accessing data

How to get the main raison behind these results?

V. extended Berkeley Packet Filter (*eBPF*)

- It is a recent **dynamic tracing technique** in *Linux*
- It could connect to **all *Linux* data sources**
- Very negligible overhead (4 ns per syscall)
- **Fits with systems in production**

An *eBPF* tool is built to evaluate the I/O access patterns:

- A **generic tool**, could be used by other systems
- It traces **all I/O requests**
- It reports **offsets, request latencies & data size**
- Its results could be filtered by **accessed files**

VI. I/O access patterns using *eBPF*

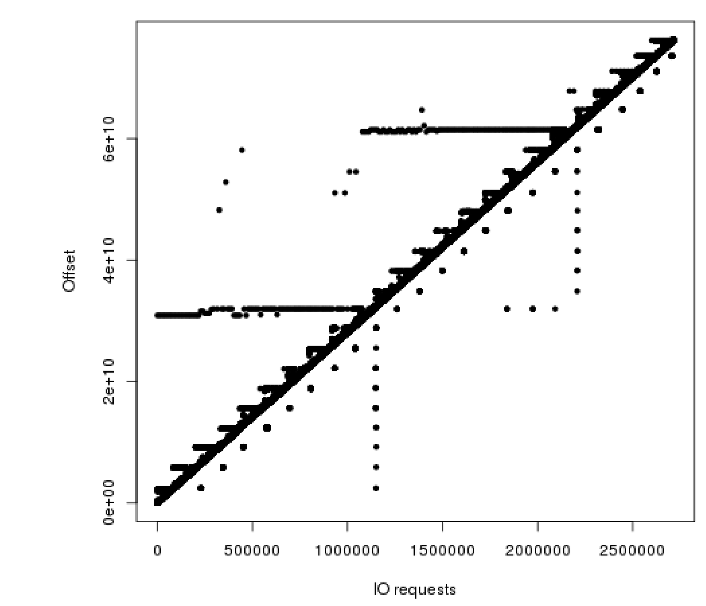

I/O access pattern on standalone

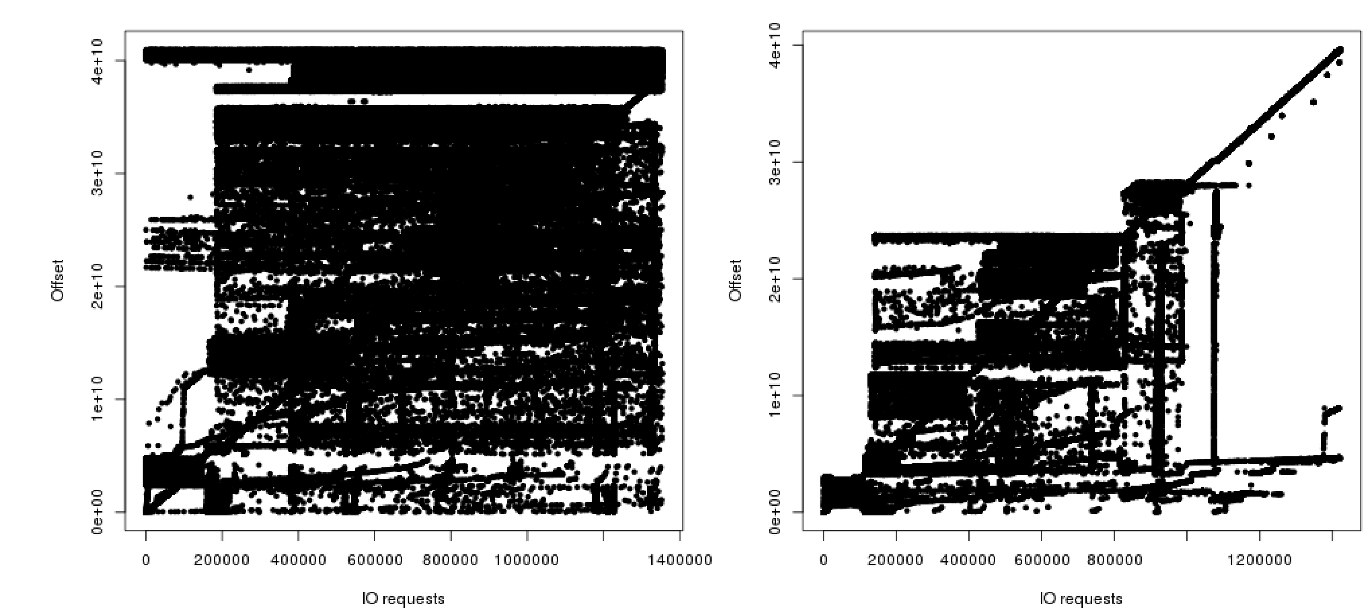

Tow shards I/O access patterns (Every shard has 50% of data

VII. Conclusion

- A **performance study on *MongoDB*** I/O access pattern is done
- A **generic *eBPF* tool for testing I/O access patterns** is developed
- A new **experimental method to go beyond benchmarking results** is introduced

Acknowledgment

This work is partially funded by the ***Xilopix SAS***, a French startup which is behind ***Xaphir*** search engine.

Robots that learn to control the physical interaction with humans

Oriane Dermy (https://members.loria.fr/ODermy/)
Supervisors: François Charpillet and Serena Ivaldi
LARSEN Team, Inria Nancy, France
Université de Lorraine, LORIA, UMR 7503, France

1) Objectives: a robot able to reach autonomously the body position desired by its partner

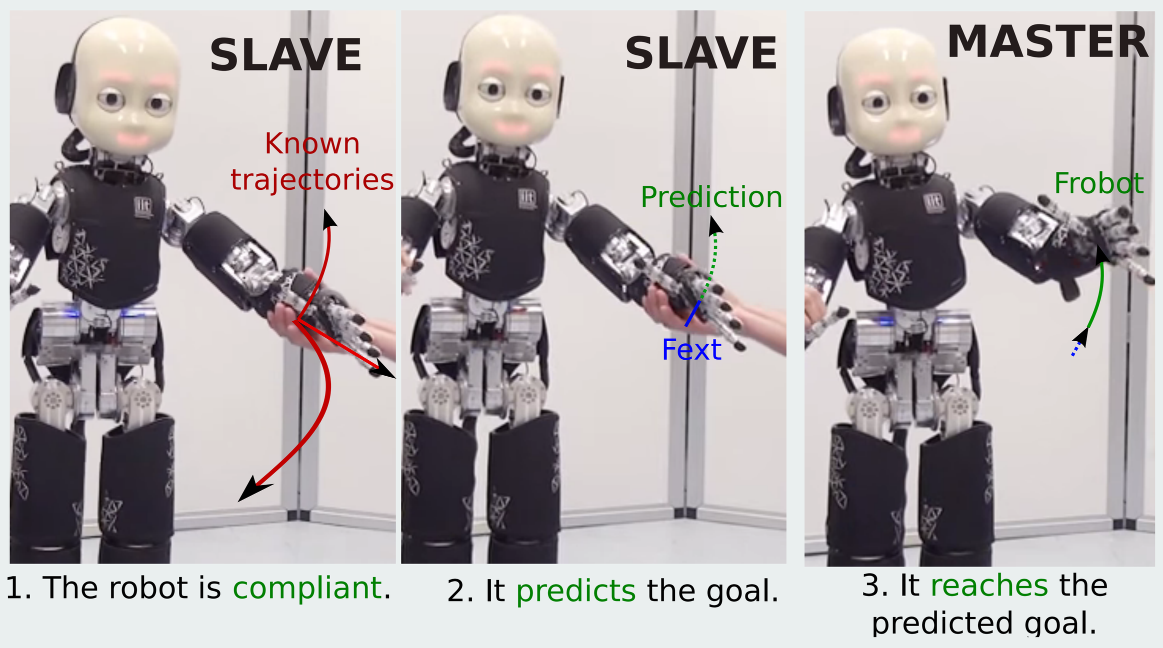

Not requiring its partner's guidance to the end.

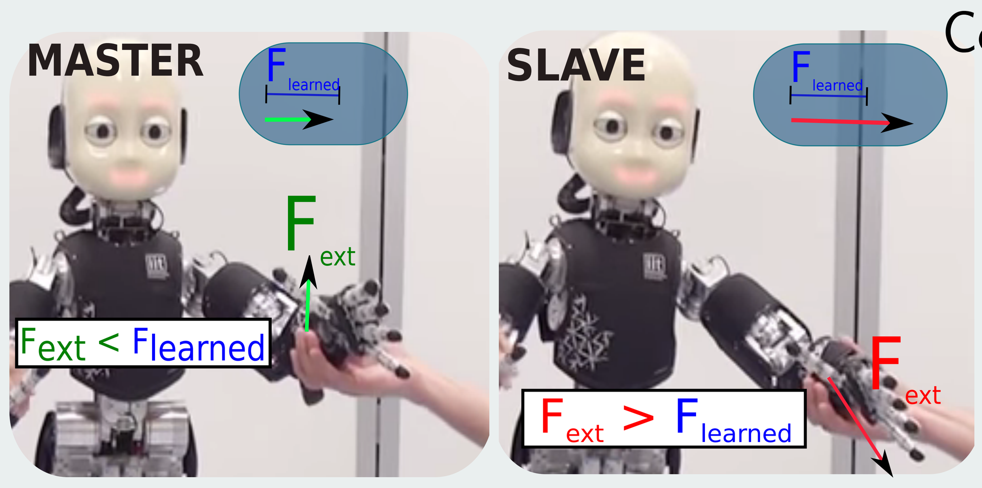

Staying alert to its partner's desires using forces information (next work).

Toolbox: WholeBodyDynamics (dynamics), Intraface
Communication between softwares: YARP.

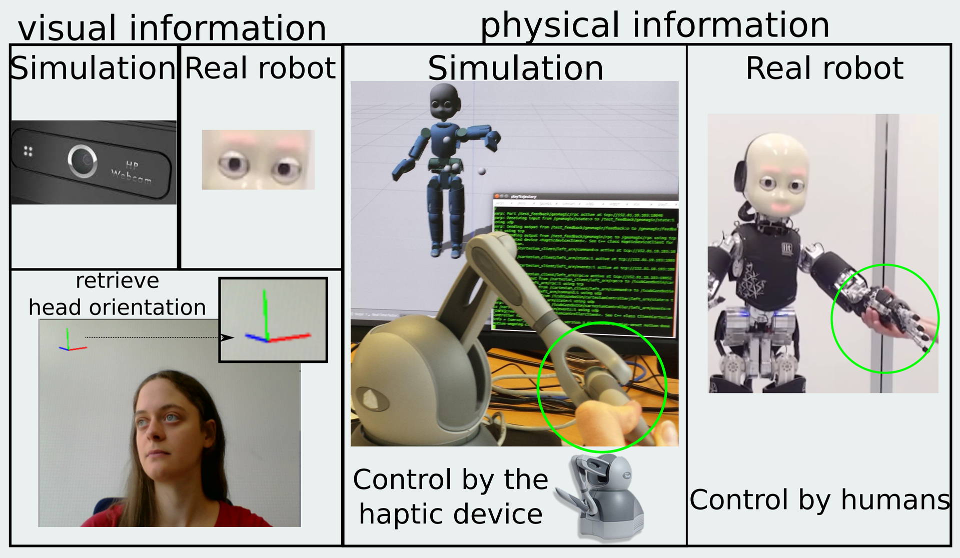

Using different modality to predict the intention.

2) Method scheme: multi-modal learning.

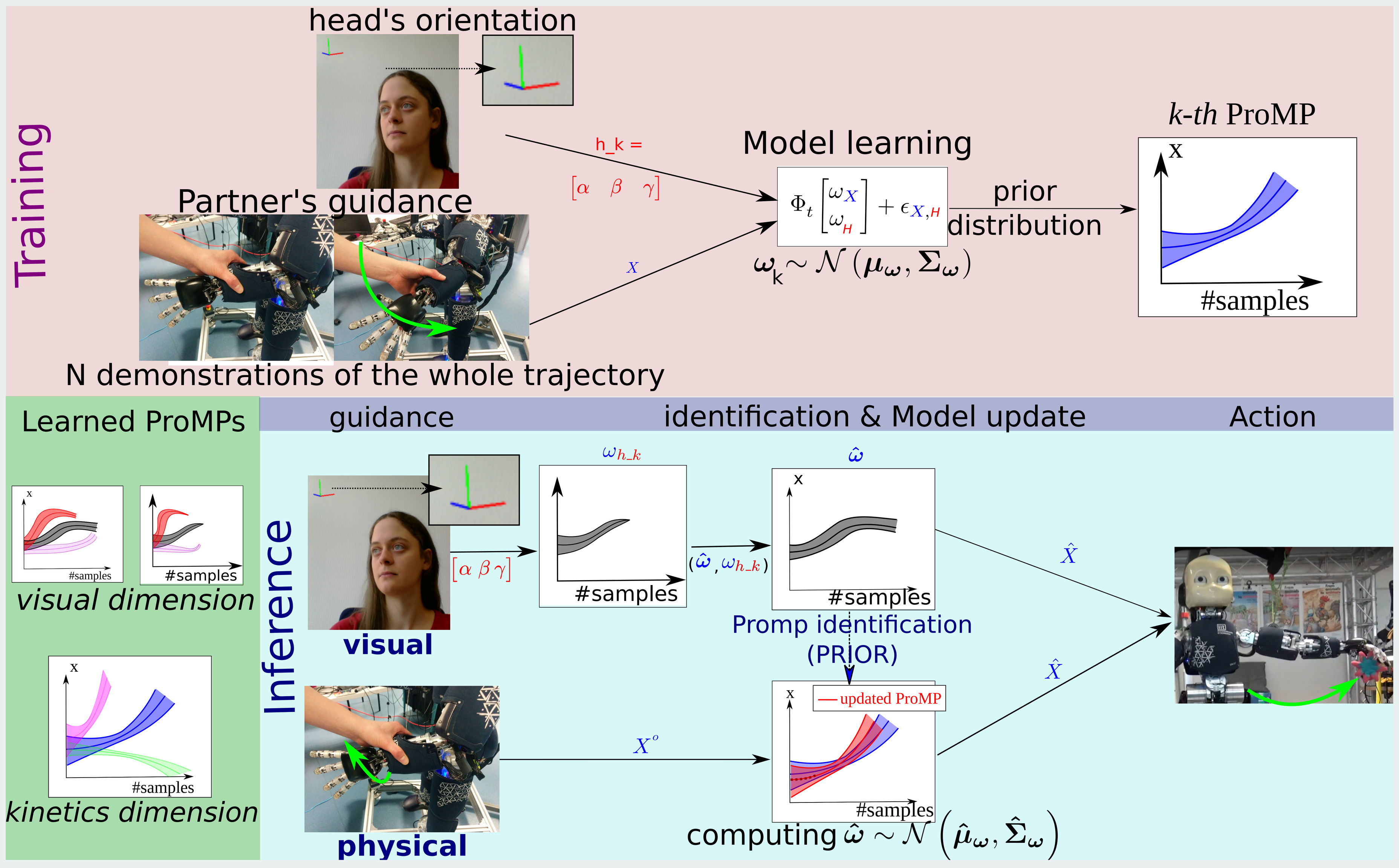

- 1st: arm movement learning.
- 2nd: whole body movement learning

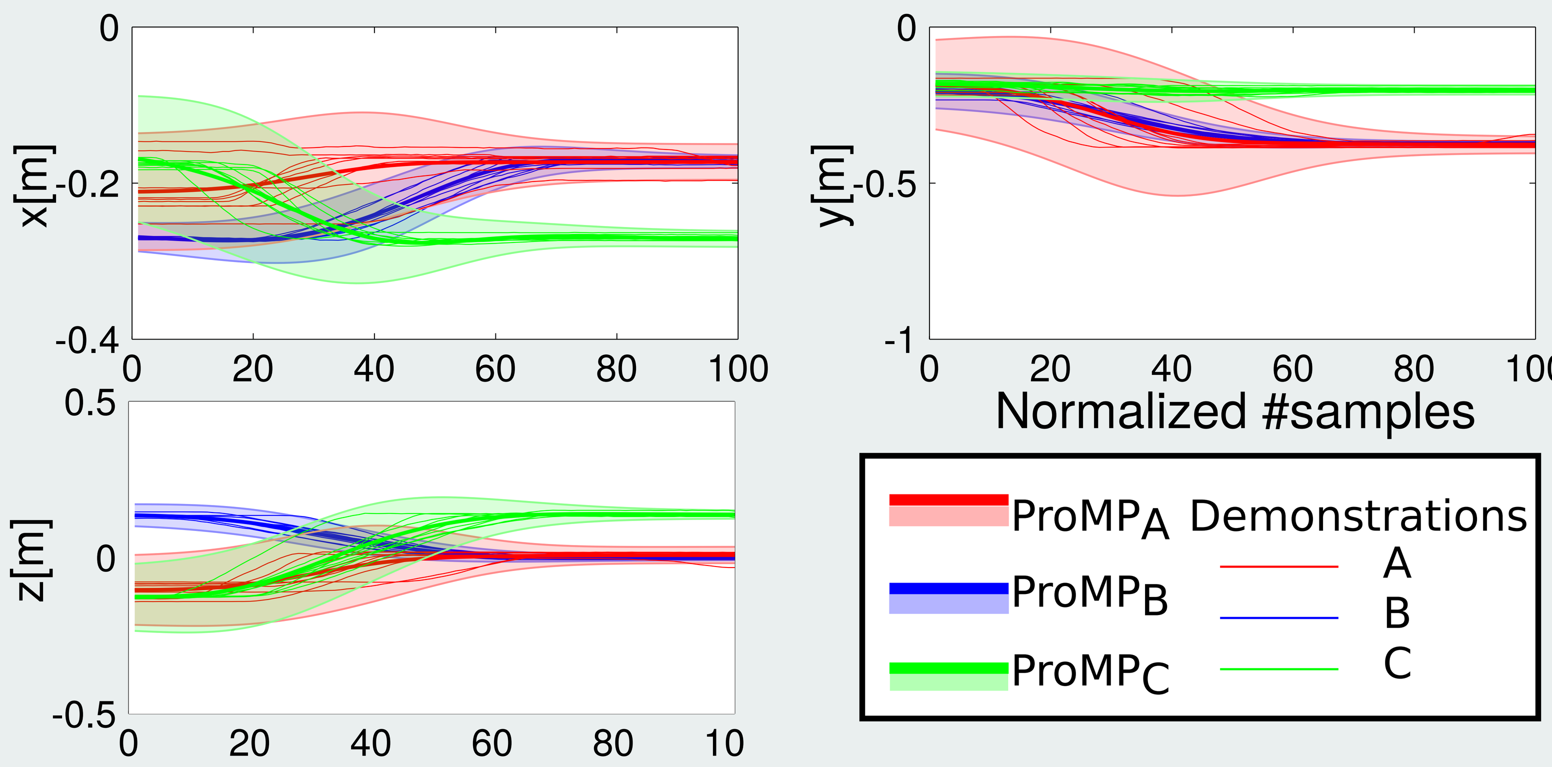

Example of Cartesian distribution learning.

4) Learning method: Probabilistic Movement Primitives (ProMPs) [2]

Bayesian parametric model

$y_t = \begin{bmatrix} X_t \\ F_t \end{bmatrix} = \Phi_{\alpha t}^{\top}\omega + \epsilon_y$

- y_t vector of variables to learn
- $\Phi_{\alpha t}$ diagonal matrix of RBFs scattered across time
- ω parameters vector
- e_y Gaussian noise of data.

Learning

* Observations $\mathcal{T} = \{\tau_1, \ldots, \tau_n\}$
* Trajectory: $\tau_i = \{y_1, \ldots, y_{tfi}\}$
* Parameters ω:
- $\forall \tau_i$: Least Squares $\rightarrow \omega_i$
- ω's distribution computed from $\{\omega_1, \omega_n\}$: $p(\omega) = \mathcal{N}(\omega|\mu_\omega, \Sigma_\omega)$.

Hypothesis: Gaussian distribution.

Modulation time α

- To learn movements independently to their time duration
- $\forall \tau_i$, $\alpha_i = \frac{t_{fi}}{Z}$ with Z a reference time.
- Model based on the idea $\dot{y} = \frac{\delta y}{t_f}$:

$\alpha = \Psi(\delta_e)^{\top}\boldsymbol{\omega}_\alpha + \epsilon_\alpha$

(Ψ: RBFs; ϵ_α: Gaussian noise; $\delta_e = y_e - y_1$.)

- ω_α's distribution computed from $\{\alpha_1, \alpha_n\}$: $p(\omega_\alpha) = \mathcal{N}(\omega_\alpha|\mu_{\omega_\alpha}, \Sigma_{\omega_\alpha})$.

Inference:

Given $D = X_{[1:e]}$, $p(\omega)$, $p(\omega_\alpha)$
We compute $\hat{\alpha} = \Psi(\delta_e)^{\top}\boldsymbol{\omega}_\alpha$
We update the distribution: $p(\omega|D) = p(\omega^{new}) = \mathcal{N}(\omega_{new}|\mu_\omega^{new}, \Sigma_\omega^{new})$:

$$\begin{cases} \mu_\omega^{new} = \mu_\omega + K(D - \Phi_{\hat{\alpha}t}^{T}\mu_\omega) \\ \Sigma_\omega^{new} = \Sigma_\omega - K(\Phi_{\hat{\alpha}t}^{T}\Sigma_\omega) \end{cases}$$

- $K = \Sigma_\omega \Phi_{\hat{\alpha}t}^{T}(\Sigma_D + \Phi_{\hat{\alpha}t}^{T}\Sigma_\omega\Phi_{\hat{\alpha}t})^{-1}$;
- Σ_D the expected data noise.

Then we follow: $y^*_{[e+1:t_{fexp}]} = \Phi_{\hat{\alpha}t}^{\top}\mu_\omega^{new}$

5) Results of the physical human robot collaboration[1]

- **Experiment**: arm movement learning with the simulated robot (haptic device) or real robot (physical guidance)

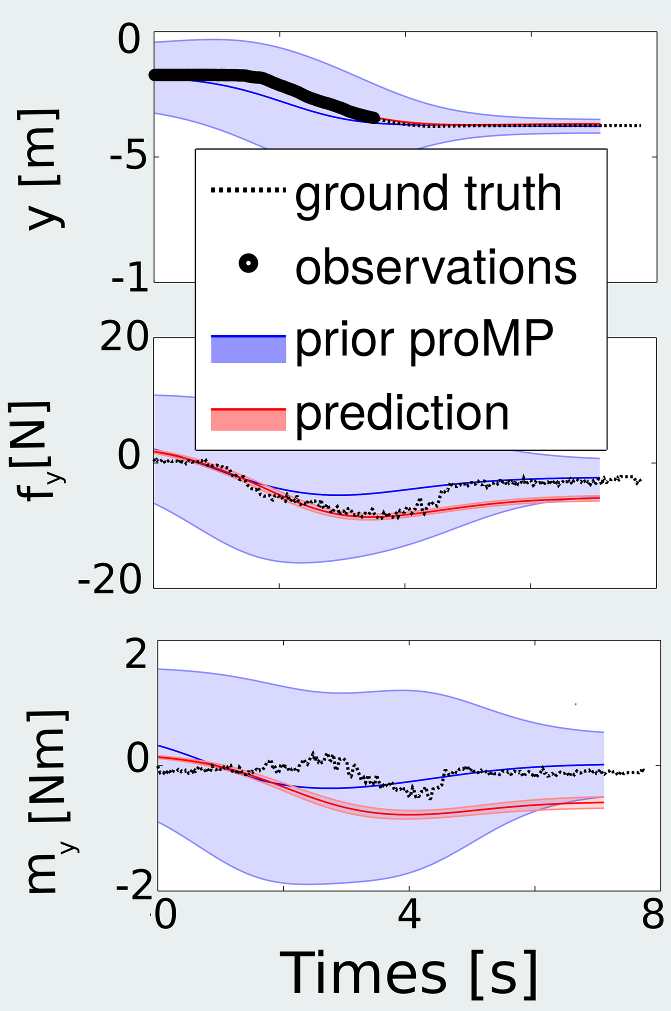

Inference representation of traj. A when the user releases the robot's arm. Without wrenches...

- **Observations**: 7 trajectories per ProMP; natural movements with different duration ($\simeq$ 4/5s).

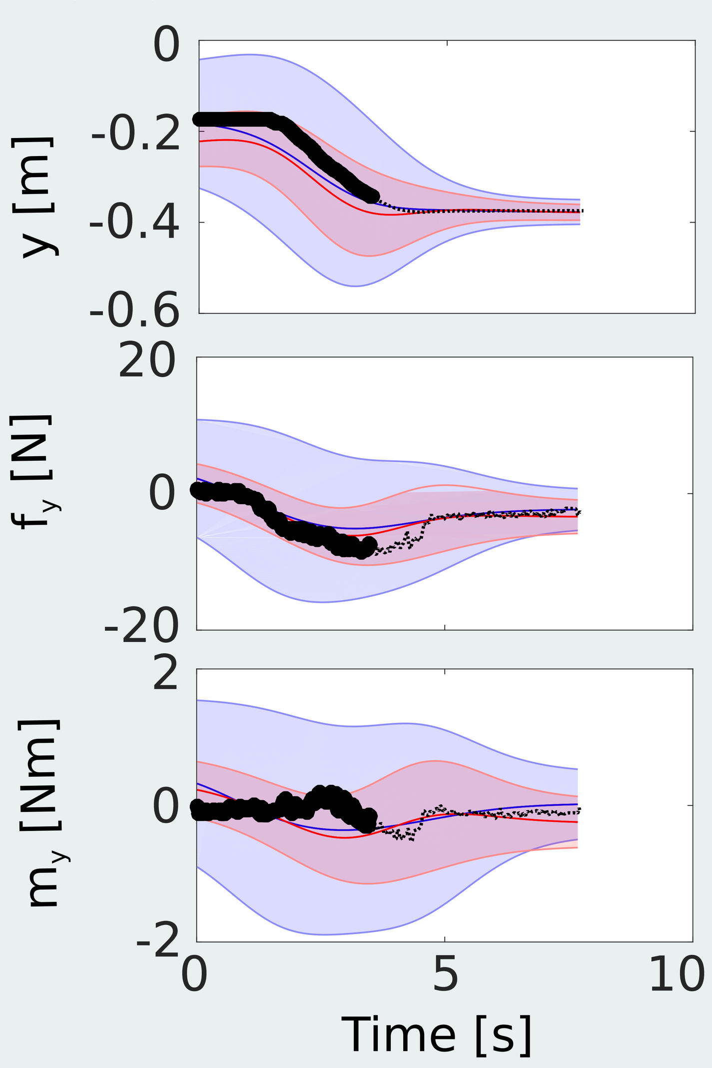

... and with wrenches...

- **Model**:
  - 5 RBF per inputs, parsed in time
  - reference time: Z= 100 samples.
- **Inference of a new trajectory**:
  - modulation time expected to be: $\alpha_{y^*} = \mu_\alpha$

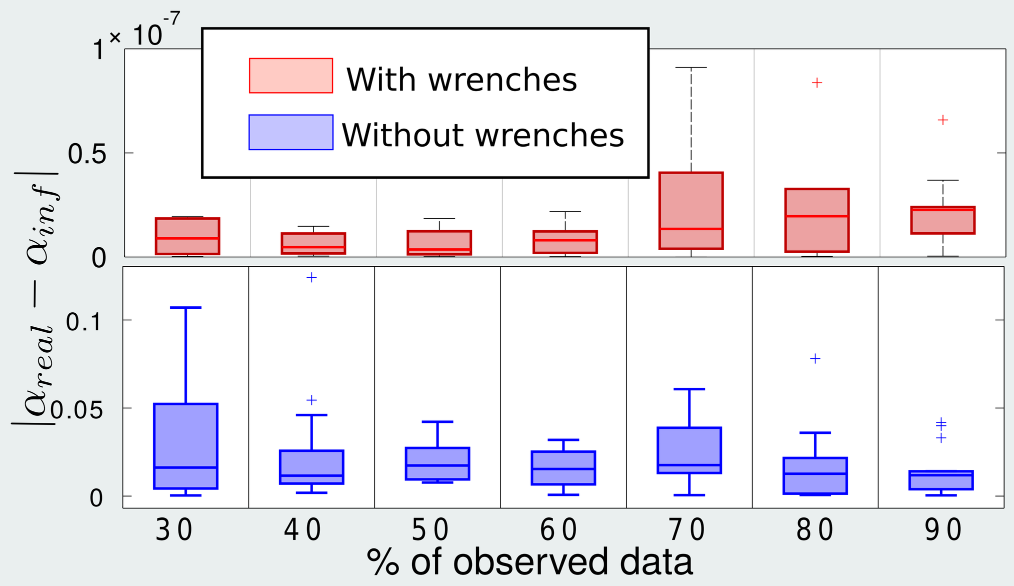

Figure: Error of alpha prediction (off-line statistics)

6) References

[1] Oriane Dermy, Alexandros Paraschos, Marco Ewerton, Jan Peters, Franois Charpillet, and Serena Ivaldi.
Prediction of intention during interaction with icub with probabilistic movement primitives.
2017.

[2] Alexandros Paraschos, Christian Daniel, Jan R Peters, and Gerhard Neumann.
Probabilistic movement primitives.
In *Advances in neural information processing systems*, pages 2616–2624, 2013.

Méthodologie d'élaboration d'un bilan de santé (performance et dégradation) de machines de production pour aider à la prise de décision en exploitation :

application à un centre d'usinage à partir de la surveillance de sa cinématique

Thomas Laloix {thomas.laloix@univ-lorraine.fr}

Thèse CIFRE

Encadrement CRAN : **Benoit Iung, Alexandre Voisin**

Encadrement Renault : **Eric Romagne, Kamel Fettih**

Contexte industriel de la thèse

CHALLENGES INDUSTRIELS

- Maîtrise de la conformité des produits sans contrôle a posteriori de leurs propriétés par contrôles statistiques
- Réduction des situations de non productivité des moyens de production par une surveillance anticipative et non pas par une réactivité de type corrective : privilégier des maintenances prédictives/prévisionnelles de type PHM (Prognostics and Healh Management)
- Optimisation des coûts globaux de possession sur l'ensemble du cycle de vie machine. Recherche d'un optimum lié à la fois aux composants produits (rebuts, non-conformité) et aux moyens de production (indisponibilité)

SITUATION DE TRAVAIL

- Usine Renault de Cléon
- Machine-outil bi-broche de type GROB G520, usinage carter-cylindre du moteur R9M
- Déploiement potentiel sur 4500 machines-outils en Europe/monde

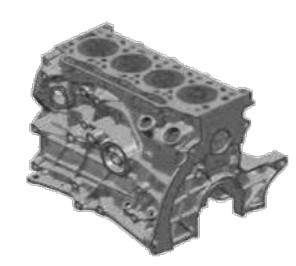

Carter cylindre R9M

Machine-outil GROB G520

VERROUS INDUSTRIELS/TECHNOLOGIQUES

1. Maitrise de la conformité du produit (propriétés de qualité, dimension géométrique, etc.) à partir d'une maîtrise en ligne des composants de la machine-outil et de leur dégradation
2. Disposer de KPI (Key Performances Indicators) pertinents de niveau système, multidimensionnels permettant d'avoir un bilan de santé de la relation produit /machine
3. Optimisation de l'aide à la décision en conduite et en maintenance à partir de ces indicateurs

Contexte scientifique

DES VERROUS TECHNOLOGIQUES AUX VERROUS SCIENTIFIQUES

1. Maîtrise de la conformité du produit à partir d'une maîtrise en ligne des composants de la machine et de leur dégradation (Laloix et al. 2016)
   - ❖ **Formalisation de règles de connaissances statiques et dynamiques reliant les propriétés de dégradation des composants aux déviations des propriétés du produit**
2. Disposer d'indicateurs pertinents (KPI), multidimensionnels permettant d'avoir un bilan de santé de la relation produit /machine
   - ❖ **Agrégation/fusion d'indicateurs fonctionnels et dysfonctionnels de niveaux d'abstraction différents voire de sémantiques différentes pour élaborer des KPI pertinents**
   - ❖ **Modélisation de l'évolution de ces indicateurs (pronostic avancé), et de l'impact de cette évolution dans une vision système (bouclage du système produit/machine)**
3. Optimisation de l'aide à la décision en conduite et en maintenance à partir de ces indicateurs
   - ❖ **Définition et fondement du concept de potentiel restant au regard des KPI multicritères, multi-dimensionels / au regard d'un système bouclé**
   - ❖ **Définition, en lien avec le potentiel restant des critères de décision / Formalisation des critères de décision, leviers d'action**

Contributions scientifiques et 1ers résultats

1. Formalisation des concepts de connaissance liés aux interactions produit/process :

La considération conjointe des aspects produit et process est basée sur la combinaison et l'extension d'approches conventionnelles d'analyses fonctionnelle et dysfonctionnelle (AMDEC et HAZOP).

Ces nouveaux concepts de connaissance permettent de relier les caractéristiques produits avec la dégradation des composants machine à travers le concept d'indicateur. La construction de ces indicateurs est formalisée par un méta-modèle dans un soucis de généricité.

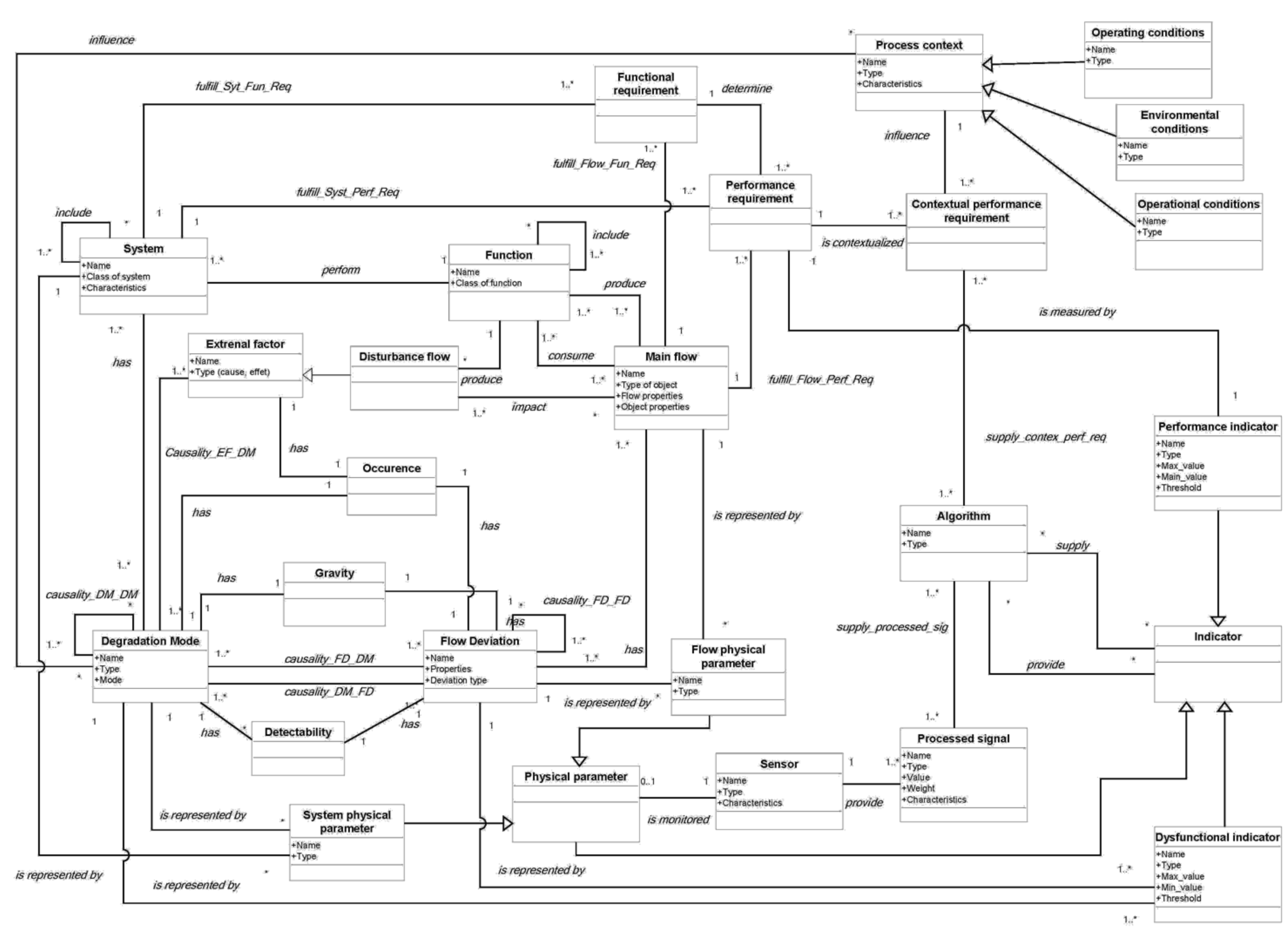

Formalisation UML du méta-modèle de construction des indicateurs de santé (Laloix et al., 2017)

L'instanciation de ce méta-modèle permet de générer un modèle de référence de type fonctionnel et technologique spécifique à la classe d'application machine-outil.

Le modèle de référence de la classe d'application machine-outil peut ensuite être particularisé à une machine donnée, par la prise en compte de son contexte opérationnel (typologie de produit, classe de machine, mission machine), et environnemental.

2. Génération d'un bilan de santé multi-niveau à partir d'indicateurs :

Basé sur les notions d'indicateur de santé introduites par [Abichou, 2013], l'indicateur de santé d'un système (E) résulte de la combinaison d'indicateurs en lien avec sa finalité (indicateurs de performance I_j^P), avec son aspect dysfonctionnel (indicateurs de dégradation I_j^D), et avec son contexte opérationnel et environnemental (indicateur de contexte I_j^C).

$$V(E) \triangleq \{I_1^P, I_2^P, \dots, I_{np_E}^P\} \cup \{I_1^D, I_2^D, \dots, I_{nd_E}^D\} \cup \{I_1^C, I_2^C, \dots, I_{nd_E}^C\}$$

Dans le but de prendre en compte un aspect multi-niveau du bilan de santé, il est nécessaire de considérer la performance des sous-systèmes impliqués dans la réalisation de la mission du système.

La construction de ces indicateur de performance est basée sur la combinaison de paramètres fonctionnels (position, vitesse, couple, etc.). 1

La prise en compte de l'impact de la dégradation des composants sur ces indicateurs de performance est assurée par un mécanisme d'agrégation des indicateurs de performance et des indicateurs de dégradation. 2

Ces indicateurs nécessitent d'être considérés au regard de la mission du système afin d'en estimer leur impact sur sa bonne réalisation. 3

Enfin, ces indicateur de santé contextualisés, de niveau sous-système, sont agrégés afin de fournir un indicateur global représentatif de l'état de santé du système. 4

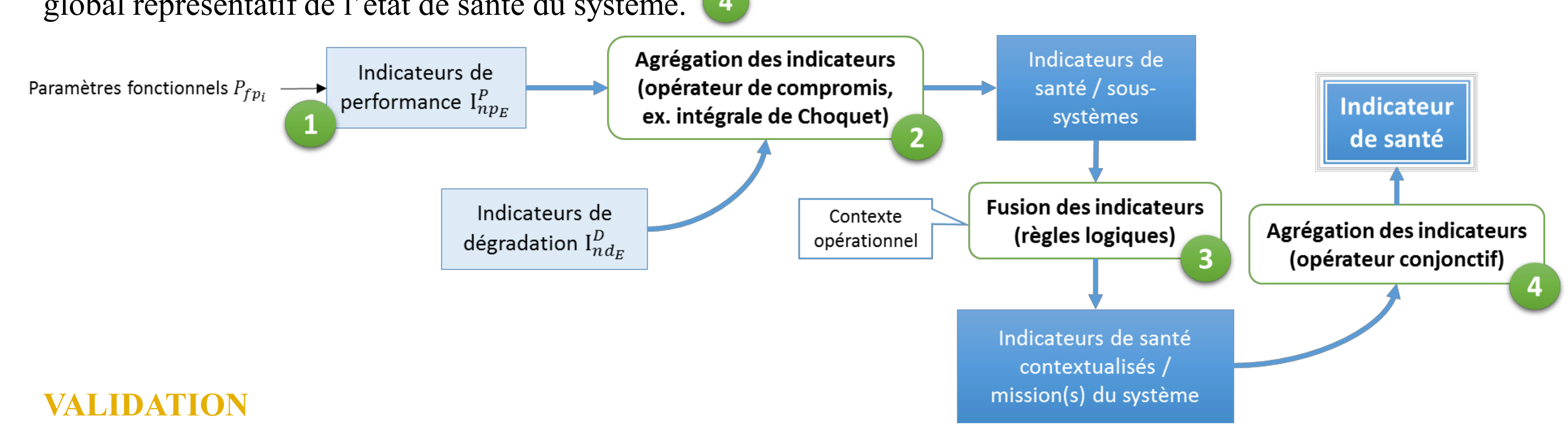

VALIDATION

Dans le cadre de l'application machine-outil, la finalité du système est de transformer une pièce. Pour ce faire, la mission de la machine–outil est divisée en trois activité correspondant aux opérations d'usinage : perçage/taraudage, alésage et fraisage, chacun ayant un impact sur la qualité de la pièce usinée. A partir de l'instrumentation de sous-ensembles fonctionnels ou technologiques clés de la machine (électro-broches, axes linéaires et rotatifs…), des indicateurs (particulièrement les indicateurs de performance) ont été identifiés et construits.

Par exemple, au regard des axes linéaires, un des indicateurs de performance est l'indicateur de *« maintien en position »,* et résulte de la construction suivante:

$I_{mp_x}^P$ = Moyenne(abs(Valeur réelle déplacement−Valeur cible déplacement))

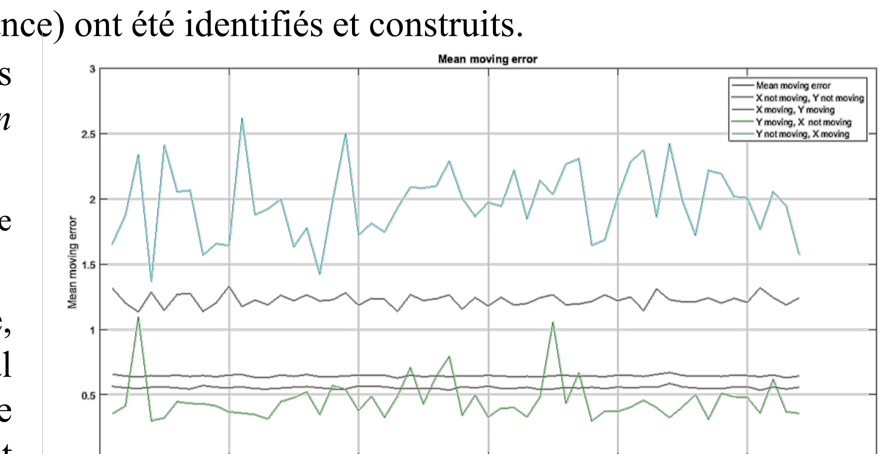

Indicateurs de performance liés au maintien en position axe X, Y et Z

Ces indicateurs, mis en regard des opérations d'usinage, peuvent être associés pour former un indicateur global lié à une considération qualité produit. Ainsi, pour une opération de perçage/taraudage, par exemple, il est nécessaire que les axes répondent aux conditions de fonctionnement suivantes:

X_maintaining & *Y_maintaining* & *Z_moving*

L'indicateur de performance de l'opération de perçage (indicateur de performance contextualisé à la mission) résulte donc d'une combinaison des indicateurs de performance des axes linéaires :

$$I_{Perç_{Axes}}^P = \cup \left(I_{mp_x}^P, I_{mp_y}^P, I_{dp_z}^P\right)$$

Avec, $I_{Perç_{Axes}}^C$: indicateur de perf. *Perçage* au regard des axes linéaires
$I_{mp_x}^P$: indicateur de perf. du maintien en position de l'axe X
$I_{mp_y}^P$: indicateur de perf. du maintien en position de l'axe Y
$I_{dp_z}^P$: indicateur de perf. de la précision de déplacement de l'axe Z

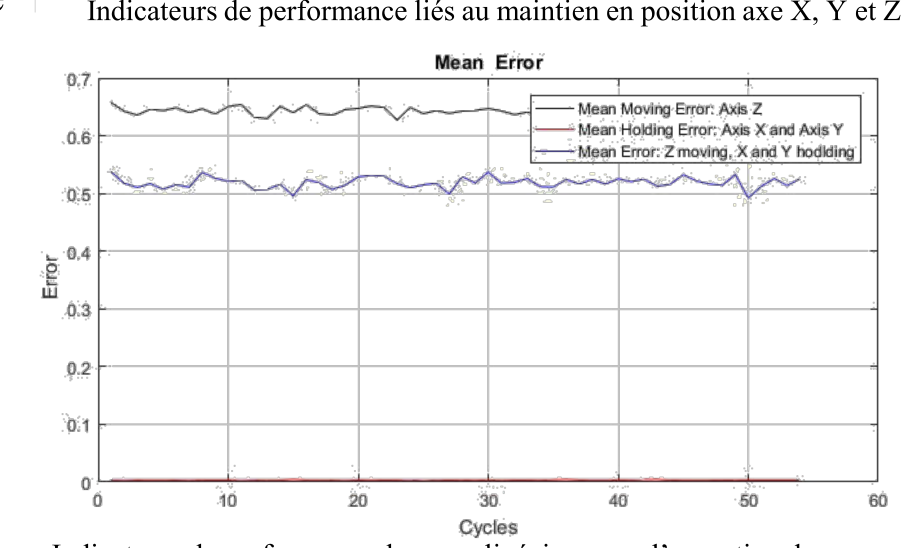

Indicateurs de performance des axes linéaires pour l'operation de perçage

Travail restant

3. Proposer les fondements d'un concept de potentiel restant relatif aux KPI de la classe d'application machine-outil.

$$REEL(t) = \left\{ E[T] : EEI^{t+T} = EEI_{Threshold} \middle| EEI^{t} < EEI_{Threshold} \right\}$$

[Calcul de potentiel restant de type efficacité énergétique (REEL) (A. Hoang, P. Do, B Iung, 2015)]

VALIDATION

- Prendre en compte l'aspect *dégradation* dans le calcul de l'indicateur de santé niveau sous-système : agrégation des indicateurs de dégradation et de performance par l'intégrale de Choquet.
- Calculer l'indicateur de santé machine : agrégation des indicateurs de santé contextualisés niveau sous-système via un opérateur d'agrégation conjonctif.
- Implanter les algorithmes au sein des outils métiers de Renault.

Publications réalisées

- Laloix T., A. Voison, S. Deeb, E. Romagne, B. Iung, F. Lorange (2017). Industrial system functioning/dysfunctioning-based approach for indicator inditification to support proactive maintenance. 20th IFAC World Congress, 7-14 July, Toulouse, France
- Laloix T., Iung B., Voisin A., Romagne R. (2016). Towards the control of product quality from the process deviation monitoring: Overview and investigation in automotive sector. 3rd IFAC Workshop on Advanced Maintenance Engineering, Service and Technology, IFAC A-Mest'16, 19-21 October, Biarritz, France
- Laloix T. (2016). Methodological framework for global performance control of manufacturing system in automotive sector. 8th doctoral Workshop on Product and Asset Lifecycle Management, 16-18 October, Saint-Jean de Luz, France

Thomas PARIS
Université de Lorraine,
LORIA, Inria
thomas.paris@loria.fr

Complex System Modeling by Composition

Supervised by Vincent CHEVRIER and Laurent CIARLETTA

Context: Modeling and Simulation (M&S) of Complex Systems

Complex Systems
Complex systems are systems composed of several heterogeneous interacting entities. Cyber Physical Systems, such as smart grids, are complex systems as they contain many entities from several domains (electrical, telecommunication, control system...).

causes

New challenges
Multi-domain, multi-perpective approaches and **new tools** need to be developped.

approach

Co-simulation
A co-simulation is a simulation where several models and their simulators synchonize their execution and exchange data. It enables to reuse models and tools.

approach

Multimodel
A multimodel is a model composed of several interacting submodels that represent together the system under study.

challenge

Composition
The composition is the ability to select and assemble simulation components (models) to create new meaningful simulation components. This is a key concept for the multi-modeling of complex system, it gives a level of abstraction that enables to reuse and make hierarchy of multimodels.

purpose

Multi-modeling co-simulation process based on the composition of models built in several heterogeneous M&S software.

Issue: Multi-modeling and Co-simulation, three levels to deal with

Technical/Integrability
We can exchange data between the simulation components.

→ **Formal/Syntactic interoperability/Simulation**
Simulation components share a common syntax, the data exchanged is structured.

→ **Conceptual/Composability/Modeling**
The composed simulation component is meaningful. It is the highest level of interoperability, it refers to the ability to validate the composed multimodel.

Proposal: Combine MECSYCO with a Domain Specific Language approach to develop a multi-modeling co-simulation framework with composition features

MECSYCO (*Multi-agent Environment for Complex SYstem CO-simulation)* is a co-simulation platform for complex system M&S. It associates the **DEVS** (*Discrete EVent Systrem specification*) formalism and a multi-agent architecture based on **AA4MM** (*Agent and Artifact for Multi-Modeling*) to handle heterogeneities and ensure modularity.

Advantages: handle integrability and syntactic interoperability
Shortfalls: no composition ability, lack of expressivity at modeling level

Development of several DSL to support the M&S process on MECSYCO
Each DSL is dedicated to one step of the multi-modeling and co-simulation process. The data about the model is separated from the data about its simulator thanks to specific keywords. DSL generates description files linked to the models. Each step can be described and reused.

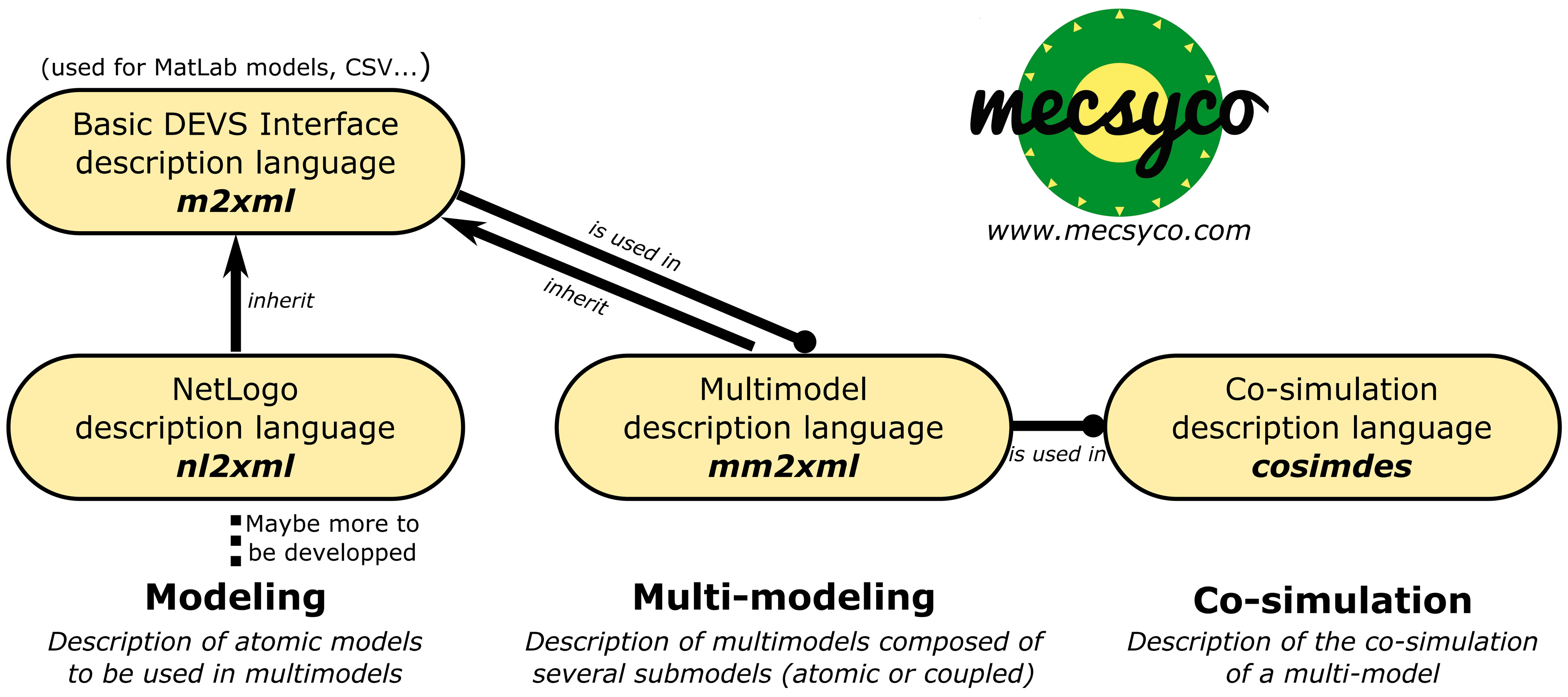

Several activity specific and interacting languages

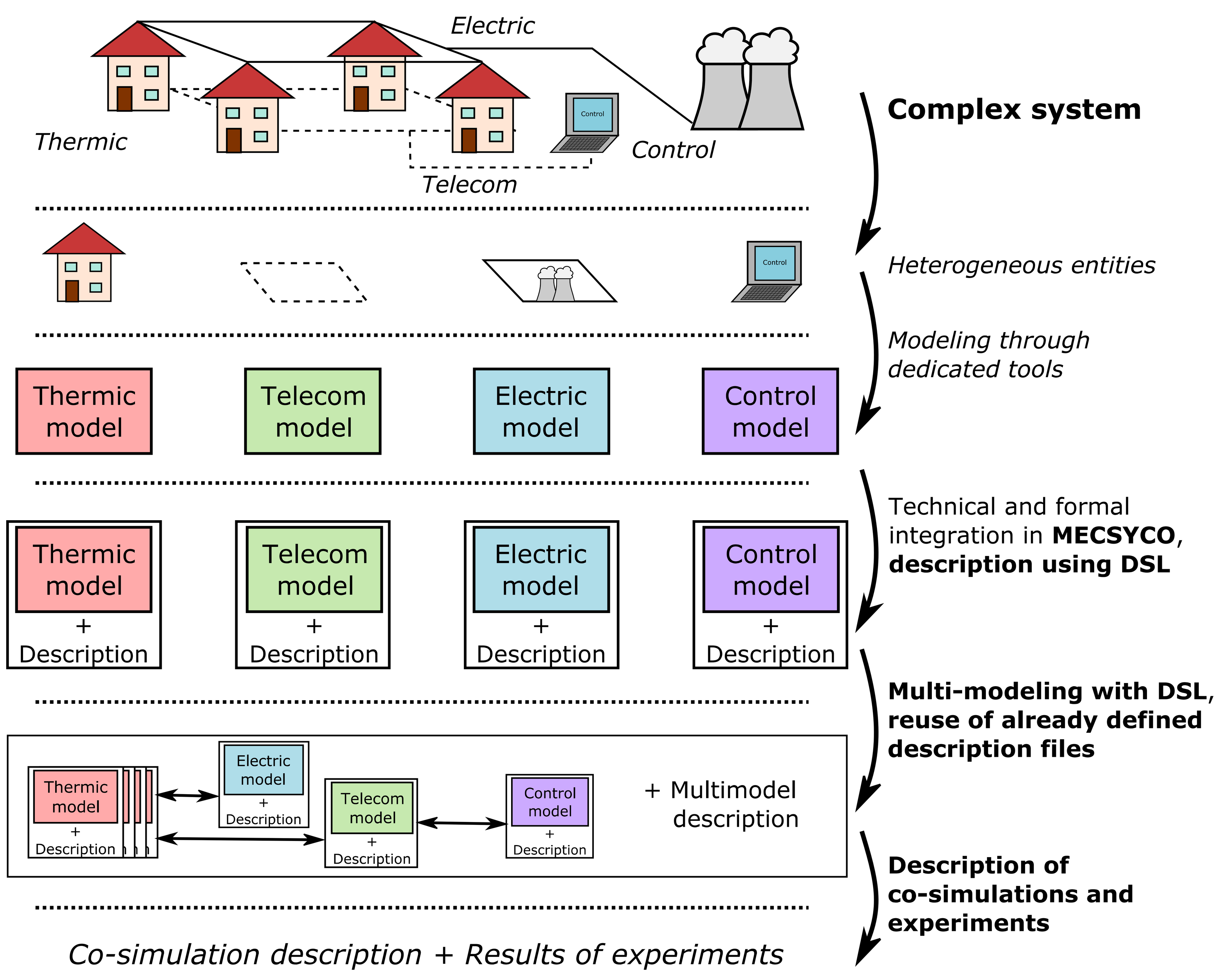

Multi-modeling process with MECSYCO and the DSL

Contributions:

-Development of a multi-modeling methodology based on the reuse of models from different M&S software and which proposes composition features
-Enhancement of MECSYCO with the ability to reuse multimodels and the expressivity of DSL
-Development of a DSL based IDE to support the multi-modeling process

*Basis for the creation of a **DEVS based co-simulation and multi-modeling framework** which relies on the integration of models from existing modeling tools and provides an approach to study the composability from a pragmatic point of view.*

Perspectives of this work can be the development of new features based on the expressivity of DSL: *semantic verification based on the description files, automation of the verification of results, design space exploration...*

Publications:

-T. Paris, L. Ciarletta, V. Chevrier. Intégration d'un simulateur multi-agent dans une plateforme de co-simulation DEVS. Journées Francophones sur les Systèmes Multi-Agents (JFSMA 2017), Jul 2017, Caen, France.
-B. Camus, J. Vaubourg, T. Paris, Y. Presse, C. Bourjot, L. Ciarletta, V. Chevrier. *Co-simulation de systèmes complexes grâce au wrapping DEVS dans MECSYCO.* Technique et Science Informatiques (TSI). (Accepted)
-T.Paris, T. Alexandre, L. Ciarletta, V. Chevrier. Study about decomposition and integration of continuous systems in discrete environment. In Spring Simulation Multi-Conference (SpringSim'16).

UNIVERSITÉ DE LORRAINE
Loria Laboratoire lorrain de recherche en informatique et ses applications
cnrs
Inria INVENTEURS DU MONDE NUMÉRIQUE

Lattice polynomials over finite distributive lattices

Quentin Brabant, Miguel Couceiro
quentin.brabant@loria.fr, miguel.couceiro@loria.fr

UNIVERSITÉ DE LORRAINE Loria

Lattices

A lattice is a partially ordered set $(L, \leq)$ in which any pair of elements has exactly one least common greater element (supremum) and one greatest lower element (infimum). Supremum of $x, y \in L$: $x \vee y$, Infimum of $x, y \in L$: $x \wedge y$, Infimum and supremum respect
commutativity: $x \vee y = y \vee x, x \wedge y = y \wedge x$,
associativity: $x \vee (y \vee z) = (x \vee y) \vee z, x \wedge (y \wedge z) = (x \wedge y) \wedge z$,
absorption: $x \vee (x \wedge y) = x, x \wedge (x \vee y) = x$.

A lattice is **distributive** if for any $x, y \in L$:

$$x \vee (y \wedge z) = (x \vee y) \wedge (x \vee z), \quad x \wedge (y \vee z) = (x \wedge y) \vee (x \wedge z).$$

Not lattices:

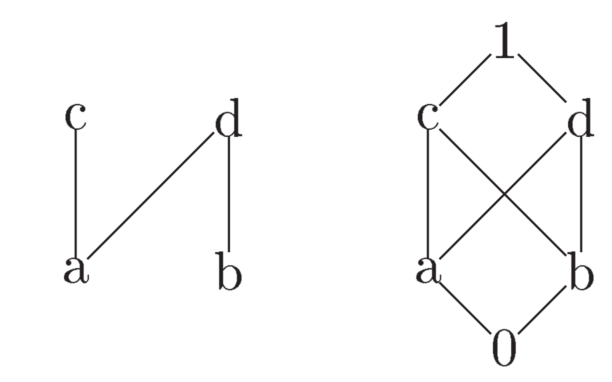

Lattices:

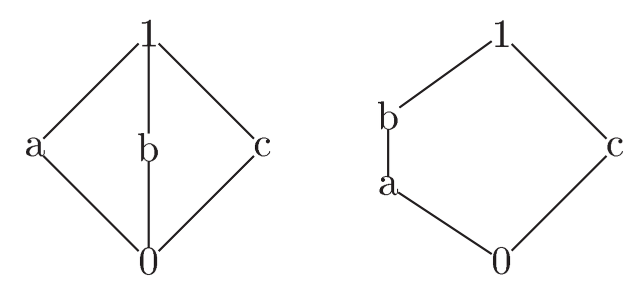

Distributive lattices:

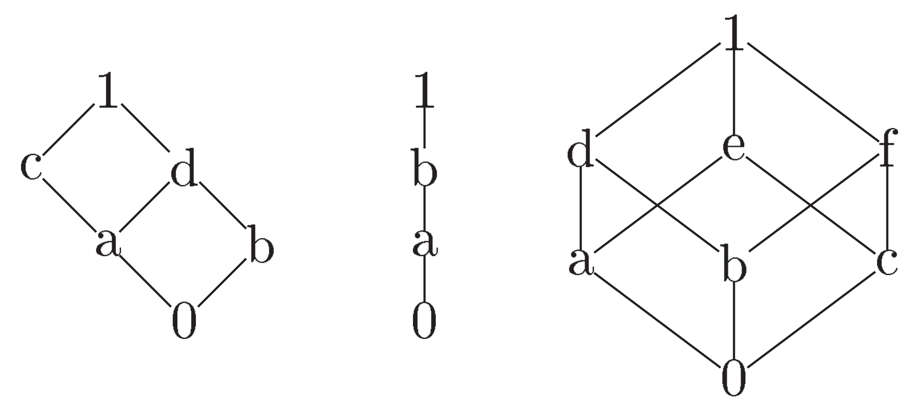

Join irreducibles and Birkhoff representation

A join irreducible is an element that is not the supremum of other elements (the bottom of the lattice is the supremum zero elements, therefore it is never a join irreducible). A finite distributive lattice can be represented as a family of sets ordered by inclusion. An easy way to get this representation is to replace each element by set containing all join irreducibles below it.

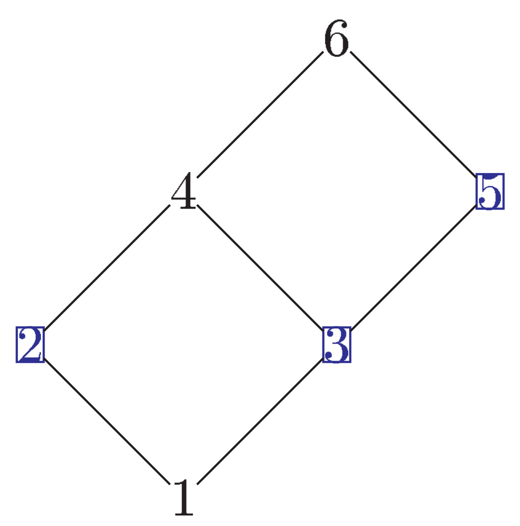

A distributive lattice $(L, \leq)$. Join-irreducibles are represented by blue squares.

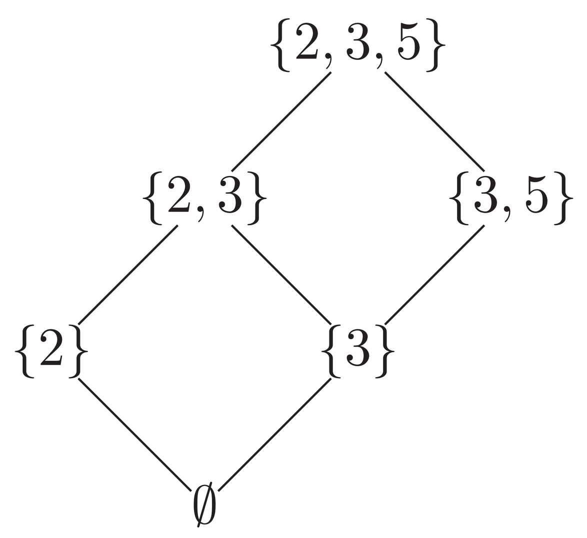

The lattice representing $(L, \leq)$ using sets of join-irreducibles.

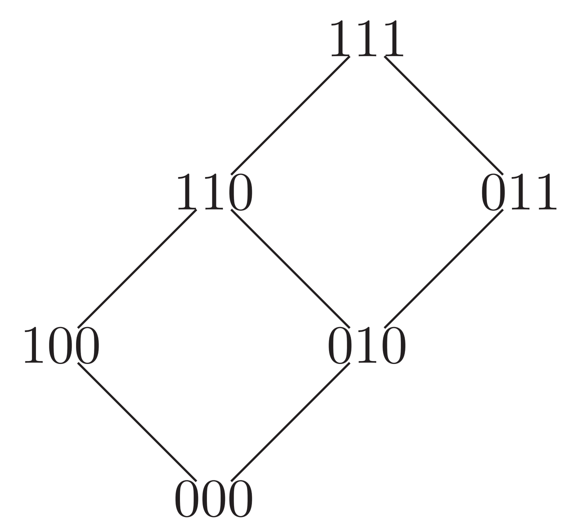

An equivalent representation, using binary tuples.

The ordering of join irreducibles determines the shape of the distributive lattice. In fact, there is a one to one correspondence between partial orders and distributive lattices.

Lattice polynomials

They are all functions that can be expressed by formulas involving only variables, constants, and the lattice operators $\vee$ and $\wedge$. Example:

$$p(x_1, x_2, x_3) = a \vee (b \wedge x_1 \wedge x_2) \vee (d \wedge x_2 \wedge x_3).$$

Formally, the class of lattice polynomials from L^n to L, denoted by $\mathcal{P}_L^n$, can be defined recursively by finitely many applications of the following rules:

1. For any $k \in [n]$, the projection $(x_1, \ldots, x_n) \mapsto x_k$ is a lattice polynomial from L^n to L.
2. For any $c \in L$, the constant function $(x_1, \ldots, x_n) \mapsto c$ is a lattice polynomial from L^n to L.
3. If $p, q \in \mathcal{P}_L^n$, then $p \vee q \in \mathcal{P}_L^n$ and $p \wedge q \in \mathcal{P}_L^n$.

Problem: interpolation and approximation of partial functions

Let $D \subseteq L^n$ and $f : D \to L$. A lattice polynomial $p : L^n \to L$ interpolates f if $\forall \mathbf{x} \in D$: $p(\mathbf{x}) = f(\mathbf{x})$.
Problem 1: Is the set of lattice polynomials interpolating f empty or not? If not, how to describe this set?
Problem 2: If the set is empty, can we find a lattice polynomial that approximately covers f?
Learning a lattice polynomial from a set of examples practically boils down to these problems.

References

[1] B.A. Davey and H.A. Priestly. *Introduction to Lattices and Order*. Cambridge University Press, Cambridge, UK, 2002.

[2] D. Dubois, J.-L. Marichal, H. Prade, M. Roubens, and R. Sabbadin. The use of the discrete Sugeno integral in decision-making: a survey. *International Journal of Uncertainty, Fuzziness and Knowledge-Based Systems*, 9(05):539–561, 2001.

[3] J.-L Marichal. Weighted lattice polynomials. *Discrete Mathematics*, 309(4):814–820, 2009.

[4] M. Couceiro, D. Dubois, H. Prade, and T. Waldhauser. Decision-making with sugeno integrals. *Order*, 33(3):517–535, 2016.

Preference aggregation

Consider the following situation: a user has to make a choice between several alternatives. She can evaluate each of these alternatives with respect to several criteria (for example, if the alternatives to chose from are flats to rent, the criteria can be the price, the localization, the surface). The evaluations are expressed by values from a totally ordered set L. For example

$$L = \{\texttt{verybad}, \texttt{bad}, \texttt{average}, \texttt{good}, \texttt{perfect}\},$$

where `verybad` < `bad` < `average` < `good` < `perfect`. Let us denote by $x_1, \ldots, x_n \in L$ her evaluations of some alternative w.r.t. criteria. A classical problem of multi-criteria decision aid (MCDA) is that of predicting from $x_1, \ldots, x_n$ a global evaluation of the alternative.
Classical aggregation operators, such as weighted means or Choquet integrals cannot be applied directly, due to the non-numerical nature of L. This is why lattice polynomials are interesting.
Moreover suppose that, additionally to the previous values, the user is enabled to evaluate a characteristic of the object by the value "I don't know" (`IDK`). In order to handle this value, we can define L' as the distributive lattice depicted in the Figure below.

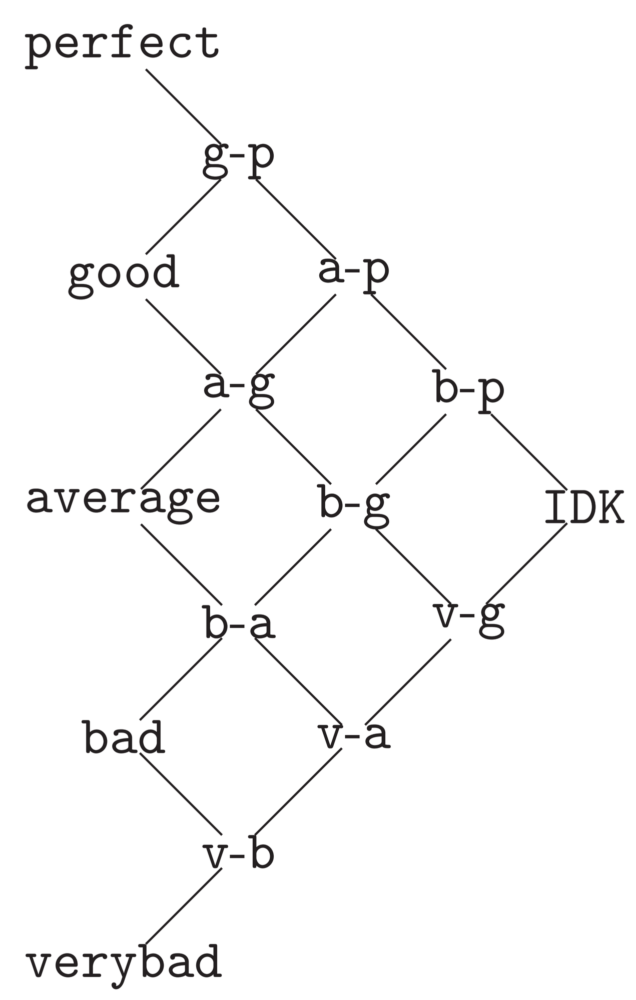

In this lattice, `IDK` represents an uncertainty, i.e., some value between `perfect` and `verybad`. For any value $x \in L$, the supremum (resp. infimum) of x and `IDK` is an element of L' representing a partial uncertainty, whose interpretation is "somewhere between x and `perfect`" (resp. "somewhere between x and `verybad`").

General consensus function

Any poset $(X, \leq)$ can be viewed as the set of ordered join irreducibles of a distributive lattice. Consider the representation of this lattice, denoted by $(L, \subseteq)$, where each element is a set of join-irreducible. For any $A \in L$, if $x \in A$ and $y \leq x$, then $y \in X$.
Therefore, when dealing with objects that can be represented as itemsets, with restrictions of the form "x implies y" between items, lattice polynomials can be used for merging objects together.
They have the following nice property: for any $X_1, \ldots, X_n, X'_1, \ldots, X'_n \in L$ and $x \in X$:
if $x \in X_i \Rightarrow x \in X'_i$ for any $i \in \{1, \ldots, n\}$,
then $x \in p(X_1, \ldots, X_n) \Rightarrow x \in p(X'_1, \ldots, X'_n)$.

Design IR-UWB transmitter and receiver based on wavelet packet transform for wireless sensor network

Christophe Hüseyin KIZIL, Camille DIOU, Camel TANOUGAST
Laboratoire LCOMS, Université de Lorraine
7 rue Marconi, 57070 Metz, France
{Christophe-huseyin.kizil, camille.diou, camel.tanougast}@univ-lorraine.fr

1. Introduction

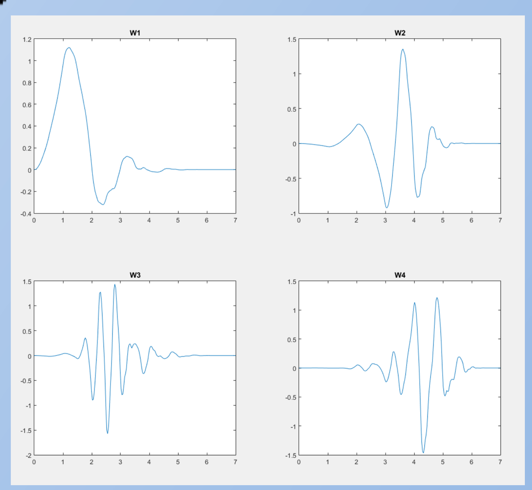

The 4 Daubechies-4 wavelet packets associated to 4 filters of wavelet.

IR-UWB (Impulse Radio Ultra Wideband) is a communication method and this kind of communication has many benefits:

- high data rate,
- better immunity to multipath propagation
- and low power spectral density [1].

However, several technical challenges must be considered such as

- the synchronization (of clocks, of DAC and ADC) at the receiver,
- performance degradation due to multiple access interference
- and high system complexity.

To overcome these drawbacks, coherent and non-coherent receivers can be considered.

- Coherent receivers: optimum solution for achieving robust performance [2] but it require accurate channel estimation: one correlator for each path and perfect synchronization for each path. So, the system complexity growth even if it allows good performance [2].
- Non-coherent receivers: low complexity and low power consumption [2] furthermore, it present low performance.

Usually, most of IR-UWB receivers are mainly based on correlator functions and energy detection while designing on ASIC technologies [3].
Our embedded communication system performs DWPT/IDWPT as carrier-less communication medium. This approach allow us to obtain better performance in terms of data rate and logic resources while maintaining a high flexibility.

2. Our architecture of E/R in parallel mode

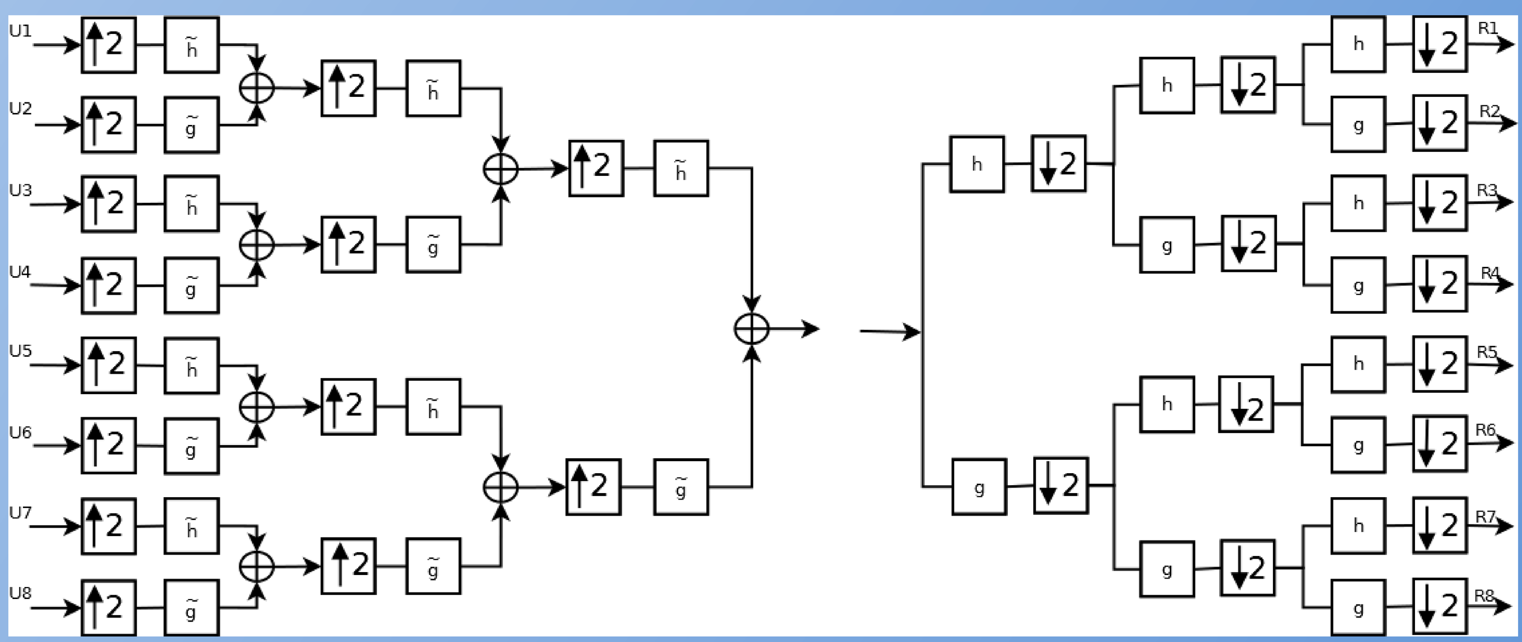

On top, architecture of emitter (left) and receiver (right) for 3 level of resolution. Each sensor send n bits in parallel. However, in this mode, sensors need the entire architecture to correctly emit.

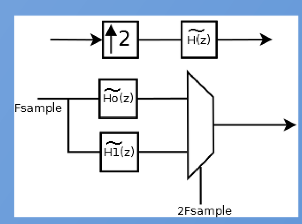

Interpolator filter in transmitter

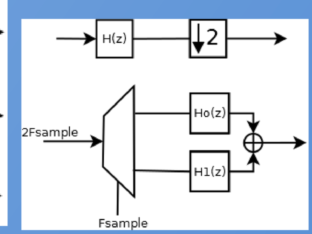

Decimator filter in receiver

3. Our architecture of E/R in serial mode

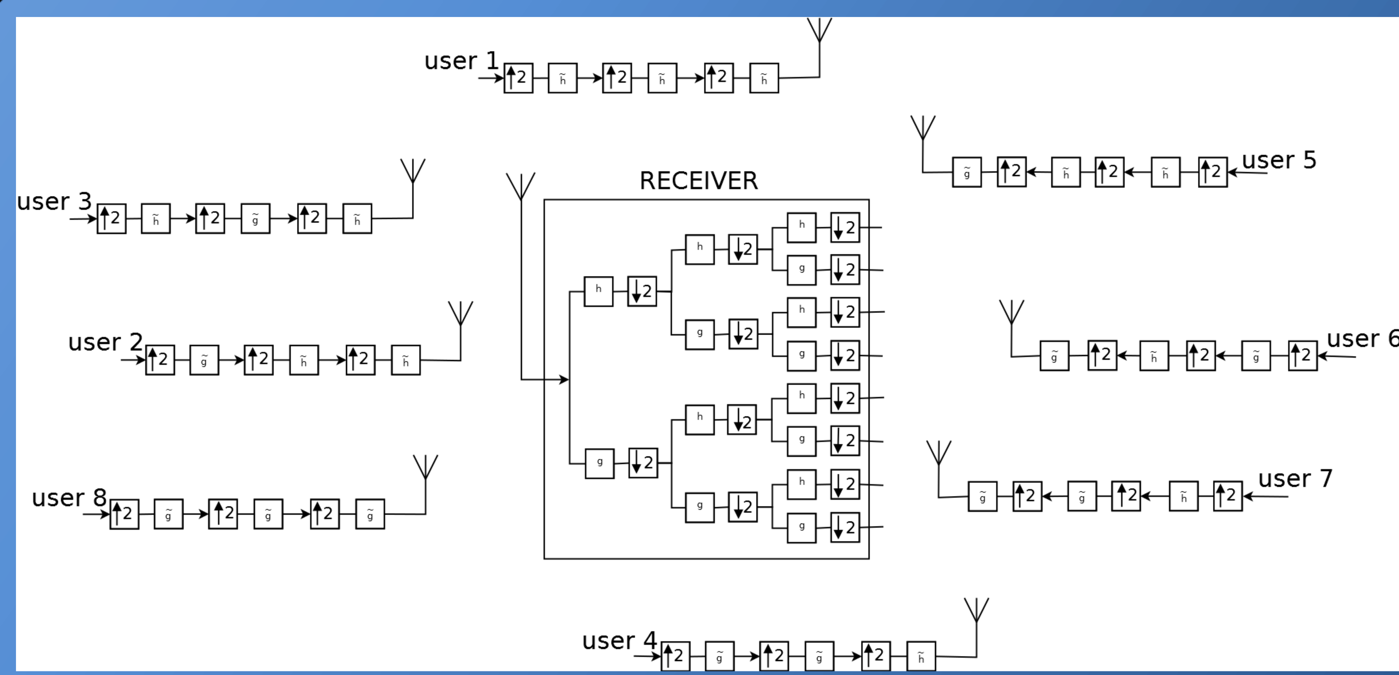

Each user is associated with a wavelet packet. In this mode, each user does not need the entire architecture to emit. Therefore, one sensor can send data with only filters and up-samplers corresponding to this sensor.

4. Implementation

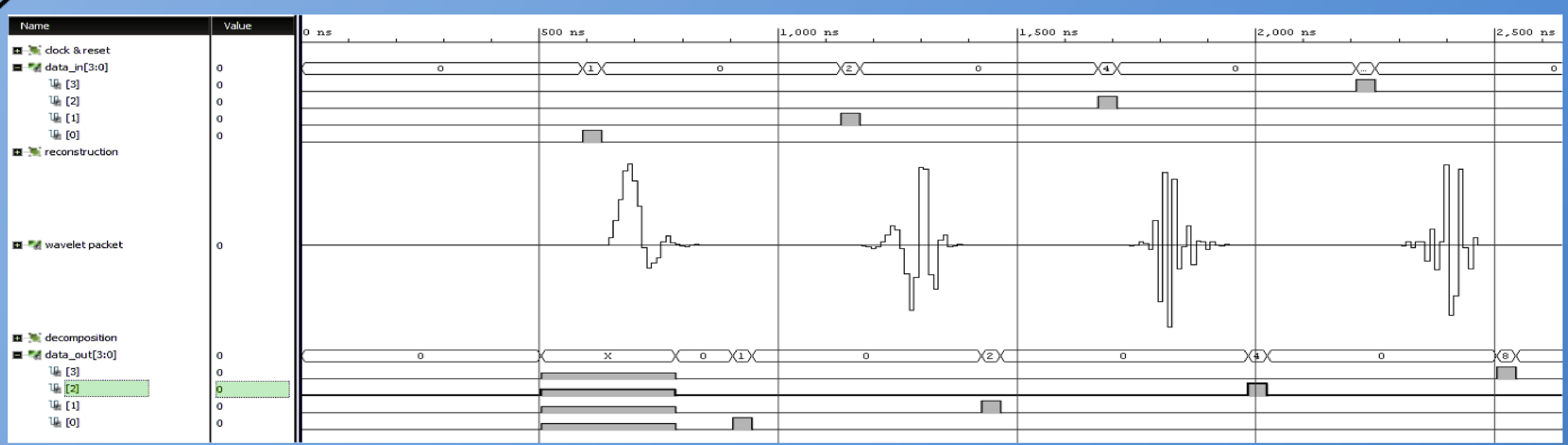

LOGIC RESOURCE UTILIZATION, CLOCK FREQUENCY AND POWER CONSUMPTION FOR TRANSMISSION PART BASED ON DB4 WAVELET.

Resolution level	1	2	3	4
FF	505	1522	3556	7622
LUT	3397	12499	30877	67608
clock (MHz)	948	204	105	99
power (W)	0.095	0.253	0.518	1.196

LOGIC RESOURCE UTILIZATION, CLOCK FREQUENCY AND POWER CONSUMPTION FOR RECEPTION PART BASED ON DB4 WAVELET.

Resolution level	1	2	3	4
FF	577	1794	4099	8708
LUT	5748	17241	40174	86105
clock (MHz)	948	204	105	99
power (W)	0.291	0.364	0.446	0.514

These designs decrease the silicon effectiveness compared to FPGA technologies although it provides low power consumption and high clock frequency. These results are for FPGA Virtex-7.

5. Binary Error Rate

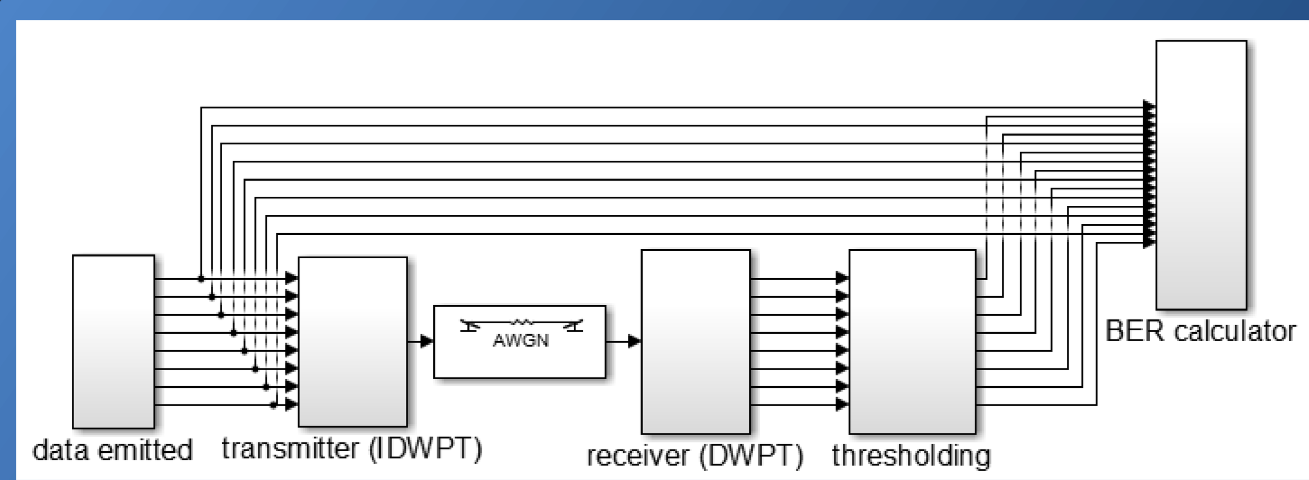

Structure of scheme in Simulink for a Transmission of 8 parallel data using different Wavelet to get BER results.

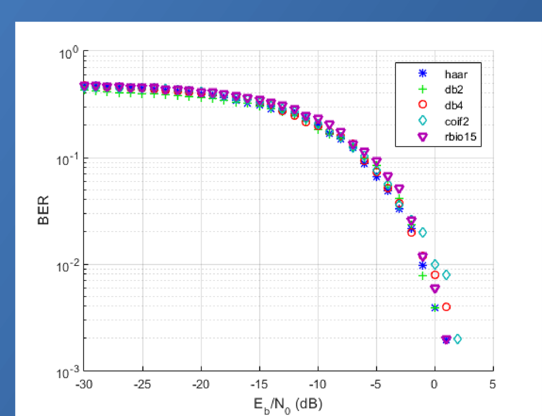

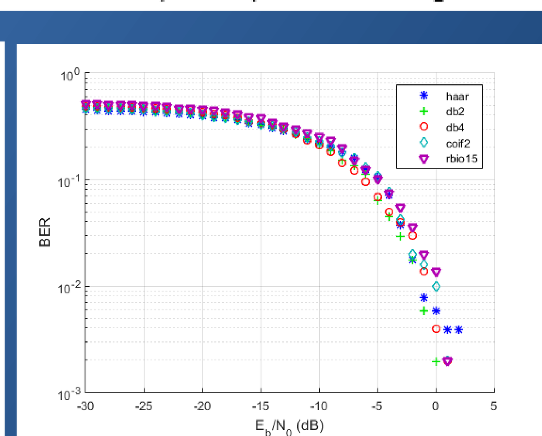

BER results for 2 data transmission and different Wavelet (Haar, Db2, Db4, Coif2, rbio1.5). The results are the same for others 6 data.

6. Matlab reception

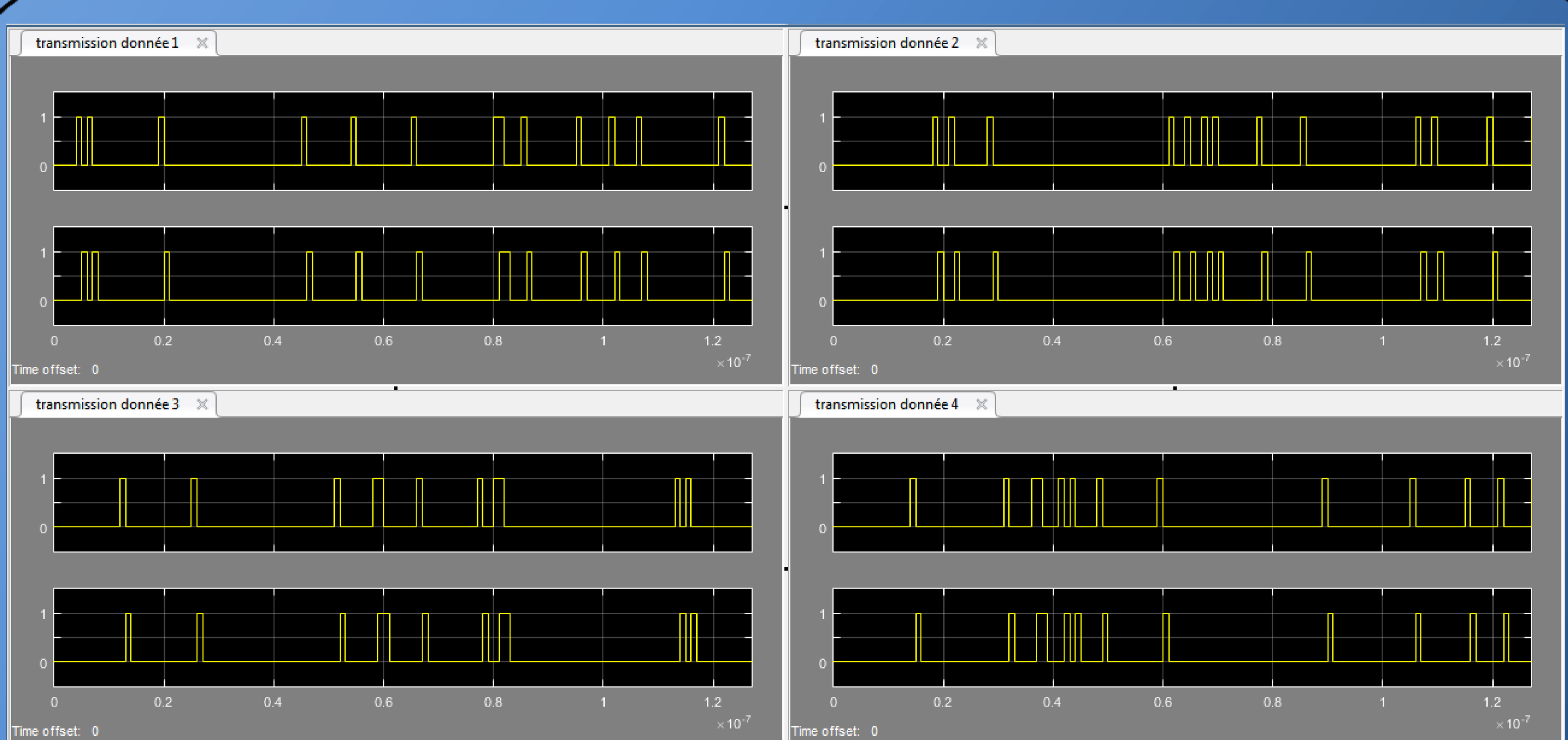

Representation of 4 data emitted and received according to the simulink scheme for one specific wavelet (Haar). These data are correctly received with a reception delay.

7. Conclusion

The proposed symmetric schemes allow us to transmit data and decode pulses. We designed an architecture which can easily change parameters such as the number of sensors (only in serial mode) and the wavelet used for transmission. In the literature, IDPWT and/or DPWT are used in many fields but never as a carrier-less communication medium in IR-UWB communications. We obtain good results for a transmission in a Gaussian AWGN channel and implementations results show us the feasibility of the architecture.

8. References

[1] M. Tabaa, C. Diou, R. Saadane and A. Dandache, "Los/Nlos identification based on stable distribution feature extraction and svm classifier for UWB on-body communications," Journal of Ubiquitous Systems and Pervasive Networks, vol. 6, 2015, pp.27-32.
[2] R. Hazra and A. Tyagi, "A Survey on Various Coherent and Non-coherent UWB-IR Receivers", Wireless Personal Communications, vol. 79, no. 3, pp. 2339-2369, Dec. 2014.
[3] J. Hu, Y. Zhu, S. Wang, and H. Wu, "An Energy-Efficient IRUWB Receiver Based on Distributed Pulse Correlator", IEEE Transactions on Microwave Theory and Techniques, vol. 61, no.6, pp. 2447-2459, Jun. 2013.
[4] Y. Youn, H. Jeon, H. Jung, and H. Lee, "Discrete wavelet packet transform based energy detector for ognitive radios", in Vehicular Technology Conference, 2007. IEEE 65th, 2007, pp. 2641-2645.
[5] W. Saad, N. El-Fishawy, S. El-Rabaie, and M. Shokair, "An efficient technique for OFDM system using discrete wavelet transform", in Advances in Grid and Pervasive Computing, Springer, 2010, pp. 533-541.

Contribution to Bearing Fault Diagnosis in Electrical Machines

Thibaud Plazenet[1,2], Cyrille Caironi[2], Thierry Boileau[1], Babak Nahid-Mobarakeh[1]
[1]GREEN-ENSEM, University of Lorraine, Nancy, France
[2]LORELEC, Pulnoy, France

Inverter Induced Bearing Faults

Bearing failures are one of the most common cause of forced outage on industrial rotating machines. Inverters creating high *dv/dt* are greatly contributing to early bearing aging. In the view to prevent and **anticipate bearing failures at early stage** to match industrial's performance objectives, condition based monitoring has to be improved. Based on **mechanical and electrical signals analysis**, new diagnosis tools has to be proposed.

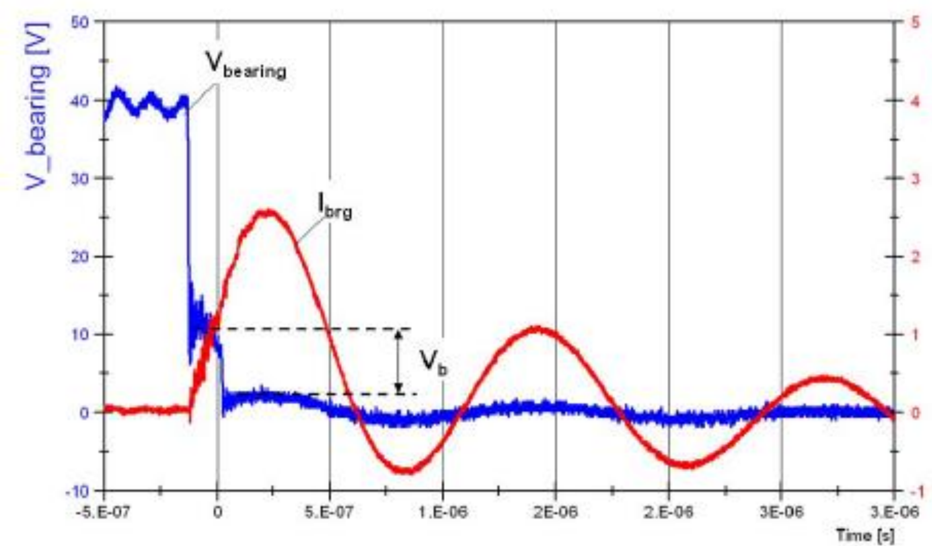

Arc voltage for an EDM bearing current

Bearing Electrical Degradation

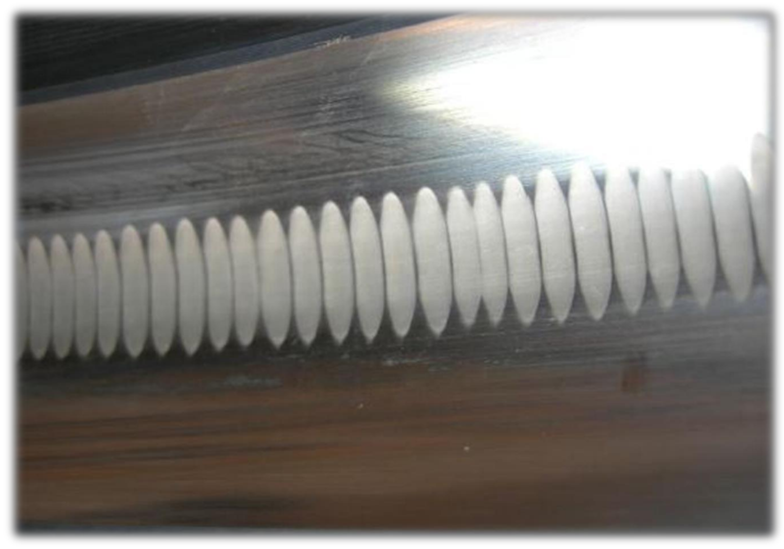

Generalized roughness or "fluting" on inner race at last stage

Bearing Fault Signal Modeling

Generalized roughness fault produce on vibration and current stator spectra, an **increase of the noise floor, stochastic broadband changes** with the absence of characteristic fault frequencies at incipient stage.

Stationary / Nonstationary signals

Synthesized Signals

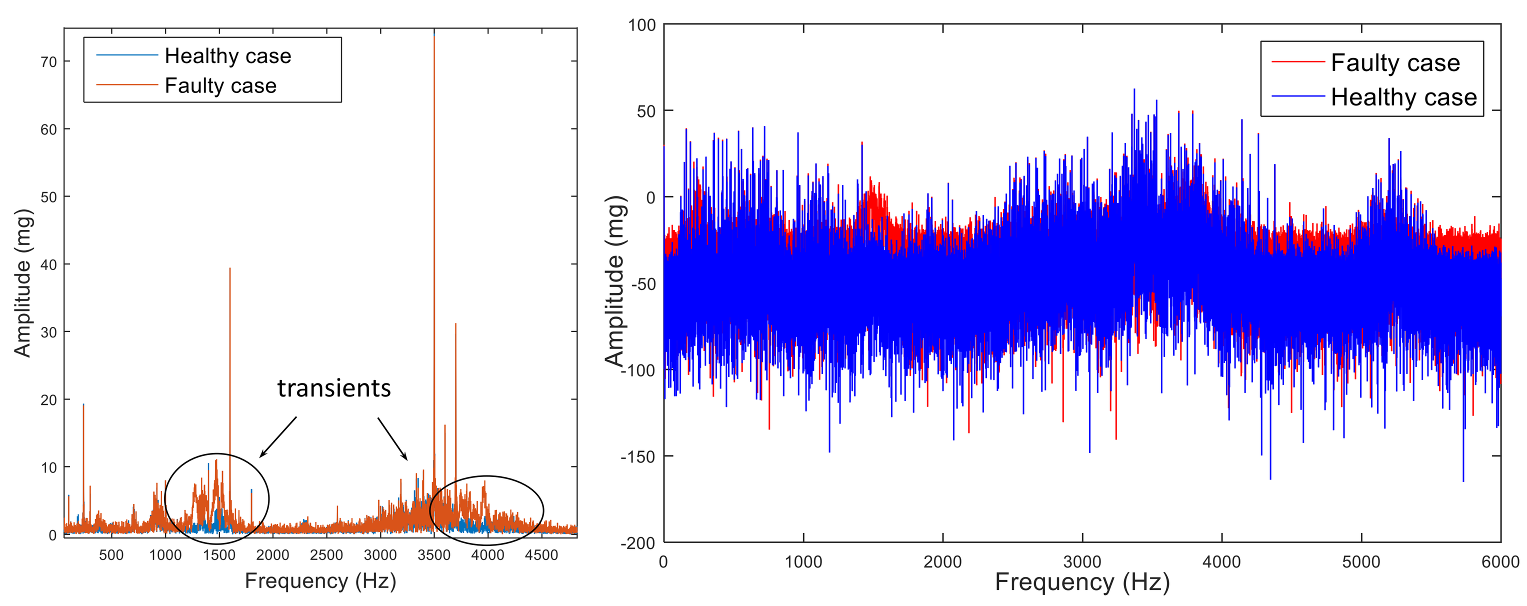

- ❑ Broadband noise amplitude increase
- ❑ Stochastic transients
- ❑ Increase of bearing characteristic frequencies at last stage
- ❑ Validation of detection algorithms

Fault Detection Improvements

This type of fault is only detectable by performing inter-state deviation analysis: parametric method based on wiener filtering & time-frequency methods based on spectral subtraction and spectral kurtosis

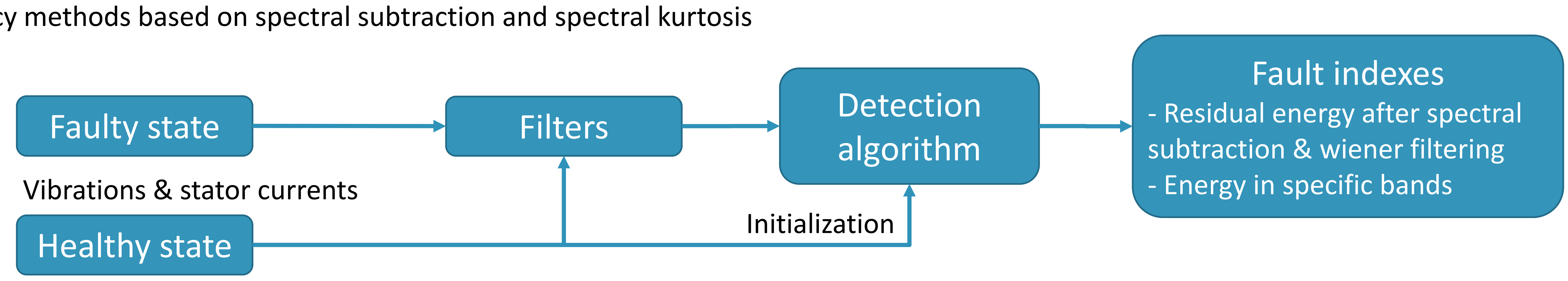

Sensibility improvements
- ❑ suppression of known spectral components in vibration & stator current spectra
- ❑ Principal component analysis on vibration tri-axial signals

Implementability & reliability
- ❑ Fast algorithms implemented in LabVIEW for use with industrial constraints
- ❑ Combination of multiple algorithms for stationary & nonstationary components detection

The purpose is to extract valuable indicators both from data reliability and implementability point of view. This work has both industrial and research interests: today no large scale diagnosis/prognosis tools are applied in industry because the development of this incipient bearing fault is complex to quantify.

Bearing Electrical Aging & Monitoring

7,5 kW motors – inverter controlled

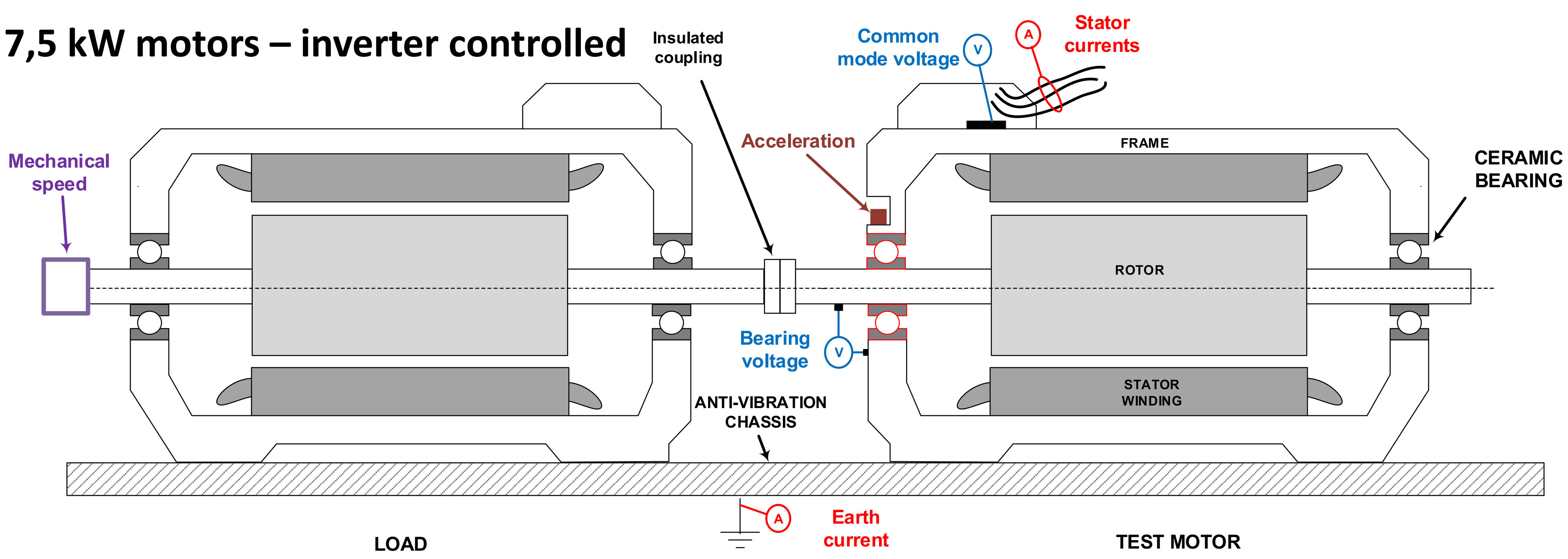

- ❑ Validation of signal models & detection algorithms
- ❑ DE bearing 6208 aging = common mode voltage artificially increased
- ❑ Unique path for bearing currents
- ❑ Vibration, stator current & bearing voltage monitoring

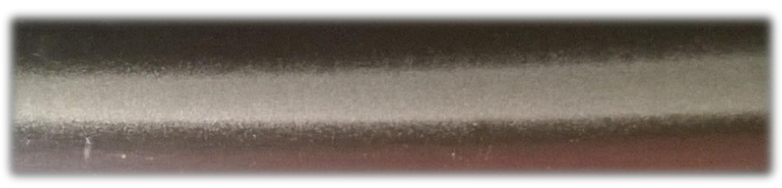

Middle stage generalized roughness

ECOLE DOCTORALE IAEM LORRAINE

UNIVERSITÉ DE LORRAINE

Modelling of Interoperability of Cyber-Physical Systems with Formal Methods

PhD candidate: Dmitry Morozov (dmitrii.morozov@univ-lorraine.fr)
Thesis supervisor: Prof. Hervé Panetto
Thesis cosupervisor: MdC. Mario Lezoche

CNRS CRAN

Research Problem

Cyber-Physical Systems (CPSs) are *systems of systems*, which involve *communication, computation, sensing, and actuating* through heterogeneous and widely distributed physical devices and computation components. Components of a CPS are connected through wired and wireless networks on a large scale and act together as a whole.

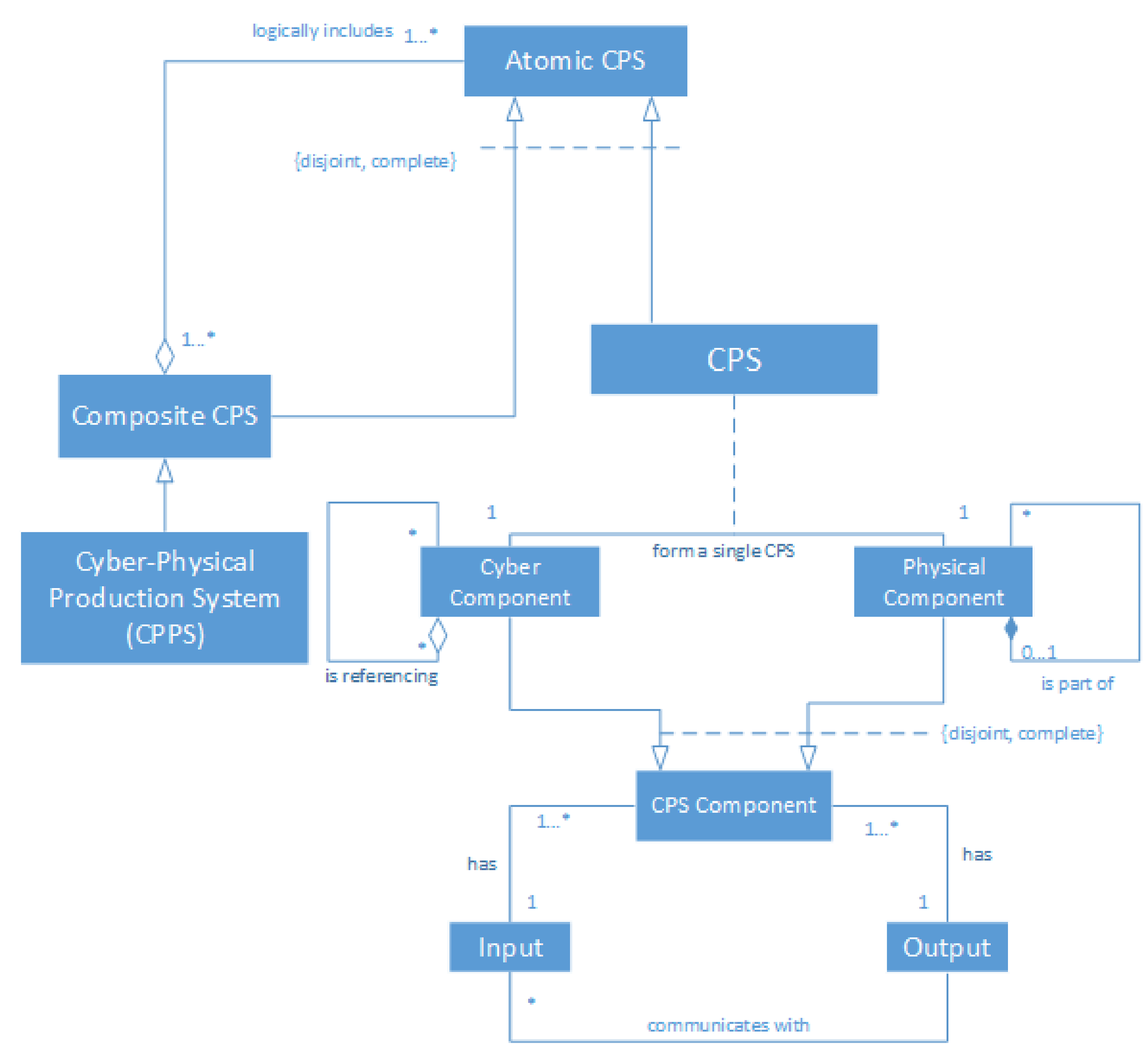

Meta-model of a composite CPS

Research Questions:

- identification of interrelationships between groups of components of CPSs from physical and cyber perspectives
- improvement of interoperability between components of CPS
- identification of redundant components of a CPS

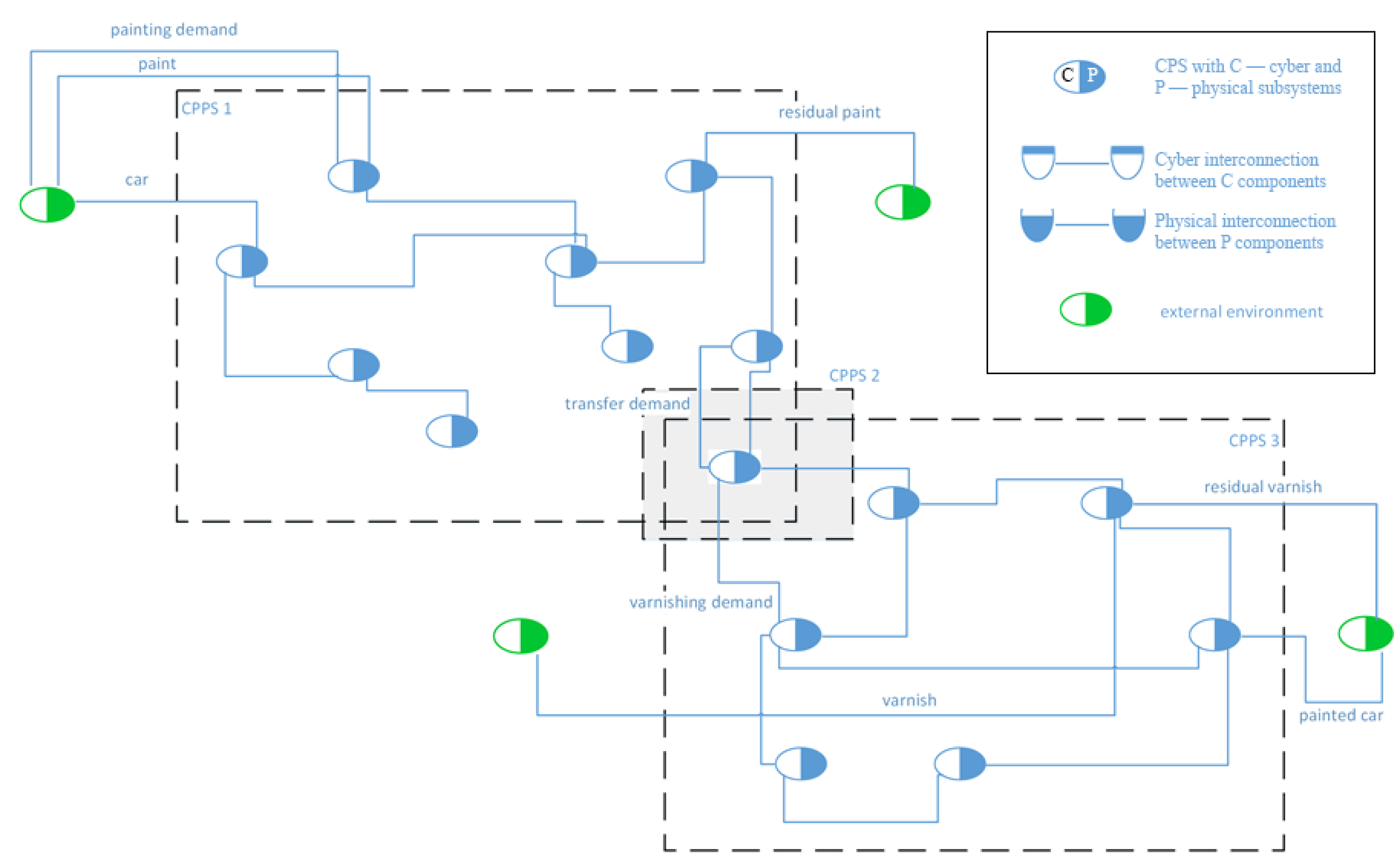

Interconnection of CPSs in cyber and physical perspectives

Formal Concept Analysis modelling

A **formal context** $\mathbb{K} = (G, M, I)$ consists of sets G – set of all objects
M – set of all attributes
and a binary relation $I \subseteq G \times M$

Derivation operators:

For $A \subseteq G$ $\quad A' \coloneqq \{m \in M | gIm \; for \; all \; g \in A\}$

For $B \subseteq M$ $\quad B' \coloneqq \{g \in G | gIm \; for \; all \; m \in B\}$

$(.)''$- **closure operator** $A''' = A' \;\; A'''' = A''$

For $A \subseteq G, B \subseteq M$ (A, B) is a **formal concept** iff $A' = B$ and $B' = A$

An implication between attributes subsets A, B ⊆ M in the context (G;M;I) is a pair of subsets A → B, such that each object g∈G that has all the attributes in A also has all the attributes in B.

Example: "Smart Light Switch" CPS

Two types of sensors:

- **Localization Sensor** – keeps track of the real-time location of the target person
- **Lighting sensor** – measures the strength of light in the room

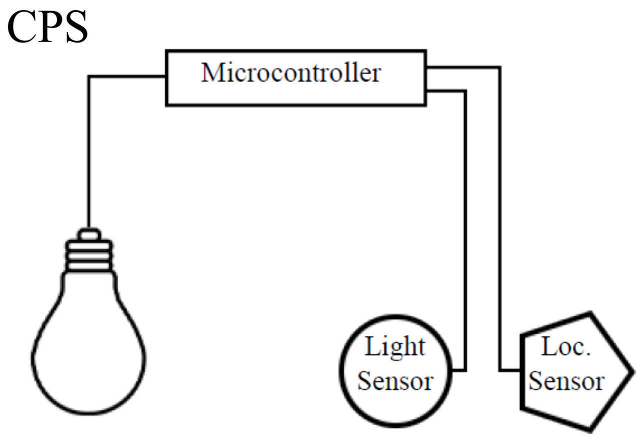

Formal context for the "Smart Light Switch" CPS

	Light Sen	Loc Sen	mC	bulb	room	…	cyber	phys
g_1	X				X	⋮	X	
g_2		X			X	⋮	X	
g_3			X		X	⋮	X	
g_4				X	X	⋮		X

(A = {g_1, g_2}, B = {room, …, cyber}, B′ = {g_1, g_2, g_3})

Characteristic implications of the formal context Table 1:

Properties specific for a particular class:
Cyber: room x = 2 y ≤ 3.5 y ≥ 2.5
Physical: room x = 0 y ≤ 3.5 y ≥ 2.5

Properties common for all components of the system:
room x ≤ 2 x ≥ 0 y ≤ 3.5 y ≥ 2.5;

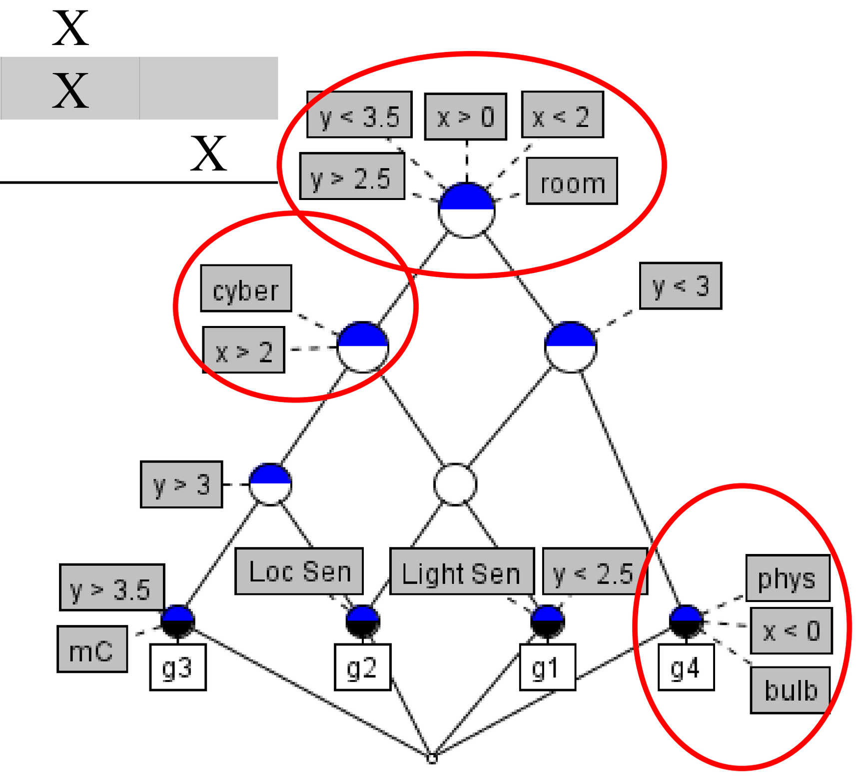

Concept Lattice for the "Smart Light Switch" CPS

Proposed Approach

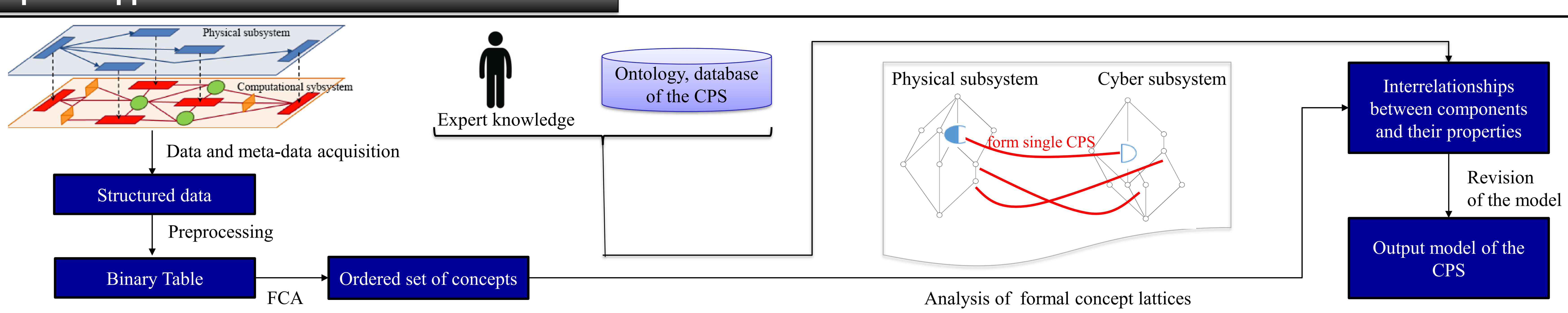

Publications:

- Morozov, D., Lezoche, M., and Panetto, H. "FCA modeling for CPS interoperability optimization in Industry 4.0." *7th International Conference on Information Society and Technology (ICIST 2017).* Vol. 1. 2017.
- Detro, Silvana Pereira, et al. "Enhancing semantic interoperability in healthcare using semantic process mining." *6th International Conference on Information Society and Techology, ICIST 2016.* Vol. 1. 2016.
- [Submitted] Morozov, Dmitry, Mario Lezoche, and Hervé Panetto. "Multi-paradigm modelling of Cyber-Physical Systems" *Journal «Enterprise Information Systems»*, Taylor & Francis Computer Science, 2017.

Case-Based Interpretation of Best Medical Coding Practices

Application to Data Collection for Cancer Registries

Michael Schnell[1,2], Sophie Couffignal[1], Jean Lieber[2], Stéphanie Saleh[1], Nicolas Jay[2,3]

[1] Luxembourg Institute of Health
[2] UL, CNRS, Inria, Loria
[3] Centre Hospitalier Régional Universitaire de Nancy

Goal

Design and integrate a **coding assistant** into the ticketing system, to answer some operator questions.
→ reduce workload for operators and coding experts
→ improve coding consistency (similar questions should receive similar answers)

Idea

Similar solutions have similar arguments
→ use **arguments** to find a suitable source case to solve the target problem

Context

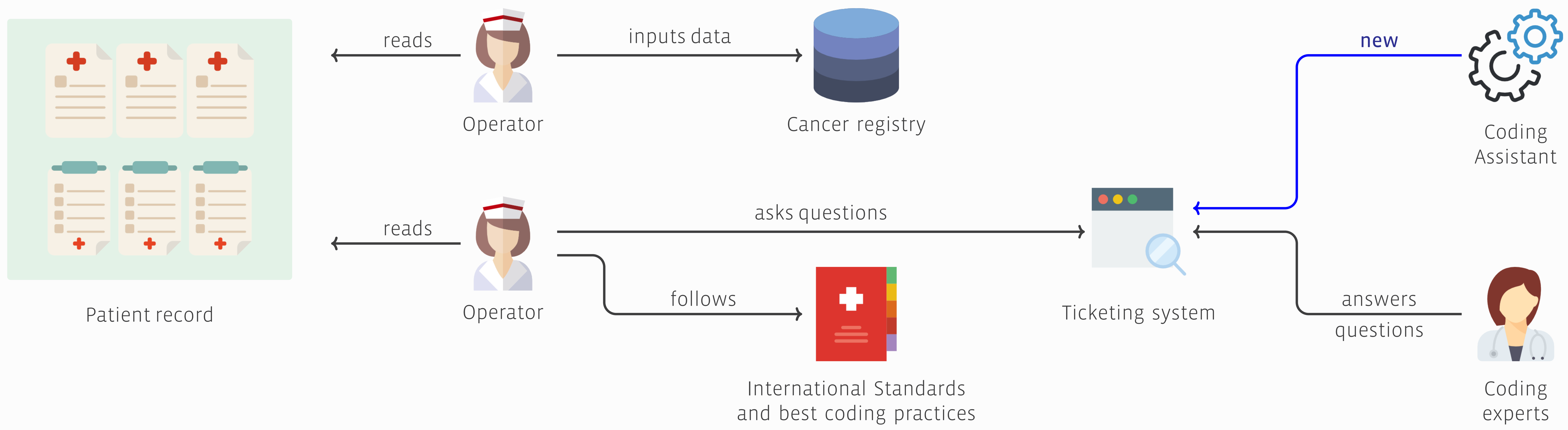

Arguments and Case-Based Reasoning

Source case: Description

Subject
What is the tumor nature of the lung cancer?

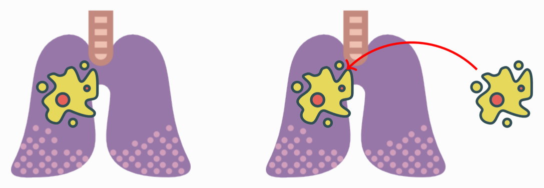

primary tumor or metastasis

Patient record (relevant features)

- Male, age 74
- 2000: prostate cancer (diagnosed, treated)
- 2014: lung cancer discovered
  - CT scan: tumor no mediastinal adenopathy
  - Tumor morphology: adenocarcinoma
  - No other tumor site found
  - Oncologist concluded a primary tumor

Answer Primary tumor (provided by the coding experts)
Explanation (key arguments)

- oncologist's conclusion (wp1)
- no other synchronous tumor was found (wp2)
- long time span between prostate cancer and lung cancer (wp3)
  (a shorter time span would have been in favor of a metastasis)
- no mediastinal adenopathy (wc1)
  (an adenopathy can only develop for primary tumor)

Argument types and applicability

wp2: No other synchronous tumor found

```
wp2(case) = ASK {
    case hasQuestion ?question .
    case concernsRecord ?record .
    ?question concernsTumor ?tumor .
    FILTER NOT EXISTS {
        ?record describesTumor ?other_tumor .
        ?tumor != ?other_tumor .
        ?tumor isSynchronousWith ?other_tumor
    }
}
```

wp2(Source 1) = true, wp2 is **applicable** to Source.

Two dimensions to distinguish arguments:

- in favor vs against
- strong vs weak

Source case: Representation using RDFS

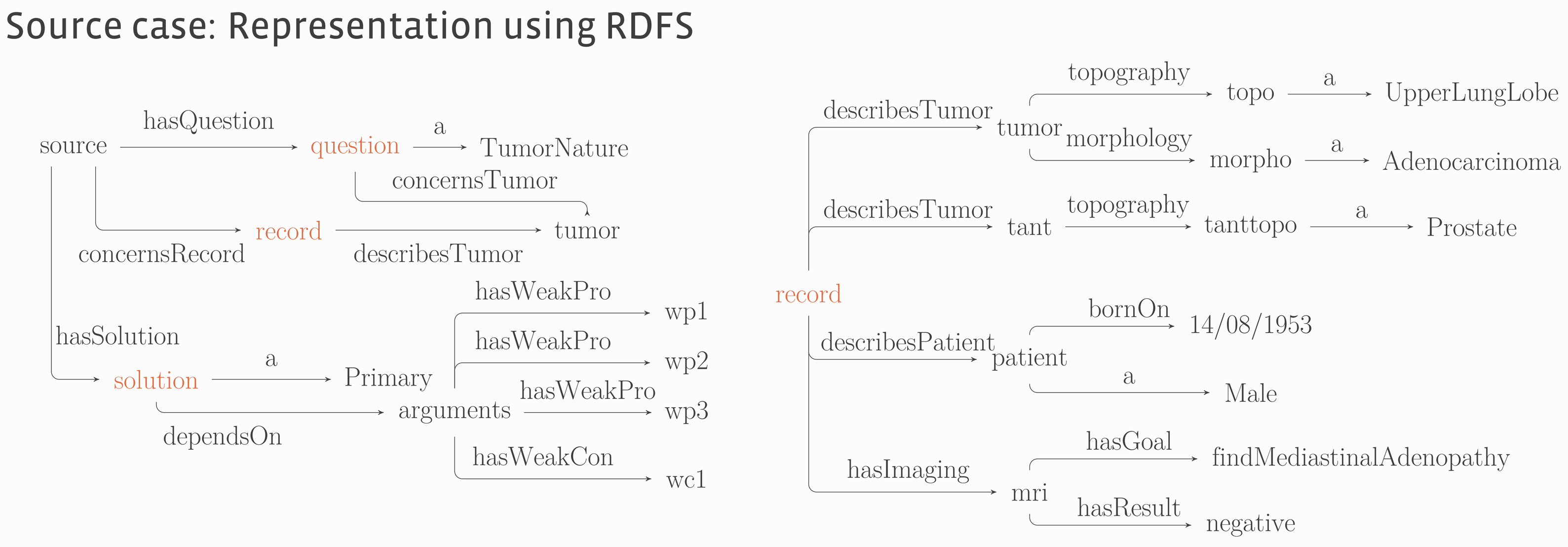

Target problem

Subject What is the tumor nature of the lung cancer? (primary tumor or metastasis)

Patient record (relevant features)

- Female, age 87
- 2006: breast cancer (diagnosed, treated)
- 2016: lung cancer discovered
  - CT scan: tumor no mediastinal adenopathy
  - Tumor morphology: adenocarcinoma
  - TTF1 is negative
  - No other tumor site found
  - Oncologist concluded a primary tumor

Solving target

Find the *most suited source case* to solve target:
→ source case with the most applicable and convincing argumentation

To choose between two source cases, use a preorder $\preccurlyeq_{Target}$ comparing:

- first the applicability of strong arguments
- then the applicability of weak arguments
- finally the patient record similarity

Current Progress

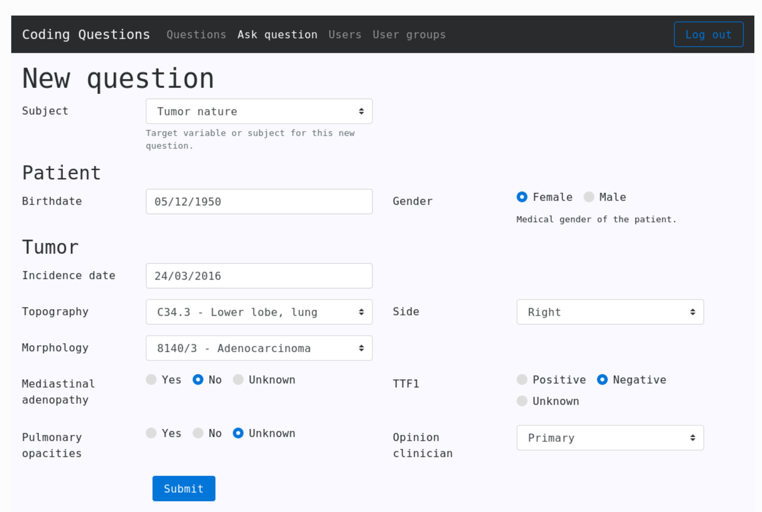

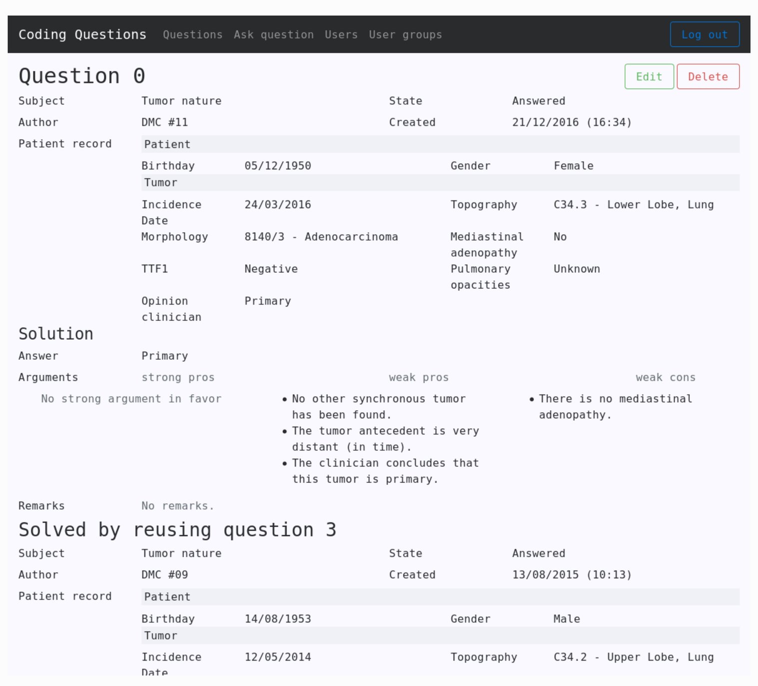

Prototype implementing the retrieve step with arguments

Future work

- Evaluation
  - Are the provided answers correct?
  - Is the method reducing the operator and expert workload?
- Problem description
  - Can we guide operators in their description of the problem?

Icons from flaticon.com, made by Freepik, Madebyoliver, Gergor Cresnar

CCPM: A Scalable and Noise-Resistant Closed Contiguous Sequential Patterns Mining algorithm

Yacine Abboud[1], Anne Boyer[1], and Armelle Brun[1]
[1]Université de Lorraine, LORIA UMR 7503, France

ABSTRACT

Mining closed contiguous sequential patterns has been addressed in the literature only recently, through the CCSpan algorithm. CCSpan mines a set of patterns that contains the same information than traditional sets of closed sequential patterns, while being more compact due to the contiguity. Although CCSpan outperforms closed sequential pattern mining algorithms in the general case, it does not scale well on large datasets with long sequences. Moreover, in the context of noisy datasets, the contiguity constraint prevents from mining a relevant result set. Inspired by BIDE, that has proven to be one of the most efficient closed sequential pattern mining algorithm, we propose CCPM that mines closed contiguous sequential patterns, while being scalable. Furthermore, CCPM introduces usable wildcards that address the problem of mining noisy data. Experiments show that CCPM greatly outperforms CCSpan, especially on large datasets with long sequences. In addition, they show that the wildcards allows to efficiently tackle the problem of noisy data.

BACKGROUND

The sequential pattern mining problem was first introduced by [Agrawal and Srikant, 1995] with the **Apriori algorithm**. Apriori is based on the **monotonicity property** "all nonempty subsets of a frequent itemset must also be frequent". **Prefixspan** [Pei and Han, 2001] algorithm uses **projected databases** to mine frequent sequential patterns. Prefixspan recursively extends a prefix sequential pattern by adding a frequent item from the projected database of this prefix. As **closed sequential patterns** lead to a more compact set of patterns but also a better efficiency, several algorithms focus their mining on such patterns: Clospan [Yan and Han, 2003], BIDE [Wang and Han, 2004]. BIDE generates new patterns with the framework of Prefixspan and uses a **BI-Directional closure checking** scheme that does not use any set of candidates, hence improves greatly both runtime and memory usage. One **major issue** in closed sequential pattern mining comes **from large databases**: the set of frequent closed sequential patterns becomes unmanageable. **CCSpan** [Zang and Wang, 2015] algorithm introduced closed contiguous sequential pattern mining which is more efficient due to the contiguity constraint. CCSpan **scales rather poorly on datasets with long sequences** and suffers from a **lack of adaptability** of the contiguity **to noisy data.**

SCIENTIFIC CHALLENGES

1) **How to improve contiguous sequential pattern mining algorithms to more accurately extract information from noisy data?**
2) **How to increase the efficiency of CCSP mining algorithms to scale with large databases and long sequences?**

CONTRIBUTIONS

1) **Second CCSP mining algorithm that significantly outperforms the first one, CCSpan**
2) **Wildcards to make CCPM noise-resistant**
3) **Experiments on large and noisy data**

CCPM ALGORITHM

CCPM is based on Prefixspan and on BIDE, two of the most efficient sequential mining and closed sequential mining algorithms. **CCPM mines closed contiguous patterns with usable wildcards**. A wildcard is a joker of one item regarding the contiguity constraint. The use of contiguous sequential patterns mining algorithm is only relevant in case of clean data but most of the time data still contains noise. In order to overcome this issue, we introduce a maximal number of wildcards per pattern. As the mined data is usually just a bit noisy, the number of wildcards allowed is often rather small. To the best of our knowledge, **CCPM is the first noise-resistant CCSP mining algorithm due to the use of wildcards**.

In addition, **CCPM allows to mine patterns starting with an item that satisfies a chosen constraint: starting item patterns**. Such patterns are interesting in many domains. In text mining, patterns starting with an action verb in order to identify competencies [Abboud et al.,2015] or in marketing, purchase patterns starting by a given category of items to establish more targeted selling strategies, etc. As a contiguous sequential starting item pattern (CSSP) can only start with a starting item, a closed contiguous sequential starting item pattern (CCSSP) is necessarily equal or included in a closed contiguous sequential super-pattern.

CCPM uses a framework that enumerates frequent contiguous sequential starting item patterns with wildcards (CSSPWs), inspired by the framework of Prefixspan to enumerate frequent sequential patterns. CCPM uses a closure scheme and a pruning technique inspired by the BI-Directional closure scheme and the Backscan method of BIDE to mine closed patterns. CCPM relies on three steps listed here: First, a **framework that mines frequent CSSPWs**. Second, a **BI-Directional checking scheme, adapted to CSSPWs**, that forms closed contiguous sequential starting item patterns with wildcards (CCSSPWs). Third, a contiguous pruning techniques used to improve the efficiency of CCPM.

EXPERIMENTS

The experiments were performed in order to evaluate the performance of CCPM, we used five real datasets that cover a wide range of distribution characteristics. Two of them are reference datasets used to evaluate sequential pattern mining algorithms (Gazelle and Mushroom). As CCPM can be set to mine CCSPs like CCSpan, we can conduct a series of experiments on the five datasets in terms of execution time and memory usage, with various relative support thresholds. Some of **these datasets share similarities on some attributes**, so we can easily compare the influence of each attribute on CCPM. **The experiment highlights the impact of both average length and number of sequences on the efficiency of CCSpan and CCPM.**

DATASET	*#SEQ*	*#ITEMS*	*AVERAGE LENGTH*
BMS1 Gazelle	59,601	497	2.4
Mushroom	8,416	119	23.0
jobs900	900	4,460	26.6
jobs1000	1,000	8,813	76.0
jobs60000	60,000	92,394	77.0

RESULTS

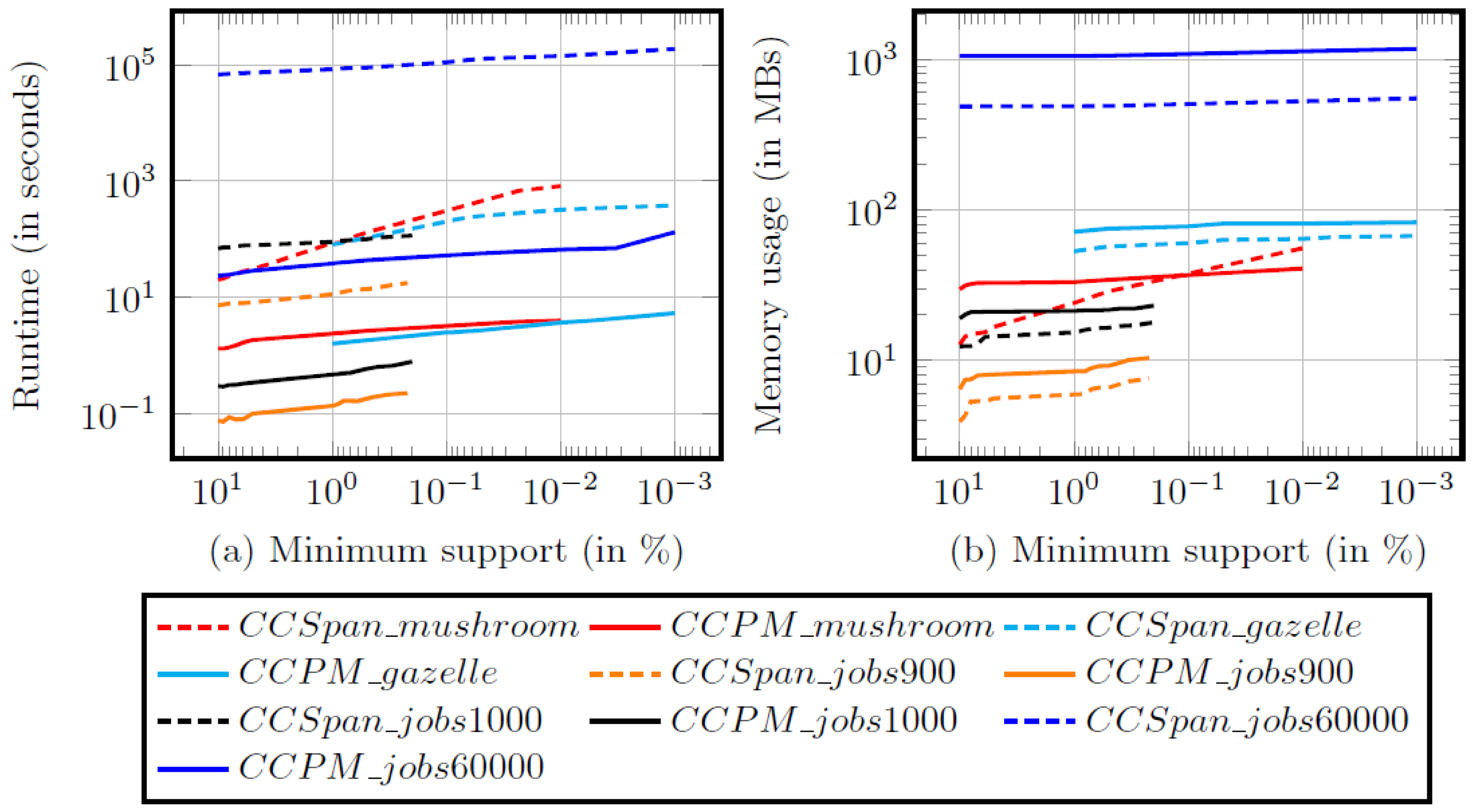

DATASETS PAIR	*RATIO OF AVERAGE LENGTH*	*RATIO OF #SEQ*	*RATIO OF RUNTIME ON CCSPAN*	*RATIO OF RUNTIME ON CCPM*
jobs900/ jobs1000	3	~1	8 **(8/3=2.7)**	3.5 **(3.5/3=1.2)**
BMS1 Gazelle/ jobs60000	32	~1	6,800 **(6,800/32 =212)**	25 **(25/32=0.8)**
jobs900/ Mushroom	~1	9	8 **(8/9=0.9)**	18 **(18/9=2)**
jobs1000/ jobs60000	~1	60	915 **(915/60=15)**	**83** **(83/60=1.4)**

This experiment has shown that **when mining CCSPs the support variation has almost no impact on both runtime and memory usage**, probably due to the contiguity constraint. In addition, the memory usage is extremely stable.

CCPM is always significantly faster than CCSpan, regardless the dataset and the support, while having memory usage in the same order of magnitude. Moreover**, the runtime of CCPM is linearly impacted by the number of sequences and their average length, contrary to CCSpan.**

CONCLUSIONS

- ✓ **CCPM efficiently mines** closed contiguous sequential patterns **in large datasets with long sequences**
- ✓ **Wildcards allows to fit noisy data** while preserving the added value of contiguity
- ✓ Starting items allows to mine a new set of patterns not included in the set of closed contiguous sequential patterns

Predictive Maintenance for Control of Energy Performance in Buildings

Collince Christian NZUKAM – 3ème Année

Encadrants: Éric Levrat, Dominique Sauter, Alexandre Voisin

CONTEXT OF THESIS

Sectors

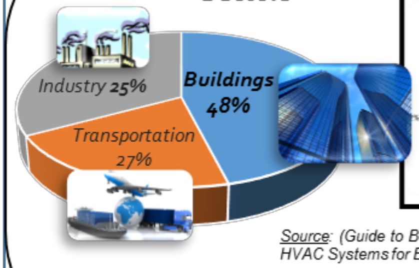

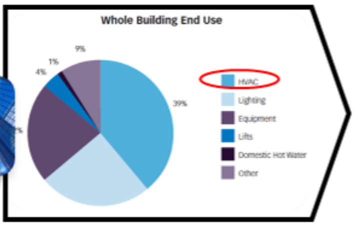

Source: (Guide to Best Practice Maintenance & Operation of HVAC Systems for Energy Efficiency, January 2012)

Objectives of Thesis

- ❑ How the coupling of diagnostic and prognostic processes can be done
- ❑ Propose a decision making approach for maintenance decision taking to help the maintenance expert taking suitable and efficient decisions.

Project Title: Simulation based control for Energy Efficiency building operation and maintenance. EIT (**Energy In Time**) architecture is decomposed in several modules among which **Predictive Maintenance Strategy** belongs. There are **13 participants** in the project from 8 countries

Predictive Maintenance Definition

- ✓ Predict when equipment failure might occur
- ✓ Prevent failure occurrence by performing maintenance. Predictive maintenance is based on three processes:

Diagnostic
- Faults identification
- Degradation/Failure Mode

Prognostic
- Remaining Useful Life (**RUL**)
- Degradation/Failure Mode
- Equipment Health state

Decision Making
- Propose Maintenance actions
- Best time to perform these maintenance actions

Results and Prospects

1- Grouping Maintenance Actions (Opportunity-Oriented Approach)

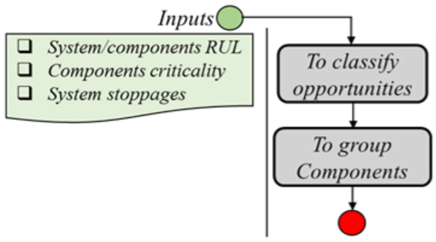

Advantages of the proposed approach

- ❑ Optimizes the availability of facility;
- ❑ Proved dynamic in group construction;
- ❑ Opportunity-oriented approach;
- ❑ Delay as far as possible maintenance interventions

❖ **To classify opportunity**

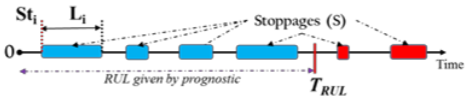

Stoppages formalism

St_i: Starting time; L_i: Length of stoppage; $Trul$: Time of failure

(E. Thomas 2009)

$$P_i = R(St_i).M(L_i)_{1<i<n}$$

$$r_i = P_i / 1 - P_i$$

$$Sum = \sum_{i=n} r_i$$

Optimal stoppage

C_3	C_1	C_2	C_3
S_4	S_3	S_4	S_3
S_1		S_2	S_2
		S_1	

- Let **G** be a set of sets such that $G = \{G_1, \dots, G_k\}_{1 \le k \le p}$
- The sum of mean time to Repair is computed

$$Sum_{G_k} = \sum_{i=1}^{cn_k} MTTR_i$$

- The aforementioned sum is compared

$$Sum_{G_k} \le L_k$$

What happen when

$$Sum_{G_1} > L_k$$

- The stoppage shift has to be minimized

$$\min\{l_{C_{i,1 \le i \le cn_k}} / cs_{i,k} = 1\}$$

- Component criticality and then component RUL

$$\min\{Crit(C_j)\}$$

$$\min\{\mathrm{RUL}(C_j)\}$$

C.Nzukam, A.Voisin, E.Levrat, D.Sauter, B.Iung. A dynamic maintenance decision approach based on maintenance action grouping for HVAC maintenance costs savings in non-residential buildings. 20th IFAC World Congress, IFAC 2017, Jul 2017, Toulouse, France

2- Impacts of uncertainties on choice of Optimal Stoppage

- ❑ In reality, the time when a stoppage will start as well as its duration is not known with accuracy.
- ❑ This lack of accuracy arises **uncertainties** that have an impact on the choice of optimal stoppage. (Prediction context)

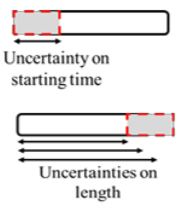

Modeling of Uncertainty

Let denote X_k, the random variable that follows a normal law with mean μ and standard deviation σ^2

$$X_k \longrightarrow N(\mu, \sigma^2)$$

3- Prospects (Further research)

- ❑ Taking into account the Probabilistic nature of RUL
- ❑ Taking into account Spares Part and Human Resources Availability
- ❑ Evaluation of grouping solution relevance (Compared to existing methods)

Studying group performance and behavior in collaborative editing

PhD Student: Hoai Le NGUYEN hoai-le.nguyen@inria.fr
Supervisors: Claudia IGNAT and Francois CHAROY

Real-time and non real-time collaborative editing

A group of people edits a shared document or a shared project simultaneously or non-simultaneously. Examples: real-time editors, version control systems.

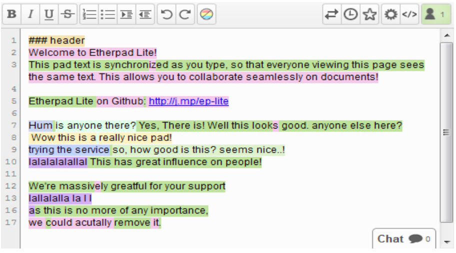

RQ1: *How often people edit in parallel?* → ***Integration rate***
RQ2: *How often parallel works result in unresolved conflicts ?* → ***Conflict rate***
RQ3: *How people try to resolve conflicts?* → ***Rollback, applying changes***

Parallelism and conflicting changes in decentralised version control systems Git [1]

RQ1, RQ2

Project name	Modified files	Integration rate on files	Conflict rate on files
Rails	117960	4.04%	16.26%
IkiWiki	37327	1.08%	50.50%
Samba	306182	0.68%	87.84%
Kernel	1278247	10.99%	4.86%

RQ3

Project name	No. of merge	Rollback Level 0	Rollback Level 1	Rollback Level 2	Rollback Level 3	Rollback rate
Rails	9728	3217	36	2	0	33.46%
IkiWiki	1037	39	13	1	1	05.11%
Samba	1281	260	2	0	0	20.45%
Kernel	38961	2016	1	0	0	05.11%

Adjacent-line conflict

Project name	Total content conflicts	Adjacent-line conflicts	Applying both changes
Rails	397	20.15%	57.50%
IkiWiki	26	15.38%	75.00%
Samba	1190	3.45%	24.39%
Kernel	1693	21.68%	85.01%

Integrations and conflicts based on Release dates

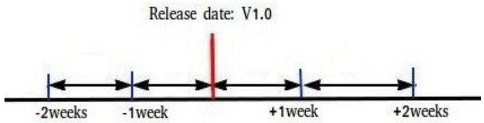

Linux kernel: Conflict rate on files

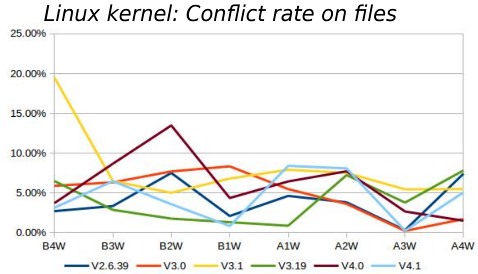

Linux kernel: Integration rate on files

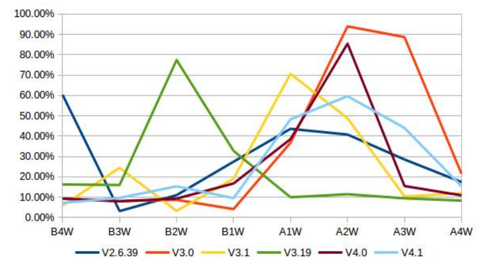

Merge

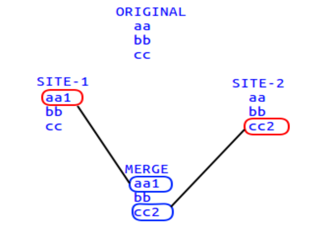

Conflict

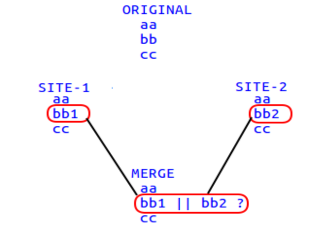

Adjacent-line conflict

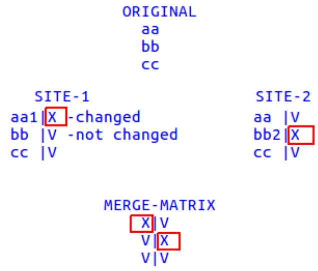

Rollback action

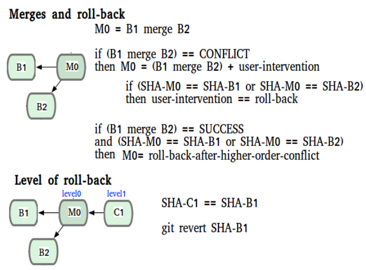

Results

+ *Conflict rate depends on how the integration process is managed*
+ *The rollback action is used more often in case of higher-order conflicts than in case of textual conflicts*
+ *Users mostly appy all changes in two adjacent lines conflicts; We propose that Git merges changes in two adjacent lines and throws a warning message instead of considering them as conflicting*

Future Work

+ *Real-time collaborative editing analysis: ShareLaTeX logs*

[1] NGUYEN H.L, IGNAT C., Parallelism and conflicting changes in Git version control systems, The Fifteenth International Workshop on Collaborative Editing Systems, IWCES'17 - ACM CSCW 2017, Portland, Oregon, USA

Structures de patrons pour classifier des triplets RDF

Justine Reynaud, Yannick Toussaint et Amedeo Napoli

INRIA – Université de Lorraine

Résumé

Objectifs

- Travailler avec des données *complexes* (RDF)
- Utliser de la *background knowledge*
- Extraire des *définitions* à partir de triplets

Travail dans la continuité de [1]

Background théorique

Web des données

Triplet `(sujet, prédicat, objet)`

RDF Exprimer des faits (ABox)

```
Poitiers rdf:type Capital
```

RDFS Structurer les données (TBox)

```
Capital rdfs:subClassOf City
cityOf rdfs:subPropertyOf hasLocation
```

Structures de patrons [2]

Permettent de classifier des objets en fonction de leurs descriptions.

$$(G, (D, \sqcap), \delta)$$

- **G** Ensemble d'objets
- **D** Ensemble de descriptions ordonnées
- **$\sqcap$** Opérateur de *similarité*
- **δ** Mappe d'un objet vers une description

On vérifie $A \sqcap B = A \Leftrightarrow A \sqsubseteq B$

Classification des triplets

Nous proposons une structure de patrons pour les triplets RDF étendant celle proposée dans [1].

```
Paris capitalOf France .
Paris cityOf Europe .
Paris subject European_Capitals .
Poitiers cityOf France .
Poitiers hasLocation Europe .
Kiev hasLocation Europe .
Kiev subject European_Capitals .
Alger hasLocation Africa .
```

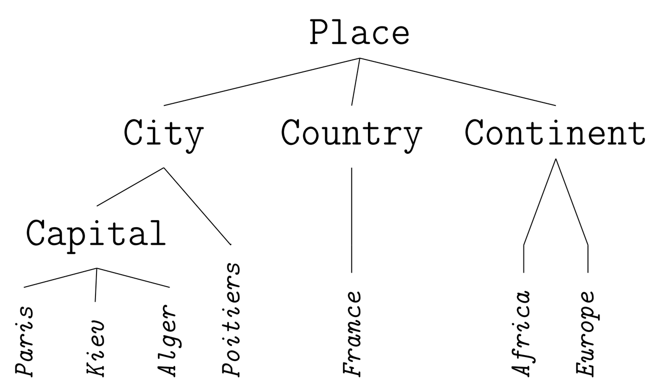

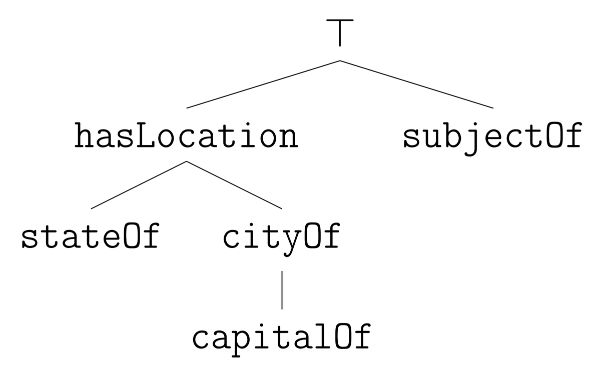

Construction de la structure de patrons

Extent Sujets des triplets

Intent $\delta(s) = \{(p, o) \mid (s, p, o) \in \mathcal{B}\}$

Similarité $\delta(s_1) \sqcap \delta(s_2) = min\,\{(lcs(p_i, p_j), lcs(o_i, o_j)) \mid \forall (p_i, o_i) \in \delta(s_1), \forall (p_j, o_j) \in \delta(s_2)\}$

- *lcs* désigne le plus petit ancêtre commun
- *min* ne conserve que les paires les plus spécifiques

$$\delta(Paris) = \{(capitalOf, France), (cityOf, Europe), (subject, European\_Capitals)\}$$
$$\delta(Poitiers) = \{(cityOf, France), (hasLocation, Europe)\}$$
$$\delta(Paris) \sqcap \delta(Poitiers) = \{(cityOf, France), (hasLocation, Europe)\}$$

Utilisation de *Range Minimum Query* (RMQ)

RMQ [3] est une approche permettant de l'antichaîne d'ancêtres communs à deux antichaînes. Lorsque les antichaînes sont de taille 1, cela revient à chercher le *lcs*.

- **N** Nœuds dans l'ordre du parcours en profondeur
  N = [Place, City, Capital, City, Place, Country, Place, Continent, Place]
- **P** Profondeur du nœud à la même position dans `N`
  P = [0, 1, 2, 1, 0, 1, 0]

$lcs(Capital, Country) = RMQ(2, 5) = 0$ en position 5 dans `P`, ce qui correspond à `Place` dans `N`

Extraction des définitions

Association Rule $A \rightarrow B$ Support : $\mid (A \cup B)' \mid$ Confidence : $\frac{|(A \cup B)'|}{|A'|}$

Implication If $A \rightarrow B$ with a confidence of 1, then $A \Rightarrow B$

Definition If $A \Rightarrow B$ and $B \Rightarrow A$, then $A \equiv B$

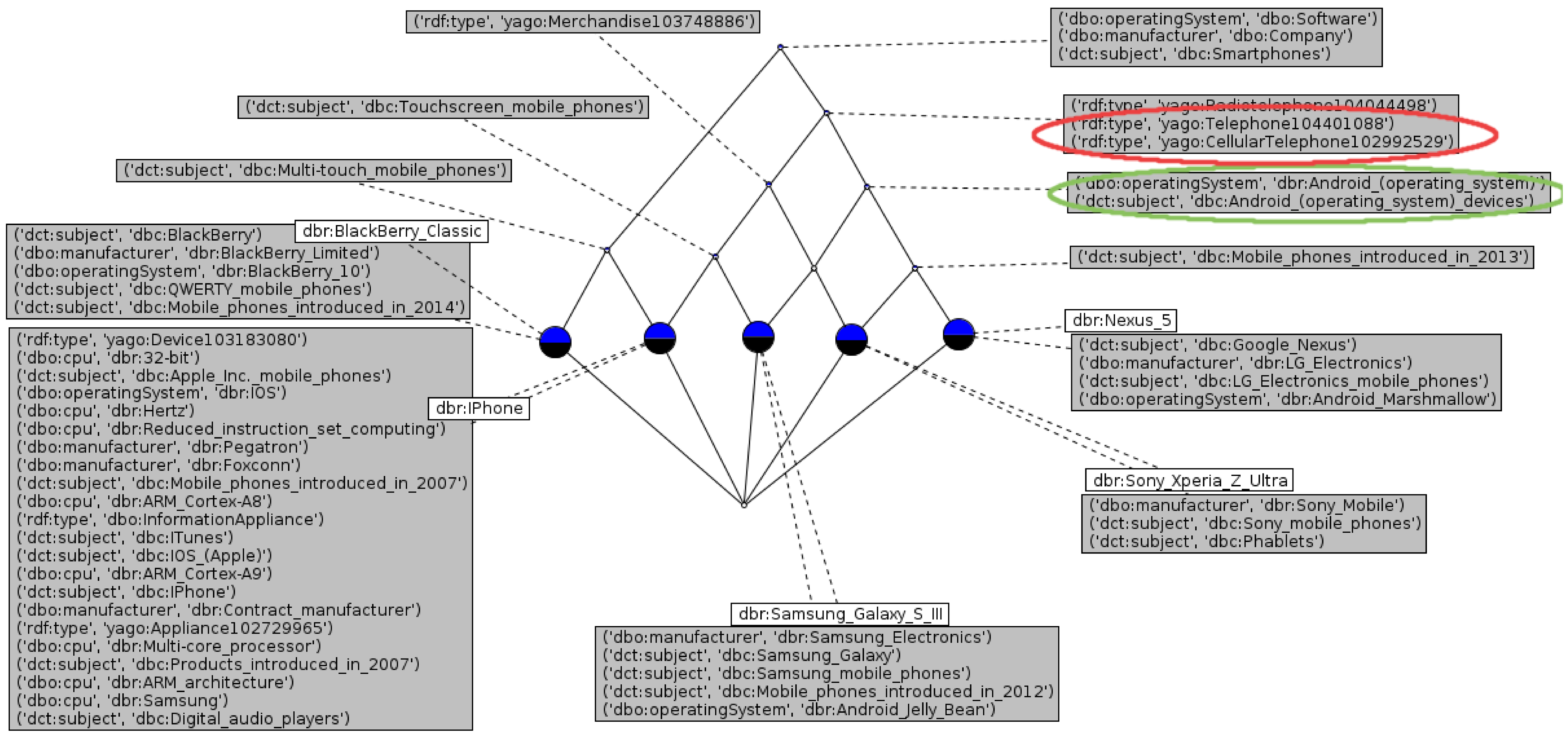

`(subject,Android_(OS)_devices)` $\equiv$ `(operatingSystem,Android_(OS))`

`(type,Telephone)` $\not\equiv$ `(type,CellularTelephone)`

Conclusion

- Structure de patrons pour les triplets
- RMQ pour l'implémentation
- Règles d'association pour les définitions

Perspectives

- Fouille de définitions dans les structures de patrons
- Prise en compte des littéraux

Remerciements

La thèse de Justine Reynaud est co-financée par la Direction Générale de l'Armement et par la Région Lorraine.

Références

[1] Mehwish Alam.
Interactive Knowledge Discovery over Web of Data.
PhD thesis, Loria & Inria Grand Est, 2015.

[2] Bernhard Ganter and Sergei O. Kuznetsov.
Pattern structures and their projections.
In *Conceptual Structures : Broadening the Base, 9th International Conference on Conceptual Structures, ICCS 2001, Stanford, CA, USA, July 30-August 3, 2001, Proceedings*, pages 129–142, 2001.

[3] Mehwish Alam, Aleksey Buzmakov, Amedeo Napoli, and Alibek Sailanbayev.
Revisiting pattern structures for structured attribute sets.
CLA 2015, page 241, 2015.

Conception d'une interface cerveau-ordinateur pour une meilleure surveillance des réveils peropératoires au cours d'une anesthésie générale

Sébastien Rimbert | Neurosys team, Inria, Villers-lès-Nancy, France

Motivation

On estime jusqu'à 1% le nombre de patients subissant un réveil peropératoire durant une anesthésie générale [1].

Les patients qui gardent des souvenirs de leur réveil peropératoire peuvent être sujet à de graves traumatismes [2].

Lorsque les patients reprennent conscience durant l'opération, leur premier réflexe est d'essayer de bouger [3]. Malheureusement, ils ne peuvent pas bouger à cause du curare qui est administré pour la bonne conduite de l'opération chirurgicale.

Il est possible de détecter une intention de mouvement grâce à la technique d'électroencéphalographie [4].

Est-il envisageable de créer une interface cerveau-ordinateur permettant de détecter les réveils peropératoires grâce à la technique d'électroencéphalographie?

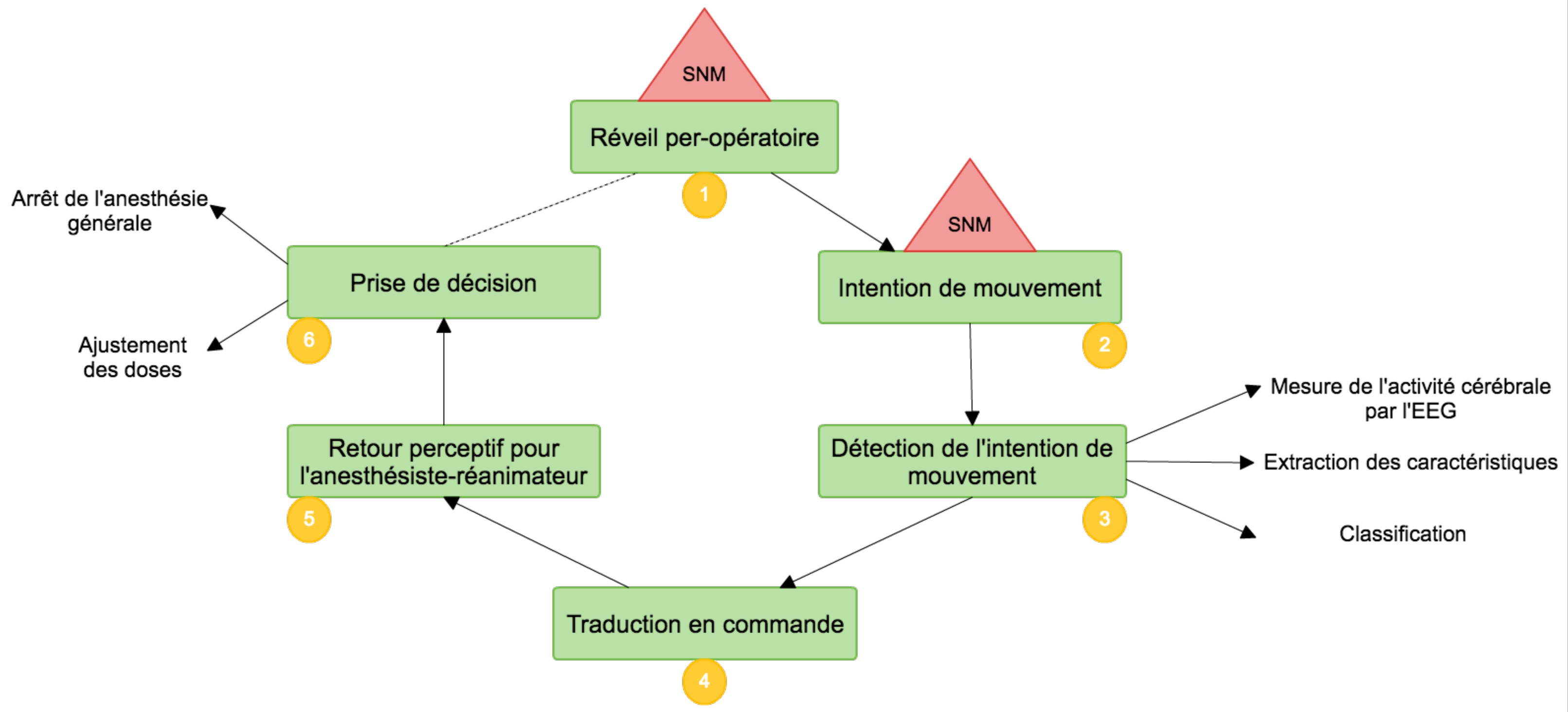

Figure 1 : Différentes étapes nécessaires au fonctionnement d'une interface cerveau-ordinateur permettant la détection de réveils peropératoire au cours de l'anesthésie générale.

Acceptation du protocole clinique

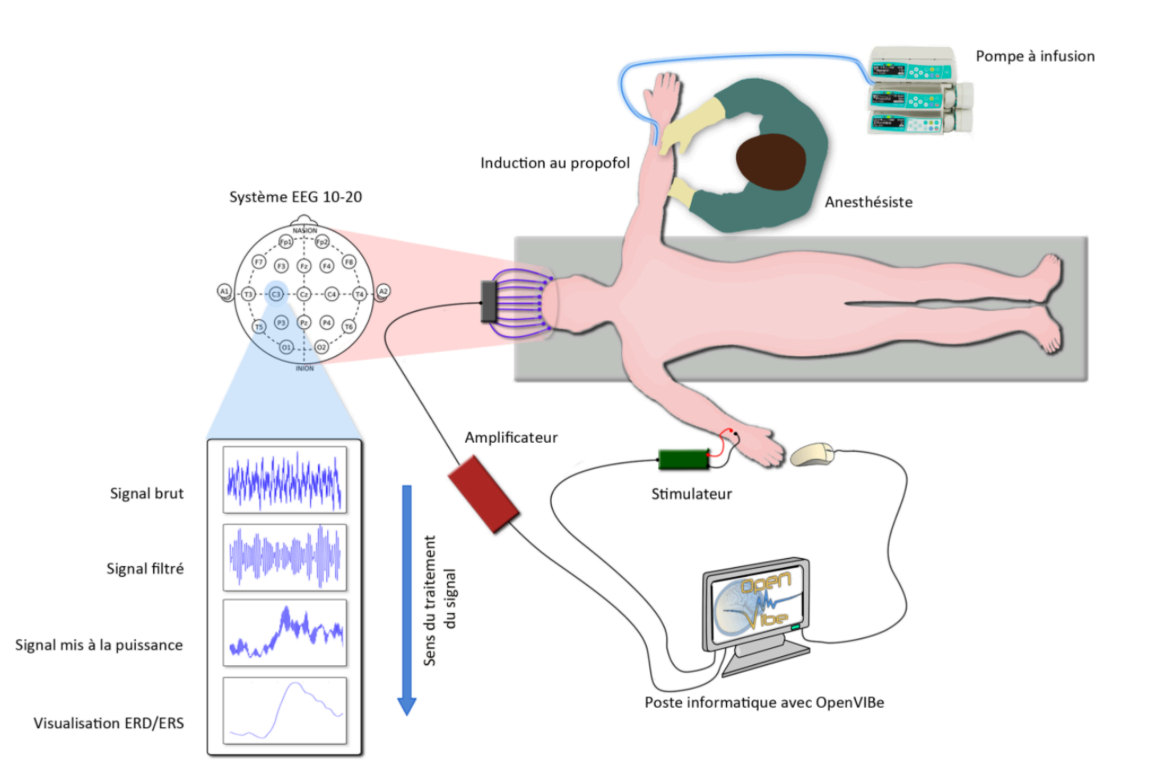

Figure 2 : Schéma descriptif de l'expérience. Le sujet volontaire sain sera allongé et équipé d'un casque EEG et les signaux seront enregistrés grâce au logiciel OpenViBe.

Le protocole clinique a été soumis en collaboration avec le service d'anesthésie-réanimation à la Direction de la Recherche et de l'Innovation, l'Agence National de Sécurité du Médicament et au Comité de Protection des Personnes. L'objectif du protocole clinique est de vérifier qu'il est possible de détecter une intention de mouvement durant une anesthésie partielle au propofol.

Apprentissage de l'imagination motrice

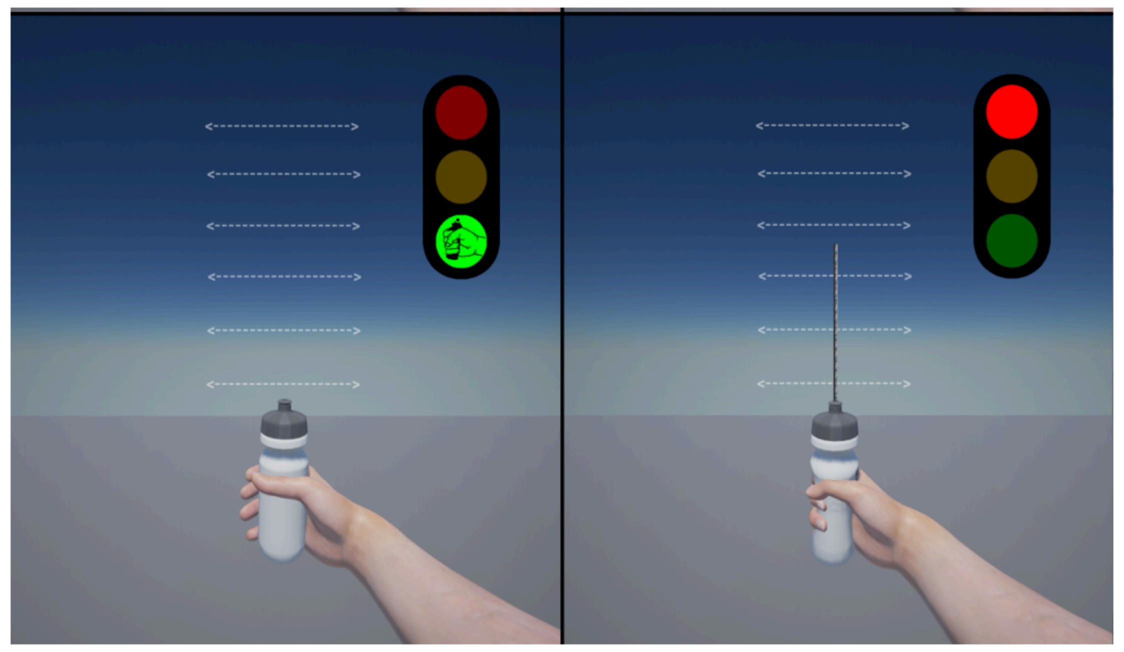

Figure 3 : Illustrations de l'interface Grasp'it permettant l'apprentissage de la tâche d'imagination motrice. Lorsque le feu est vert, l'utilisateur est invité à réaliser la tâche d'IM. Puis, une pression sur la gourde et un jet d'eau apparaît proportionnel à la réussite de la tâche. Une absence de jet correspond à une modulation cérébrale trop faible [5].

Les sujets sains et volontaires qui participeront au protocole clinique doivent connaître et maîtriser la tâche d'imagination motrice. Imaginer un mouvement sans réellement l'effectuer est une tâche complexe qui nécessite un entraînement spécifique [5]. Grasp'it est une IHM qui vise à favoriser l'apprentissage de la tâche d'imagination motrice. Elle supporte un apprentissage progressif, ludique et affordant de la tâche d'IM et permet de s'entraîner avec un neurofeedback visuel.

Imagination motrice discrète et continue

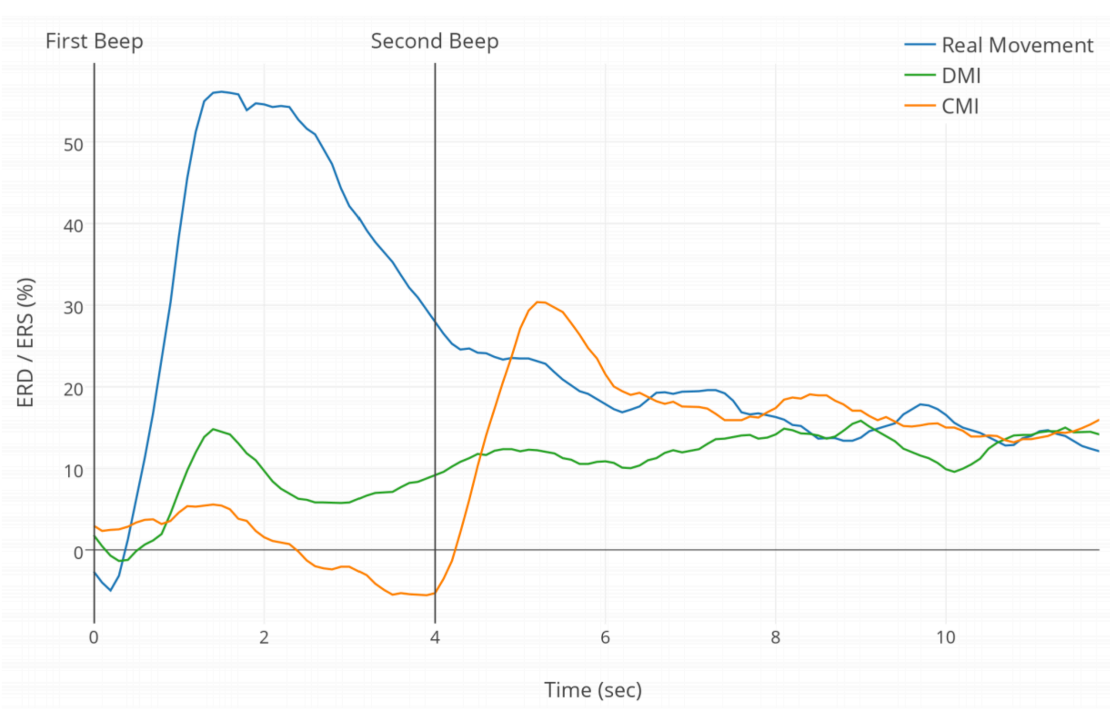

Figure 4 : Grand moyennage des courbes d'ERD/ERS% pour un mouvement réel (RM en bleu), une IM discrète (DMI, en vert) et une IM continue (CMI, en orange) dans la bande de fréquence alpha+bêta (8-30 Hz) [6].

Présence d'un ERS et d'un ERD pour les tâches de mouvement réel, d'imagination motrice discrète et d'imagination motrice continue. L'imagination motrice discrète pourrait donc être utilisée par une BCI.

Adaptation de la BCI pour les utilisateurs

	Frequency Bands		
	Alpha	Beta	Alpha + Beta
Subject	ERD [0-6 sec]	ERS [6-12 sec]	ERD [0-6 sec]
1	88,75 ±6,29	56,25 ±10,31	88,75 ±2,5
2	68,75 ±4,79	83,75 ±6,29	68,75 ±10,31
3	95 ±5,77	58,75 ±2,5	95 ±4,08
4	58,75 ±11,09	73,75 ±4,79	61,25 ±2,5
5	53,75 ±9,46	76,25 ±8,54	51,25 ±2,5
6	56,25 ±7,5	68,75 ±4,79	61,25 ±21,75
7	61,25 ±17,02	80 ±7,07	61,25 ±21,75
8	75 ±4,08	61,25 ±14,36	76,25 ±13,15
9	91,25 ±4,79	33,75 ±11,09	92,5 ±2,89
10	97,5 ±2,89	60 ±5,77	95 ±10
11	97,5 ±5	53,75 ±6,29	98,75 ±2,5
12	60 ±10,8	73,75 ±6,29	73,75 ±10,31
13	96,25 ±7,5	42,5 ±2,89	92,5 ±11,9
14	90 ±9,13	82,5 ±8,66	77,5 ±2,89
15	87,5 ±9,57	88,75 ±19,31	91,25 ±11,09
AVG	78,5 ±7,71	66,25 ±7,93	79,41 ±8,33
AVG OPT	94,58 ±6,51	76,04 ±6,30	90,42 ±6,035

Figure 5 : Résultats de performances obtenues par une analyse linéaire discriminante (LDA) et en utilisant un algorithme CSP pour deux classes (IM main gauche et IM main droite) [7].

Détection d'imaginations motrices combinées

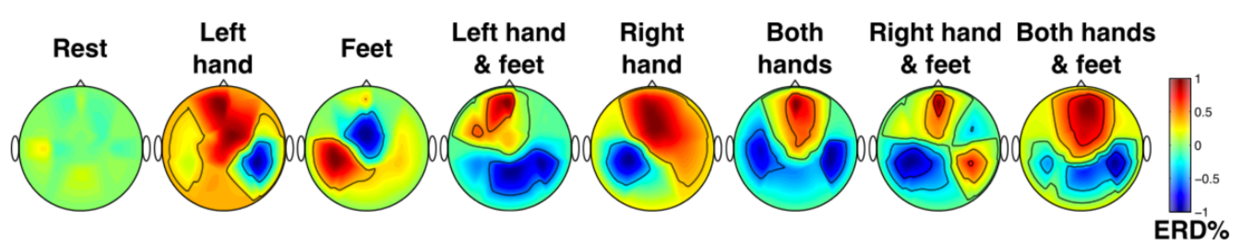

Figure 6 : Puissance oscillatoire relative au niveau du cortex sensorimoteur pour différentes tâches d'IMs.

Perspectives

Les données électroencephalographiques sous anesthésiants doivent être prochainement enregistrées. Elles nous permettront de vérifier si il est possible de détecter correctement l'intention de mouvement d'une personne après une induction de propofol.

Bibliographie

[1] Schwender D, Klasing S, Daunderer M, Madler C, Poppel E, Peter K. (1995). Awareness during general anesthesia. Definition, incidence, clinical relevance, causes, avoidance and medico legal aspects. Anesthesist. 44 (11): 743-54.

[2] Janet, E, Hopper, J, Heran, J, Keane, T, and Kolk, A. (1998). Awareness under anesthesia and the development of post-traumatic stress disorder. 14th Annual Meeting of the International Society for Traumatic Stress Studies, Washington,

[3] Ghoneim M, Block R, Haffarnan M, Mathews M (2009) Awareness during anesthesia: Risk factors, causes and sequelae: A review of reported cases in the literature. Anesth Analg 108: 527–35.

[4] Blokland M, Farquhar J, Mourisse J, G S, Lerou J, and Bruhn J. (2012). Towards a novel monitor of intraoperativeawareness: Selecting paradigm settings for a movement-based brain-computer interface. Br J Anaesth, (101): 178–85.

[5] Rimbert S, Bougrain L, Orhand R, Nex J, Gaborit S and Fleck S. (2017) Grasp'it : une interface cerveau-ordinateur pour l'amélioration de l'apprentissage d'une tâche d'imagination motrice kinesthésique. *29ième conférence francophone sur l'Interaction Homme-Machine*, Poitiers, France (accepted).

[6] Rimbert S, Avilov O, and Bougrain L. (2017) Discrete motor imageries can be used to allow a faster detection. *7th Graz Brain-Computer Interface Conference 2017*, Graz, Austria.

[7] Rimbert S, Lindig-León C, and Bougrain L. (2017) Profiling BCI users based on contralateral activity to improve kinesthetic motor imagery detection. *8th Internationl IEEE EMBS Conference On Neural Engineering*, Shanghai, China

APIL'17

THÈSE

VERS UNE CONCEPTION ARCHITECTURALE AGILE

EXPÉRIMENTATIONS BIM-AGILES EN CONCEPTION COLLABORATIVE

HENRI-JEAN GLESS, ARCHITECTE ET DOCTORANT EN SCIENCES DE L'ARCHITECTURE

1/ UN PROCESSUS TROP RIGIDE

Le processus de conception collaborative en architecture est un processus rigide car orienté activité et production, et non pas équipe et coordination, mieux adaptées à une conception BIM (Building Information Modeling)[1].

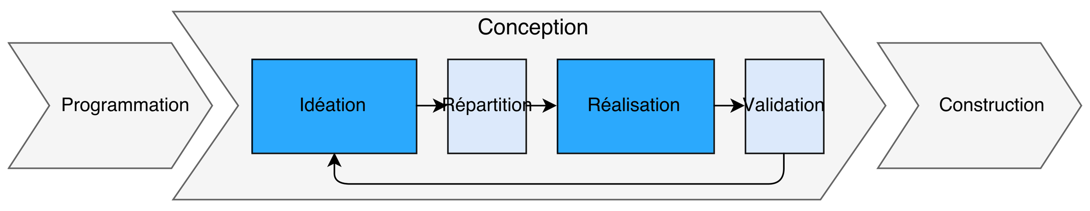

Figure 1 - Processus rigide de conception collaborative

En effet, la technologie BIM de part sa nature aux multiples échelles de conception et à son processus incrémental[1,2], nécessite des méthodes de gestion de projet adaptées et repensées. Par ailleurs, nous avons identifié lors d'entretiens avec des architectes plusieurs manques dans ce processus de conception, tels que la mauvaise communication des intentions architecturales entre tous les acteurs d'un projet, ou encore le faible renseignement des tâches de conception. Ainsi, il s'agit de redéfinir le processus de conception tout en améliorant les activités de coordination et de production.

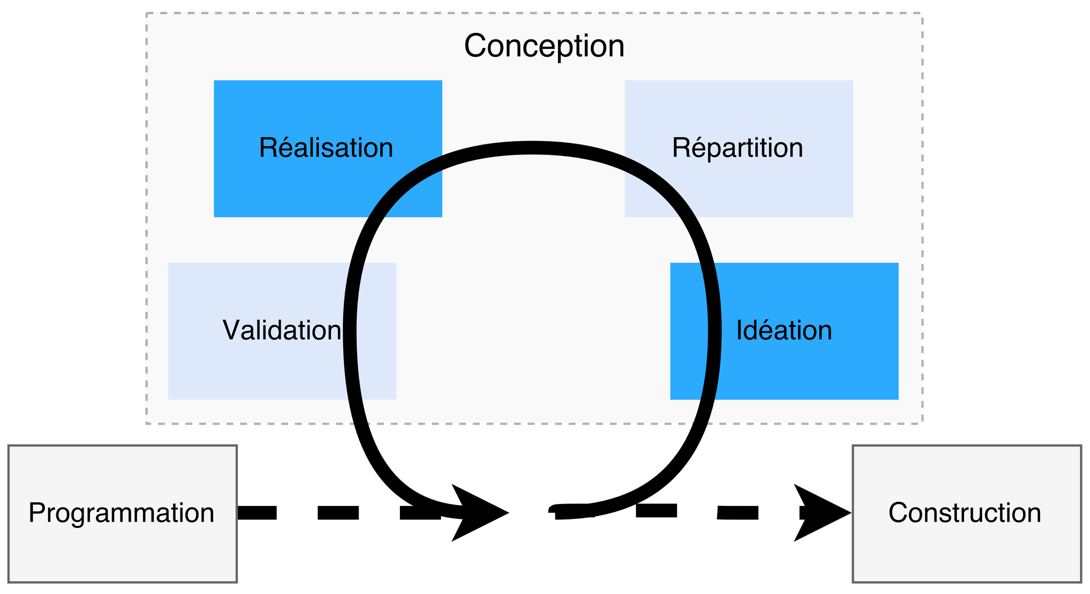

Figure 2 - Processus agile de conception collaborative

2/ UN BESOIN D'ÉLICITATION

En insérant des pratiques dites agiles[3] dans le processus de conception, entre, ou au sein des activités de production ou de coordination, on améliore la communication et donc les chances pour les acteurs du projet de mieux cerner les intentions de tout le monde[4,5]. Ainsi, nous avons imaginé une matrice conceptuelle que les concepteurs peuvent remplir collaborativement suite à l'activité d'idéation. Cette matrice, permet de positionner chaque concepteur au niveau des autres.

		Extrants (visual representation, words)				
		Ground plane		Functional diagram		Keywords
Intrants (programming, needs, constraints)	Boat center			Boats size Boats stockage Dimensions depends capacity High seiling		visibility
	Seminar center	- cohesion between project buildings - private access for delivery	- facilitated visibility and access for external people	- spaces versality ex: same kitchen for club house and intership	links with intership	panorama
	Intership		- calm and privacy - private exterior spaces		- keep night and day spaces distinct - closer spaces for kids	centered
	Club house		- lake access - panoramic terrace - facilitated visibilité and access for external people		- restaurant in links with panoramic terrace - office near the dock	introspection

Figure 3 - Matrice de conception d'un groupe d'étudiants lors d'un projet de conception architecturale.

La figure 3 montre la matrice conceptuelle sous forme de tableur en ligne. Nous trouvons en lignes les intrants[6]. Il s'agit des éléments programmatiques d'un projet, ou encore les besoins ou les contraintes du client. En colonnes nous trouvons les extrants[6]. Ce sont les représentations visuelles, schématiques ou sémantiques tels que les mots-clés, qui servent d'artefacts de sortie, de livrables à montrer au client ou permettant une validation de l'équipe. Les intersections correspondent alors aux traductions verbales des intrants pour les extrants.

3/ ET DE TÂCHES RAFFINÉES

Une fois les intentions des concepteurs clairement définies, il s'agit de les traduire en tâches, avant de les répartir. Il est ainsi nécessaire pour les concepteurs de bien cerner le périmètre de définiton d'une tâche, ainsi que les compétences de chacun. Nous avons donc formalisé la définition d'une tâche selon son nom, sa complexité, sa durée, et son propriétaire.

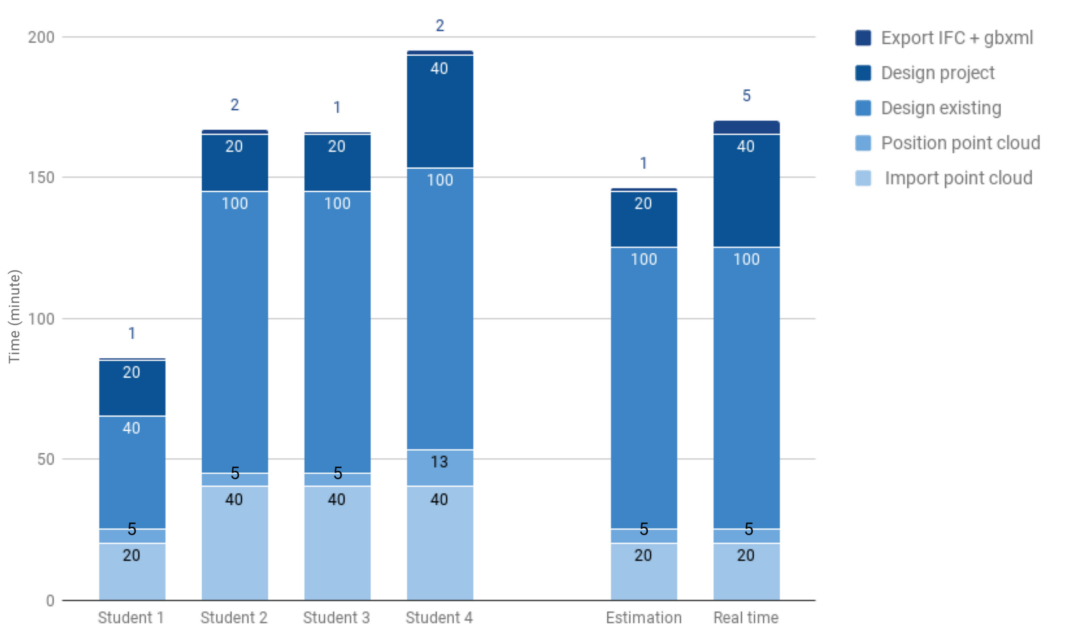

Figure 4 - Estimations d'un groupe d'étudiants grâce au planning poker lors d'un projet de conception architecturale.

Ces caractéristiques sont définies lors d'un serious game, le planning poker, utilisé en génie logiciel.

Il s'agit d'un jeu de cartes, dont les valeurs vont de 1 à 100 (1, 2, 3, 5, 8, 13, 20, 40 et 100) et que chaque joueur dévoile devant lui en même temps que les autres. Les valeurs servent donc à exprimer son avis quant à la durée ou à la complexité d'une tâche.

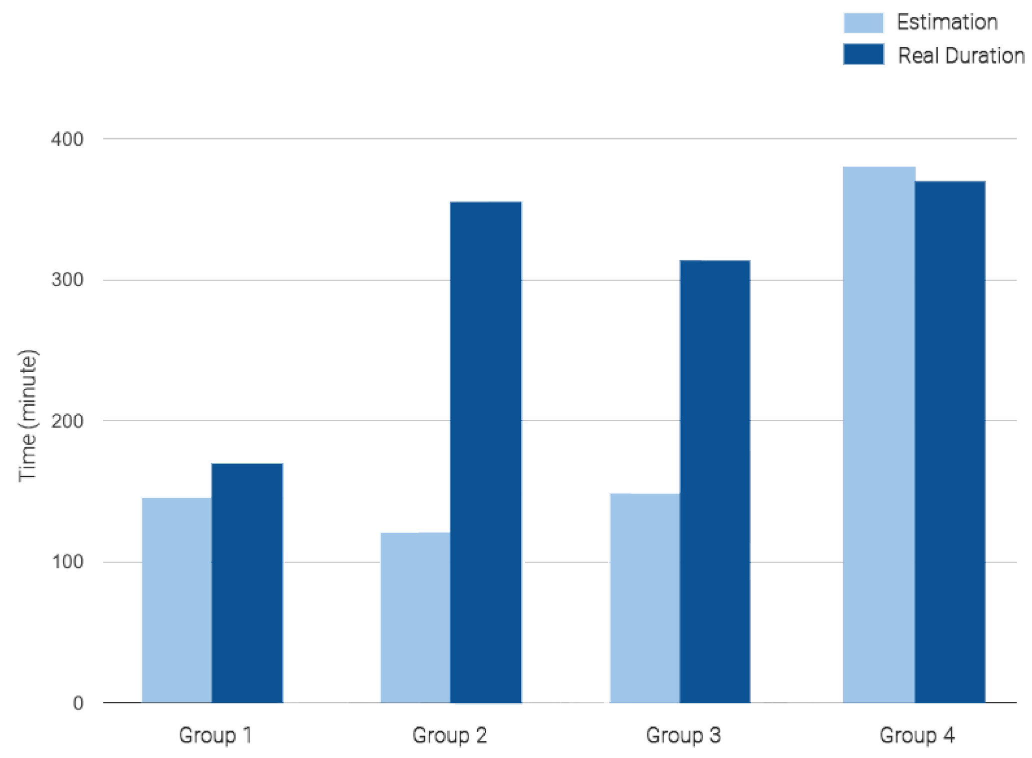

Figure 5 - Estimations et durées réelles mesurées par tous les groupes d'étudiants lors du même projet.

L'objectif est de permettre à chacun de s'exprimer « en même temps » et d'éviter le phénomène du « premier parleur ». Même si les estimations sont erronées, elles permettent aux acteurs, tout comme la matrice conceptuelle, de négocier et d'échanger quant à la quantité de travail d'une tâche ou de qui a les compétences pour la réaliser.

4/ TESTER L'ORIENTÉ CLIENT

Ce travail d'identification et d'insertion de pratiques agiles dans le processus de conception architectural se poursuit ce semestre avec les étudiants du M2 AME. Ces deux pratiques orientées équipe ont évolué pour devenir plus simples à appréhender tandis qu'une pratique orientée client sont également testée : les étudiants sont accompagnés par un facilitateur « BIM et projet » leur permettant de se concentrer sur la conception, le facilitateur se chargeant de résoudre les problèmes dit externes et les besoins clients.

RÉFÉRENCES

[1] Halin G, Hanser D, Bignon J-C (2004) User adaptive visualization of cooperative architec-tural design. International Journal of Architectural Computing, Issue 01 Vol. 02- March 2004, pp. 89-107. doi:10.1260/1478077041220188

[2] Succar B (2009) Building information modeling framework: A research and delivery foun-dation for industry stakeholders. Automation in Construction 18 (2009) pp. 357-375. doi:10.1016/j.autcon.2008.10.003

[3] Beck K et al. (2001) Manifesto for agile software development http://agilemanifesto.org

[4] Dupin P (2014) LEAN applied to construction: How to optimize project management and reduce costs and delays in building? Publisher: Eyrolles; ISBN 978-2212138320

[5] Womack J, Jones D (2003) Lean Thinking: Banish Waste and Create Wealth in Your Cor-poration, Revised and Updated. Publisher: Free Press; Edition: 2 Rev Upd (10 juin 2003) ISBN 978-0743249270

[6] Suh N (2001) Axiomatic Design: Advances and Applications. Publisher: Oxford University Press; ISBN 978-0195134667

Centre de Recherche en Architecture et Ingénierie
UMR n° 3495 - Modèles et simulations pour l'Architecture et le Patrimoine
École Nationale Supérieure d'Architecture de Nancy
ARCHITECTURE NANCY
UNIVERSITÉ DE LORRAINE

A Post-Nonlinear Mixture Model Approach to Binary Matrix Factorization

Mamadou Diop[1,3], Sebastian Miron[3], Anthony Larue[2], David Brie[3]

[1]CEA Tech Grand-Est Metz Technopole, [2] CEA LIST, 91191 Gif sur Yvette, France

[3] CRAN, UMR7039, Université de Lorraine, CNRS, Vandœuvre-lès-Nancy, F-54500, France

1. Introduction: Binary Matrix Factorization (BMF)

- BMF problem:
  The principle of BMF is to factorize a binary matrix $\mathbf{X}$ of size $N \times M$ into two binary matrices $\mathbf{W}$ et $\mathbf{H}$ of respective sizes $N \times K$ and $M \times K$ as:

$$\mathbf{X} = \mathbf{W} \odot \mathbf{H}^T \text{ with } x_{ij} = \bigvee_{k=1}^{K} (w_{ik} \wedge h_{jk})$$

  where $(\vee)$ and $(\wedge)$ are OR and AND logical operators, respectively.
- Example of application : Discrete event system surveillance

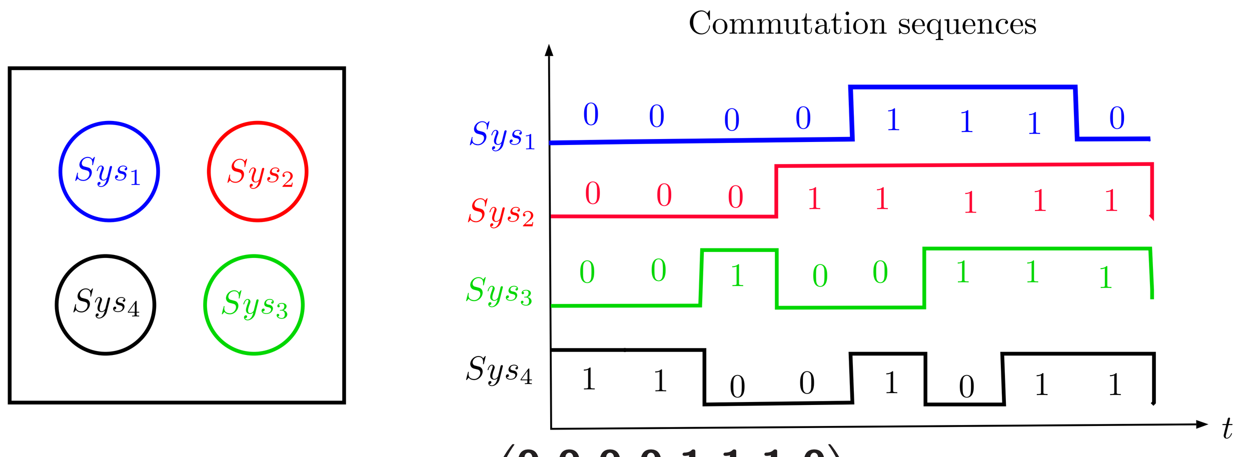

$$\mathbf{X} = \begin{pmatrix} 0&0&0&0&1&1&1&0 \\ 0&0&0&1&1&1&1&1 \\ 0&0&1&0&0&1&1&1 \\ 1&1&0&0&1&0&1&1 \end{pmatrix}$$

Goal: Factorize matrix $\mathbf{X}$ in order to identify common behaviors of different systems or to detect atypical behaviors $\rightsquigarrow$ fault prediction.

- Other applications of BMF: Energy monitoring of buildings, Extraction of population characteristics , Recommendation systems (Google, IMDB, $\cdots$), Gene expressions analysis, etc.
- Inverse problem:

$$\{\mathbf{W}^*, \mathbf{H}^*\} = \underset{\mathbf{W},\mathbf{H} \in \{0,1\}}{\arg\min} \|\mathbf{X} - \mathbf{W} \odot \mathbf{H}^T\|_F^2$$

NP complete problem [1] $\rightsquigarrow$ reformulations (e.g., [2])

2. BMF linear mixture model $\rightsquigarrow$ PF (Penalty Function) algorithm

Replace binary matrix produit $(\odot)$ by the classical matrix product $(\cdot)$

Inverse problem:

$$\{\mathbf{W}^*, \mathbf{H}^*\} = \underset{\mathbf{W},\mathbf{H} \in \{0,1\}}{\arg\min} \|\mathbf{X} - \mathbf{W} \cdot \mathbf{H}^T\|_F^2$$

Cost function with binarity penalty:

$$J(\mathbf{W},\mathbf{H}) = \sum_{i,j} \left(\mathbf{X}_{ij} - (\mathbf{W} \cdot \mathbf{H}^T)_{ij}\right)^2 + \frac{1}{2}\lambda \sum_{i,k} \left(\mathbf{W}_{ik}^2 - \mathbf{W}_{ik}\right)^2 + \frac{1}{2}\lambda \sum_{j,k} \left(\mathbf{H}_{jk}^2 - \mathbf{H}_{jk}\right)^2$$

To minimize this cost function, a gradient descent method with multiplicative update rules, similar to NMF is used.

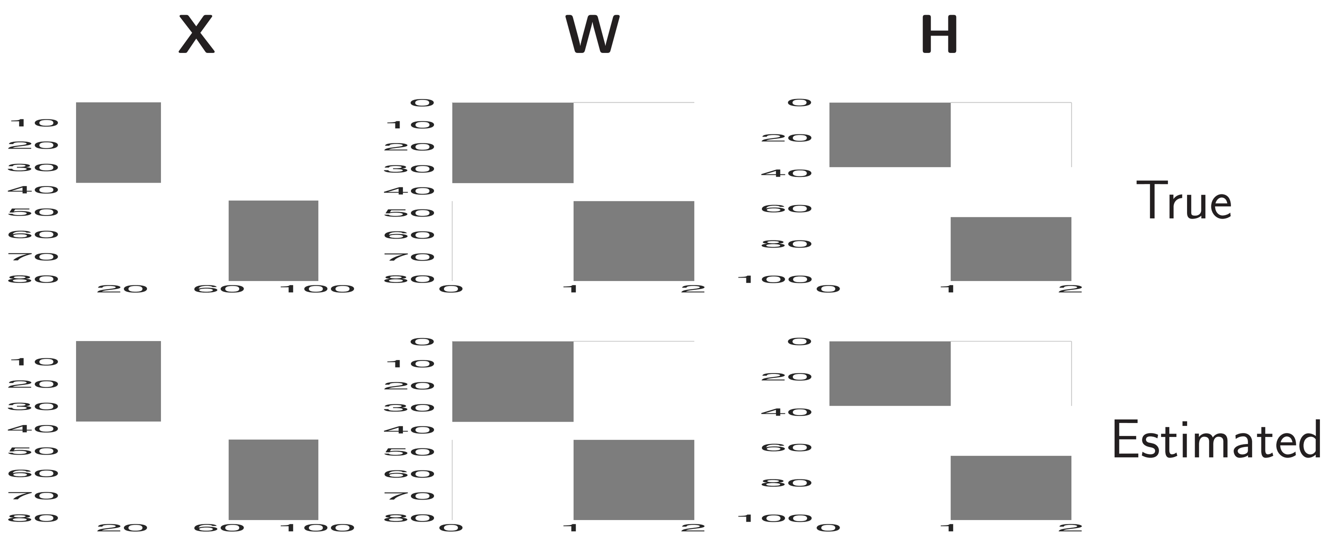

Behavior of PF algorithm for the case of 2 uncorrelated sources

Correct estimation of $\mathbf{X}$, $\mathbf{W}$ et $\mathbf{H}$

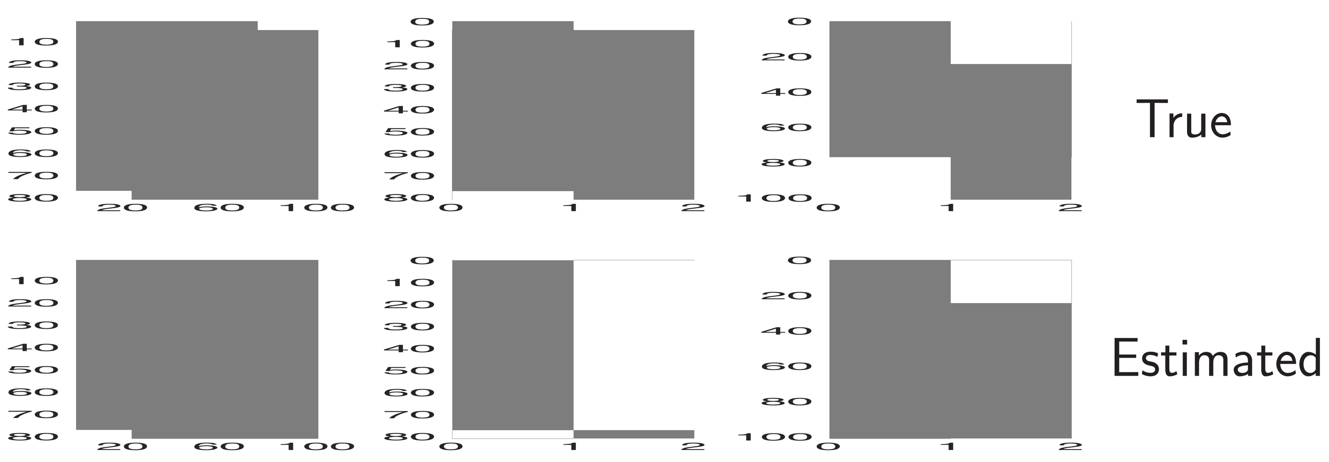

Behavior of PF algorithm for the case of 2 correlated sources

Bad estimation of $\mathbf{W}$, $\mathbf{H}$ and $\mathbf{X}$ because $(\cdot) \neq (\odot)$ in the correlated case.

6. Conclusion

- We proposed a post-nonlinear mixture model for BMF and developed two algorithms
- We provided an identifiability condition for the BMF model
- We compared the proposed algorithms in simulations with the state of the art methods

References

[1] Mamadou Diop, Anthony Larue, Sebastian Miron, and David Brie.
A post-nonlinear mixture model approach to binary matrix factorization.
In *25th European Signal Processing Conference, EUSIPCO 2017*, Kos Island, Greece, August 2017.

[2] Mamadou Diop, Anthony Larue, Sebastian Miron, and David Brie.
Factorisation en matrices binaires par modèle de mélange post non-linéaire.
In *XXVIe Colloque GRETSI Traitement du Signal & des Images, GRETSI 2017*, Juan-les-Pins, France, September 2017.

3. Post-NonLinear (PNL) mixture model $\rightsquigarrow$ PNL-PF algorithm

We introduce a nonlinear function $\mathbf{\Phi(X)}$ which guarantees the binarity of product $\mathbf{W} \cdot \mathbf{H}^T$.

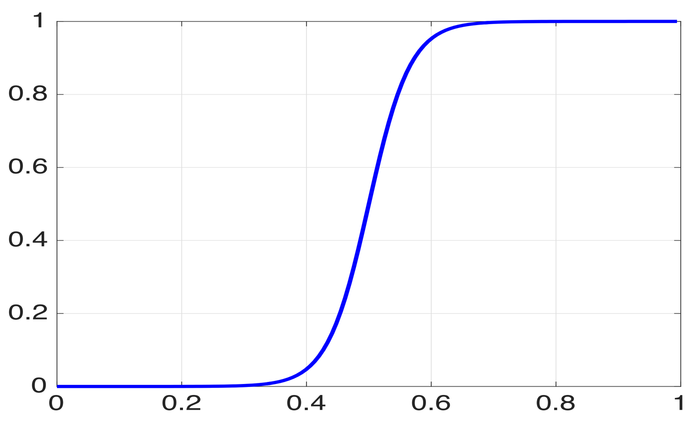

Function $\mathbf{\Phi(X)} = \frac{1}{1+e^{-\alpha(x-0.5)}}$

Inverse problem:

$$\{\mathbf{W}^*, \mathbf{H}^*\} = \underset{\mathbf{W},\mathbf{H} \in \{0,1\}}{\arg\min} \|\mathbf{X} - \mathbf{\Phi}(\mathbf{W} \cdot \mathbf{H}^T)\|_F^2$$

Cost function:

$$G(\mathbf{W},\mathbf{H}) = \sum_{i,j} \left(\mathbf{X}_{ij} - \mathbf{\Phi}(\mathbf{W} \cdot \mathbf{H}^T)_{ij}\right)^2 + \frac{1}{2}\lambda \sum_{i,k} \left(\mathbf{W}_{ik}^2 - \mathbf{W}_{ik}\right)^2 + \frac{1}{2}\lambda \sum_{j,k} \left(\mathbf{H}_{jk}^2 - \mathbf{H}_{jk}\right)^2$$

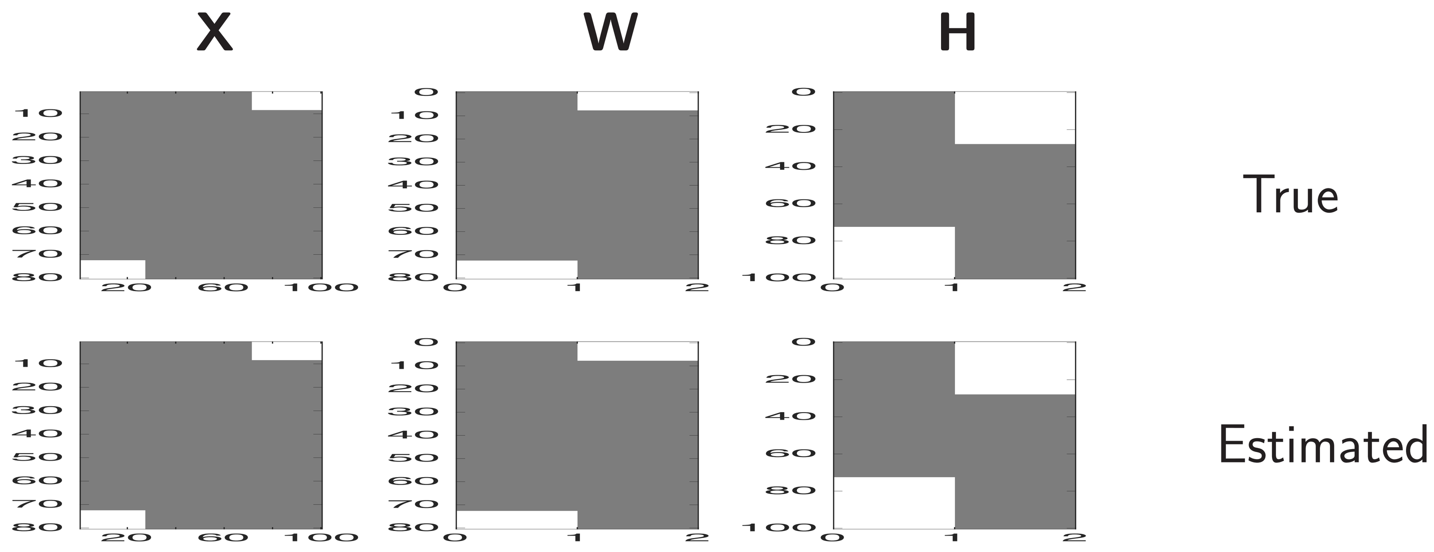

Behavior of PNL-PF algorithm for the case of 2 correlated sources

Correct estimation $\mathbf{W}$, $\mathbf{H}$ and $\mathbf{X}$

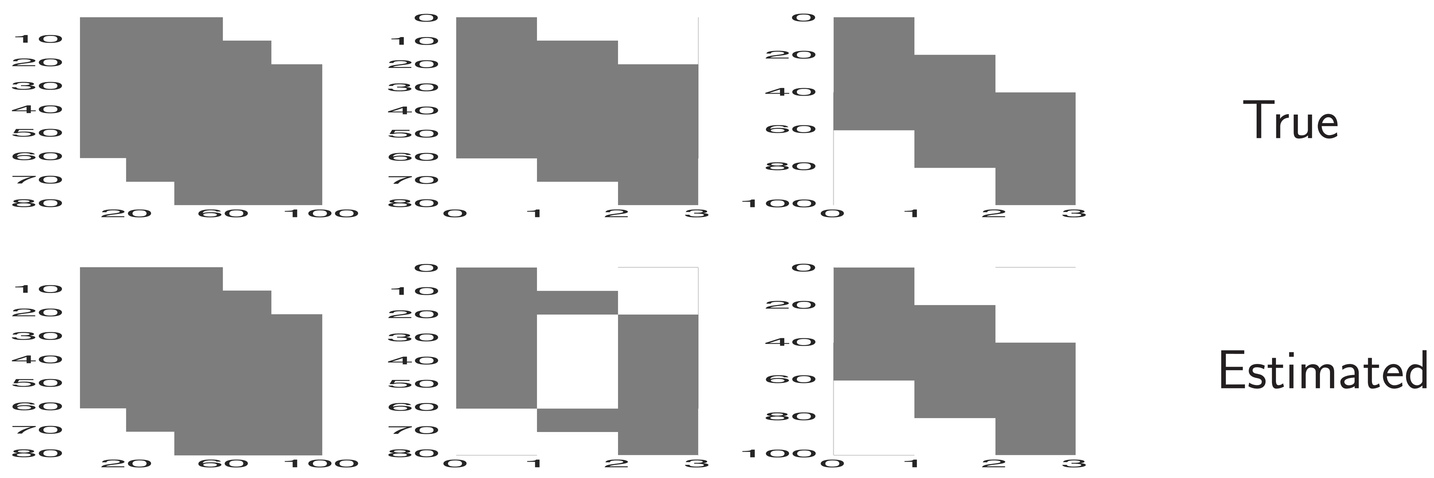

Behavior of PNL-PF algorithm for the case of 3 correlated sources

Correct estimation of $\mathbf{X}$ and $\mathbf{H}$ but not of $\mathbf{W}$ (uniqueness problem).

4. Uniqueness condition for the BMF decomposition

Theorem *[Diop et al., 2017]*

The ℓ^{th} column of $\mathbf{W}$ *i.e.*, $\mathbf{W}_\ell$ can be uniquely estimated from $\mathbf{X}$ iff:

$$\forall n = 1, \ldots, N, \text{ with } \mathbf{W}_\ell(n) \neq 0, \, supp\left(\mathbf{e}_n \odot \mathbf{H}_\ell^T\right) \not\subseteq \bigcup_{k \neq \ell}^{K} supp(\mathbf{X}_k),$$

with $\mathbf{e}_n = [0, \cdots, 1, \cdots, 0]^T$ the n^{th} vector of the canonical basis of $\mathbb{R}^N$.

5. Constraint post-nonlinear mixture model $\rightsquigarrow$ C-PNL-PF algorithm

To regularize the BMF decomposition, we choose to maximize the support of the rank-one terms (sources):

$$L(\mathbf{W},\mathbf{H}) = G(\mathbf{W},\mathbf{H}) + \lambda_1 \frac{1}{\sum_k \left(\sum_{i,j} \mathbf{W}_{ik}\mathbf{H}_{jk}\right)}$$

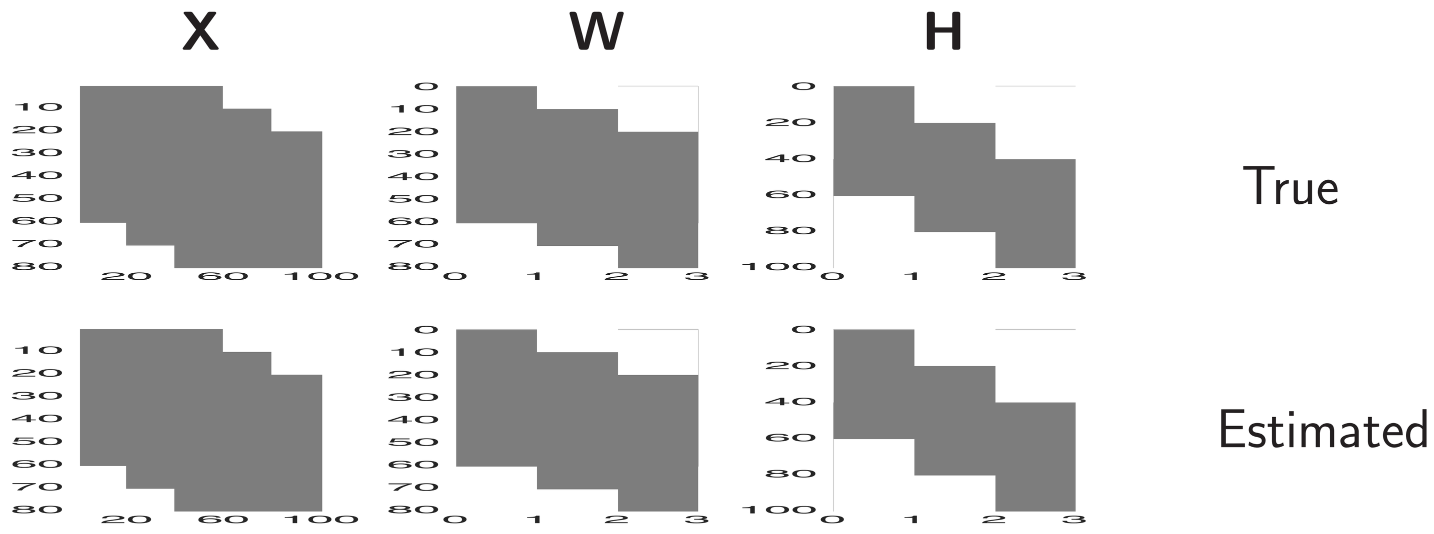

Behavior of C-PNL-PF algorithm for the case of 3 correlated sources

Correct estimation of $\mathbf{X}$, $\mathbf{W}$ and $\mathbf{H}$.

Numerical simulation (5 sources with **55%** of "1")

	X	W	H
TH	20.7 [3.4 37.2]	5.65 [0.4 10.8]	3.64 [0.1 8.3]
PF	19.3 [6.7 36.2]	5.74 [0.9 11.4]	3.2 0[.04 8.3]
PNL-PF	12.6 [1.1 32.2]	3.40 [0.05 9.1]	2.1 [0.0 7.3]
C-PNL-PF	4.3 [0.1 13.7]	1.86 [0.9 3.9]	1.5 [0.8 3.5]

The mean, minimum and maximum of the estimation error rate of $\mathbf{W}$ and $\mathbf{H}$ columns and $\mathbf{X}$ ($N = 120$, $M = 150$, $\gamma = 170$, $\lambda = 800$, $\lambda_1 = 10^8$)

ECOLE DOCTORALE IAEM LORRAINE

Optimisation de la planification d'un système d'assemblage à deux niveaux sous une politique de maintenance

Zouhour GUIRAS[1], Sadok TURKI[2], Nidhal REZG[3]

[1] Doctorante, LGIPM
[2] Maître de conference, Université de lorraine
[3] Professeur des universités, Université de lorraine

Description du problème :

- ❑ Système d'assemblage à deux niveaux.
- ❑ Une seule machine d'assemblage qui traite toutes les opérations d'assemblage des deux niveaux qui est soumise à des pannes aléatoires.
- ❑ Le système est face à des incertitudes: Délais d'approvisionnement, pannes de la machine.
- ❑ Risque de pertes de profit dû au retard dans la livraison de la commande.

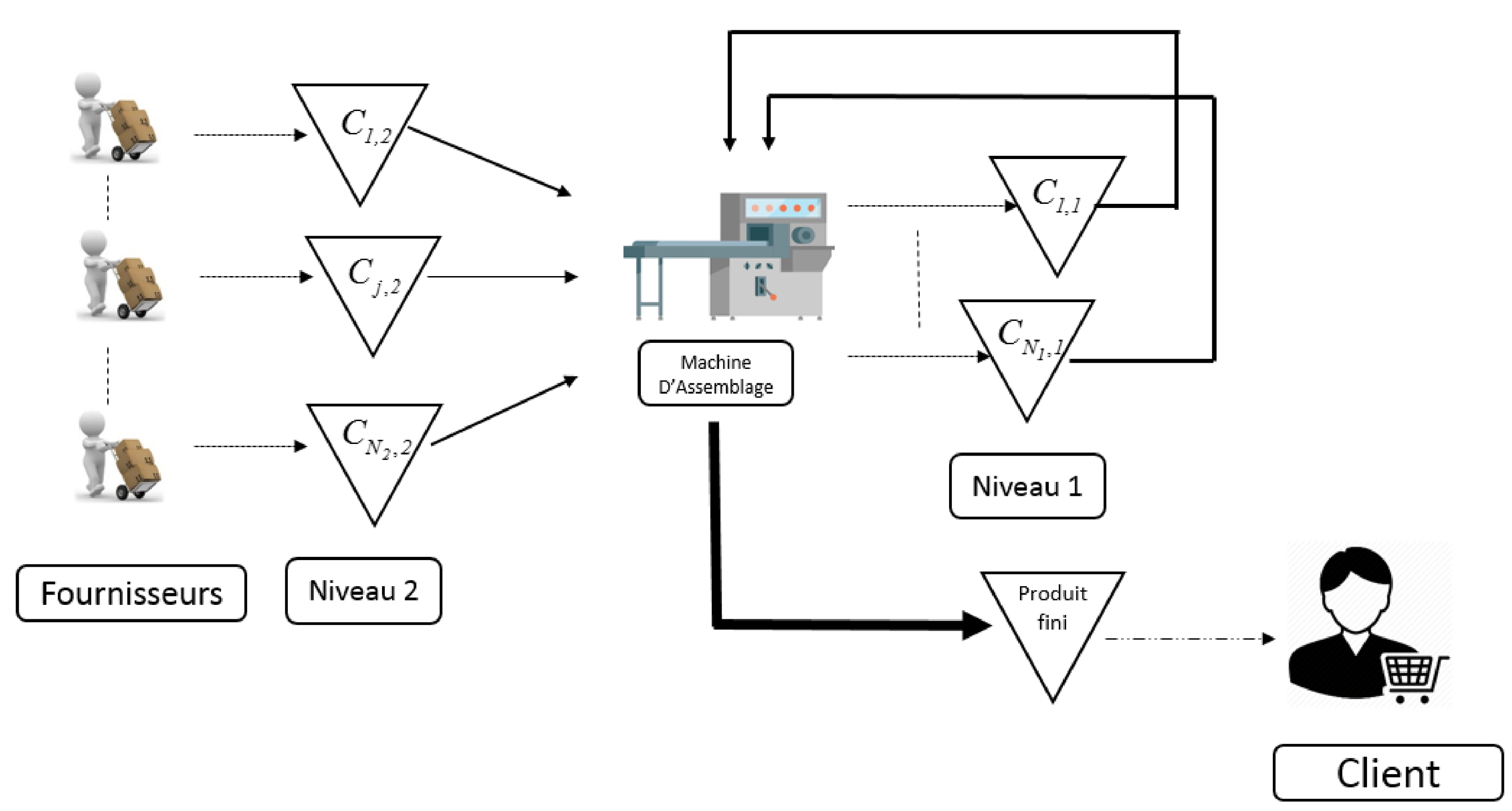

→ Le but est l'optimisation de la planification d'un système d'assemblage à deux niveaux en prenant en compte les contraintes de délais d'approvisionnement et les défaillances de la machine.

→ Étudier le risque de perte de profit dû aux défaillances de la machine qui a un impact sur le délai de livraison du produit fini.

Méthodologie :

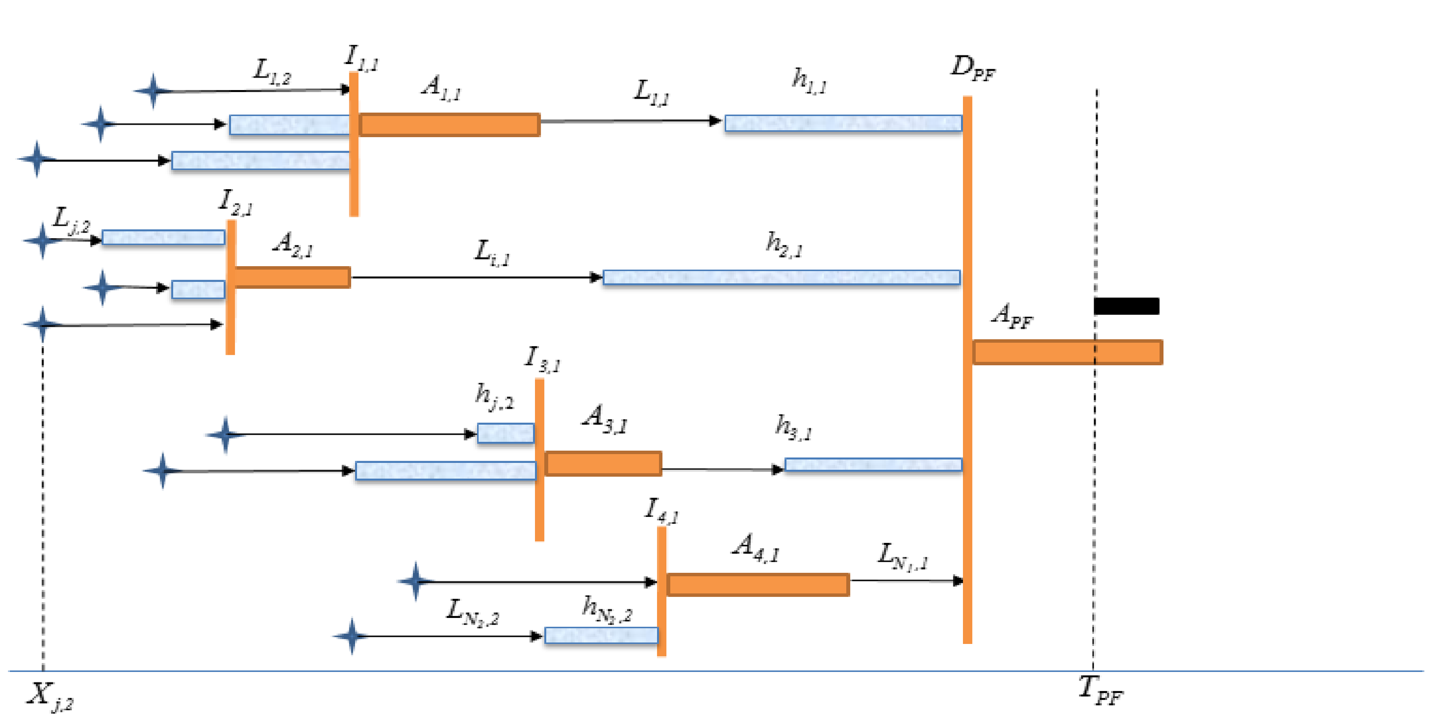

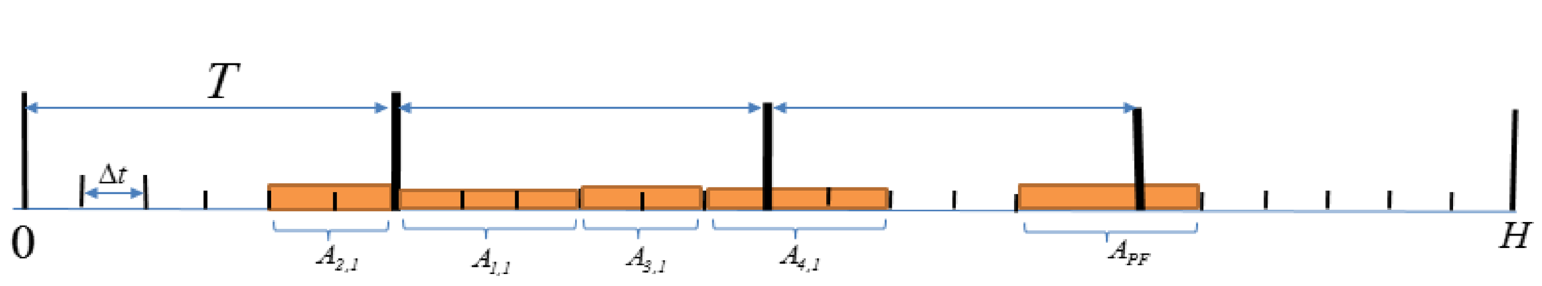

→ Adopter une stratégie séquentielle, on cherche dans un premier temps un plan optimal de dates de lancement d'ordres aux fournisseurs, puis, on détermine un plan de maintenance optimal utilisant le premier plan trouvé.

❑ Modélisation Mathématique :

- **Fonction objective :** Minimiser (Coût de stockage des composants de niveau 2 + coût de stockage des composants de niveau 1 + coût de stockage ou de rupture du produit fini + coût des actions de maintenance)

- **Variables de decision :**

$X_{j,2}$: Date de lancement d'ordre au fournisseur du composant $C_{j,2}$.

N: nombre d'actions de maintenance préventive au cours de l'horizon fini de travail *H*.

❑ Implémentation :

- Pour trouver le plan optimal des dates de lancement d'ordres aux fournisseurs, on a développé une heuristique avec le langage JAVA, on obtient le plan ci- dessous :

j	1	2	3	4	5	6	7	8	9	10
$X_{j,2}$	7	6	5	7	7	4	7	7	2	4

- On utilise le plan trouvé dans la détermination du nombre d'actions de maintenance préventive, la courbe ci-dessous représente l'évolution du coût par rapport au nombre d'actions de maintenances préventives.

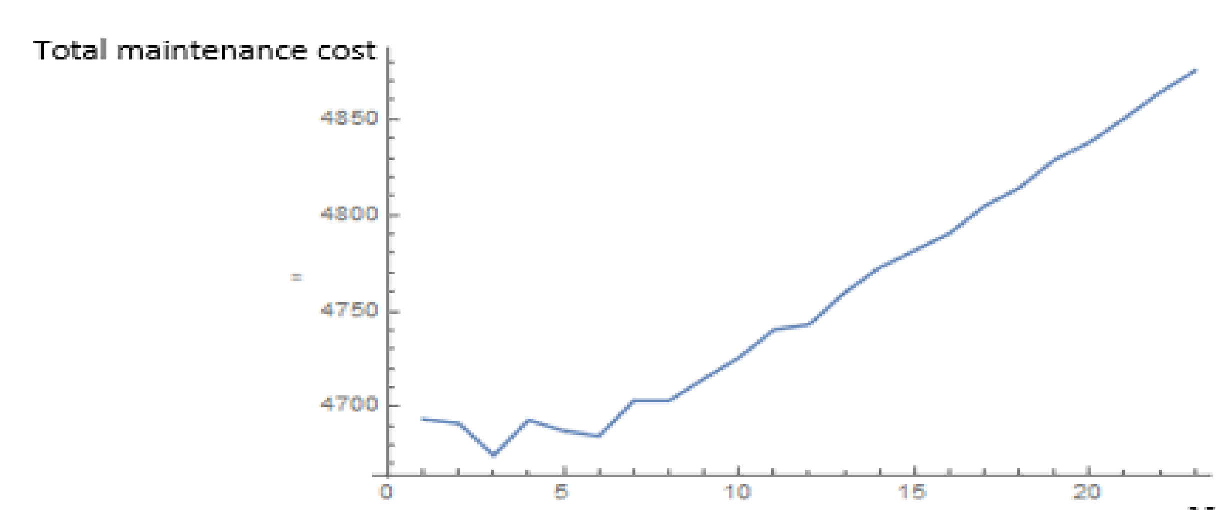

❑ Etude de risque :

L'évaluation des risques dans notre étude consiste à calculer la période seuil pour laquelle la somme du temps de réparation pour toutes les pannes ne dépasse pas cette période. D'autre part, dans le cas où le temps de réparation dépasse le délai de livraison, nous devrons calculer le risque de perte de profit (LPR).

Conclusion :

Contribution scientifique : **Guiras, Z., Turki, S., Rezg, N. and Dolgui, A., 2016, December. Optimal supply planning for two-levels assembly system with stochastic lead-times and maintenance actions. In *Industrial Engineering and Engineering Management (IEEM), 2016 IEEE International Conference on* (pp. 551-556). IEEE.**

- Développer une stratégie séquentielle pour trouver un plan de dates de lancement d'ordres aux fournisseurs optimal et un plan de maintenance préventif optimal.
- Etudier le risque de pertes de profit pour l'exemple proposé en calculant la période seuil de réparation de pannes de la machine.

Authenticated Snapshot in Peer-to-Peer Collaborative Systems

Victorien Elvinger (victorien.elvinger@loria.fr), Gérald Oster, François Charoy

Participants edit their own **copy of co-authored document**

Alice edits the document
Then she shares her change

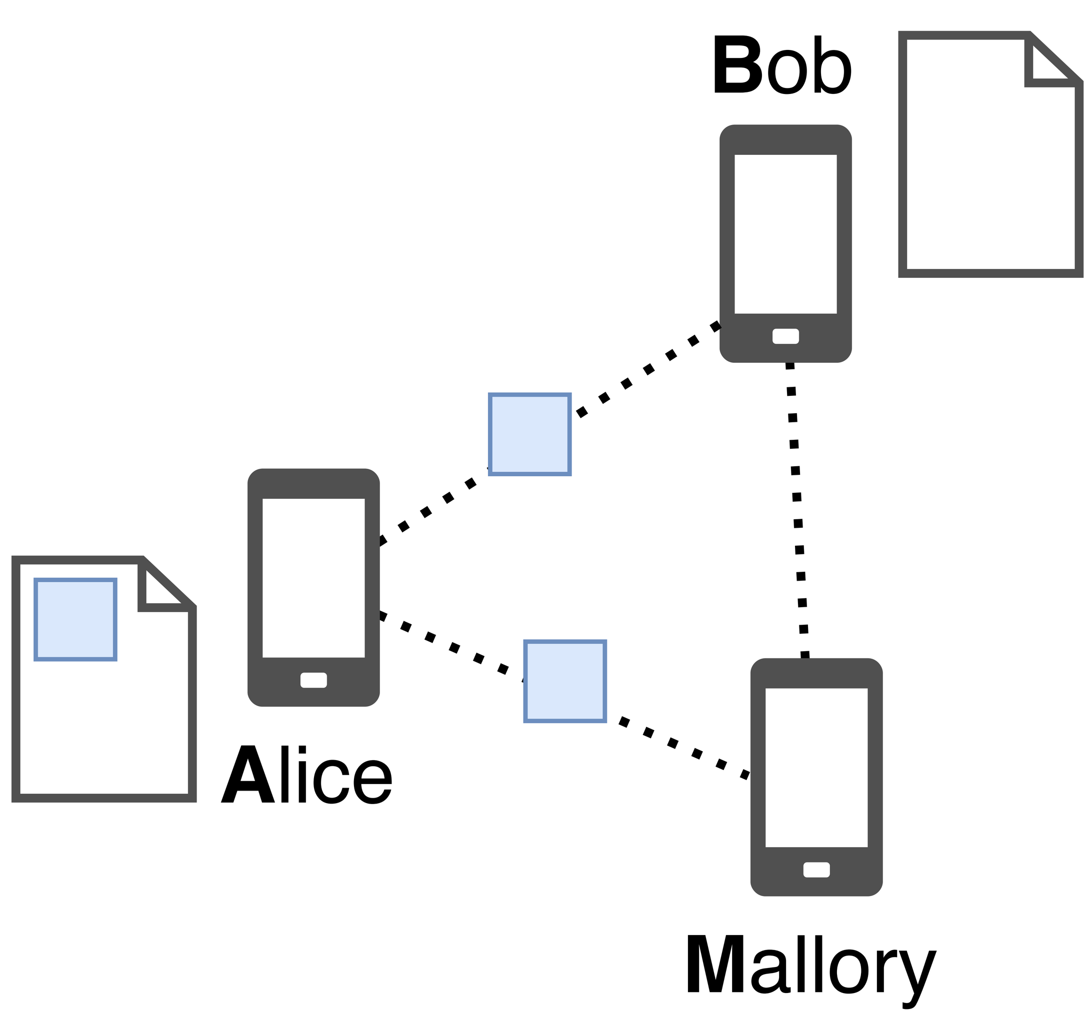

Mallory is **malicious**
She shares **distinct changes**

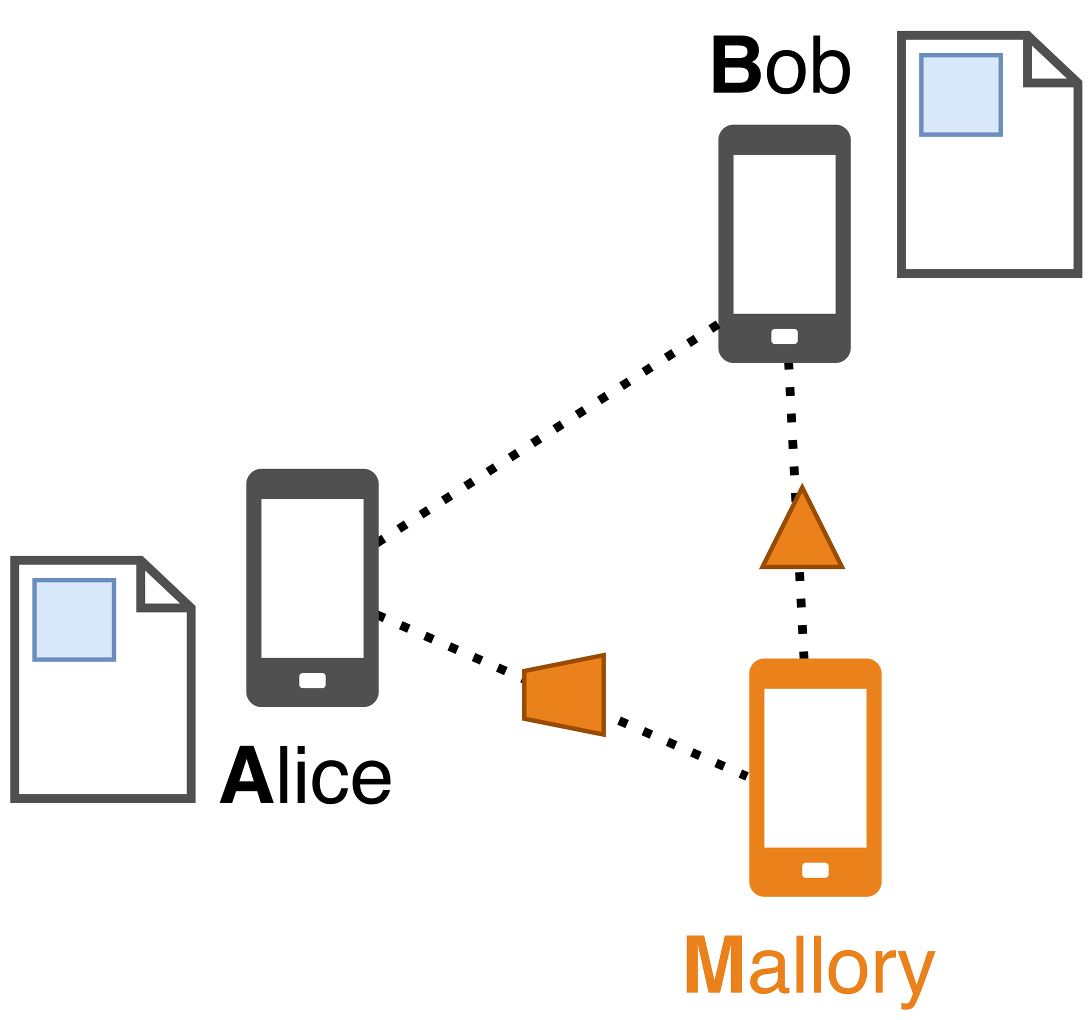

Alice & Bob converge, despite misbehaviors. Dave **joins** the group

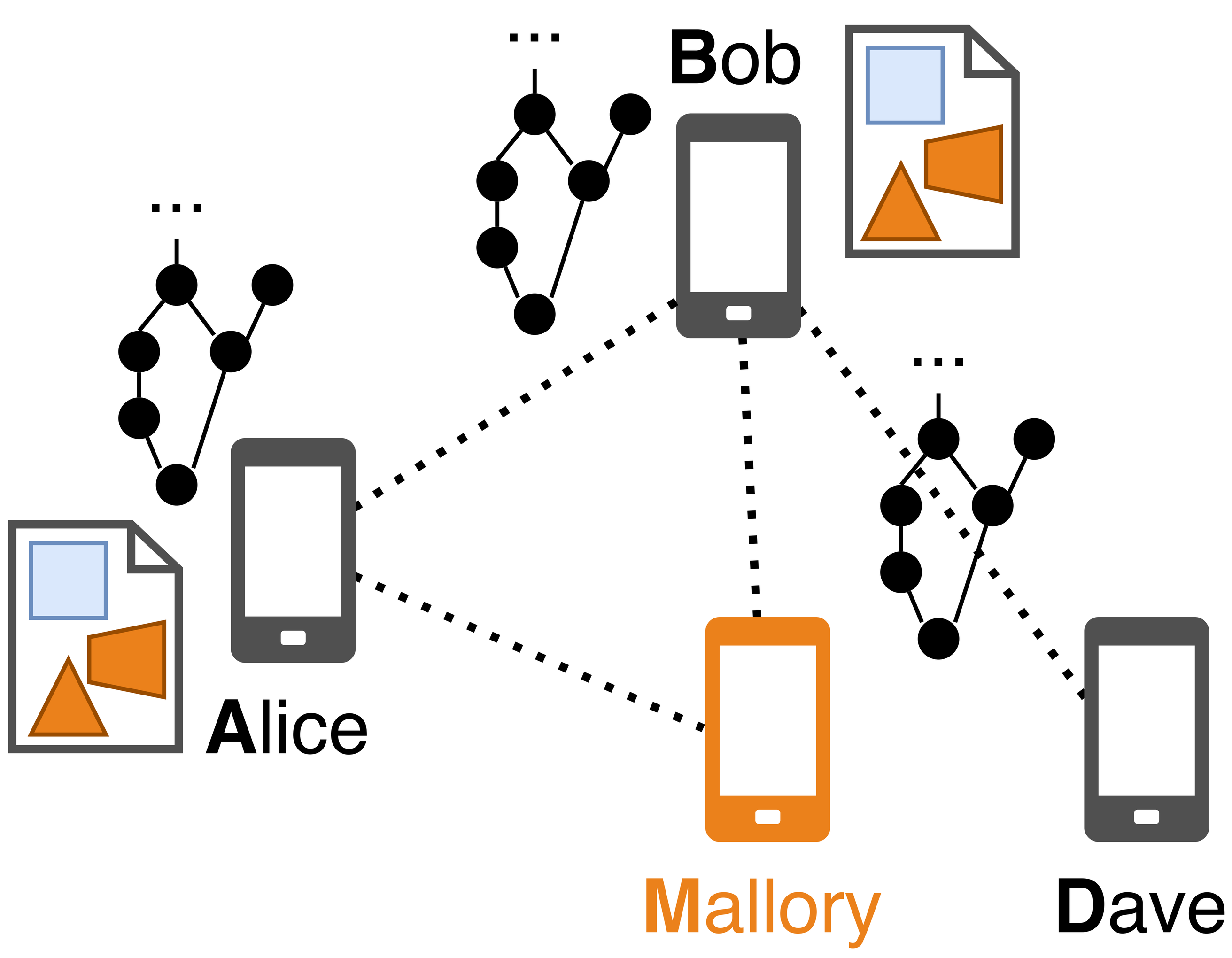

Copies **diverge then converge**, **except under misbehaviors**

VFJC logs make misbehaviors evident & ensure convergence
But, they lead to **large storage, communication and computation overheads**

How to reduce overheads of VFJC logs in dynamic groups ?

1 Prune the log

Participants **prune** their log by removing **VFJC stable** changes

A change is VFJC stable once **no more concurrent** changes cannot be **honestly accepted**

Pruned logs **reduce storage overhead**
But, joining participants, such as Dave, can no longer get the document state

2 Authenticate a snapshot using trust

Dave retrieves a **pruned log** and a **snapshot**
This reduces communication and computation

Invitations embed a **fingerprint** of the document
Participants verify embedded fingerprints

Dave trusts fingerprints verified by a **trusted set**

Dave computes the snapshot fingerprint
If **fingerprints match**, the snapshot is **authentic**

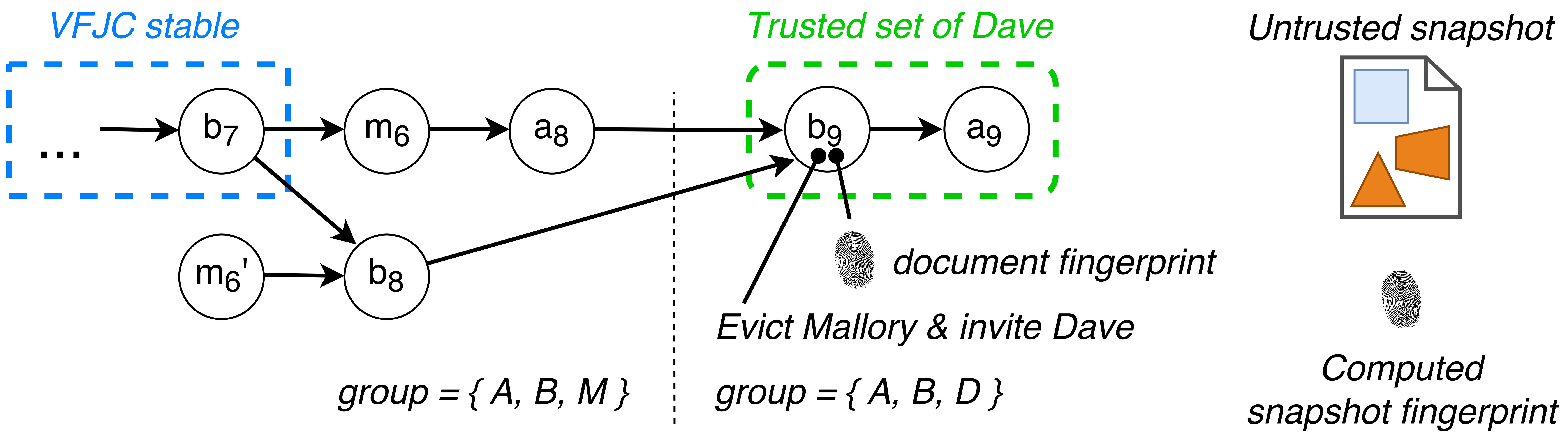

Adaptive deconvolution for pushbroom hyperspectral imaging systems

Yingying Song

Directeur de thse : David Brie

Co-directeur de thse : El-Hadi Djermoune

Abstract: This paper introduces a framework based on the LMS algorithm for sequential deconvolution of hyperspectral images acquired by pushbroom imaging systems. Considering a sequential model of image blurring phenomenon, we derive a sliding-block regularized LMS algorithm with spatial and spectral regularizers. The transient behavior of the algorithm is analyzed in the mean and mean-square sense. The role of each hyper-parameter is discussed. The performance of the algorithm is evaluated using simulated and real hyperspectral data.

Pushbroom hyperspectral imaging systems

Pushbroom imaging system

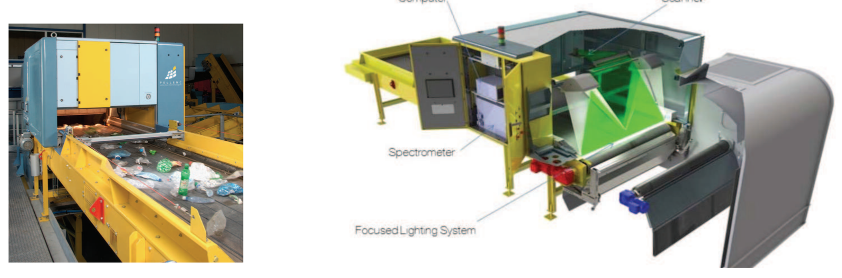

NIR (Near Infrared Spectroscopy) analysis

Data acquisition

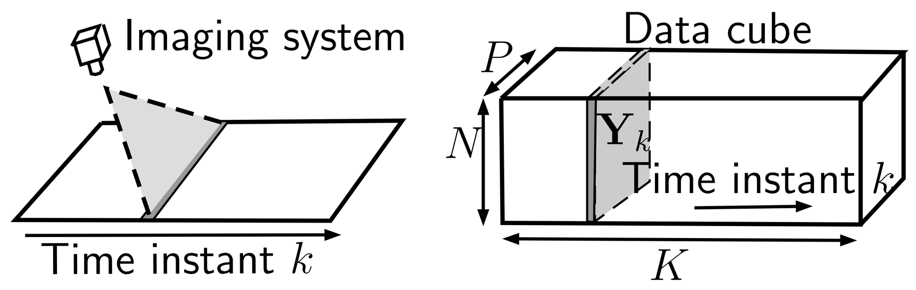

Blurring of the image.

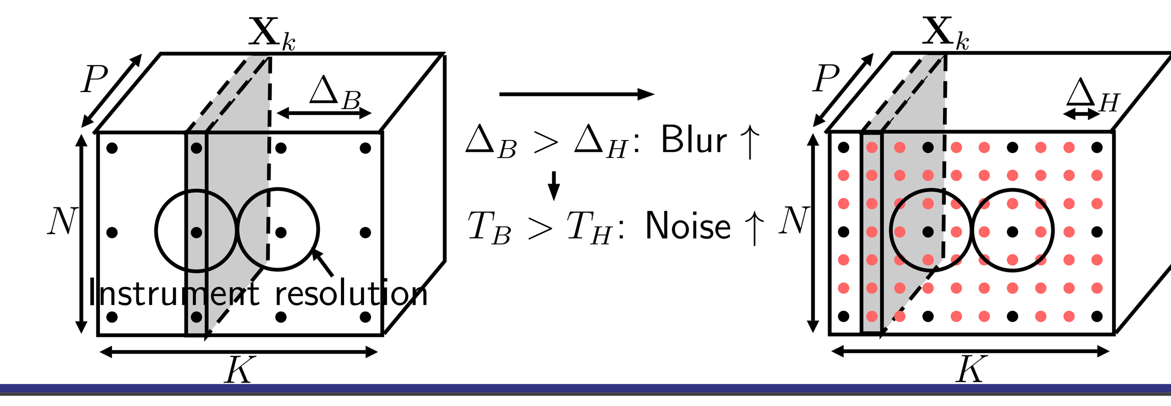

Adaptive image deconvolution

Causality of convolution kernel and associated estimates

2D convolution for each wavelength λ_p, $p = 1, \dots, P$:

$$\mathbf{Y}^p = \mathbf{H}^{*p} * \mathbf{X}^p + \mathbf{Z}^p$$

Causality of convolution kernel:

$$\tilde{\mathbf{y}}_k^p = \mathbf{y}_{k-(L-1)/2}^p = \sum_{\ell=1}^{L} \mathbf{H}_\ell^p \mathbf{x}_{k-\ell+1}^p + \mathbf{z}_k^p$$

Causality of the estimation process of $\mathbf{x}_k^p$:

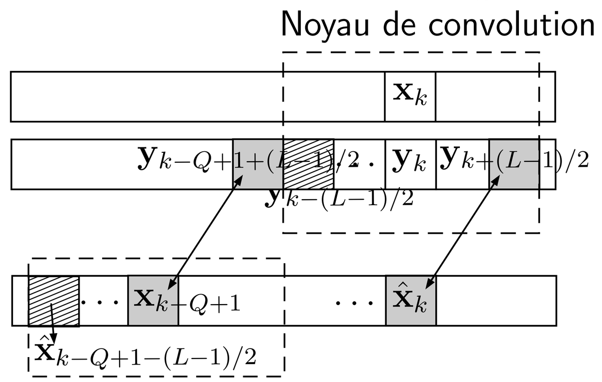

Adaptive hyperspectral image deconvolution

- SBR-LMS Criterion for 2D image:

$$\mathcal{J}(\mathbf{x}_k^p, \dots, \mathbf{x}_{k-Q-L+2}^p) = \sum_{q=1}^{Q} \mathbb{E}\|\mathbf{y}_{k-q+1}^p - \sum_{\ell=1}^{L} \mathbf{H}_\ell^p \mathbf{x}_{k-q-\ell+2}^p\|^2 + \eta_z \sum_{q=1}^{Q} \|\mathbf{x}_{k-q+1}^p\|_1 + \eta_s \sum_{q=1}^{Q} \|\mathbf{D}_N^p \mathbf{x}_{k-q+1}^p\|_1$$

- Instantaneous gradient:

$$\nabla \mathcal{J} \triangleq \left(\frac{\partial \mathcal{J}}{\partial \mathbf{x}_k^p}, \dots, \frac{\partial \mathcal{J}}{\partial \mathbf{x}_{k-Q+1}^p}, \mathbf{0}_{N\times 1}, \dots, \mathbf{0}_{N\times 1} \right)$$

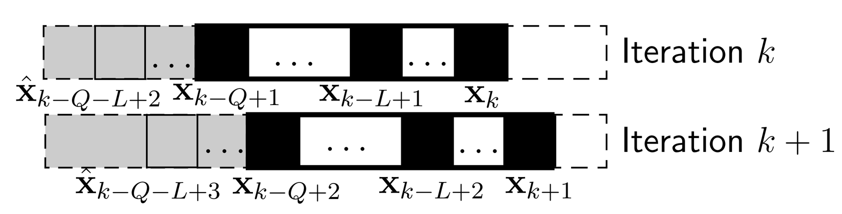

Adaptive hyperspectral image deconvolution

- Vectorization of data:

$$\mathbf{x}_k' \triangleq \mathrm{col}\left\{ \mathrm{col}\{\mathbf{x}_{k-q+1}^p\}_{q=1}^{Q+L-1} \right\}_{p=1}^{P}$$

- Criterion for the hyperspectral image:

$$\mathcal{C}(\mathbf{x}_k') = \sum_{p=1}^{P} \mathcal{J}(\mathbf{x}_k'^p) + \|\mathbf{\Lambda}_\lambda \mathbf{x}_k'\|^2$$

- SBR-LMS for hyperspectral images:

$$\hat{\mathbf{x}}_{k+1}' = \mathbf{\Omega}\hat{\mathbf{x}}_k' - \frac{\mu}{2}\nabla\mathcal{C}(\hat{\mathbf{x}}_k') = \mathbf{\Omega}\hat{\mathbf{x}}_k' + \mu\mathbf{\Phi}(\mathbf{y}_k' - \mathbf{G}\hat{\mathbf{x}}_k') - \rho_z \mathbf{\Gamma}\mathrm{sign}(\hat{\mathbf{x}}_k') - \rho_s \mathbf{\Lambda}_s^\top \mathrm{sign}(\mathbf{\Lambda}_s \hat{\mathbf{x}}_k') - \mu\eta_\lambda \mathbf{\Lambda}_\lambda^\top \mathbf{\Lambda}_\lambda \hat{\mathbf{x}}_k'$$

- Selecting of the Q-th block: $\hat{\mathbf{x}}_{k-Q+2} = \mathbf{S}\hat{\mathbf{x}}_{k+1}'$ with $\mathbf{S} \triangleq \mathbf{I}_P \otimes [\mathbf{0}_{N\times(Q-1)N}, \mathbf{I}_N, \mathbf{0}_{N\times(L-1)N}]$

Stochastic analysis

- Mean behavior:

$$\mathbb{E}\{\hat{\mathbf{x}}_{k+1}'\} = \mathbf{A}\mathbb{E}\{\hat{\mathbf{x}}_k'\} + \mu\mathbf{\Phi}\mathbf{G}\mathbf{x}_k' - \rho_z \mathbf{\Gamma}\,\mathbb{E}\{\mathrm{sign}(\hat{\mathbf{x}}_k')\} - \rho_s \mathbf{\Lambda}_s^\top \mathbb{E}\{\mathrm{sign}(\mathbf{\Lambda}_s \hat{\mathbf{x}}_k')\}$$

$$\mathbb{E}\{\hat{\mathbf{x}}_{k-Q+2}\} = \mathbf{S}\mathbb{E}\{\hat{\mathbf{x}}_{k+1}'\}$$

- Mean square error:

$$\mathbb{E}\|\boldsymbol{\epsilon}_k\|^2 = NP\sigma_z^2 + \mathrm{trace}(\mathbf{G}^\top\mathbf{S}^\top\mathbf{S}\mathbf{G}\mathbb{E}\{\hat{\mathbf{x}}_k'\hat{\mathbf{x}}_k'^\top\}) + \mathbf{x}_k'^\top\mathbf{G}^\top\mathbf{S}^\top\mathbf{S}\mathbf{G}\mathbf{x}_k' - 2\mathbf{x}_k'^\top\mathbf{G}^\top\mathbf{S}^\top\mathbf{S}\mathbf{G}\mathbb{E}\{\hat{\mathbf{x}}_k'\}$$

- First-order approximation

Effects of the parameters

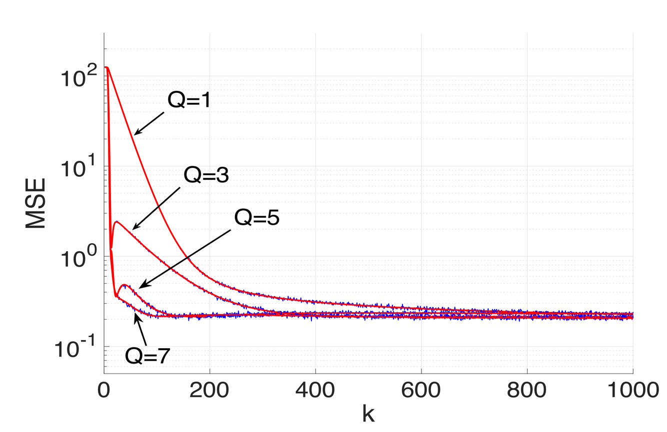

Influence of the block size Q

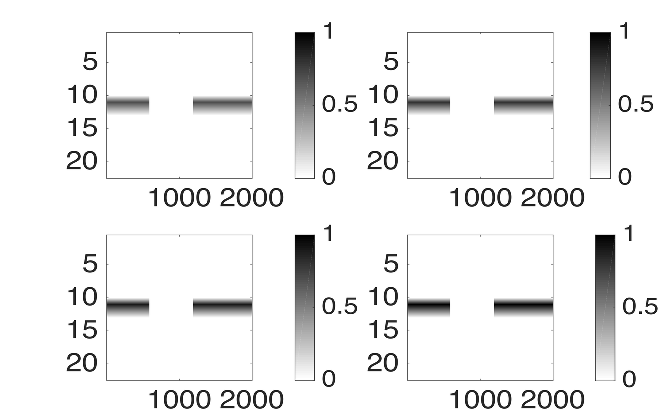

Simulated image with 4 wavelengths

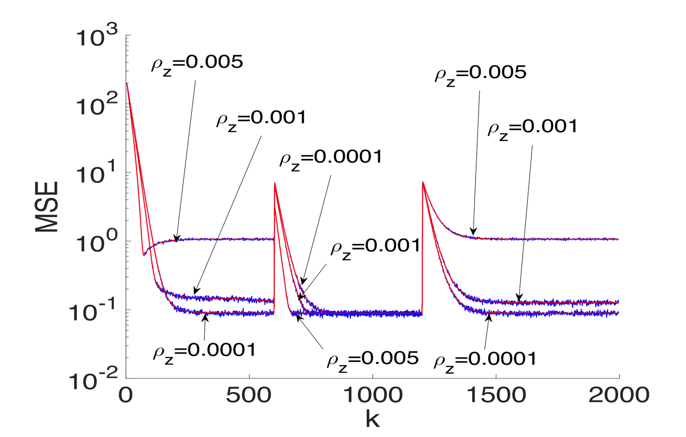

Influence of the zero-attracting regularization paramter ρ_z

Experiments

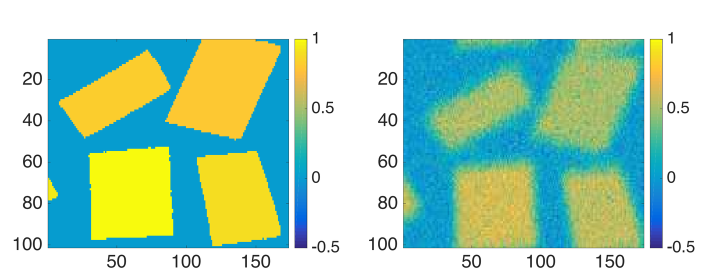

Original image Noisy blurred image

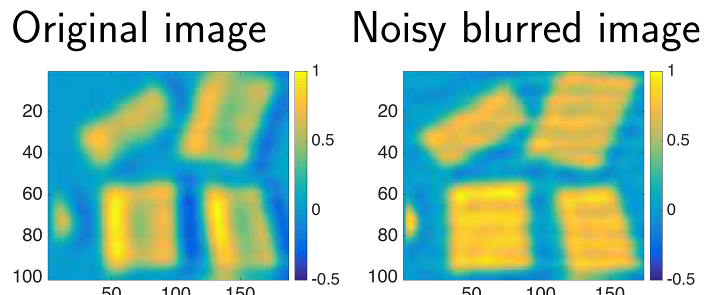

ZA-LMS SB-LMS

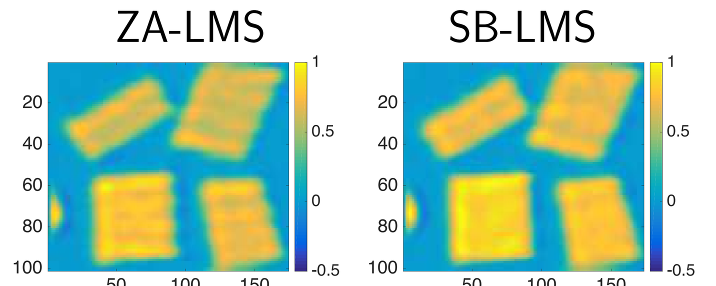

SBZA-LMS SBR-LMS

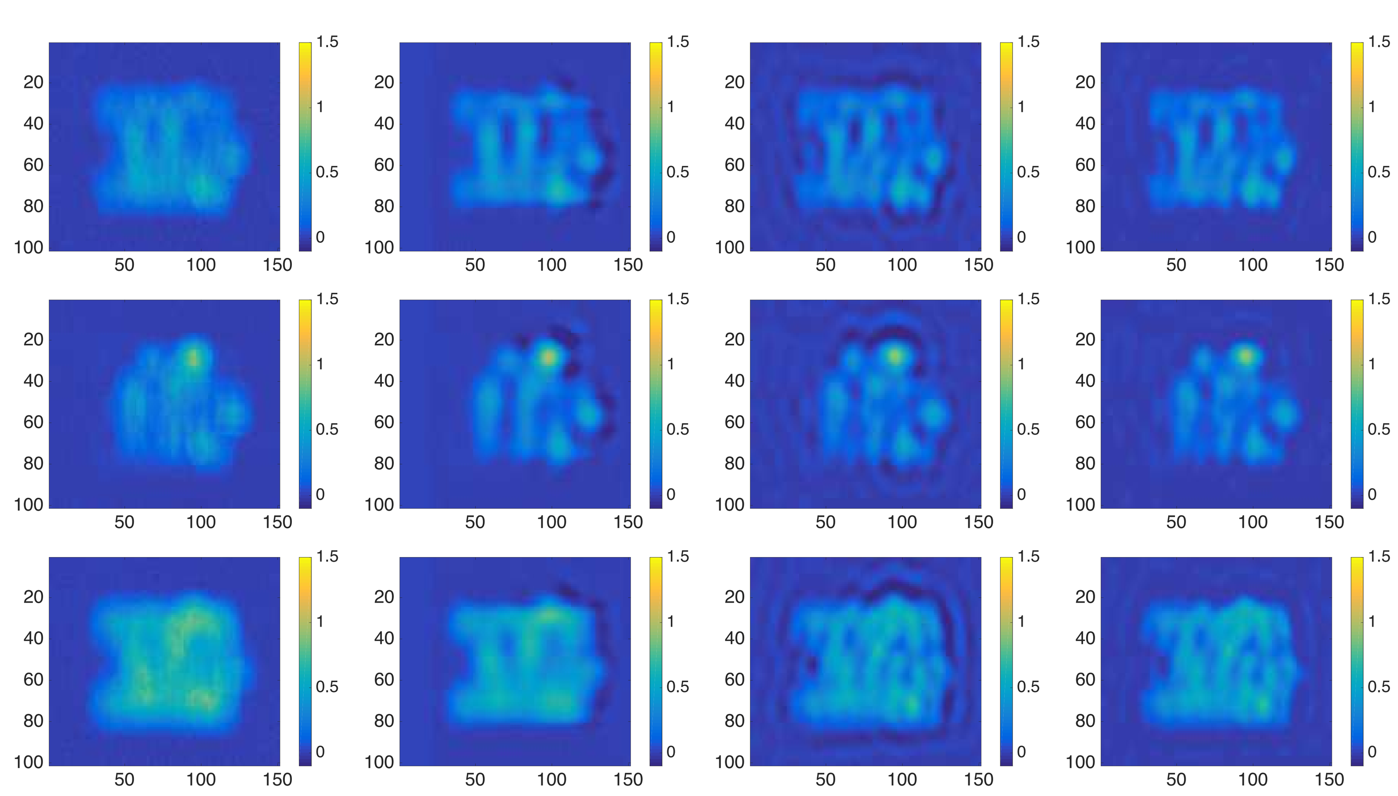

Restauration of hyperspectral images (from left to right : observed hyperspectral image, estimated image (SBR-LMS), estimated image (Tikhonov), estimated image (Non-negative Tikhonov)

Conclusion

- Proposal of the SBR-LMS algorithm for adaptive deconvolution of images collected by a pushbroom imaging system.
- Discussion of issues related to the non-causality of the convolution kernel and the estimation model
- Analysis of the transient behavior of the SBR-LMS algorithm taking into account high order correlations introduced by convolution kernel.
- Stability condition and computational burden
- Future works: development of an algorithm for on-line source separation.

References:

Yingying Song, El-Hadi Djermoune, Jie Chen, Cdric Richard, David Brie. Dconvolution en ligne d?images hyperspectrales pour les imageurs de type pushbroom, GRETSI 2017, XXVIeme Colloque, Juan-Les-Pins, France, 5-8 Septembre 2017

Jie Chen, Cdric Richard, Yingying Song, David Brie, Transient performance analysisof zero-attracting LMS, IEEE Signal Processing Letters, 2016

Trusternity: Auditing Key-Transparency server with Blockchain

Long Nguyen hoang-long.nguyen@loria.fr

Claudia-Lavinia Ignat claudia.ignat@inria.fr

Olivier Perrin olivier.perrin@loria.fr

LORIA, Université de Lorraine / Inria / CNRS

- End-to-End encrypted systems rely on **key servers** to distribute Public Keys.
- A **Key-Transparency** server uses a **Merkle tree** and **gossiping** for efficient auditing

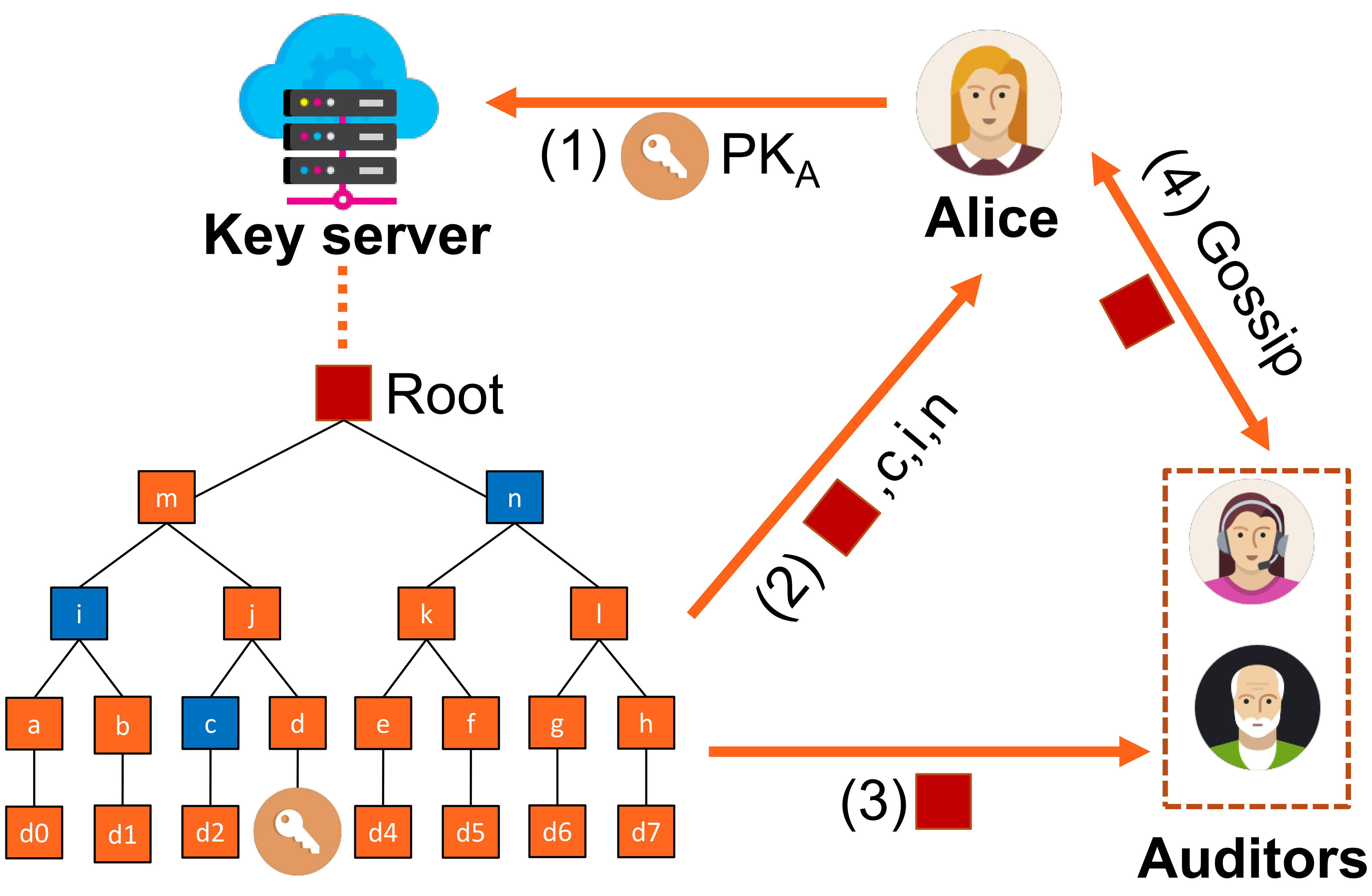

1. Users upload public keys
2. Users **monitor** their own keys
3. Auditors keep track of **Root**
4. Users & Auditors **gossip** Root

- ***Gossip protocol***
  - Short epochs
  - Incentive
  - Malicious clients

Proposal: Trusternity - auditing with Blockchain

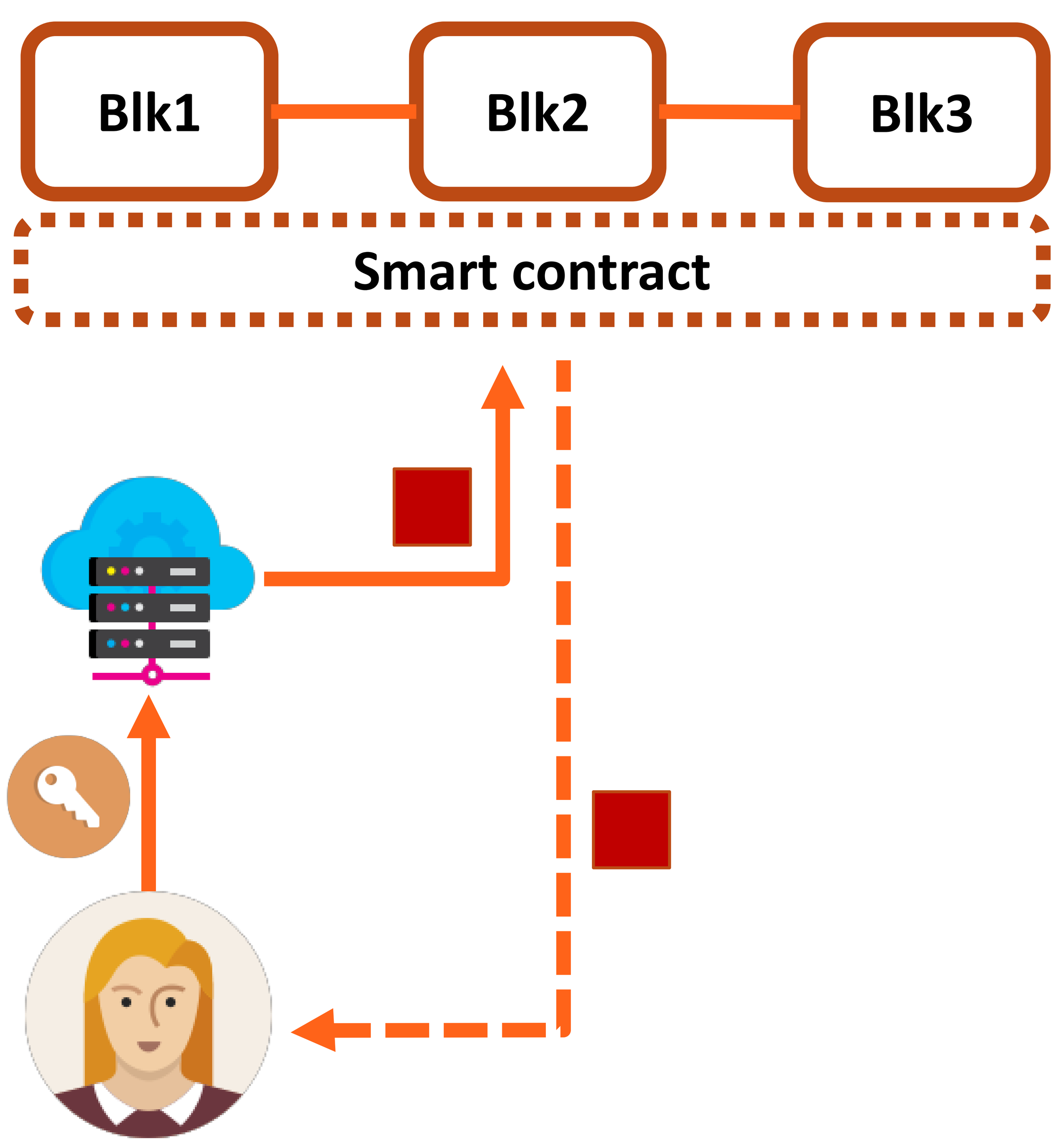

Trusternity extension to CONIKS [1]

1. Ethereum **smart contract** enforces policy
2. Publishing & Querying Root from the **blockchain**

Compared to state of the art (EthIKS [2])

1. **Thin client** architecture
2. Much **cheaper** storage ~ 80 times

[1] Melara, M S., et al. "CONIKS: Bringing Key Transparency to End Users." *Usenix Security*. 2015.

[2] Bonneau, J. "EthIKS: Using Ethereum to audit a CONIKS key transparency log." *International Conference on Financial Cryptography and Data Security*. Springer Berlin Heidelberg, 2016.

https://github.com/coast-team

Audio Source Localization with Alpha-Stable Models

Mathieu Fontaine[1], Charles Vanwynsberghe[2], Antoine Liutkus[1], Roland Badeau[3]

[1]Inria, multispeech team (LORIA, UMR 7503), Université de Lorraine, 54600 Villers-lès-Nancy, France.
[2]Institut Jean le Rond d'Alembert, Saint-Cyr l'École, France.
[3]Institut Mines-Télécom, Télécom ParisTech, CNRS LTCI, France.

mathieu.fontaine@inria.fr

Problem Statement

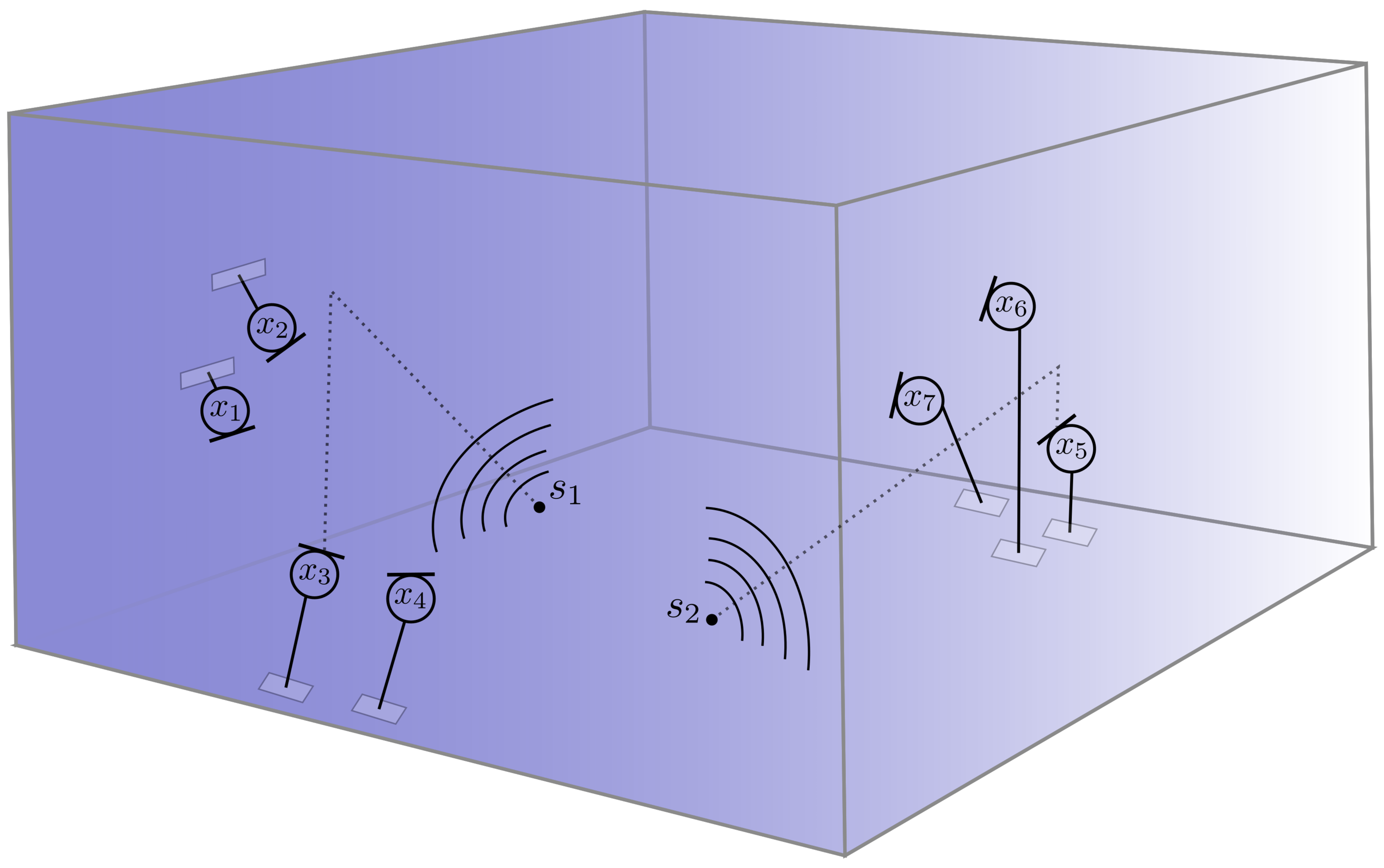

- Given several microphones $x_1, \dots, x_K$ randomly positioned.
- Localize audio sources $s_1, \dots, s_L$ by estimating their magnitudes.

Sources and acoustic model

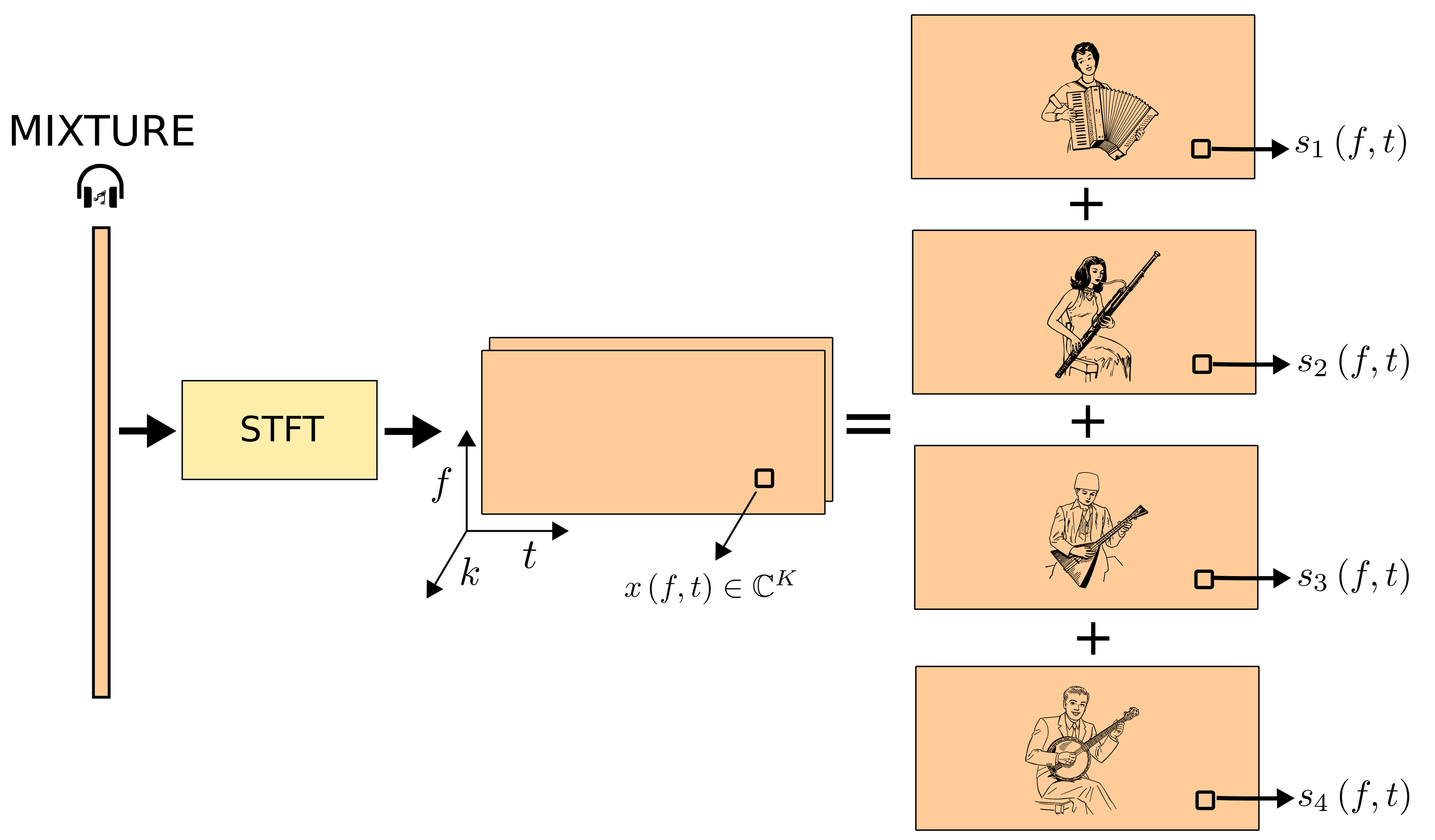

Each source s_l is an α-harmonizable process with $\alpha \in (0,2]$. Thus, for all l, f, t as mutually independent

$$s_l(f,t) \sim S_\alpha S_c(\sigma_l^\alpha).$$

- $s_l(f,t)$ is called an **isotropic α-stable distribution**.
- The **characteristic exponent** α describes the impulsivity of an audio source.
- It is characterized by a **scale parameter** which could be understood as the amplitude of the potential source.

The classical far field region assumption yields the modeling below

$$\forall (f,t), \; \boldsymbol{x}(f,t) = \sum_{l=1}^{L} \boldsymbol{A}_l(f) s_l(f,t).$$

- $\boldsymbol{A}_l(f)$ depends on the knowing position of microphones, speed of the air, and the frequency band f

Doing so, some sources may be found out as negligible while others as significantly active.

How use the α-stable theory to estimate DoAs?

Spatial measure for DoAs estimation

The chf. of the distribution of $\boldsymbol{x}(f,t)$ for any t and a given frequency f is

$$\forall \boldsymbol{\theta} \in \mathbb{C}^K, \; \varphi_f(\boldsymbol{\theta}) = \exp\left(-\int |\langle \boldsymbol{\theta}, \boldsymbol{a}\rangle|^\alpha d\Gamma_f(\boldsymbol{a})\right),$$

A fast calculation using Levy exponents $I_f(\boldsymbol{\theta}) \triangleq -\ln(\varphi_f(\boldsymbol{\theta}))$ and particular form of φ_f involves

$$I_f(\boldsymbol{A}_{l'}(f)) = -\sum_{l=1}^{L} \underbrace{\sigma_l^\alpha}_{\Upsilon_l} \underbrace{|\langle \boldsymbol{A}_{l'}(f), \boldsymbol{A}_l(f)\rangle|^\alpha}_{[\Psi_f]_{l',l}}$$

- $\boldsymbol{\Upsilon} \triangleq [\Upsilon_1, \dots, \Upsilon_L]^\top$ is defined as the **spatial measure** and gives exactly the amplitude of sources.
- Can be estimated by sampling the 3d-space.

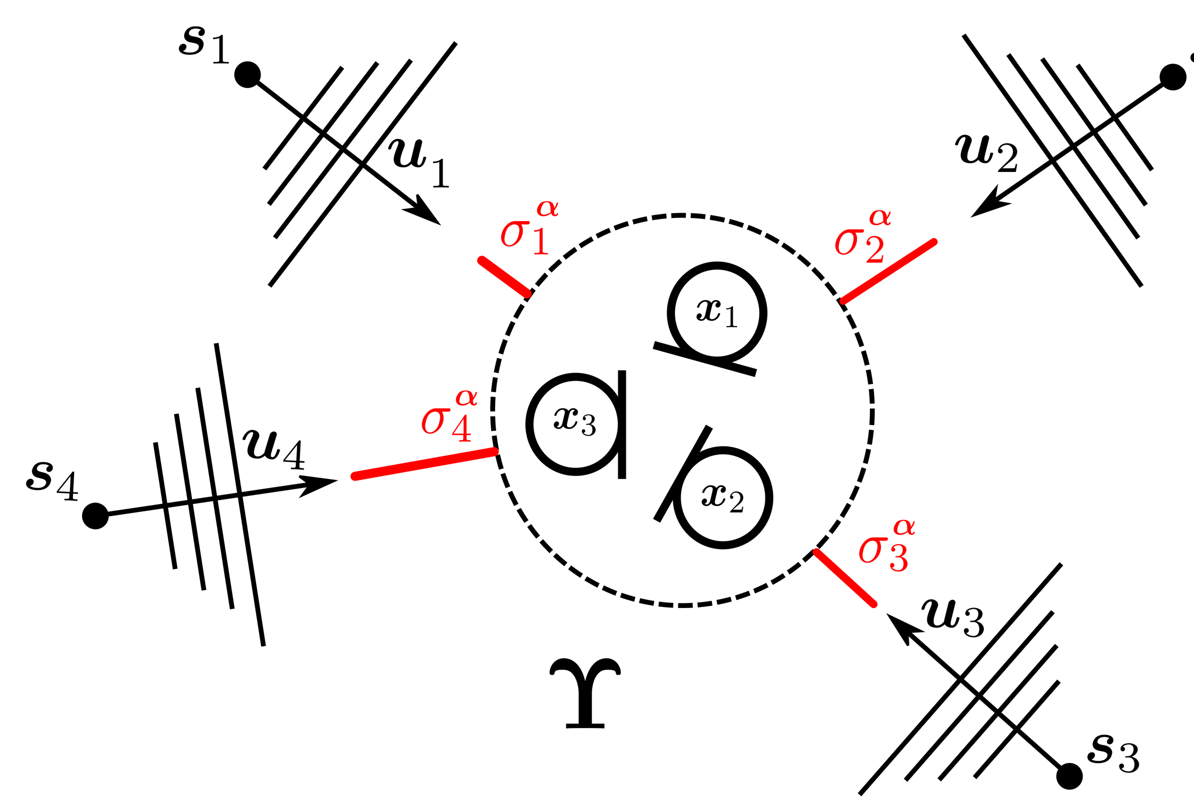

The convex problem obtained by gathering all Ψ_f and I_f is

$$\boldsymbol{I} = \boldsymbol{\Psi}\boldsymbol{\Upsilon}$$

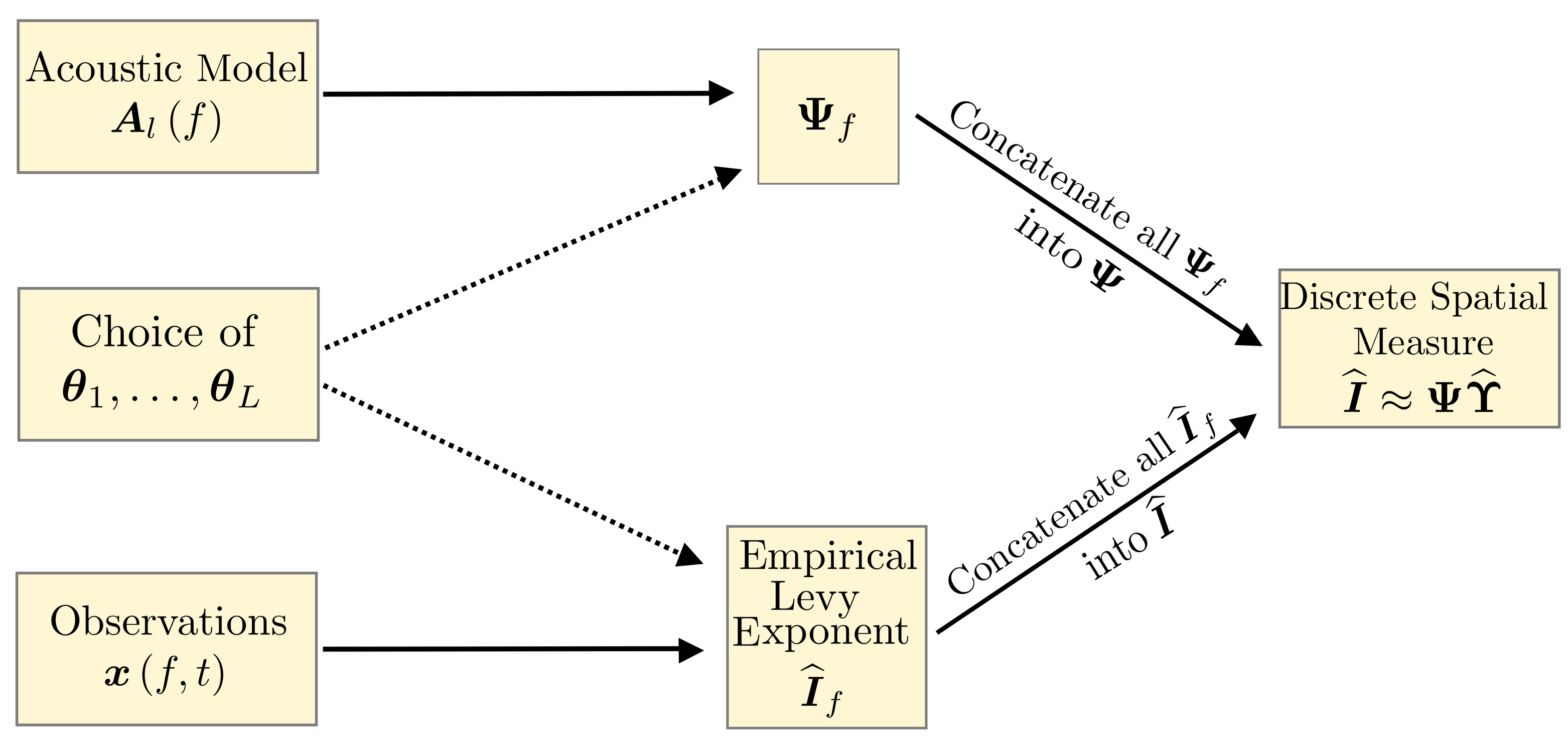

Estimation and Evaluation

- **Estimation Method**
  → Estimate $\boldsymbol{I}$ by using a nonnegative empirical chf.

$$\forall \boldsymbol{\theta} \in \mathbb{C}^K, \; \hat{\varphi}_f(\boldsymbol{\theta}) = \left|\frac{1}{T}\sum_{t=1}^{T} \exp\left(i\frac{\Re\langle \boldsymbol{\theta}, \boldsymbol{x}(f,t)\rangle}{2^{1/\alpha}}\right)\right|^2.$$

  → Minimize the discrepancies between the left and right-hand sides of the previous equation using a nonnegative matrix factorization approach.
- **Results**

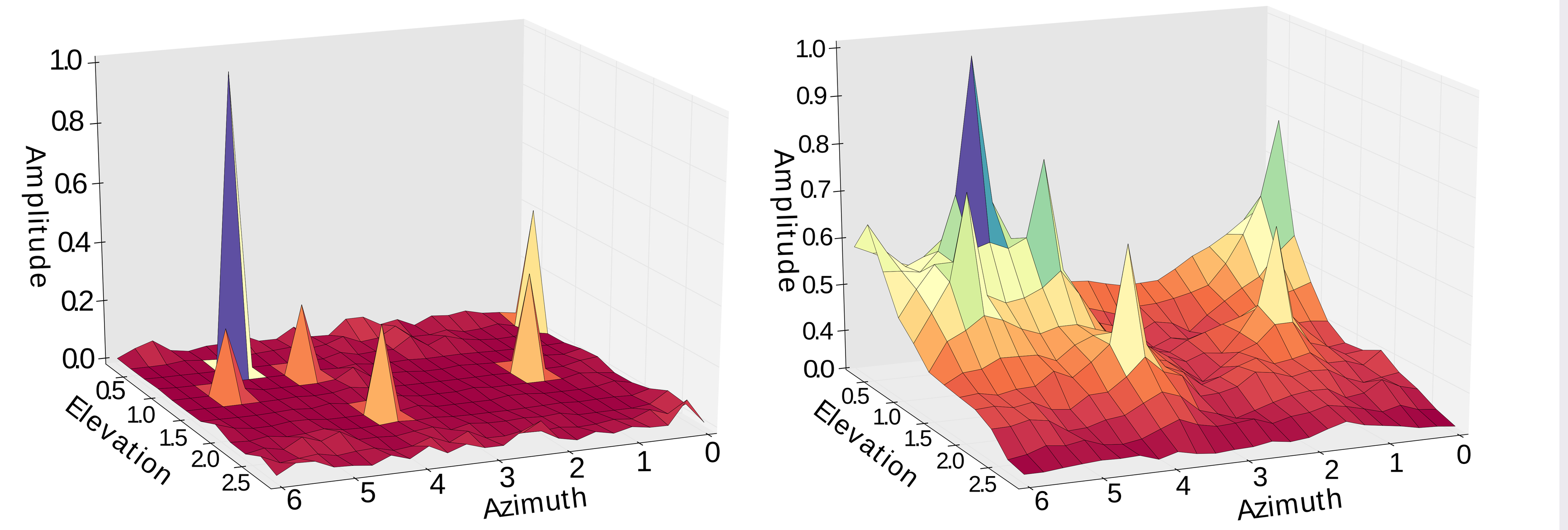

Localization between the spatial measure (left) and the steering response power (right)

This work was partly supported by the research programme KAMoulox (ANR-15-CE38-0003-01) funded by ANR, the French State agency for research.

Faisceau minimal sur Bun_G pour G de type G_2

Lizao YE, IECL
lizao.ye@univ-lorraine.fr
26. oct. 2017

Motivation et Analogue Physique

- Une chose qu'on fait en physique consiste à filtrer une lumière selon les différentes fréquences, et on appelle cette procédure *analyse spectrale*.
- Souvent, les photons dedans de la plus basse fréquence, correspondant à l'état le plus stable, est facile à retenir, et ne donne pas beaucoup de renseignements sur les particularités du matériel.
- Ce qu'on appelle *état minimal* correspond au *premier état d'excitation*.
- La mécanique quantique modélise les états comme vecteurs propres de l'*opérateur hamiltonien* dans un espace hilbertien, genre $\mathrm{L}^2(\mathcal{M})$, l'ensemble des fonctions de carré intégrables sur une variété $\mathcal{M}$.

Qu'est ce que c'est qu'un faisceau ?

- La procédure dite de *géométrisation* ou de *catégorification* consisite à promouvoir l'ensemble $\mathrm{L}^2(\mathcal{M})$ en une catégorie, dont les objets sont baptisés :

"faisceaux".

- L'essentielle différence d'une catégorie par rapport à un ensemble est qu'on peut parler des *morphismes* entre les objets, et en particulier, des *automorphismes* d'un objet.
- Pour un faisceau, on s'intéresse aussi à sa *perversité*.
- Notre outil principal est la *tranformation de Fourier géométrique*.

Cadre Physique	Notre Cadre
variété $\mathcal{M}$	Bun_G
hamiltonien	opérateurs de Hecke
état minimal	faisceau minimal

Notre Context

Soit G le groupe exceptionnel de type G_2. Soit X une courbe projective lisse. On fixe un Borel B de G et un tore maximal T dans B, ainsi le système de racines par rapport à cet épinglage. On note α la racine simple longue et β la courte. Et notons P_α le parabolique standard maximal contenant $-\alpha$, Z_α le centre du radical unipotent de P_α. Les groupes correspondants pour la racine β sont notés P_β, Z_β. Pour toute racine γ, on désigne par U_γ le sous-groupe unipotent de dimension un de G qui lui corresponde. Notons par $\mathcal{F}_{\min}$ le faisceau minimal sur Bun_G, l'espace de module de G-fibrés principaux sur X. On cherche à décrire le "P_α-modèle" du faisceau minimal. Voici le diagramme des champs concernés :

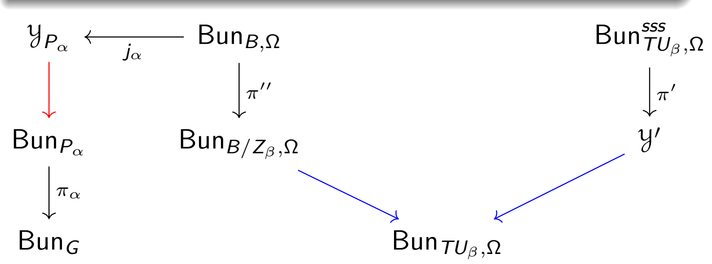

Ici $\mathcal{Y}_{P_\alpha}$ classifie $\mathcal{F}_{P_\alpha} \in \mathrm{Bun}_{P_\alpha}$ mini de $Z_{\alpha\mathcal{F}_{P_\alpha}} \to \Omega$. Les pairs de flèches au-dessus d'une même base sont des fibrés vectoriels duaux. $\mathrm{Bun}^{sss}_{TU_\beta,\Omega}$ classifie $\mathcal{F}_{TU_\beta} \in \mathrm{Bun}_{TU_\beta,\Omega}$ muni de trois réductions s_1, s_2, s_3 dans $\mathrm{Bun}_{T,\Omega}$. Il admet ainsi une action du groupe S_3. L'indice Ω désigne leur changement de base par rapport au morphisme $\mathrm{Bun}_{T,\Omega} \to \mathrm{Bun}_T$ où $\mathrm{Bun}_{T,\Omega}$ classifie $\mathcal{F}_T \in \mathrm{Bun}_T$ muni de $Z_\alpha/Z_{\beta\mathcal{F}_T} \xrightarrow{\sim} \Omega$. Le morphisme j_α est une immersion ouverte. Le morphisme π' est fini et S_3-invariant. Désignons par Four la transformation de Fourier identifiant la catégorie des faisceaux sur un fibré avec celle sur son dual.

Théorème

On a $j_\alpha^*\mathrm{Four}(\pi_\alpha^*\mathcal{F}_{min}) \xrightarrow{\sim} \pi''^*\mathrm{Four}(\pi'_*\bar{\mathbb{Q}}_\ell)$. *Et c'est un faisceau pervers sur* $\mathrm{Bun}_{B,\Omega}$.

Remarque

La S_3-symétrie de $\mathcal{F}_{\min}$ suggérée par le Théorème 1 vient en fait de la S_3-invariance de la *représentation minimale* de Spin_8(voir [1]), mais il n'est pas facile de le voir sur sa géométrisation construite dans [2] via le *theta lifting*.

[1] W. T. Gan, N. Gurevich, D. Jiang, *Cubic unipotent Arthur parameters and multiplicities of square integrable automorphic forms*, Inventiones Mathematicae, 2002, vol. 149, issue 2, pp. 225-265

[2] V. Lafforgue, S. Lysenko, *Geometrizing the minimal representations of even orthogonal groups*, Reprensentation Theory, An Electronic Journal of AMS, Volume 17, Pages 263–325 (May 28, 2013) S 1088-4165(2013)00431-4, errata : page webe de Sergey Lysenko.

Modélisation de réseaux de télécommunication et Processus de contact

Tom Riblet, sous la direction d'**Olivier Garet** et de **Régine Marchand**.

1 Modélisation de réseaux de télécommunication

1.1 Introduction

Un réseau de télécommunication peut être modélisé par un graphe, c'est à dire un ensemble de sommet représentant les antennes ou les sites du réseau et un ensemble d'arètes qui signifient que deux sites communiquent.

Exemple: La grille $\mathbb{Z}^2$ munie de son ensemble d'arètes usuel:

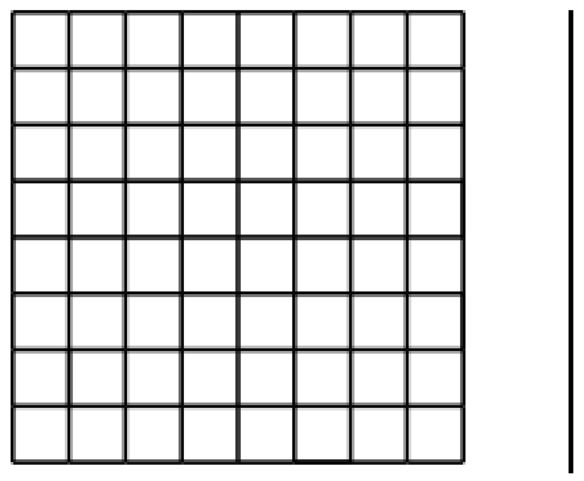

Mais ce graphe est très régulier et potentiellement peu réaliste donc nous allons nous intéresser à des graphes aléatoires qui semblent plus naturels pour modéliser des réseaux de télécommunication.

1.2 Percolation de Bernoulli

Une façon naturelle de crer un graphe aléatoire est de le rèaliser comme sous-graphe d'un graphe déterministe connu. Par exemple dans cette section, on présente un graphe aléatoire obtenu à partir du graphe $\mathbb{Z}^2$ précédent. (En fait, plus généralement tout ceci se généralise au cas des dimensions supérieures mais la dimension 2 est plus visuelle.)

Définition 1.1 (Percolation de Bernoulli). *Soit $p \in]0,1[$, on dit qu'on réalise une percolation de Bernoulli de paramètre p lorsque l'on crée un sous graphe de $\mathbb{Z}^2$ en conservant indépendamment chacune des arètes avec probabilité p.*

Exemple: Pour $p = 0.3$

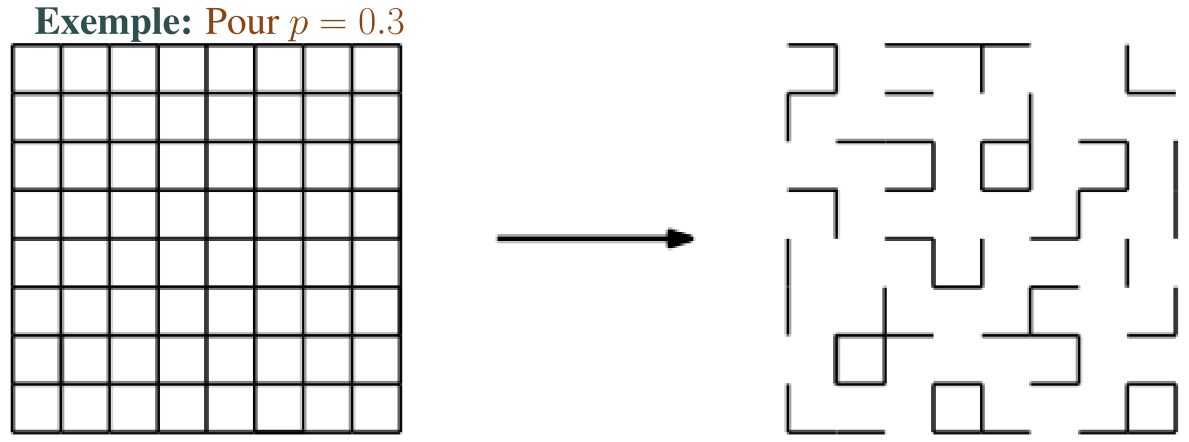

Théorème 1.2 (Éxistence et non-trivialité du seuil-critique, voir [3]). *Il existe une valeur $p_c(d)$ où d désigne la dimension de l'espace, comprise strictement entre 0 et 1, telle que:*

- *Pour tout $p < p_c(d)$, presque-sûrement, toutes les composantes connexes du graphe de Bernoulli sont finies.*
- *Pour tout $p < p_c(d)$, presque-sûrement, il existe une unique composante connexe infinie pour la percolation de Bernoulli.*

En outre, $p_c(2) = 1/2$.

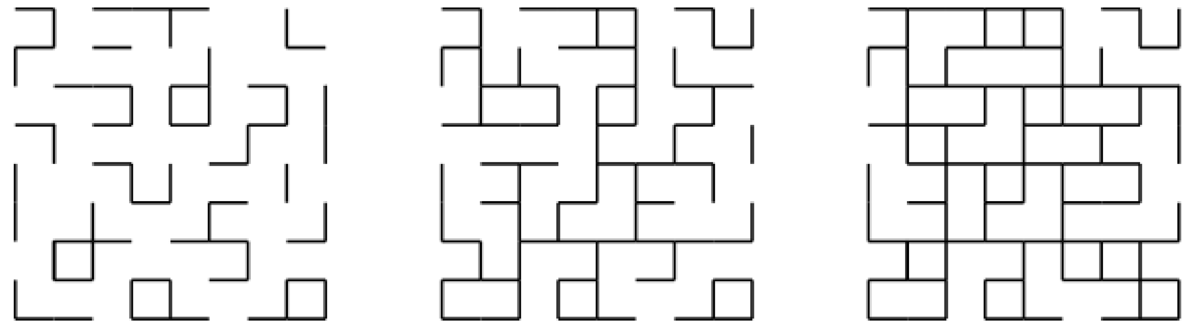

$p = 0.3$ $p = 0.6$ $p = 0.8$

Remarque. *La Percolation est un domaine de recherche très dynamique en théorie des probabilités. Beaucoup de questions très intéressantes et naturelles se posent au sujet du graphe aléatoire obtenu, par exemple:*

- *Que se passe-t-il au seuil critique? À-t-on l'existence d'un amas infini?*
- *Dans chacun des régimes sur et sous-critique, quelle est la taille typique d'un amas fini?*
- *Quelles sont les valeurs de $p_c(d)$ pour $d \neq 2$?*

1.3 Percolation Booléenne

Nous voulons maintenant crer un graphe aléatoire dont les sommets sont situés eux aussi aléatoirement dans l'espace (ou le plan en dimension 2). Jusqu'à maintenant ils étaient contraints à avoir des coordonées entières. Pour cela, nous allons utiliser un outil probabiliste appelé processus ponctuel de Poisson. C'est une façon de tirer aléatoirement des points qui a de bonnes propriétés dans son étude mathématiques (pour plus de détails voir [4]).

Définition 1.3 (Graphe Booléen). *Le graphe Booléen de rayon $R > 0$ est un graphe obtenu à partir de l'ensemble de ces sommets donné par un processus ponctuel de Poisson homogène et tel que deux sommets communiquent si leur distance est plus petite que R.*

Théorème 1.4 (voir [7]). *En fonction de l'intensité du processus ponctuel, il existe un rayon critique à partir duquel il existe presque-sûrement une unique composante connexe infinie.*

Remarque. *Ce nouveau graphe aléatoire est très intéressant notamment parce qu'il n'est à priori pas à degré borné.*

Illustrations:

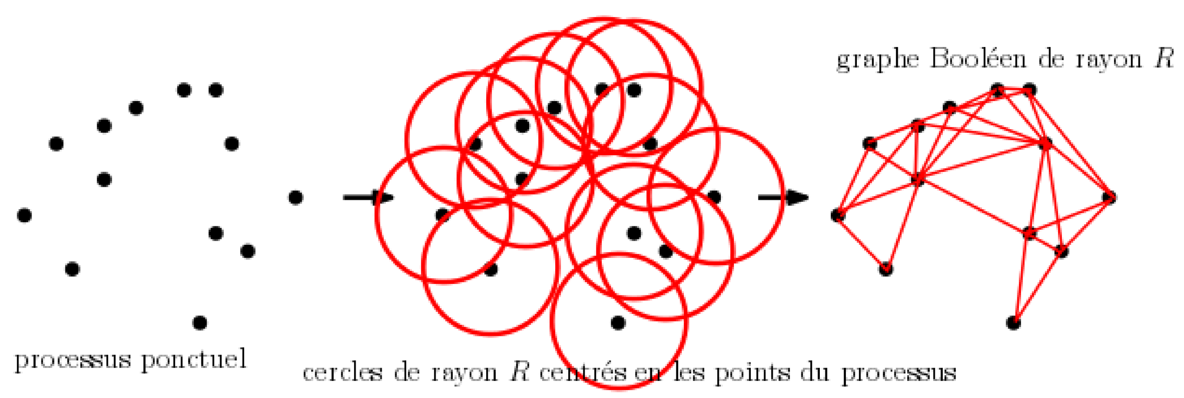

Remarque. *La percolation Booléenne est elle aussi très étudiée et le même genre de questions que pour la percolation de Bernoulli se posent. Cependant, ce graphe contrairement au précédent présente une certaine forme de continuité dans sa construction et cela permet d'envisager de nouveau outils dans létude de cet objet. Par exemple, il existe un certain nombre de transformations continues et aléatoires du graphe qui laissent sa mesure de construction invariante.*

2 Processus de contact

Le processus de contact est un système de particules en intéractions modélisant la propagation d'une maladie ou le développement d'une population par exemple. Ce processus vit sur un graphe et il a notamment été beaucoup étudié sur les graphes $\mathbb{Z}^d$ (voir [6] et [5]). Dans ce système, une particule infecté (ou vivante) peut donner naissance à une particule qui sera située sur l'un des sommets voisins du graphe mais une particule peut aussi mourrir. Dans l'étude du processus de contact, on s'intéresse à la probabilité de survie notamment ainsi qu'á la façon dont la population (ou la maladie) évolue et voyage sur le graphe au fil du temps. En particulier, ce processus possède un paramètre $\lambda > 0$ caractérisant la fertilité de la population (ou la virulence de la maladie).

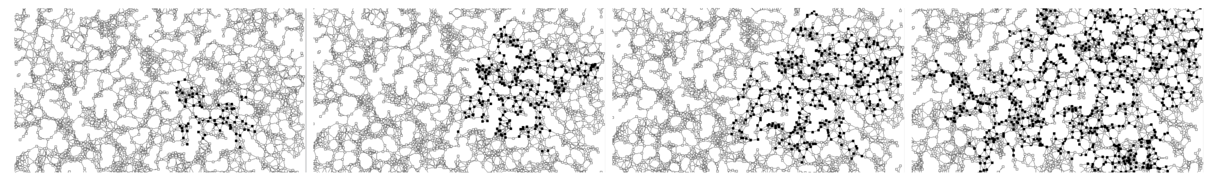

2.1 Résultats

Définition 2.1. • *On dit que le processus de contact survit lorsque pour tout $t > 0$ l'ensemble des points vivants (ou infectés) est non-vide. Sinon, on dit qu'il s'éteint.*

• *On dit que le processus de contact survit fortement si tout site du réseau né (ou est infecté) un nombre infini de fois au cours du temps.*

Proposition 2.2. *Pour le processus de contact évoluant en environnement aléatoire sur un amas de Percolation de Bernoulli ou sur un graphe Booléen (sur-critique), il existe un seuil critique λ_c non-trivial (dépendant des paramètres de l'environnement) tel que:*

- *Pour tout $\lambda < \lambda_c$, le processus de contact s'éteint presque-sûrement.*
- *Pour tout $\lambda > \lambda_c$, le processus de contact survit avec probabilité strictement positive.*

La preuve de ce résultat repose essentiellement sur des propriétés de monotonie et sur des comparaisons stochastiques avec d'autres modéles.

Proposition 2.3. *Il existe un seuil-critique pour le paramètre λ à partir duquel le processus de contact survit fortement. En outre, ce seuil coïncide avec λ_c et est donc non-trivial.*

2.2 Objectifs

L'objectif principal est de formuler un théorème dit de Forme asymptotique pour le processus de contact conditionné à la survie. sur les environnements aléatoires précédents.

Théorème 2.4 (De forme asymptotique). *Pour tout λ suffisament grand, il existe un ensemble convexe déterministe $B \subset \mathbb{R}^2$ qui dépend des paramètres de l'environnement aléatoire, tel que pour tout $\epsilon > 0$;*

$$\mathbb{P}\left(\exists T > 0,\ \forall t \geq T,\ (1-\epsilon)\,B \subset \frac{\bar{H}_t}{t} \subset (1+\epsilon)\,B\right)$$

où $\bar{H}_t$ désigne l'ensemble des points qui ont déjà vécu (ou été infectés) au temps t.

Remarque. *Les théorèmes de formes asymptotiques sont des résultats classiques dans beaucoup de modèles de systèmes de particules en intéractions et en particulier pour le processus de contact dont un certain nombre de variantes ont déjà été étudiées. Pour établir ce résultat, je m'inspire des articles de O.Garet et R.marchand [1] et [2] qui ont montré un théorème de forme asymptotique pour le processus de contact en environnement aléatoire mais lorsque le graphe lui restait déterministe.*

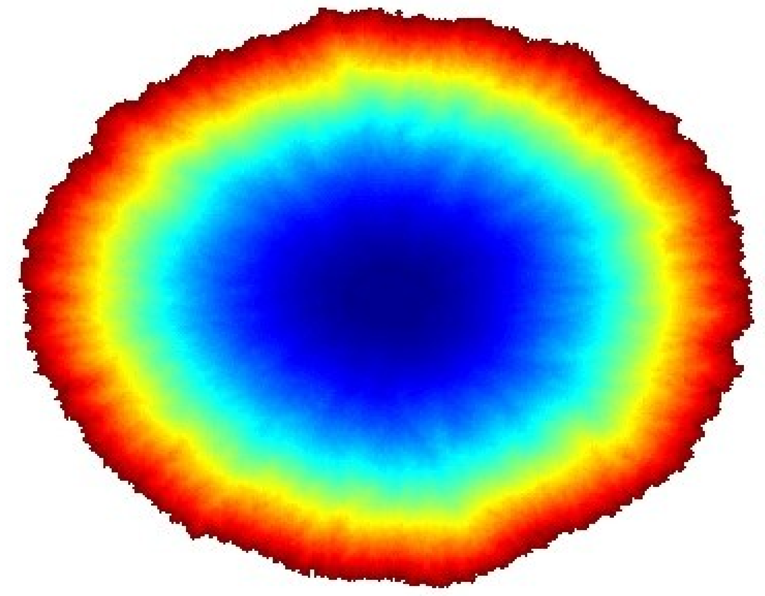

References

[1] Olivier Garet and Régine Marchand. Asymptotic shape for the contact process in random environment. *Ann. Appl. Probab.*, 22(4):1362–1410, 2012.

[2] Olivier Garet and Régine Marchand. Growth of a population of bacteria in a dynamical hostile environment. *Adv. in Appl. Probab.*, 46(3):661–686, 2014.

[3] G. Grimmett. *Percolation*. Springer, Berlin, 1999.

[4] J. F. C. Kingman. *Poisson processes*, volume 3 of *Oxford Studies in Probability*. The Clarendon Press, Oxford University Press, New York, 1993. Oxford Science Publications.

[5] Thomas M. Liggett. *Stochastic interacting systems: contact, voter and exclusion processes*, volume 324 of *Grundlehren der Mathematischen Wissenschaften [Fundamental Principles of Mathematical Sciences]*. Springer-Verlag, Berlin, 1999.

[6] Thomas M. Liggett. *Interacting particle systems*. Classics in Mathematics. Springer-Verlag, Berlin, 2005. Reprint of the 1985 original.

[7] Roy R. Meester R. *Continuum Percolation*. Cambridge Tracts in Mathematics. Cambridge University Press, 1996.

ECOLE DOCTORALE IAEM LORRAINE

UNIVERSITÉ DE LORRAINE

Titre de la thèse: Analyse et optimisation de la durabilité des systèmes de production de biocarburants oléagineux en Afrique de l'ouest : cas du Burkina Faso et du Mali

Nom Prénoms : BAMBARA Linda Dominique Fabiola

Directeur de thèse : ANCIAUX Didier

Co-directeur de thèse : *R Daniel*

lgipm Laboratoire de Génie Industriel, de Production et de Maintenance

Problématique et objectifs

- Engouement pour les biocarburants depuis les années 2000 en Afrique
- Nombreux projets biocarburants développés au Burkina Faso et au Mali

Constat une dizaine d'année après:

- Faible rentabilité de ces projets
- Projets focalisés uniquement sur l'exploitation du jatropha
- Rares d'études sur l'optimisation de la chaine logistique des systèmes de production de bioénergies dans le contexte ouest Africain

Objectifs:

- Concevoir un modèle d'optimisation de la chaine logistique (CL) amont et de la chaine logistique Inverse (CLI) des systèmes de production de biocarburant oléagineux en Afrique de l'ouest
- Déterminer les conditions de durabilité des systèmes de production de biocarburant oléagineux en Afrique de l'ouest

Modélisation

Le problème modélisé concerne une unité de production de biocarburant (UPB) oléagineux. Cette UPB doit être approvisionnée en biomasse et souhaite valoriser les coproduits générés de sorte à satisfaire les objectifs ci-dessous:

Objectif économique : minimiser les coûts totaux de la production et de l'approvisionnement de la biomasse et de la valorisation des coproduits
Objectif social : minimiser la quantité de travail totale engendrée par la production et l'approvisionnement de la biomasse et par la valorisation des coproduits
Objectif environnement : minimiser les impacts environnementaux (IE) liés à la production et à l'approvisionnement de la biomasse et à la valorisation des coproduits

La valorisation des coproduits est supposé générer un gain économique, environnemental et social

Le système modélisé possède 3 niveaux

- Niveau 1 : sites de production de la biomasse (SPB)
- Niveau 2 : points de rassemblement intermédiaires (PR)
- Niveau 3 : unité de production de biocarburants (UPB)

3 localisations possibles du prétraitement:
niveau 1 c'est-à-dire sur les sites de production de la biomasse
niveau 2 c'est-à-dire aux PR
niveau 3 c'est-à-dire à l'unité de production de biocarburant.

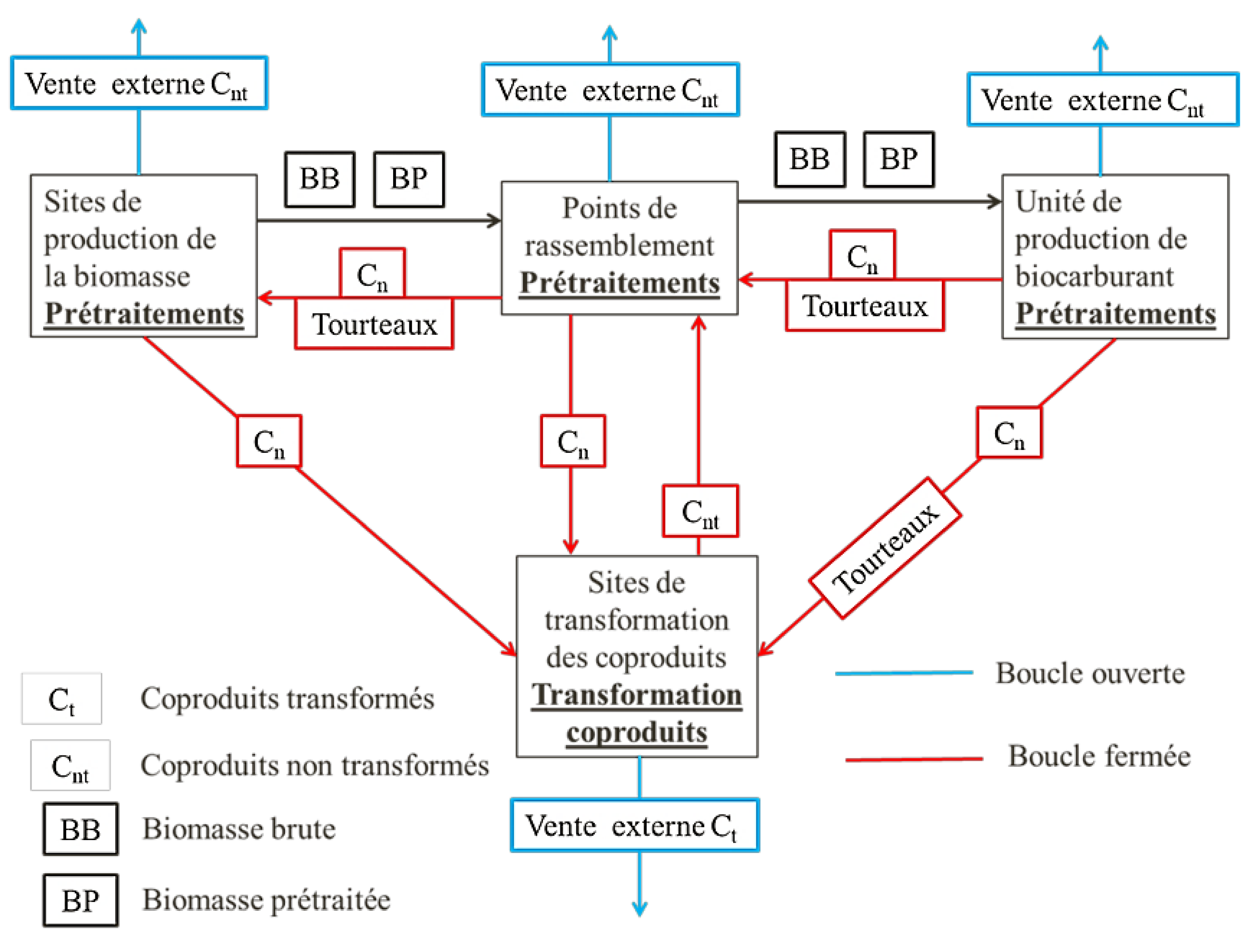

Schéma du réseau logistique avec les flux de matière pour la chaine directe et la chaine inverse

- Plusieurs itinéraires technique de culture pour la production de la biomasse
- Plusieurs moyens de transport de la biomasse
- Demande saisonnière en biomasse de l'UPB
- Post traitement possible pour les coproduits

Programme linéaire à variable mixtes

La fonction économique :

coûts culture + coûts récolte + coûts transport biomasse entre SPB et PR + coûts transport biomasse entre PR et l'UPB + coûts prétraitement + coûts transport coproduits + coûts post traitement coproduits – Gain

La fonction environnement:

IE culture + IE récolte + IE transport biomasse entre SPB et PR + IE transport biomasse entre PR et l'UPB + IE prétraitement + IE transport coproduits + IE post traitement coproduits – Gain environnement

La fonction social :

quantité de travail de culture + quantité de travail de récolte + quantité de travail transport entre les SPB et les PR + quantité de travail transport entre les PR et l'UPB + quantité de travail prétraitement + quantité de travail transport coproduits + quantité de travail post traitement coproduits – Gain social

Les contraintes

Capacité de production des SPB
Capacité d'accueil saisonnière des PR
Capacité de charge des moyens de transport
Distance de voyage des moyens de transport
Demande de l'UPB

Résultats

Le modèle détermine pour chaque fonction:

- Le nombre de SPB parmi un ensemble de SPB préalablement identifié
- La superficie de chaque SPB à allouer à la culture énergétique
- L'itinéraire technique de culture
- La période de transport de la biomasse
- Le nombre optimal de PR à ouvrir parmi un ensemble de sites de PR préalablement identifié
- L'affectation de chaque ouvert à un ou plusieurs PR
- Les quantités optimales à transporter entre chaque SPB et chaque PR ouvert
- Les quantités optimales à transporter entre chaque PR ouvert et l'UPB
- La localisation optimale du prétraitement qui permet de minimiser les coûts de transport, d'ouverture des PR et d'ouverture des unités de prétraitement.
- La quantité de coproduit à valoriser afin de réduire le prix de revient de la biomasse

Conclusion et perspectives

- Construction d'un modèle d'optimisation des coûts, de la quantité de travail et des impacts environnementaux de la chaine logistique amont et inverse des systèmes de production de biocarburant oléagineux en Afrique de l'ouest
- Implémentation de la fonction économique

- **Perspectives pour la 2ième année**
- Implémentation de la valorisation des coproduits (Chaine inverse)
- Implémentation des fonctions environnement et social

Scheduling and Polynomial Approximation

Gais ALHADI, Imed KACEM, Pierre LAROCHE, and Izzeldin M. OSMAN
Université de Lorraine, LCOMS, F-57045 Metz, France
{alhadiba1, imed.kacem, pierre.laroche}@univ-lorraine.fr

Introduction

Scheduling problem is one of the problems that have been the subject of extensive research for over fifty years. In this research project, we aim to study of a family of scheduling problems.

The main objective of our study is to deal with NP-hard problems, and propose analytical characteristics for this family of problems. From a methodological point of view, we will consider the study of exact methods. In addition, we are also considering the development of heuristics and lower bounds. A performance evaluation at worst case will prove the effectiveness of these approaches based on analytical proofs.

Lateness Minimization on Two Parallel Machines without Release Dates

We consider the two-parallel machines scheduling problem, as we can see in Figure.1.

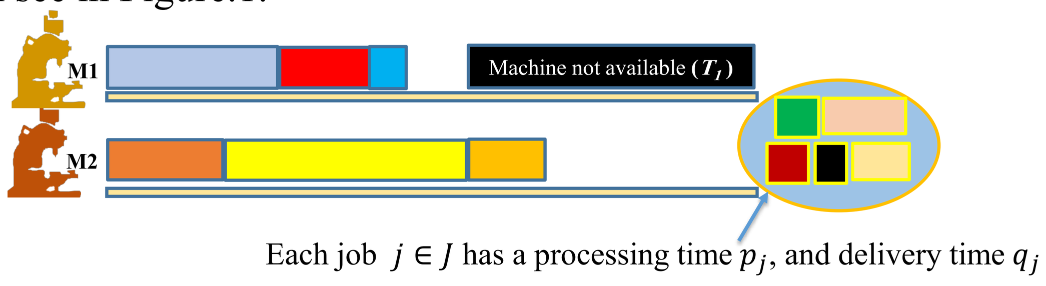

Figure.1 Illustrates the definition of the problem

The problem is to find a sequence of jobs, with the objective of minimizing the maximum lateness $L_{max} = max_{1 \le j \le n}\{C_j(s) + q_j\}$ where $C_j(s)$ the completion time of job j in sequence S. With no loss of generality, we consider that all data are integers and that jobs are indexed in nonincreasing order of their delivery times ($q_1 \ge q_1 \ge \cdots q_n$) (i.e., according to Jackson's order).

Constant Approximation Heuristics

We consider the two constructive heuristics in the worst-case.

i) The first heuristic:

The first heuristic (H') is to put all the available jobs as soon as possible on the second machine.

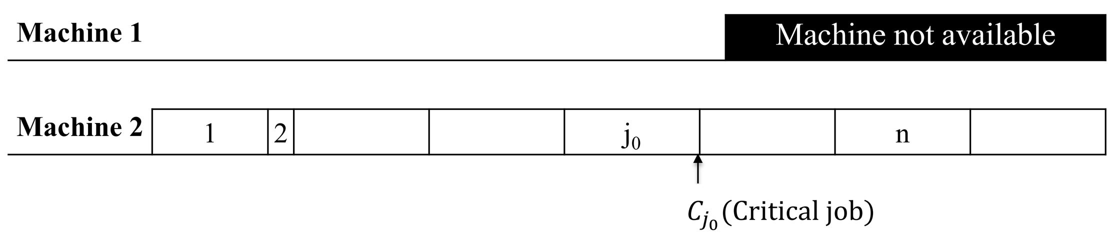

Figure.2 Illustration of heuristic H'

Lemma 1:

Any assignment of jobs to the machines is a constant approximation with a standard ratio no more than 3.

Proof For any instance I, we have:

$$OPT(I) \ge P/2$$

Now, let $j_0$be the job such that $C_{j_0} + q_{j_0} = L_{max}$ as it show in figure.3, then we have:

$$L_{max} \le P + q_{j_0}$$

Therefore, $L_{max} \le 2OPT(I) + OPT(I) \le 3.OPT(I)$

ii) The second heuristic:

The second heuristic H is to put all the available jobs as soon as possible on the most available machine, according to Jackson's rule.

1. For $n = 1$, H is optimal.

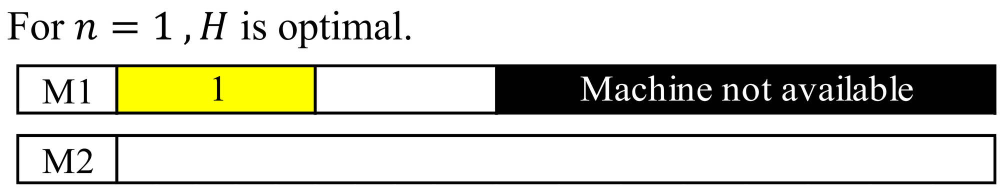

2. For $n = 2$, H is optimal.

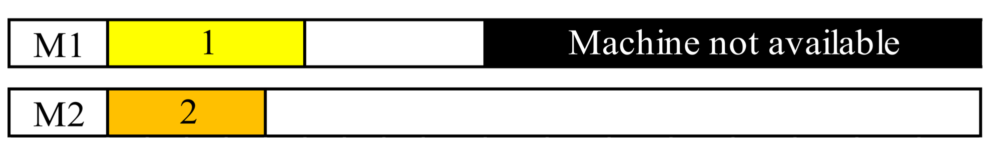

3. For $n = 3$, H is not optimal.

Let us consider the three jobs instance defined as follows:

$p1 = z;\ q1 = 1 + 2\varepsilon;\ p2 = z;$
$q2 = 1 + \varepsilon;\ p3 = 2z;\ q3 = 1$
where $\varepsilon > 0$.

Constant Approximation Heuristics…

For this instance the solution obtained by the heuristic as follows:

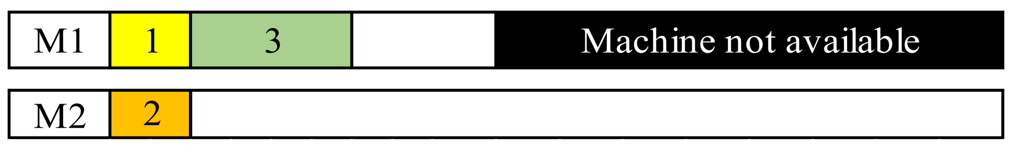

$$L_{max} = p1 + p3 + q3 = 3z + 1$$

While the optimal solution as follows

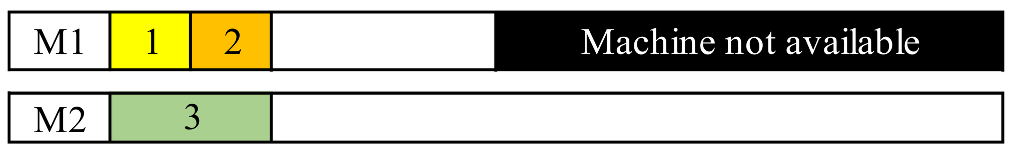

$$L_{max} = p3 + q3 = 2z + 1$$

Therefore, for n=3, the heuristic is not optimal.

Dynamic programming algorithm

The following dynamic programming (DP) algorithm A^{ε}, can be applied for solve this problem optimally. Note that, variable t denotes the completion time of the last job scheduled on the first machine before *T1* and f is the maximum lateness of the corresponding schedule.

Algorithm A^{ε}

i. Set $Q'_0 = \{[0,0]\}$.
ii. For j ∈{1, 2, 3, … , n},
For every state [t, f] in Q'_{j-1}
1) Put $[t, max\{f, \sum_{i=1}^{j} p_i - t + q_j\}]$ in Q'_j
2) Put $[t + p_j, max\{f, t + p_j + q_j\}]$ in Q'_j (if $t + p_j \le T_1$)
Remove Q'_{j-1}

iii. $L^*_{max}(P) = \min_{[t,f] \in Q'_n}(f)$

FPTAS

In our FPTAS we should remove a special part of the states generated by the DP algorithm to produce an approximation solution instead of the optimal solution. The comparison of the execution of algorithms A^{ε}, and $A^{\varepsilon\prime}$produce the analysis of worst-case for the FPTAS.

Given an arbitrary $\varepsilon > 0$, we define

$$LB = \frac{2L^{A^{\varepsilon\prime}}_{max}(p)}{3}, \quad \beta = \frac{3n}{2\epsilon}, \quad \text{and } \gamma = \frac{L^{A^{\varepsilon\prime}}_{max}(p)}{\beta}.$$

We divide the interval *[0, L_{max}]* into β equal sub intervals $I_h = [(h-1)\gamma, h\gamma]_{1 \le h \le \beta}$ of length γ. The algorithm $A^{\varepsilon\prime}$described below produces reduced the sets $Q^{\#\prime}_j$ instead of sets Q'_j.

Algorithm $A^{\varepsilon\prime}$

i. Set $Q^{\#\prime}_0 = \{[0,0]\}$.
ii. For j ∈{1, 2, 3, … , n},
For every state [t, f] in $Q^{\#\prime}_{j-1}$
1) Put $[t, max\{f, \sum_{i=1}^{j} p_i - t + q_j\}]$ in $Q^{\#\prime}_j$
2) Put $[t + p_j, max\{f, t + p_j + q_j\}]$ in $Q^{\#\prime}_j$ (if $t + p_j \le T_1$)
Remove $Q^{\#\prime}_{j-1}$
Let [t, f]h be the state in $Q^{\#\prime}_j$ such that $t \in I_h$ with the smallest possible t (we choose the state which have the smallest f). Set $Q^{\#\prime}_j = \{[t,f]_h | 1 \le h \le \beta\}$.

iii. $L^{A^{\varepsilon\prime}}_{max}(P) = \min_{[t,f] \in Q^{\#\prime}_n}(f)$.

Lemma 2:

For every state $[t,f] \in Q'_j$ *there exists at least one approximate state* $[t^{\#}, f^{\#}] \in Q^{\#\prime}_j$ *such that:*

$$t^{\#} \le t$$

and

$$f^{\#} \le f + j\gamma$$

Results

For the DP and FPTAS algorithms, we all randomly generate 7000 jobs, and, for each job, p_j and q_j are sets to be an integer randomly selected from [1 ; 50]. Noteworthy, the values of processing times, delivery times, epsilon, and the availability of machine plays an important role in the results. The results of the experiments showed that:

- The capacity of the DP algorithm does not exceed 30 jobs (after 30 jobs becomes very slow).
- For the FPTAS, We can see that:
  - The proposed FPTAS has a strongly polynomial running time.
  - The results are better with a larger T_1 .
  - The FPTAS become faster when epsilon is larger and also when T_1 is smaller.
  - Moreover, when using larger values for p and q, the running time increase, and L_{max} become a large.
  - Table 1 Shows the results for some instances (N=800 jobs, values of p between 40 and 50, and values of q between 20 and 30).

T_1	*Epsilon*	*Lmax*	*Time (seconds)*
P/3	0.3	23993	206.814
P/3	0.9	23994	66.55
P/7	0.3	30842	92.446
P/7	0.9	30846	31.043

Table.1 The results for some instances (N=800 jobs)

- We can also see in Figure 3 the effect of epsilon on running time for the some instances that have been tested (for DP and FPTAS).

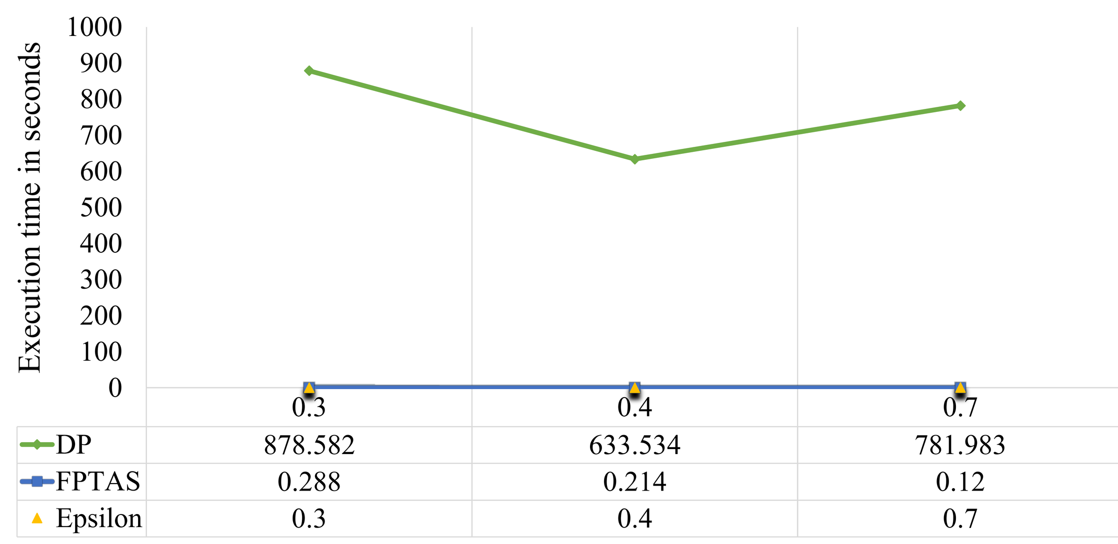

Figure.3 Effect of Epsilon on running time for some instances that have been tested

Conclusion

In this work, we established the existence of a constant approximation for the studied problem. One variant of heuristics is obvious (with a guaranteed ratio of 3). Then, we designed a dynamic programming algorithm capable to solve exactly the problem in O(n.T) time, where *n* is the number of jobs and *T* is the length of the availability period. Finally, we converted the dynamic programming method into an FPTAS with a strongly polynomial time complexity. We also improved the result by exploiting the so-called "*merging technique*".

In our future works, we look forward to extend these results to other variants of this problem, and add other constraint release dates, additional criteria (for example, makespan, maximum tardiness, etc.). Also, we aim to finish the current work on multi-objective optimization by writing a journal paper and running several experimental results in order to evaluate our work. The whole work will be submitted to an international journal if we are successful.

References

- I.Kacem and M. Hifi, "Makespan Minimization On Two Parallel Machines With Release Dates," pp. 296–299, 2009.
- I.Kacem and M. Haouari, "Approximation algorithms for single machine scheduling with one unavailability period," *4or*, vol. 7, no. 1, pp. 79–92, 2009.
- Kacem. Approximation algorithm for the weighted flow-time minimization on a single machine with a fixed nonavailability. Computers & Industrial Engineering, 54:3, 401-410, 2008.
- I. Kacem and C. Chu, "Worst-case analysis of the WSPT and MWSPT rules for single machine scheduling with one planned setup period," *Eur. J. Oper. Res.*, vol. 187, no. 3, pp. 1080–1089, 2008.

PRISE EN COMPTE DES EXIGENCES SUR LES ESPACES DANS LES PRATIQUES BIM

Aida Siala, Gilles Halin, Najla Allani, Mohamed Bouattour

Espace & exigences

L'architecte donne à l'espace non seulement une forme, mais aussi des aspects de **topologie, d'accessibilité** et de **confort**. Cette production est basée sur un ensemble d'**exigences** définies en phase de programmation : des exigences **quantitatives**, mais aussi et surtout **qualitatives.**

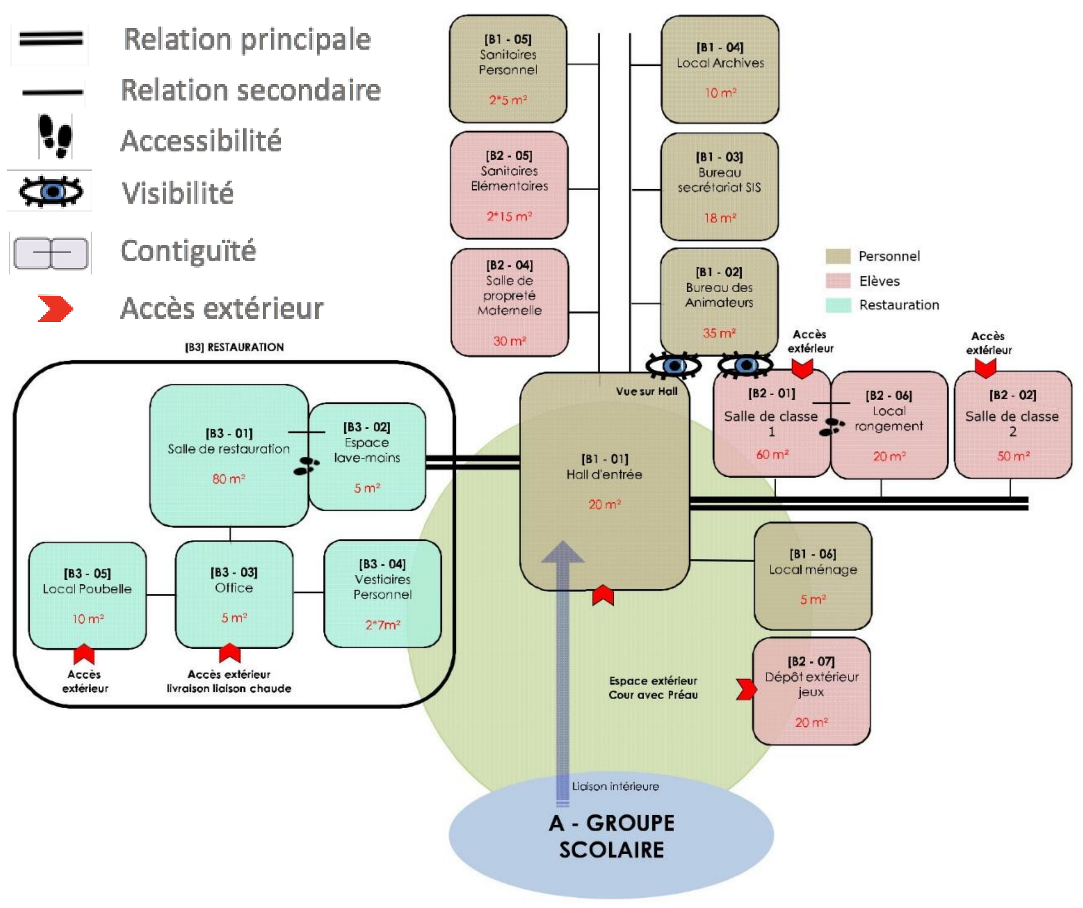

Exemple des exigences de topologie et d'accessibilité du Groupe scolaire de Vany, 2013

➡ **Exigences indispensables** en phase de conception, qui sont **implicitement connues** par les architectes (retour format papier).

Modèles d'espace existants

Méthode : Divers modèles récents ont été analysés pour identifier leurs abilité à inclure ces exigences

Résultats :

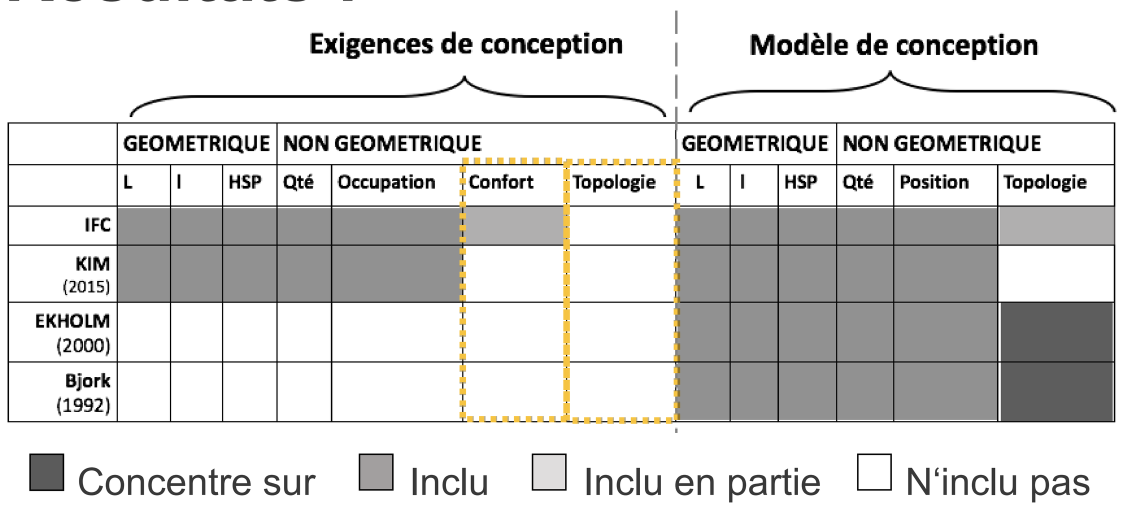

Identification des exigences spatiales

Méthode : Analyse de contenu (Wanlin 2007) de 10 documents de programmation architecturale

Catégorisation et typologie
Groupement des mots décrivant les espaces avec leurs descriptions et élaboration de grille de catégories

Calcul des fréquences
Remplissage des grilles

Condensation des résultats
Les descriptions <5% sont considérées non significatives.

Résultats :

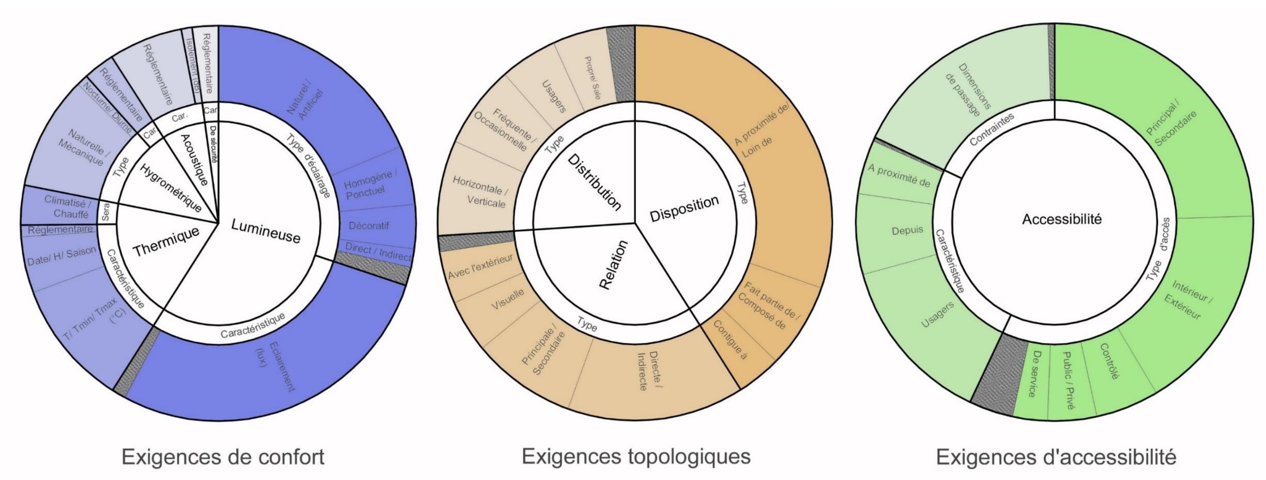

Vérification : Tester sur un nouveaux document : Résultats similaires (différences <6%)

Proposition d'un Modèle

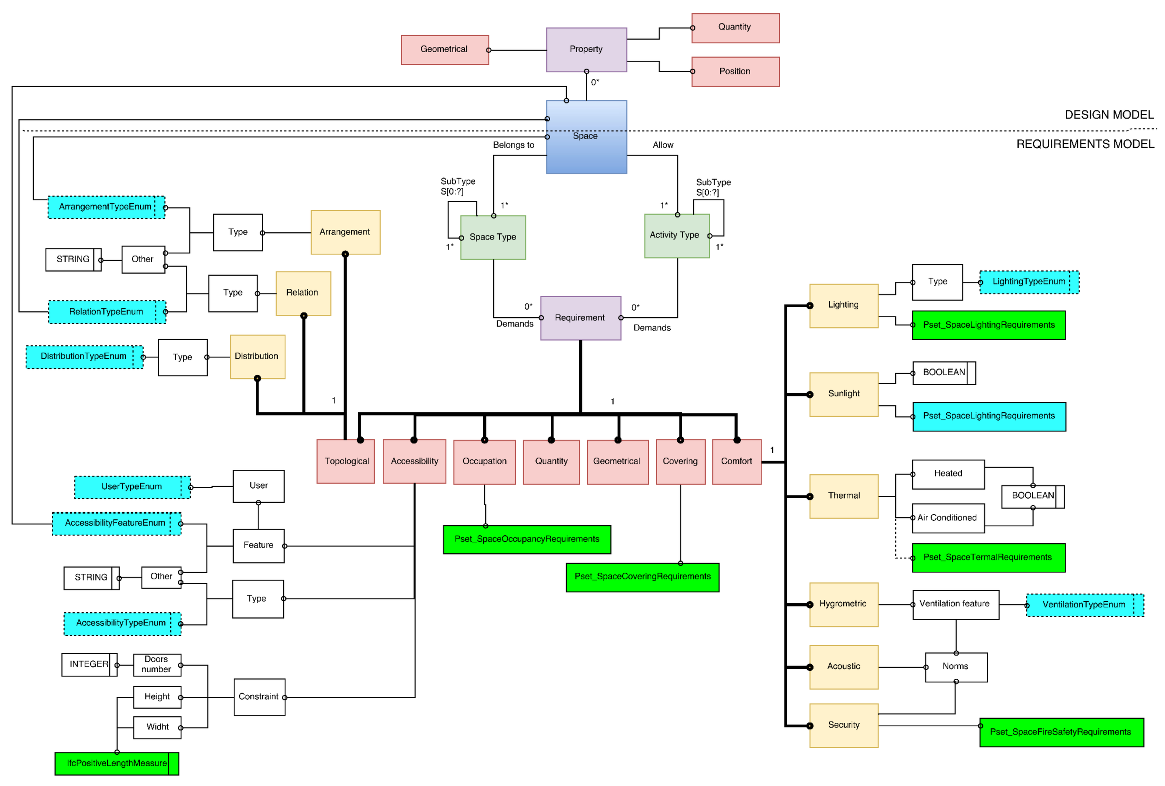

Pratiques et outils BIM et prise en compte des exigences

Démarche BIM : basée sur des standards traduisant toute l'information sur le bâtiment en **données essentiellement quantitatives**, ce qui ne permet pas de prendre en compte les **exigences spatiales qualitatives.**

➡ Pour identifier le besoin d'une nouvelle vision pour les espaces, divers outils BIM ont été investigué.

Méthode : 1- Concevoir des espaces. **2-** Définir des tâches de conception (tâches possibles sur les ouvrages). **3-** Essayer de les appliquer sur les espaces.

Résultats :

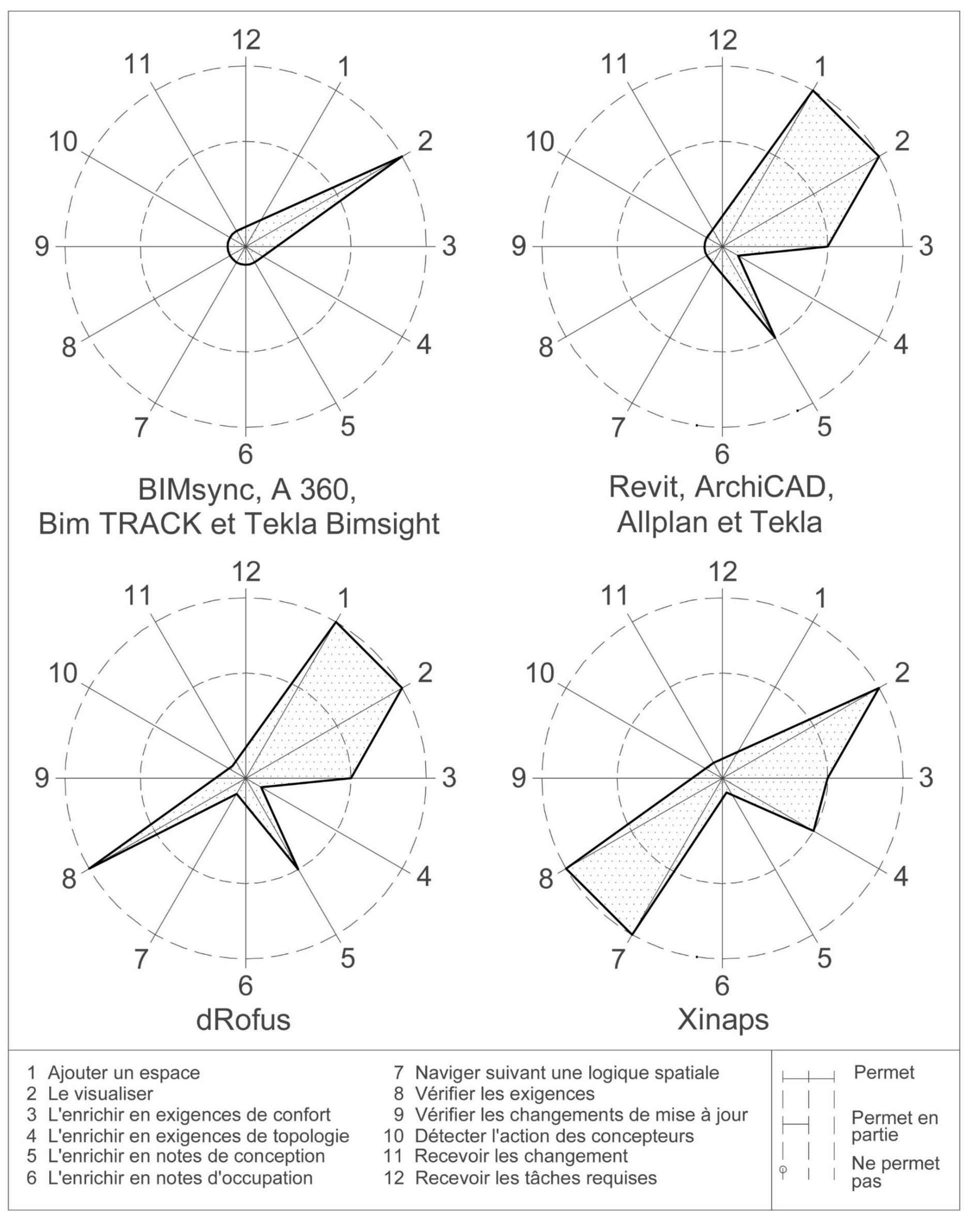

Proposition d'un outil integrant le modèle proposé

Méthode (3 étapes) **:**

1. Saisie des exigences sur Excel

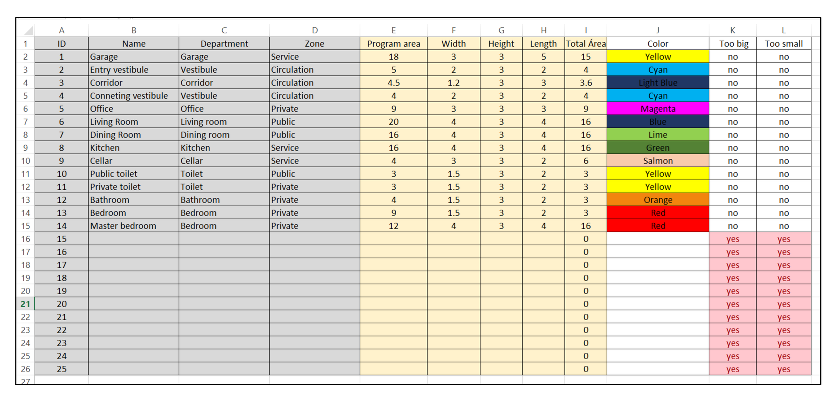

2. Conception : Dynamo/ Revit

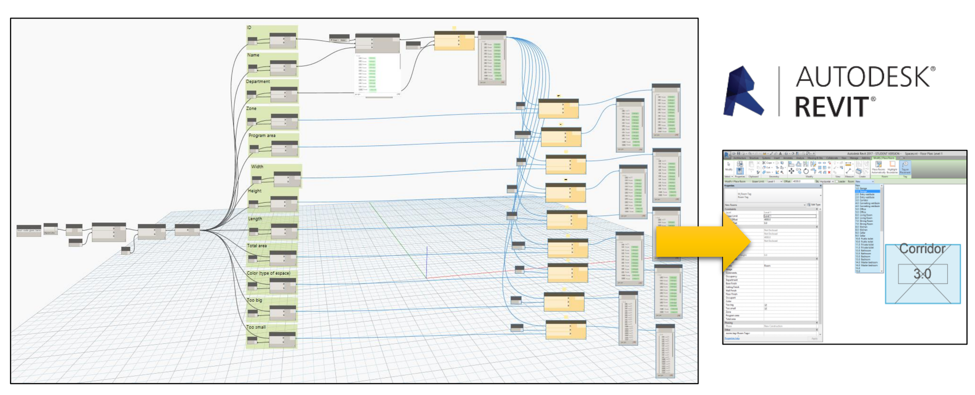

3. Vérification : Comparaison automatique Dynamo/ affichage des exigences non respectées sur Revit.

• Références :

Anders, Ekholm and Sverker, Fridqvist 2000, `A concept of space for building classification, product modelling and design', Automation In Construction, 9, pp.315-328
Bo-Crister, Bjork 1992, `A conceptual model of spaces, space boundaries and enclosing structures', Automation In Construction, 1(3), pp. 193-214
Kim, Tae Wan, Youngchul, Cha, Seung Hyun and Fischer, Martin 2015, `Automated updating of space design requirements', Automation In Construction, 50, pp. 102-110
Wanlin, Philippe 2007, `L'analyse de contenu comme méthode d'analyse qualitative d'entretiens : une comparaison entre les traitements manuels et l'utilisation de logiciels', in Recherches qualitatives, ARQ (eds) 2007

Université de Carthage University of Carthage
UMR 3495 Ministère Culture Communication
UNIVERSITÉ DE LORRAINE

Annual PhD students conference IAEM Lorraine 2017

Étude de nouvelles techniques d'interaction en situation de mobilité avec les lunettes électroniques pour le domaine de santé

CONEXTE

CONTEXTE

Smartglasses :

- Un nouveau dispositif avec des mains libres
- Plusieurs capteurs ⇒ Beaucoup de possibilités
- Près des yeux⇒ données en temps réel

Mais…

- Dispositif mobile⇒ Sensibilité au contexte
- Petit écran⇒ Difficulté de visualisation d'un grand espace de données

Domaine de santé:

- Les professionnels ont montrer un intérêt pour les avantages potentiels des lunettes électroniques selon "HL7 standards" (spécialistes en médecine et technologies).
- Beaucoup de tâches à réaliser avec les lunettes électroniques (chirurgie, documentation détaillée, collaboration…).

VISUALISATION

INTERFACE À BASE DE TUILES

Utilisé sur windows

Intègre les propriétés de sensibilité au contexte

ADAPTATION | FLEXIBILITÉ | INTERCONNECTION | PLACEMENT

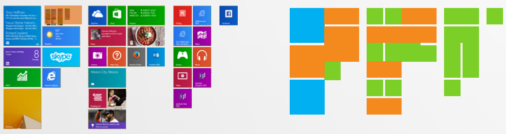

MOTIVATION

- Une interface classique ne peut pas répondre aux attentes de l'utilisateur.
- Une ergonomie, une interface conviviale et un confort visuel doivent être apportés sur ces lunettes: réduire au le temps et l'effort fournis par l'utilisateur.

PROBLÉMATIQUE

- Représenter un grand nombre de tuiles dans un espace limité.
- Garder toutes les tuiles dans la même vue.
- lier les services entre eux.

VUE FISHEYE

Permet de donner une vue détaillée tout en gardant le contexte général.

Point fort: Elle est caractérisée par sa fonction de degré d'intérêt qui mesure l'intérêt de chaque information pour la présenter à l'utilisateur.

PROPOSITION

- Utilisation des relations sémantiques des informations contenues dans les tuiles à travers un modèle.
- Reformulation de la fonction du degré d'intérêt.

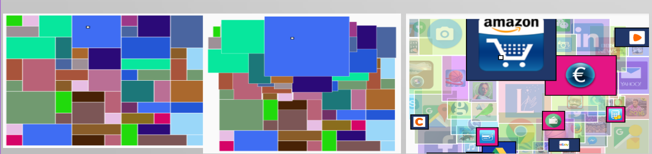

ESPACE DE CONCEPTION

PROBLÉMATIQUE

- La visualisation des dossiers patients reste un problème complexe.
- Il manque un réel soutien au concepteurs de systèmes de visualisation des dossiers patients.

PROPOSITION

- Fournir un cadre pour guider les concepteurs d'applications permettant d'accéder à un dossier patient.
- Un espace de conception à huit dimensions pour trouver des solutions aux problèmes et manques dans les systèmes existants

DIMENSIONS

Les dimensions de notre espace de conception sont tirées de la méthode 5W1H utilisée pour la collecte des informations.

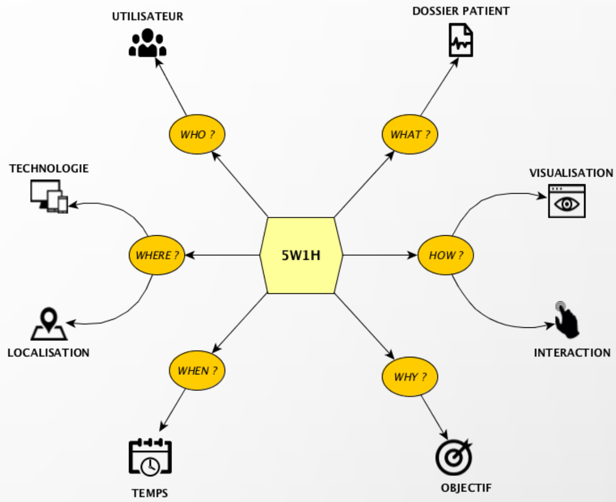

INTERACTION EN ENTRÉE

PROBLÉMATIQUE

- Identifier les techniques de pointage qui peuvent être utilisé dans un contexte de mobilité sur les lunettes électroniques pour naviguer dans le dossier patient.

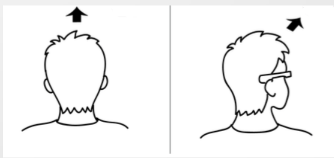

Orientation de la tête

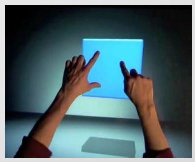

Gestes

Touchpad

MÉTODOLOGIE

- Test de ISO 9241-9 multidirectionnel pour comparer les différentes techniques
- Questionnaire de type SUS

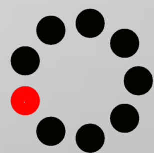

chist-era · UNIVERSITÉ DE LORRAINE · loria · eGlasses

Déterminants et Quantificateurs Généralisés Dynamiques

Objectifs

- Définir formellement la notion de déterminant
- Étudier la sémantique formelle des déterminants [1]
- Modéliser les déterminants à l'aide de quantificateurs généralisés dynamiques [2]
- Classer les déterminants en fonction de leurs propriétés dynamiques relatives à l'introduction de référents [3]
- Proposer des λ-termes dénotant les déterminants en tenant compte des propriétés mises en évidence [4]

Qu'est-ce qu'un déterminant ?

- Approche linguistique
  - Distribution
  - Actualisateur de nom
- Approche formelle
  - Quantificateur généralisé $(e \to t) \to (e \to t) \to t$
  - Conservatif $\mathcal{D}AB \Leftrightarrow \mathcal{D}A(A \cap B)$

Pourquoi de la dynamicité ?

- Accès au contexte
  - Références inter-phrastiques
  - Références au monde

Dynamicité interne

- $\mathcal{D}$ joueur(s) qui pioche(nt) **[un As]** **[le]** retourne(nt) sur la table
  - *Un* joueur qui pioche **[un As]** **[le]** retourne sur la table
  - ⋘ Pas d'exemple négatif ⋙

Dynamicité externe

- Si $\mathcal{D}$ joueur(s) pioche(nt) **[un As]**, le croupier **[le]** retirera du jeu
  - Si *trois* joueurs piochent **[un As]**, le croupier **[le]** retirera du jeu
  - *Si *tout* joueur pioche **[un As]**, le croupier **[le]** retirera du jeu

Dynamicité intrinsèque

- Si [$\mathcal{D}$ **joueur(s)]** pioche(nt) un As, **[il(s)]** remporte(nt) le point
  - Si **[*certains* joueurs]** piochent un As, **[ils]** remportent le point
  - *Si **[*aucun* joueur]** ne pioche un As, **[il]** remporte le point

Classes dynamiques de déterminants

déterminants	*dynamique interne*	*dynamique externe*	*intrinsèquement dynamique*	*exemple de déterminant*
quantificateurs	+	−	−	*aucun, tout*
spécifiques	+	+	−	*le, ce, son*
généraux	+	+	+	*un, cinq, certains*

Déterminants généraux

- $Q_{\mathrm{w}}\,A\,B := \lambda ek.\,\mathbf{q}\,(\lambda x.\,A\,x\,e\,(\lambda e.\,\top))\,(\lambda x.\,((A\,x) \mathbin{/\!\!\!\wedge} (B\,x))\,(x :: e)\,k)$
- $Q_{\mathrm{s}}\,A\,B := \lambda ek.\,\mathbf{q}\,(\lambda x.\,A\,x\,e\,(\lambda e.\,\top))\,(\lambda x.\,((A\,x) \Rightarrow (B\,x))\,(x :: e)\,k)$

Déterminants quantificateurs

- $Q_{\mathrm{w}}\,A\,B := \diamond(Q_{\mathrm{w}}\,A\,B)$
- $Q_{\mathrm{s}}\,A\,B := \diamond(Q_{\mathrm{s}}\,A\,B)$

Avec $\diamond A := \lambda ek.\,(A\,e\,(\lambda e.\,\top)) \wedge (k\,e)$

Bibliographie

[1] R. Montague. The proper treatment of quantification in ordinary English. In J. Hintikka e.a., editor, *Approaches to Natural Language*, pages 221–242. Reidel, 1973.

[2] J. Barwise and R. Cooper. Generalized quantifiers and natural language. *Linguistic & Philosophy*, 4(2):159–219, 1981.

[3] C. Beysson. Déterminants et quantificateurs généralisés dynamiques. *TALN*, 2017.

[4] C. Beysson, S. Blind, Ph. de Groote, and B. Guillaume. Generalized quantifiers and dynamicity, preliminary results. *QUAD workshop, ESSLLI*, 2017.

Clément Beysson

Sous la direction de Philippe de Groote et de Bruno Guillaume

Équipe Sémagramme, Loria, Université de Lorraine, CNRS, Inria Nancy Grand Est

Loria

Numerical Analysis and Parallelization of a Domain Decomposition Method for the Full-Wave Simulation in cold Plasma.

Rihab Daadaa
Supervisors: Jean R. Roche and Simon Labrunie
Institut ÉLIE CARTAN de Lorraine

Introduction

Heating tokamak plasma to a very high temperature can be achieved by many techniques, among them injection of electromagnetic waves. The aim of this poster is to present a numerical simulation of the propagation of electromagnetic waves near the so-called lower hybrid (LH) frequency in a strongly magnetized plasma. This is a challenging issue because of the short wave length with respect to the machine size.

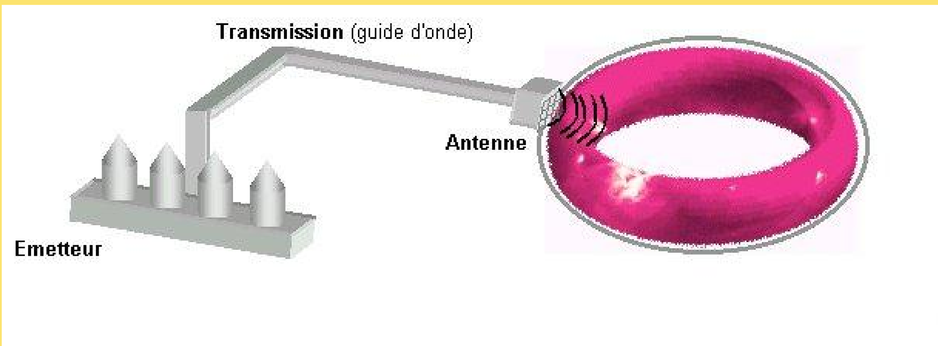

Model Problem

We consider the time-harmonic, inhomogeneous, anisotropic Maxwell equations with absorption, for an excited wave frequency $\omega > 0$. The electric field is the solution to:

$$\mathbf{rot}\,\mathbf{rot}\, E - k^2 \underline{K} E = 0 \quad \text{in } \Omega,$$
$$\operatorname{div}(\underline{K} E) = 0 \quad \text{in } \Omega,$$

where $k = \frac{\omega}{c}$, c is the speed of light. The *plasma response matrix* K is the following.

$$\underline{K} = \underbrace{\begin{pmatrix} S & -\imath D & 0 \\ \imath D & S & 0 \\ 0 & 0 & P \end{pmatrix}}_{\text{"permittivity"}} + \underbrace{\frac{\imath \gamma_e}{\varepsilon_0 \omega} \begin{pmatrix} 0 & 0 & 0 \\ 0 & 0 & 0 \\ 0 & 0 & 1 \end{pmatrix}}_{\text{Landau damping}}$$

The boundary $\Gamma = \partial\Omega$ is made of the antenna Γ_A and the remainder $\Gamma_C = \Gamma \setminus \Gamma_A$. On the antenna there holds:

$$\mathbf{rot}\, E \times n = \imath \omega \mu_0 J_A \quad \text{on } \Gamma_A,$$

where J_A is a current source equivalent to the electric field excited at the antenna. Elsewhere, the field satisfies the perfect conductor condition:

$$E \times n = 0 \quad \text{on } \Gamma_C.$$

Domain Decomposition

Introduce a non overlapping geometrical domain decomposition $\overline{\Omega} = \bigcup_{i=1}^{m} \overline{\Omega}_i$ and $\Omega_i \cap \Omega_j = \varnothing$ if $i \neq j$. We denote $\Sigma_{i,j} = \overline{\Omega_i} \cap \overline{\Omega_j}$ the interfaces between two subdomains, and $\Gamma^i = \Gamma \cap \partial\Omega_i$ the exterior boundary. Let $\Sigma = \cup_{i,j} \Sigma_{i,j}$ be the "skeleton of interfaces". On each subdomain we have the following problem: $E_i = E_{|\Omega_i}$ solves

$$\mathbf{rot}\ \mathbf{rot}\ E_i - \frac{\omega^2}{c^2} \underline{K} E_i = f_i \quad \text{in } \Omega_i,$$
$$\operatorname{div}(\underline{K} E_i) = g_i \quad \text{in } \Omega_i,$$
$$E_i \times n = 0 \quad \text{on } \Gamma^i.$$

In addition there are transmission conditions to preserve $H(\mathbf{rot}, \Omega)$ and $H(\operatorname{div} \underline{K}, \Omega)$ regularity and equivalence with the original problem:

$$[E \times n]_{\Sigma_{i,j}} = 0, \quad [\underline{K} E \cdot n]_{\Sigma_{i,j}} = 0$$
$$\mathbf{rot}\ E \times n_{\Sigma_{i,j}} = 0.$$

where $[F_i]_{\Sigma_{i,j}} = F_i - F_j$ is the jump across $\Sigma_{i,j}$.

Varational Formulation

We introduce the mixed augmented formulation for the multi-domain equations. The function spaces associated to our domain decomposition framework are the following:

$$W = \{v \in L^2(\Omega) : v_{|\Omega_i} \in H(\mathbf{rot}, \Omega_i) \cap H(\operatorname{div} \underline{K}, \Omega_i)\},$$
$$W_0 = \{v \in W : v \times n = 0 \text{ sur } \Gamma\},$$
$$S_\Sigma^W = \{\varphi \in H^{-1/2}(\Sigma) : \exists\, v \in X_N(\underline{K}, \Omega) \text{ such that } \varphi_{|\Sigma} = v_{|\Sigma}\}.$$

We obtain the following formulation: find $(E, p, \lambda) \in W_0 \times L^2(\Omega) \times (S_\Sigma^W)'$ such that

$$\sum_i \left[a_{i,s}(E_i, F_i) + b_i(F_i, p_i) \right] + \langle \lambda_n, [\underline{K} F \cdot n] \rangle_\Sigma$$
$$+ \langle \lambda_\top, [F \times n] \rangle_\Sigma = \sum_i L_i(F_i), \quad \forall F \in W_0,$$
$$\sum_i b_i(E_i, q_i) = \sum_i l_i(F_i), \quad \forall q_i \in L^2(\Omega_i), \quad (1)$$
$$\langle \mu_n, [\underline{K} E \cdot n] \rangle_\Sigma + \langle \mu_\top, [E \times n] \rangle_\Sigma = 0, \quad \forall \mu \in (S_\Sigma^W)'.$$

where we set, for $s \in \mathbb{C}$:

$$a_{i,s}(E_i, F_i) := (\mathbf{rot}\ E_i | \mathbf{rot}\ F_i) - k^2(\underline{K} E_i | F_i) + s(\operatorname{div}(\underline{K} E_i) | \operatorname{div}(\underline{K} F_i)),$$
$$b_i(F_i, p) := (\operatorname{div}(\underline{K} F_i) | p),$$
$$L(F_i) := i\omega\mu_0 (J_A | F_i)_{\Gamma_A},$$

The multi-domain problem is equivalent to the one-domain problem.

Numerical Results

The domain Ω is axisymmetric. We use a Fourier expansion in the angular coordinate, and a finite element method in the meridian section. The approximation scheme is known as the Taylor-Hood P_2-iso-P_1 finite element method; it is generally used to solve Navier Stokes equations.

The computational domain is a circle of radius 1m centered at $(3, 0)$. The external magnetic field $\mathbf{B}_0$ is invariant in time and orthogonal to the tokomak cross-section. The frequency is $\omega = 1.3117 \times 10^{10} rd/s$ and the external magnetic field $\mathbf{B}_0 = 3.2T$.

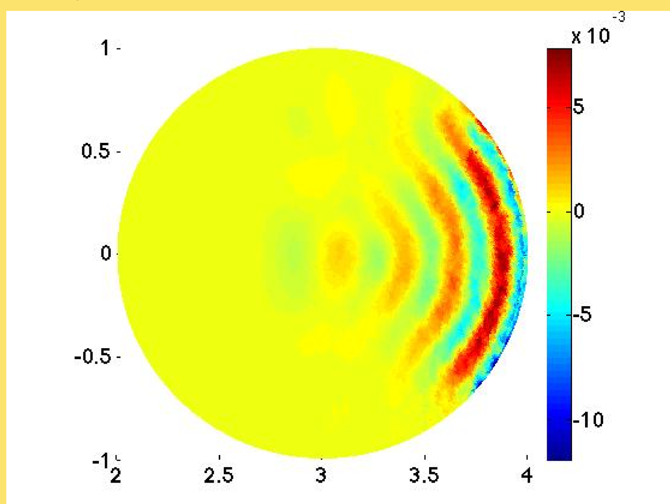

Figure 1: Value of the real part of the Fourier coefficient $\nu = 125$ of E_R, when $\omega = \omega_{LH}/4$

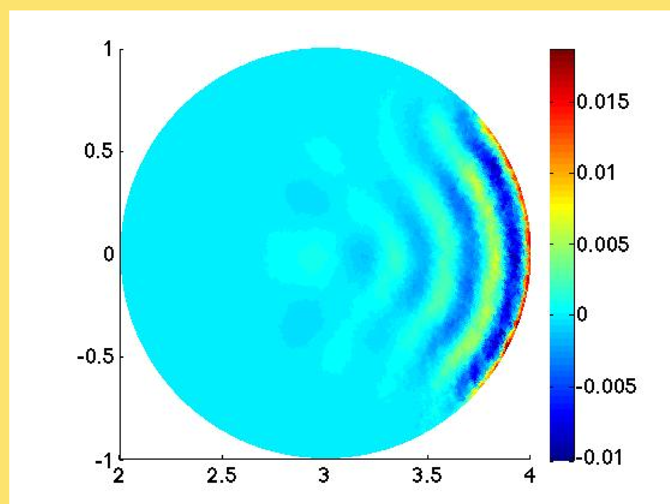

Figure 2: Value of the imaginary part of the Fourier coefficient $\nu = 125$ of E_R, when $\omega = \omega_{LH}/4$

Références

[1] Back A. R. Daadaa S. Labrunie J.-R. Roche P. Bertrand.
Numerical full wave simulation in a tokamak plasma.
ISH-2017, 2017.

[2] Back A. T. Hattori S. Labrunie J.-R. Roche P. Bertrand.
Electromagnetic wave propagation and absorption in magnetise plasmas : variational formulation and domain decomposition.
M2AN, 49:1239–1260, 2015.

[3] T. Hattori.
Décomposition des domaines pour la simulation Full-Wave dans un plasma.
PhD thesis, University of Lorraine, 2014.

rihab.zammit-chatti@univ-lorraine.fr

Design of HF power supplies for driving piezoelectric transducers operating in the 1-3 MHz range

Hamidreza Zandi,
Université de Lorraine, GREEN, Vandœuvre-lès-Nancy, 54500, France

Piezoelectric effect

- ➜ Generation of electrical voltage due to mechanical constraint
- ➜ Crystals with no inversion symmetry
- ➜ Reversible effect

High Frequency Power transducers

- Oil extraction (dozen of kHz and kW);
- Welding (dozens of kHz and some kW) ;
- Mixing (some MHz and dozen of Watts);
- Cleaning (dozens of kHz and dozens of Watts).

Power Supply topologies

Linear power supplies

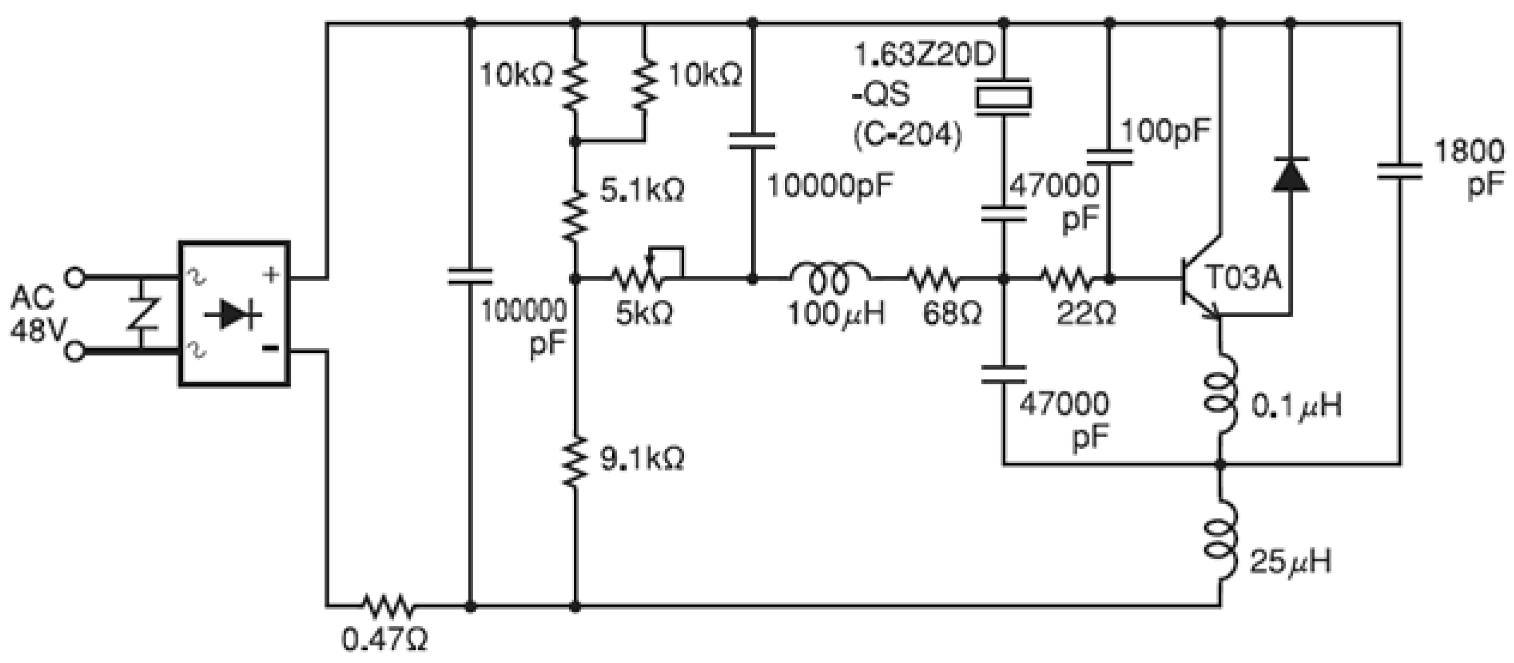

A feed-backed oscillator based structure proposed by Fujicera Co.

Switched mode power supplies

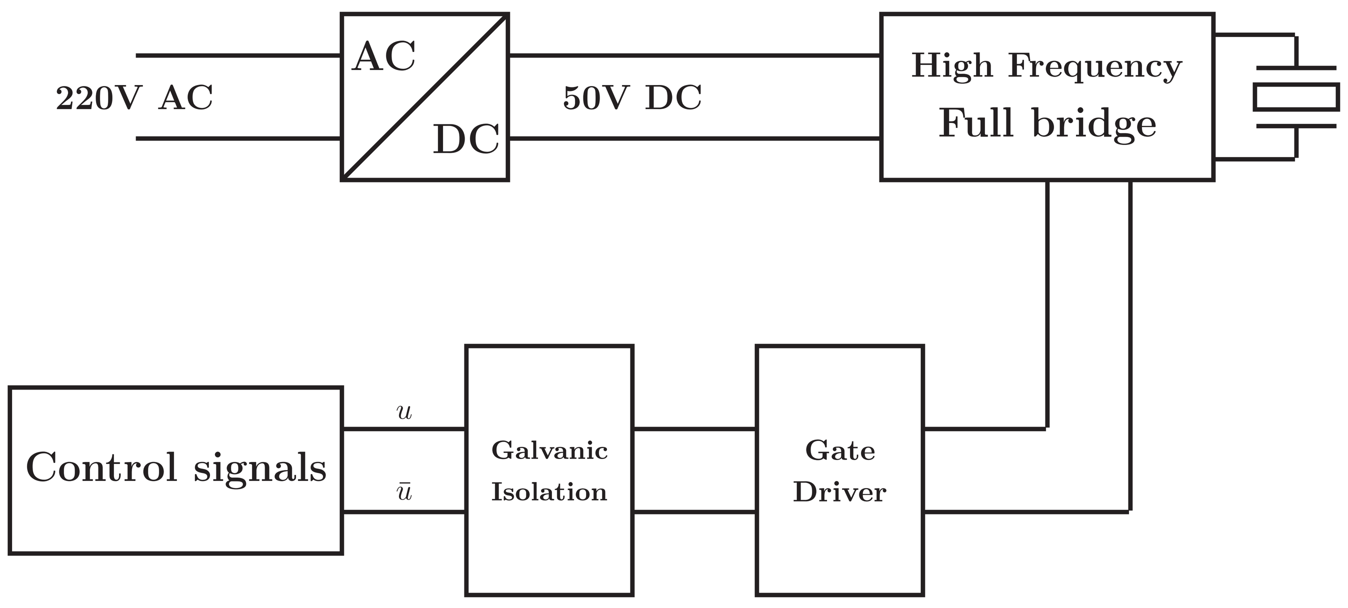

A Full bridge inverter system for driving PT.

Waveform comparison

Oscillator based power supply

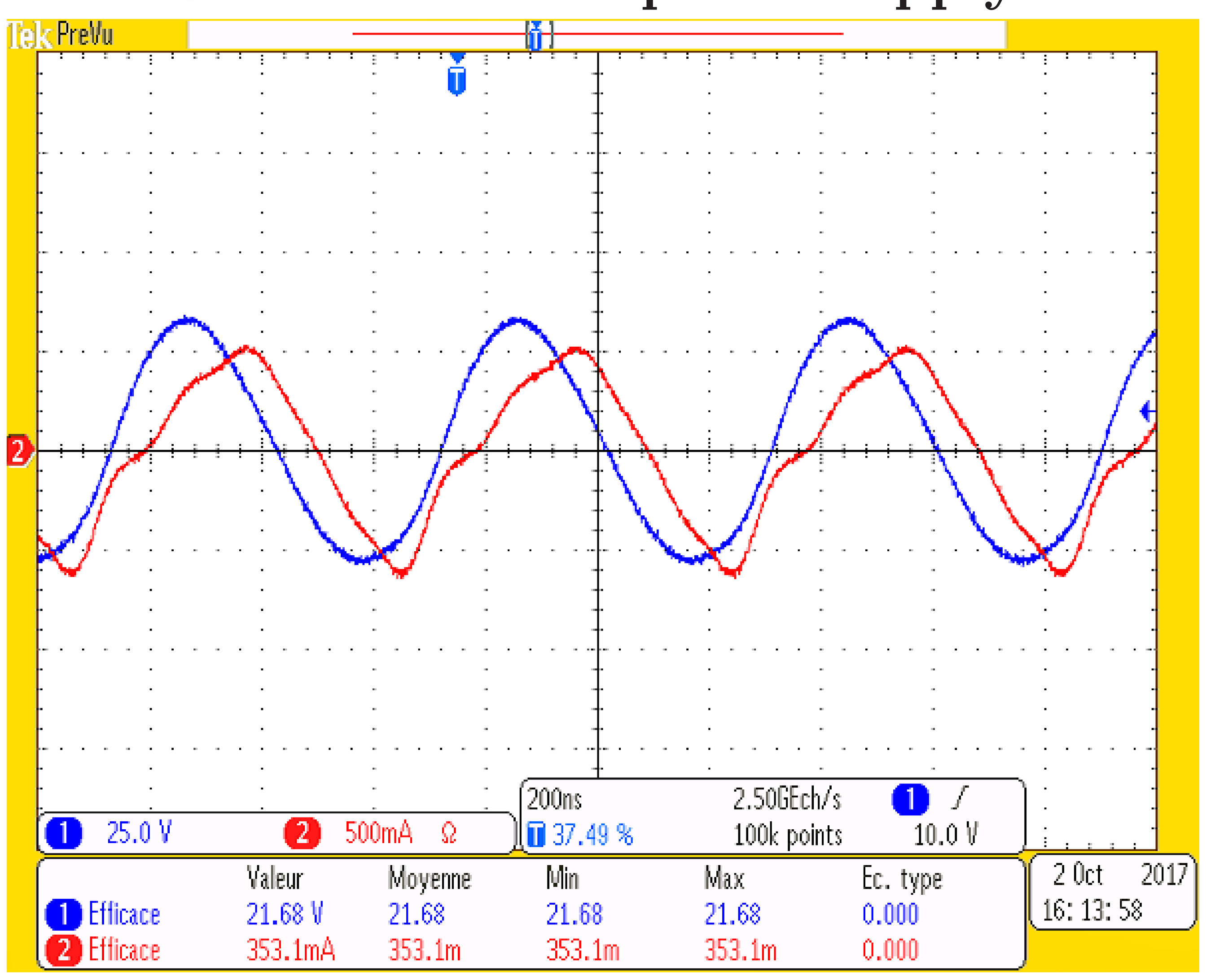

Voltage across the transducer and the delivered current

High frequency SMPS

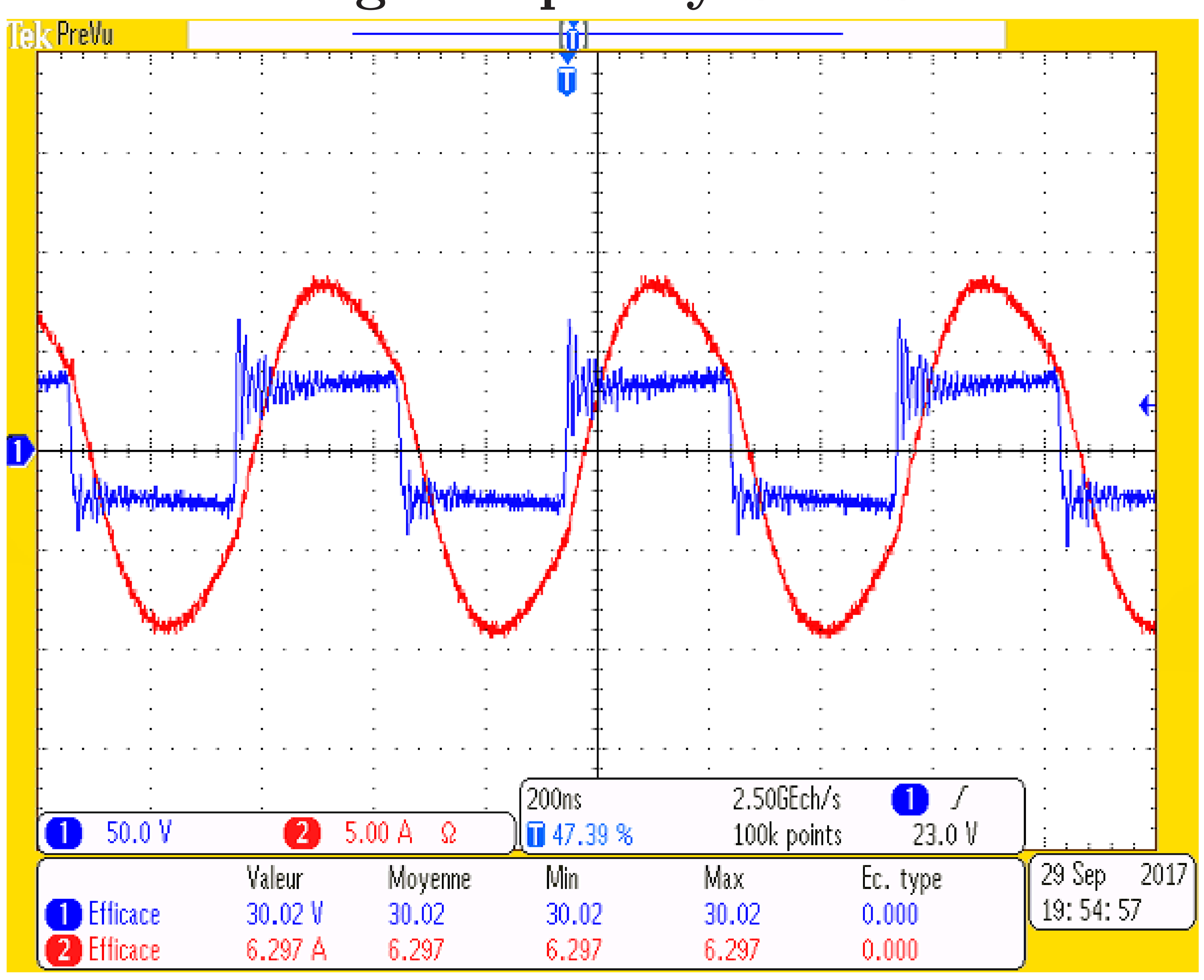

Inverter output voltage and the delivered current

Power Fast Switching

- ➜ Important Gate Drive Current
- ➜ EMI/EMC protection
- ➜ Ringing and overvoltage
- ➜ DC bus instabillity
- ➜ Connections and loop L reduction

Summary of the new power supply

- ➜ More than 5x more power transfer (eg. 200 W at a 1,7 MHz).
- ➜ Finer resonance tracking with the possibility of choosing the resonance mode in case of several exisiting modes.
- ➜ Covering the whole 1-3 MHz frequency range.
- ➜ High electrical efficiency and minimized losses (98% efficieny)
- ➜ Possible use of feed-back loops with PLL, DDS, DSP or FPGA.

Conclusion

- With the emergence of ultra-fast power switching devices an SPMS can be used to drive megasonic power PTs.
- SPMS guarantee a finer resonance tracking and makes one able to maximize the output power. However they require complicated control techniques.

ANNEXE 2 – Liste des participants

PARTICIPANTS AU FORUM FCH-ENTREPRISES
LORIA - 18/01/2018

ALTMEYER	Sophie	sophie.altmeyer@hydreos.fr		Pôle Hydréos
ALVAREZ	Rodrigo	rodrigo.alvarez@arcelormittal.com		Arcelormittal Global R&D
BARBIER	Florent	florent.barbier@predict.fr		PREDICT
BAYLE	Bernard	bernard.bayle@unistra.fr		Icube
BEATRIX	Alexis	alexis.beatrix@thewiw.com		WiW
BELLET	Jean-Baptiste	jean-baptiste.bellet@univ-lorraine.fr	IECL	
BELLOCCHIO	Jean-Baptiste	jb.bellocchio@minich-sas.fr		MINICH SAS
BENARAB	Djamel	djamel-eddine.benarab@univ-lorraine.fr	CRAN	
BESANCON	Franck	franck.besancon@crai.archi.fr	MAP-CRAI	
BODIN	Jonathan	jonathan.bodin@alsace-biovalley.com		Pôle Alsace Biovalley
BOLSHAKOVA	Veronika	bolshakova.veronika@gmail.com	MAP-CRAI	
BOLTCHEVA	Dobrina	dobrina.boltcheva@univ-lorraine.fr	LORIA	
BOUMAHDI	Mohamed	mb@cditech.fr		CDI Technologies
BRENTAN	Bruno	bruno.brentan@univ-lorraine.fr	CRAN	
BRIL	Hind	Hind.El-Haouzi@univ-lorraine.fr	CRAN	
CAGNINA	Yann	yann.cagnina@fibres-energivie.eu		Pôle Fibres Energivie
CALDINI-QUEIROS	Céline	celine.caldini-queiros@cemosis.fr	CEMOSIS/IRMA	
CASSINIS	Frédérique	fcassinis@gmail.com		ACROTIR
CERISARA	Christophe	christophe.cerisara@inria.fr	LORIA	
CIARLETTA	Laurent	laurent.ciarletta@loria.fr	LORIA	
CLAUSEL	Marianne	marianne.clausel@univ-lorraine.fr	IECL	
CONTASSOT-VIVIER	Sylvain	sylvain.contassotvivier@loria.fr	LORIA	
CRIQUI	Olivier	o.criqui@bouygues-construction.com		Bouygues Bâtiment Nord Est
CROMPIN	Jean-Michel	jean-michel.crompin@univ-lorraine.fr	ICEEL	
DA SILVA SERAPIO LEAL	Gabriel	gabriel.da-silva-serapiao-leal@univ-lorraine.fr	Doctorante	
DAADA	Rihab	rihab.zammit-chatti@univ-lorraine.fr	Doctorante	
DAUNOIS	Thierry	thierry.daunois@univ-lorraine.fr	Direction des Partenariats	
DEACONU	Madalina	madalina.deaconu@univ-lorraine.fr	INRIA	
DE BENOIST	Augustin	sdebenoist@iso-top.net		Iso-Top
DE BENOIST	Stanislas	sdebenoist@iso-top.net		Iso-Top
DE CHEFDEBIEN	André	andre.dechefdebien@groupe-lesage.fr		Groupe Rector-Lesage
DERIGENT	William	william.derigent@univ-lorraine.fr	CRAN	
DERMY	Oriane	oriane.dermy@gmail.com	Doctorante	
DE SANTIS	Giulia	giulia.de-santis@inria.fr	INRIA	
DEVIGNES	Marie-Dominique	marie-dominique.devignes@loria.fr	LORIA	
DRAPIER-BECHE	Stéphane	stephane.drapierbeche@bpifrance.fr		Bpifrance
DUJARDIN	Jean-Louis	dujardin@weris-energie.fr		Weris Energie
ELBAR	Fabienne	fabienne.elbar@inria.fr	INRIA	
FICK	Michel	michel.fick@univ-lorraine.fr	VP Partenariats	
FOURNIER	Damien	damien.fournier@cribois.net		CRITT Bois
FREVILLE	Tristan	contact@drone-alsace.fr		Drone Alsace
GEGOUT-PETIT	Anne	anne.gegout-petit@univ-lorraine.fr	IECL	
GLESS	Henri-Jean	gless@crai.archi.fr	MAP-CRAI	
GOTHIE	Emmanuel	emmanuel.ghotie@inria.fr	INRIA	
GOUYON	David	david.gouyon@univ-lorraine.fr	CRAN	
GUENARD	Adrien	adrien.guenard@loria.fr	LORIA	
GUERRIERO	Annie	annie.guerriero@list.lu		LIST
HALIN	Gilles	halin@crai.archi.fr	MAP-CRAI	
HANS	Jérôme	j.hans@jbtecnics.com		JBT PLAST
HENAFF	Patrick	patrick.henaff@loria.fr	LORIA	
HENROT	Antoine	antoine.henrot@uiv-lorraine.fr	IECL	
HOCHSCHEID	Elodie	elodie.3h@gmail.com	MAP-CRAI	
IUNG	Benoit	benoit.iung@univ-lorraine.fr	CRAN	
IVALDI	Serena	serena.ivaldi@loria.fr	LORIA	
JACGLIN	Philippe	philippe.jacglin@fibres-energivie.eu		Pôle Fibres Energivie
JORDAN	Philippe	philippe.jordan@fibres-energivie.eu		Pôle Fibres Energivie
KADHIM	Sadeq	sadeq.kadhim@univ-lorraine.fr	IECL	
KERAUTRET	Bertrand	bertrand.kerautret@univ-lorraine.fr	LORIA	
KOLANEK	Daniel	kolanekd@grandest.ffbatiment.fr		FFB Grand Est
LAHMADI	Abdelkader	abdelkader.lahmadi@loria.fr	LORIA	
LAPRIE	Yves	yves.laprie@loria.fr	Pôle AM2I	
LAURAIN	Vincent	vincent.laurain@univ-lorraine.fr	CRAN	
LEBER	Florence	florence.leber@engees.unistra.fr	ENGEES	
LEVRAT	Eric	eric.levrat@univ-lorraine.fr	CRAN	
LIEBER	Jean	jean.lieber@loria.fr	LORIA	
MARANGE	Pascale	pascale.marange@univ-lorraine.fr	CRAN	
MARION	Jean-Yves	jean-yves.marion@loria.fr	LORIA	
MARZIN	Pierre	pierre.marzin@siemens.com		SIEMENS
MAUMY-BERTRAND	Myriam	mmaumy@math.unistra.fr	CEMOSIS/IRMA	
MEFIRE	Séraphin	seraphin.mefire@univ-lorraine.fr	IECL	
MICHEL	Jérôme	jerome.michel@realtimeatwork.com		RTaW
MONARD	Gérald	gerald.monard@univ-lorraine.fr	Explor	
MONNEZ	Jean-Marie	jean-marie.monnez@univ-lorraine.fr	IECL	
MONNIN	Maxime	m.monnin@vize.io		Vize Software
MOUGEL	Jérôme	j.mougel@odymail.fr		ODYSSEE Environnement
MOUREAUX	Jean-Marie	jean-marie.moureaux@univ-lorraine.fr	CRAN	
NATAF	Emmanuel	emmanuel.nataf@loria.fr	LORIA	
NGATCHOU WANDJI	Joseph	joseph.ngatchou-wandji@univ-lorraine.fr	IECL	
PENA	Dorian	dorian.pena@univ-lorraine.fr	EXPLOR	
PEREZ	Laurent	laurent-l.perez@edf.fr		EDF
PERRINO	Alexi	alexi.perrino@materalia.fr		Pôle Matéralia
PERROT	Alexandre	alexandre.perrot@ac-process.com		A&C Process

PINCON	Bruno	bruno.pincon@univ-lorraine.fr	IECL	
POIROT	Yan	yan@poirot-construction.fr		Groupe Poirot
PONSART	Jean-Christophe	jean-christophe.ponsart@univ-lorraine.fr	CRAN	
PRACCHIA	Bruno			UIMM Lorraine
PRUD'HOMME	Christophe	christophe.prudhomme@agence-maths-entreprises.fr		AMIES
RADOUX	Jean-Pierre	jeanpierre.radoux@altran.com		ALTRAN
RAGOT	José	jose.ragot@univ-lorraine.fr	CRAN	
RAMDANE CHERIF	Wahiba	ramdanec@loria.fr	LORIA	
RIBLET	Tom	tom.riblet@gmail.com	Doctorant	
RIMBERT	Sébastien	sebastien.rimbert@univ-lorraine.fr	Doctorant	
ROCHE	Jean-Rodolphe	jean-rodolphe.roche@univ-lorraine.fr	IECL	
SAUDER	Laurent	laurent.sauder@univ-lorraine.fr	EXPLOR	
SCHAEFFER	Philippe	philippe.schaeffer@inria.fr	INRIA	
SEGHIR	Sakina	sakina.seghir@materalia.fr		Pôle Matéralia
SIRONI	Damien	damien.sironi@thewiw.com		WiW
SONG	Yingying	yingying.song@univ-lorraine.fr	Doctorant	
SONG	Ye-Qiong	ye-qiong.song@loria.fr	LORIA	
STOICA	Radu	radu-stefan.stoica@univ-lorraine.fr	IECL	
SZATKOWSKI	Cécilia	cecilia.szatkowski@hydreos.fr		Pôle Hydréos
THOMAS	André	andre.thomas@univ-lorraine.fr	CRAN	
TRAN	Nguyen	nguyen.tran@univ-lorraine.fr	Ecole de Chirurgie	
TURCK	Yann	yturck@grundfos.com		Pompes Grundfos
VALENTIN	Claude	claude.valentin@haha.fr		HAHA Architecture
VALLOIS	Pierre	pierre.vallois@univ-lorraine.fr	IECL	
VANDERMEERSCHEN	Julien	julien@drone-alsace.fr		Drone Alsace
VINCENT	Emmanuel	emmanuel.vincent@inria.fr	INRIA	
VOISIN	Alexandre	alexandre.voisin@univ-lorraine.fr	CRAN	
ZEGARRA-FLORES	Jesus	jesus.zegarraflores@altran.com		ALTRAN